STUDIES ON
ALANINE AMINOTRANSFERASE
FROM PIG HEART

A THESIS

Presented in part fulfilment of the requirements
for the degree of Doctor of Philosophy

of the

University of Warwick

by

Ian Maxwell Austin

B.Sc. Birmingham

Department of Molecular Sciences

University of Warwick

March 1974

ACKNOWLEDGEMENTS

The author wishes to express his gratitude to Dr. B. E. P. Swoboda, for help and encouragement throughout the course of this work.

The author also wishes to thank Professor V. M. Clark, for providing the facilities necessary for the research.

Thanks are due to all the members of Dr. Swoboda's research group for their helpful advice.

A grant from the Science Research Council is gratefully acknowledged.

ABBREVIATIONS

A_λ	Absorbance at wavelength λ
AB	α Aminobutyrate
Ala	Alanine
Ala AT	Alanine aminotransferase
AS	Ammonium sulphate
Asp AT	Aspartate aminotransferase
DEAE cellulose	Diethylaminoethyl cellulose
EDTA	Ethylene diamine tetraacetate
Glu	Glutamate
KB	α Ketobutyrate
KG	α Ketoglutarate
K_i	Inhibition constant
K_m	Michaelis constant
λ	Wavelength
LDH	Lactate dehydrogenase
MDH	Malic dehydrogenase
ME	β Mercaptoethanol
M.W.	Molecular weight
NADH	Reduced β nicotinamide adenine dinucleotide
PM	Pyridoxamine
PMP	Pyridoxamine 5' phosphate
PL	Pyridoxal
PLP	Pyridoxal 5' phosphate
Pyr	Pyruvate
TNM	Tetranitromethane
TSC	Thiosemicarbazide
v	Reaction velocity

SUMMARY

Ala AT was purified from pig heart by a new procedure, which consisted of an homogenisation, ammonium sulphate fractionation, heat treatment and a second AS fractionation, followed by DEAE cellulose and Sephadex G200 chromatography.

The purified enzyme had a specific activity of 450 units/mg protein, and appeared to be at least 95 % pure, from electrophoresis.

Sodium dodecyl sulphate - polyacrylamide gel electrophoresis indicated a subunit molecular weight of 52 000. The concentration of the coenzyme was measured: it was 1 mole/54 000 gm protein.

The kinetic parameters for four different assays and the inhibitor constants for several inhibitors were determined, at 25°C, at several pHs. These parameters were found to vary considerably with buffer concentration. For this reason, the values of these parameters were extrapolated to zero buffer concentration.

From a study of the affinities of several different inhibitors for ala AT, at pH 8.0, it seems that the α carboxyl and side groups of the substrate, (as well as the α amino and α keto groups), are involved in binding to the enzyme.

A Dixon analysis of the results shows the existence of certain catalytically important pKs in the free forms of the enzyme, the enzyme-substrate complexes, and the enzyme-inhibitor complexes.

The nature and role of the enzyme groups that are involved in substrate binding are deduced, in part.

Visible absorption spectra were recorded at 25°C. PL-ala AT shows a spectral pK at pH 7.6. This pK is raised to about pH 8 by fumarate or acetate binding. The dissociation constants obtained are similar to the inhibition constants. TSC binding produces an intense absorbance peak at 390 nm: a similar result has been obtained with asp AT.

Substrates were titrated with ala AT and spectra of the enzyme-substrate complexes were calculated. An absorbance peak at 490 nm is observed. It is very probably a deprotonated, (highly conjugated), complex: i.e. there are separate deprotonation and protonation steps. A rough estimate is made for the relative concentrations of the different spectral forms of the enzyme-substrate complex, at pH 7.0.

The pH dependence of the L alanine-pyruvate equilibrium enzyme-substrate complex spectrum was studied. The changes between pH 5.5 and 10.5 can be ascribed to three pKs, and were used to explain the pKs of the complex, that were shown by kinetic analysis.

The inactivation of the enzyme was studied using heat, (65°C), 5.6 M urea, formaldehyde, nitrite, TNM, and photo-oxidation by rose bengal and methylene blue.

Both methylene blue photo-oxidation and TNM inactivation of ala AT give results similar to those obtained by Martinez-Carrion, for asp AT.

Wtih methylene blue, an essential residue is modified, which has a low pK and is believed to be a catalytic base; it is probably a histidine.

With rose bengal photo-oxidation, nitrite and TNM, inactivation is incomplete and the nature and role of the modified residue is

most uncertain.

The results with formaldehyde inactivation suggest that it inactivates by a reaction at the active site: the possibility that this reagent cross-links a histidine and a lysine group is discussed.

The inactivation results, all together, indicate that two different conformational changes can occur, when substrate is bound to ala AT. The nature of these changes and their relation to the kinetic results are discussed.

A detailed model of the catalytic activity of ala AT is presented.

INDEX

CHAPTER 1

INTRODUCTION

1.1 ALANINE AMINOTRANSFERASE

The systematic name of alanine aminotransferase, (ala AT), is pyruvate - oxoglutarate - aminotransferase, (E.C. 2.6.1.2.). It catalyses the reversible transfer of an amino group between pyruvate and ∝ketoglutarate in the following reaction:

L alanine + ∝ketoglutarate $\rightleftharpoons$ pyruvate + L glutamate

1.1(a) Physiological Role

Ala AT has been found in all animals, plants and bacteria, investigated (38, 57, 69, 210). With aspartate aminotransferase, (asp AT), it seems to account for most of the transaminase activity. This gives the principal transamination pathways shown.

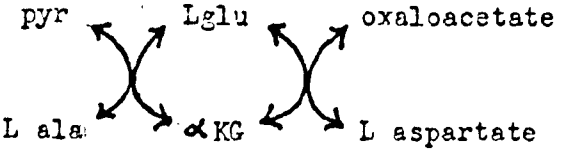

The three keto-acids are intermediates in carbohydrate degradation. L Glutamate and L aspartate are the precursors for several other amino-acids; L alanine is not. However, ala AT has another role besides the synthesis of alanine.

Grodzenskii (71) studied glycolysis in pig muscle and showed that adding glutamate caused a rise in alanine concentration,

with a fall in lactate, (whether oxygen was present or absent). Experiments with drugs that increase brain concentrations of ammonia suggested that L alanine production acts as a major ammonia-regulating system in rat brain (79). Mallette, Exton and Park (121) have reviewed evidence that; (A) alanine is the main contributor to the amino-acid output of muscle, heart, and kidney; (B) alanine is the chief amino-acid utilised in gluconeogenesis and(C) alanine is the only amino-acid for which the blood level responds to glucose or to insulin. They suggested that there is a physiologically important alanine cycle: this allows the catabolism of other amino-acids in the tissues, while the surplus, toxic ammonia is transported in the blood in the form of alanine. Although alanine constitutes less than 10% of the protein amino-acid of muscle and less than 10% of the free amino-acid of blood, it provides 35-40% of the total amino-acid flux between the liver and other tissues. Ala AT is central to such a role(55).

1.1(b) Clinical Significance

When a disease causes cell damage, enzymes are released into the blood from the damaged tissues. Measurement of the (normally low) blood levels of ala AT and asp AT is used to monitor, or even diagnose, diseases, especially those of the liver. The ratio of the activities of these two enzymes is the most reliable parameter and is sensitive to the tissue's nature, and the extent of damage.

1.1(c) Discovery of Alanine Aminotransferase

The first transamination was carried out in a non-enzymic

system by Herbst and Engel, in 1934 (84). In 1937 Braunstein and Kritsman postulated the existence of enzymic transamination in plants and pigeon muscle (23). Cohen, in 1942, demonstrated transamination in a variety of organisms and suggested that most of this activity could be accounted for by two specific enzymes, ala AT and asp AT (38). These two enzymes were separated and partially purified in 1945, by Green, Leloir and Nocito (69). Both have been completely purified since then (67, 93). Also, several other transaminases have been demonstrated.

1.1(d) Coenzyme

Lysine decarboxylase has been resolved into the apoenzyme and codecarboxylase: this coenzyme was assayed in several organisms and tissues (65, 66). Its structure is pyridoxal 5' phosphate, (PLP) (11). Green, Leloir and Nocito found it at high concentrations in their ala AT and asp AT preparations (69). It is believed to be an essential component, (or substrate), of all transaminases and several other enzymes with amino-acid substrates. Recent experiments show that it is bound to the protein in stoichiometric quantities (67, 156, 170).

1.1(e) Kinetics

Ala AT has never been shown to catalyse any reaction other than a transamination, but the possibility of slow alternative reactions has not been properly investigated. With appropiate substrates, asp AT gives deamination and β elimination (107, 108, 122, 194).

In the presence of an amino-acid and its corresponding keto-

acid, (e.g. L alanine and pyruvate), no change was seen. If the keto-acid was labelled with ^{14}C the appearance of a labelled amino-acid was observed (171).

The activity of ala AT has been studied with the substrate pairs:- pyruvate plus L glutamate, and L alanine plus ∝keto-glutarate. In each case, for rat liver (96), and pig heart (171) enzymes, the results at low substrate concentrations were analysed to give an equation of the form:

$$v^{-1} = \phi_0 + \phi_1 S_1^{-1} + \phi_2 S_2^{-1}$$

where v is the initial rate of formation of one of the products.

S_1 and S_2 are the concentrations of each substrate

ϕ_0, ϕ_1 and ϕ_2 are constants

There is no mixed S_1S_2 term - indicating no interaction between the substrates, which suggests a ping-pong mechanism, as does the isotope exchange experiment. At high substrate concentrations, substrate inhibition was observed.

From these studies the mechanism of figure 1.1. was deduced.

1.1(f) Spectral Properties

The mechanism of figure 1.1. postulates two distinct free forms of ala AT: these can be prepared and show totally different visible absorption spectra, (figure 1.2.)(67, 170).

The form, E_M, has an absorption peak at 330 nm. and is pH independent. The E_I form, at high pH, has a peak at 360 nm. and at low pH, has peaks at 340 nm. and 430 nm., with a spectral pK at pH 7.4. Comparison with free vitamin B_6 derivatives (58, 81, 82 139, 155), suggests that E_M is saturated and E_I is unsaturated at

FIGURE 1.1

A simple ping-pong model of alaAT activity. E_M and E_L are free forms of the enzyme: ES_1 and ES_2 are enzyme-substrate complexes.

FIGURE 1.2

The absorption spectra of rat liver ala AT, between 300 and 500 nm, as obtained by Gatehouse, Hopper, Schatz and Segal (67).

—— the pyridoxamine form at pH 8.3

--- the pyridoxal form at pH 8.3

—— the pyridoxal form at pH 5.0

FIGURE 1.3

The visible absorption spectra of pig heart ala AT, in 50 mM pH 9.2 tetraborate buffer, as obtained by Jenkins (100).

—— with 0.3 M L alanine

—— with 0.01 M pyruvate

--- with 0.3 M L alanine and 0.01 M pyruvate

TABLE 1.1

Kinetic constants for pig heart ala AT, at 37°C, with 20 mM pH 8.0 tris chloride buffer, 50 mM amino-acid, and 10 mM keto-acid, as obtained by Saier and Jenkins.(171).

The first two columns compare the transaminase activity for L alanine or L glutamate with that for other amino-acids.

The next two columns show the inhibition, when 50 mM amino-acid is added to an assay containing 50 mM L alanine or L glutamate.

In the last column, a dissociation constant is given, on the assumption that the amino-acids are simple competitive inhibitors.

FIGURE 1.1.

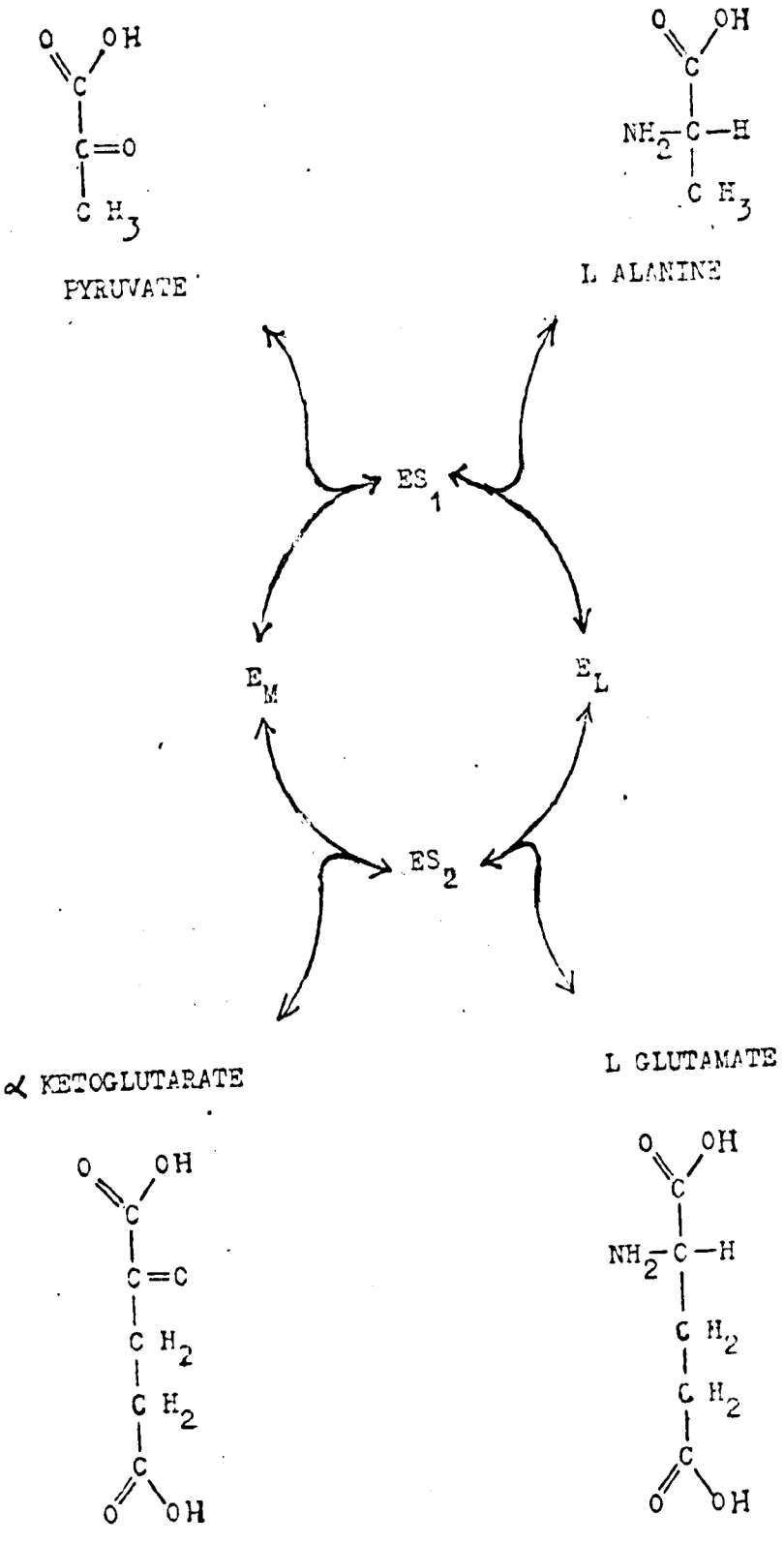

FIGURE 1.2.

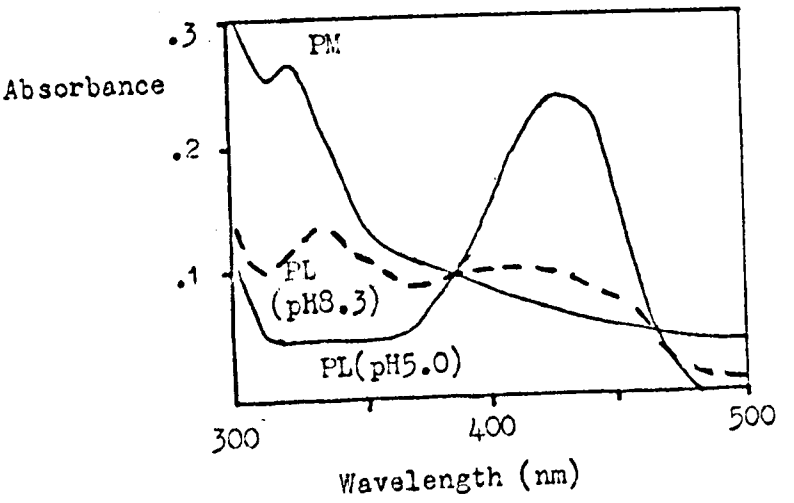

FIGURE 1.3.

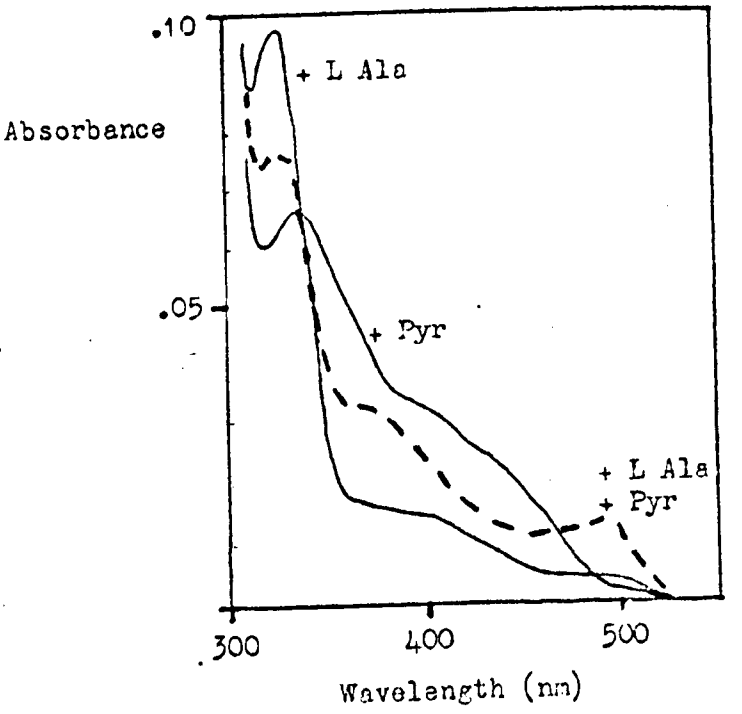

TABLE 1.1.

Amino-acid	Activity %		Inhibition %		Dissociation Constant (mM)
	+ KG	+ Pyr	Ala	Glu	
L ∝ aminobutyrate	1.4	1.5	28	29	30
L Alanine	100			45	28
L Norvaline		.2	34	32	70
L Norleucine	.08		53	50	30
L Ornithine	.04	.02	27		
L Aspartate	.13	.16	6	7	550
L Glutamate		100	60		25
DL β Hydroxy Glutamate		.5	30		
L ∝ Amino Adipate		.36	28	17	90
Glycine			7	10	500
L Leucine			20		
L Serine			17		
D Glutemate			0	0	
L Asparagine			19		
L Glutamine			8		
DL ∝ Methyl Glutamate			35	40	
γ Aminobutyrate			3	3	
Glutarate			3		
D Alanine			3	5	

the C_4, carbon of the coenzyme.

Reduction of E_L with sodium borohydride fixed the coenzyme to the apoenzyme, while lowering the absorption peak to about 330 nm. After digestion, pyridoxyl ϵ N lysine was isolated(156). Hence E_M probably contains pyridoxamine 5'phosphate(PMP), and is called the pyridoxamine form; E_L probably contains a PLP-ϵN lysine imine and is called the pyridoxal form.

Addition of substrates or inhibitors alters the absorption spectrum. In particular, with L alanine plus pyruvate, a separate peak at 490 nm. appears which seems to be an intermediate enzyme-substrate complex (99, 100, 101).

1.1(g) Substrate Specificity

The substrate specificity varies with the source of the ala AT. For pig heart the relative rates for different amino-acids (in 50mM, pH8, tris chloride, at 37°), are given in table 1.1.

1.1(h) Inhibition

Table 1.1. also gives the inhibition produced by different amino-acids, (with calculated inhibitor constants). The enzyme discriminates between amino-acids mainly at the catalytic step (171).

Other inhibitors are L cycloserine (10, 24), cyanide, hydroxylamine, sodium borohydride, succinate, maleate, fumarate, glutarate, p chloromercuribenzoate, mercury(II) chloride, acrylonitrile (188), formate, acetate, pyruvate, α ketoglutarate, L glutamate,(171), and phosphopyridoxyl-amino-acids (175). Aminooxyacetate and acrylate have only been tested on rat liver ala AT (174).

1.1(i) Activation

Formate decreased the % of the L alanine-α ketoglutarate assay and of the L alanine-pyruvate isotope exchange (171). Perhaps it accelerates the L ala $\rightarrow$ pyr step, by binding to a site that also binds the γ carboxyl group of α ketoglutarate and L glutamate - henceforth called the γ carboxyl site.

1.1(j) Physical Properties

Estimates of the molecular weight are: 82 000 (9), 91 000 (195), and 115 000 (170), for pig heart; 112 000 for rat liver (67); and 79 000 for Cheepewa seed ala AT (46). In general, the ultracentrifuge results are higher than the Sephadex results.

The rat liver ala AT has two moles of coenzyme per mole of enzyme (67): the highest estimate for pig heart is 1.5 (170).

The fluorescence yields for both forms of the enzyme are low, rising about tenfold on denaturation. The polarisation of fluorescence of PM ala AT shows a considerable coenzyme rotation that is almost independent of the viscosity of the medium - i.e. it is due to motion of the coenzyme within the enzyme (37).

The coenzyme has been reversibly dialysed from the Cheepewa seed enzyme - the apoenzyme is inactive(46). The pig heart enzyme can only be resolved by denaturing the protein (37, 156).

1.2 ASPARTATE AMINOTRANSFERASE

Asp AT is similar in many ways to ala AT. Considerably more results have been obtained with it, which can suggest possible properties in ala AT.

The molecular weight is about 90 000 (13, 34, 49, 56, 93, 95)

1.1(i) Activation

Formate decreased the Øo of the L alanine-∝ketoglutarate assay and of the L alanine-pyruvate isotope exchange (171). Perhaps it accelerates the L ala → pyr step, by binding to a site that also binds the ϒ carboxyl group of ∝ ketoglutarate and L glutamate - henceforth called the ϒ carboxyl site.

1.1(j) Physical Properties

Estimates of the molecular weight are: 82 000 (9), 91 000 (195), and 115 000 (170), for pig heart; 112 000 for rat liver (67); and 79 000 for Cheepewa seed ala AT (46). In general, the ultracentrifuge results are higher than the Sephadex results.

The rat liver ala AT has two moles of coenzyme per mole of enzyme (67): the highest estimate for pig heart is 1.5 (170).

The fluorescence yields for both forms of the enzyme are low, rising about tenfold on denaturation. The polarisation of fluorescence of PM ala AT shows a considerable coenzyme rotation that is almost independent of the viscosity of the medium - i.e. it is due to motion of the coenzyme within the enzyme (37).

The coenzyme has been reversibly dialysed from the Cheepewa seed enzyme - the apoenzyme is inactive(46). The pig heart enzyme can only be resolved by denaturing the protein (37, 156).

1.2 ASPARTATE AMINOTRANSFERASE

Asp AT is similar in many ways to ala AT. Considerably more results have been obtained with it, which can suggest possible properties in ala AT.

The molecular weight is about 90 000 (13, 34, 49, 56, 93, 95)

It can be reversibly dissociated into two subunits, each with one mole of coenzyme (161). The holoenzyme can be resolved and reformed (137).

Thus the coenzyme can be replaced by analogues. It has been shown that the phosphate, phenol, formyl groups and the pyridine nitrogen are all necessary (19, 64, 80, 144). N.B. In Tryptophan synthetase, 4,nitrosalicaldehyde can replace PLP (149), as well as in model systems (89, 138). The kinetics of coenzyme binding have been studied (4, 6, 35, 36, 50, 151).

The spectra of the free enzyme (92) and the basic kinetics (200) are qualitatively the same as for ala AT.

Addition of substrates gives a complex spectrum with only a very slight peak at 490 nm. (96, 103, 104,). With PL asp AT, dicarboxylic acids raise the spectral pK considerably,(59, 78, 94, 105) while β erythro, hydroxy aspartate gives a very large peak at 492 nm., which has been ascribed to a semiquinoid structure (97, 102).

Both protein and coenzyme show optical activity. Substrate binding has a profound effect on the coenzymic circular dichroic spectrum,which has been interpreted as a rotation of the coenzyme 25, 52, 53, 90, 91, 190,191).

T-jump experiments with substrates and their analogues (40,54, 72, 75, 76, 77)show that there are a large number of distinct forms of the enzyme-substrate complex, Up to eight equilibria have been found for hydroxy aspartate; their mechanistic signifance is most uncertain.

Treatment with sodium borohydride (88), and β bromo-propionate (147, 152)demonstrated the presence of the pyridoxal-ϵN lysine imine at the active site.

Photooxidation experiments showed that one histidine residue is essential for catalysis but not for substrate binding (127, 129, 130). Its location at the active site is suggested by other experiments (111, 112, 117, 196).

A cysteine and a tyrosine residue are also involved but their functions are most uncertain (16, 17,18, 20, 33, 39, 110, 159, 162 178, 179, 189, 192, 193, 198).

Extensive comparisons have been made between cytoplasmic and mitochondrial asp AT and between their isozymes. No differences in the mechanism of activity or gross physical structure have been recorded (5, 15, 43, 83, 125, 126, 128, 131, 143, 143, 181,182, 186).

The most detailed theories of enzymic transamination are based on our knowledge of asp AT. It is desirable to experiment on other transaminases in order to obtain a more balanced picture and also because they may be more suitable for certain experiments. Of the other transaminases the most work has been carried out on ala AT and the most convenient source for large quantities is pig heart.

The object of the work presented in this thesis was: (A), to purify pig heart ala AT; (B), to study the kinetic and spectral properties of the active enzyme and (C), to modify the enzyme with specific reagents. It was hoped that the results would be useful for comparison with asp AT and might form the basis of an independent model of transamination.

CHAPTER 2

MATERIALS AND METHODS

2.1 ALANINE AMINOTRANSFERASE

This was prepared from pig heart by the method described in chapter 4. It was stored at 4°C, at pH 7.5, in 5 mM EDTA and 5 mM ME, at a concentration of about 1 mg/ ml. However, for the rose-bengal photo-oxidation experiments a partially purified enzyme was used, (about 35 % pure).

Experiments were carried out in such a way that each assay contained about 0.1 units of ala AT.

2.2 REAGENTS

The following reagents were obtained from the Sigma Chemical Company:-

pig heart malic dehydrogenase, (free from ala AT and asp AT), pig heart asp AT, (free from ala AT), pyridoxal 5' phosphate, pyridoxamine 5' phosphate, crystalline bovine serum albumin, 2 mercaptoethanol, sodium pyruvate, ∝ ketoglutaric acid, ∝ ketobutyric acid, Trizma base, Trizma chloride, and all the amino-acids used.

The following reagents were obtained from Boehringer:-

rabbit muscle lactate dehydrogenase, (free from ala AT), the gel electrophoresis standards, (catalase, aldolase, trypsin, and RNase), and reduced /3 nicotinamide adenine dinucleotide, (NADH).

The following analytical reagents were obtained from Fisons:-

potassium phosphates, sodium acetate, urea, and hydroxylamine.

The following laboratory reagents were obtained from British Drug Houses:-

rose bengal, methylene blue, thiosemicarbazide, sodium fumarate, glutaric acid, acetic acid, sodium dodecyl sulphate, and tetraethyl methylene diamine.

Analar EDTA and formaldehyde (plus 12 % methanol) were obtained from Hopkins and Williams.

Sodium formate and maleic acid were obtained from May and Baker.

Tetranitromethane (A.R.) was obtained from Koch Light.

$^{14}C_1$-pyruvate was obtained from the Radiochemical Centre, Amersham.

Acrylamide was obtained from Fluka.

N^1N^1methylene bisacrylamide was obtained from Eastman Kodak.

DEAE Cellulose, (DE23), was obtained from Whatman.

Sephadex G200 was obtained from Pharmacia.

All other chemicals were reagent grade.

All solutions were made up in distilled water and stored at 4°C. Solutions used in assays were made up fresh, each time.

2.3 MEASUREMENT OF ENZYME ACTIVITY

This is described in chapter 3.

2.4 MEASUREMENT OF PROTEIN CONCENTRATIONS

Protein concentrations were determined by three methods.

A) The absorbance at 280 nm, (A_{280}), was measured in a Zeiss PMQ II spectrophotometer. It was assumed that;

A_{280} = protein concentration (mg/ ml)

B) The Biuret method of Gornall, Bardawill and David. The A_{540} was measured on an Eppendorf photometer (68).

C) The Folin method of Lowry, Rosebrough, Farr and Randall. The A_{691} was measured on the Eppendorf photometer (119).

The Folin assay was used with the pure enzyme; the other methods were employed during the preparation, (see table 4.2).

2.5 ABSORPTION SPECTRA

The ala AT preparation, at about 1 mg/ ml protein, was centrifuged, at 20 000 g for 30 minutes. Then, the visible absorption spectra were obtained on a Unicam SP 1800 recording spectrophotometer, using quartz cells with a 1 cm light path and 2.5 mm internal width. The slit width was .3 mm. A double beam arrangement was used, in which the ala AT plus reagents was compared with the buffer plus those reagents.

2.6 POLYACRYLAMIDE GEL ELECTROPHORESIS

The electrophoresis was performed, using the apparatus supplied by Shandon. 5.6 % polyacrylamide gels were prepared as described by Davis (42). Gels were run in the pH 8.3 buffer.

They were subjected to 4.5 mA per tube for 40 minutes. 50 - 100 µg of protein were applied to each tube and the gels were run at 3 mA per tube for 90 min. at room temperature. (N.B. Bromothymol blue came through after about 40 min.).

Gels were stained for an hour, in 1 % amido-black and 7 % acetic acid and were destained for a few days in 7 % acetic acid.

The destained gels were analysed, using a gel-scanning apparatus connected to a Gilford 2000 spectrophotometer. The recordings were taken at 600 nm.

For analysis of ala AT activity, the gel was not stained but was quickly frozen to -20°C. It was cut into 1 mm slices. Each slice was added to .25 ml of 20 mM pH 7.5 phosphate buffer, 5mM ME and 5 mM EDTA. It was broken up with a glass rod and left at 4°C for 5 days. 0.2 ml samples were taken and assayed by the standard assay.

2.7 SUBUNIT WEIGHT DETERMINATION

Ala AT, RNase, aldolase, catalase and trypsin in 5 % SDS, 2 % ME, were boiled for 2 min and then run on 5 cm, 5.6 % SDS, polyacrylamide gels, according to the method of Weber and Osborn (202). They were stained in .25 % Coomassie blue, 10 % acetic acid and 45 % methanol, for 6 hours. They were destained in 7 % acetic acid, for 5 days, and were scanned in the Gilford at 600 nm. The results were analysed according to the formula;

$$\log (MW) \propto \text{distance moved} \qquad (177)$$

2.8 ESTIMATION OF ENZYMIC PYRIDOXAL 5' PHOSPHATE

A sample of .95 mg/ ml ala AT and a sample of 2.5×10^{-5} M PLP were treated identically.

To a 400 µl sample, 1 µl of 0.2 M α-ketoglutarate was added, and then 100 µl of 25 % trichloracetic acid. The mixture was centrifuged at 20 000g for 30 min. The absorption spectrum of the supernatant was recorded.

To 360 µl, were added 40 µl of 5N sodium hydroxide. A

second spectrum was recorded and adjusted for this dilution : i.e. the absorbance was multiplied by 10/9.

The difference between the two spectra was calculated and used to estimate the PLP content, as described in appendix 2.

2.9 ESTIMATION OF DISSOCIABLE ENZYME PYRIDOXAMINE 5' PHOSPHATE

A sample of PM-ala AT in 50 mM formaldehyde, at pH 7, was assayed after 5 min and after 240 min incubation at 25°C.

To 100 µl samples were added 30 mg of guanidine and after 15 minutes, 125 µl of 0.5 M ammonium sulphate, at pH 5. After 2 hours, it was centrifuged at 20 000g, for 30 mins. The supernatant was diluted by a factor of two and the absorption spectrum was recorded.

2.10 PHOTO-OXIDATION

The apparatus was shielded from external light. The enzyme sample was contained in a glass cell, which was held in a metal jacket, through which water was pumped. A 250 W lamp illuminated the cell through a fixed slit and air was blown onto the surface of the sample.

The geometry of the system was fixed for a series of experiments. Quantitative comparisons should not be made between the results in different figures, unless otherwise stated.

The temperature in the cell, itself, was measured.

In the experiments described, no inactivation occurred in the dark, except at pH 4.6.

2.11 CALCULATION PROCEDURES

Few of the linear graphs used had sufficient points to make a least mean squares calculation useful. It was assumed that the probable percentage error was the same for each point. The best straight line was that in which the percentage deviation of the point with the highest percentage deviation was reduced to a minimum. For log plots, it was the absolute deviation of the function that was considered.

Calculation of pKs was carried out by the Dixon analysis, where stated (44, 45). Otherwise, the pK was taken as the pH at which the value of a parameter was equal to the mean of the appropriate maximum and minimum values. This second method was used in the inactivation experiments, where the parameter was a rate constant.

N.B. pK determinations were not very good when two pKs were close together: in some cases the pK given is only reliable to within 0.4 pH units.

CHAPTER 3

ACTIVITY ASSAYS

3.1 INTRODUCTION

Ala AT can give a measurable trans-amination or the exchange of a ^{14}C label when any one keto-acid substrate and any one amino-acid substrate are present. Six different assays were employed using, L alanine + ∝ ketoglutarate, pyruvate + L glutamate ∝ aminobutyrate + ∝ketoglutarate, ∝ ketobutyrate + L glutamate, and L alanine + pyruvate.

In the standard, forward and aminobutyrate assays, the production of pyruvate by ala AT was coupled to the oxidation of NADH by LDH.

In the reverse and ketobutyrate assays the ∝ ketoglutarate produced by ala AT was coupled to the production of oxaloacetate from aspartate by asp AT; and this was coupled to the oxidation of NADH by MDH.

The oxidation of NADH caused a fall in A_{366}.

3.2 STANDARD ASSAY

The mixture used in this assay was:
.4 M DL alanine, 50 mM pH7.5 phosphate buffer, 10 mM ∝ keto-glutarate, 500 μg NADH and 50 μg LDH, plus the enzyme sample, all made up to 3 ml.

All the solutions without the enzyme were mixed in a glass cell which was allowed to equilibrate in a 25°C water-bath. The

ala AT was added; the mixture was well stirred with a plunger and the cell was placed in an Eppendorf spectrophotometer - with a 25°C temperature control and a 366 nm filter. The absorbance was recorded on a Photovolt recorder (on LOG setting). The graph was invariably linear with time. The gradient was measured and converted to moles pyruvate/ min.

This assay was used to monitor the purification of the enzyme or the inactivation, unless otherwise stated.

3.3 FORWARD ASSAY

This was the same as the standard assay except that the nature of the buffer, its pH and concentration were varied and the concentration, (and pH), of the substrates were varied.

At pH 9.5 and pH 10.0, 100 μg of LDH were used, (because LDH activity is much lower at high pH). For the same reason, the assays at these pHs were not linear for the first one or two minutes, so that the gradient was measured after three minutes, when the assay was linear.

3.4 α AMINOBUTYRATE ASSAY

The mixture used in this assay was;
200 μg NADH, 50 μg LDH, and variable quantities of DL α amino-butyrate, α ketoglutarate and buffer, plus the enzyme sample, made up to 1 ml. The procedure was the same as for the standard assay At pH 9.5 and 10.0, the gradient was measured only in the linear region of the graph.

3.5 REVERSE ASSAY

The mixture used in this assay was 500 μg NADH, 50 μg MDH, 5 μg asp AT, 20 mM L aspartate, and variable quantities of pyruvate, L glutamate and buffer, plus the enzyme sample, all made up to 3 ml.

All the solutions without the enzyme were mixed and left for at least 5 minutes in a 25^{0}C water-bath. The A_{366} was recorded (as for the standard assay), for a few minutes. The enzyme sample, (a small volume), was added and stirred and the A_{366} was recorded again.

The gradient of the first graph, (which never exceeded 10% of the second gradient), was subtracted from the gradient of the second, and converted into μmoles αketoglutarate/ minute.

This procedure minimises and takes account of a slow, non-linear fall in A_{366} that occurs in the absence of ala AT.

3.6. α KETOBUTYRATE ASSAY

The mixture used in this assay was:
200 μg NADH, 25 μg MDH, 5 μg asp AT, 20 mM L aspartate, and variable quantities of α ketobutyrate, L glutarate and buffer, and the ala AT, made up to 1 ml. The procedure was the same as that for the reverse assay.

All five assays were linear with time, (except as stated), until the NADH was almost exhausted, (at A_{366} less than 0.3). The forward, reverse, aminobutyrate,(AB), and ketobutyrate,(KB), assays were tested in pH 5.0 acetate, pH 7.5 tris chloride and pH 10.0 glycine buffers. The activity varied linearly with the volume of the enzyme sample in every case. The assays were

tested to greater activities than those used in later experiments.

3.7 ISOTOPE EXCHANGE ASSAY

The mixture used in this assay was:
.4 M L alanine, 50mM pH 7.5 phosphate buffer and 2 μCi $^{14}C_1$-pyruvate in 10 mM pyruvate, plus the enzyme sample, made up to 1 ml.

The solutions without the pyruvate were stirred and equilibrated at 25°C in a water-bath. The pyruvate was added and stirred. At different times 50 μl samples were withdrawn and mixed with 10 μl of 24% trichloracetic acid. To this, 10 μl of 1.6N sodium hydroxide were added.

50 μl samples were applied to a thin layer alumina plate and dried. The chromatograms were run in 10 mM pH 7.5 phosphate, in a tank already saturated with water vapour. The plate was removed, dried and left in an iodine tank for 30 minutes. The spots were marked and the plate was left, to allow the iodine to evaporate. Two separate spots were always seen, corresponding to the alanine and pyruvate standards. These were scraped off and added to 0.5g of thixotropic silica and 10 ml of scintillation fluid. The radioactivity was measured in a liquid scintillation counter. The fraction of the total activity found in the alanine, (A'), was calculated. Using the results of appendix 2, $\log_{10}(1 - A'[1 + \text{pyr/L ala}])$ was plotted against time. The gradient was equal to $\frac{\text{pyr}^{-1} + \text{L ala}^{-1}}{2.303} \times$ activity.

Chromotography of pyruvate gave one visible spot, but two quite distinct radioactive spots - for two different ^{14}C-pyruvate preparations. The lesser, (invisible), radioactive spot fell within the L alanine spot. Hence A' was significantly above 0% at zero-time. However, making adjustments on this basis

TABLE 3.1

The isotope exchange assay.

For one assay, the calculation of $\log_{10}(1 - A^*(A + P)/A)$ from initial radioactivity counts is shown.

FIGURE 3.1

The isotope exchange assay. The results of one assay.

(A) A graph of ala* with time.

(B) A graph of $\log_{10}(1 - A^*(A + P)/A)$ with time.

FIGURE 3.2

The isotope exchange assay.

A graph of activity in the isotope assay against activity in the standard assay.

FIGURE 3.1.

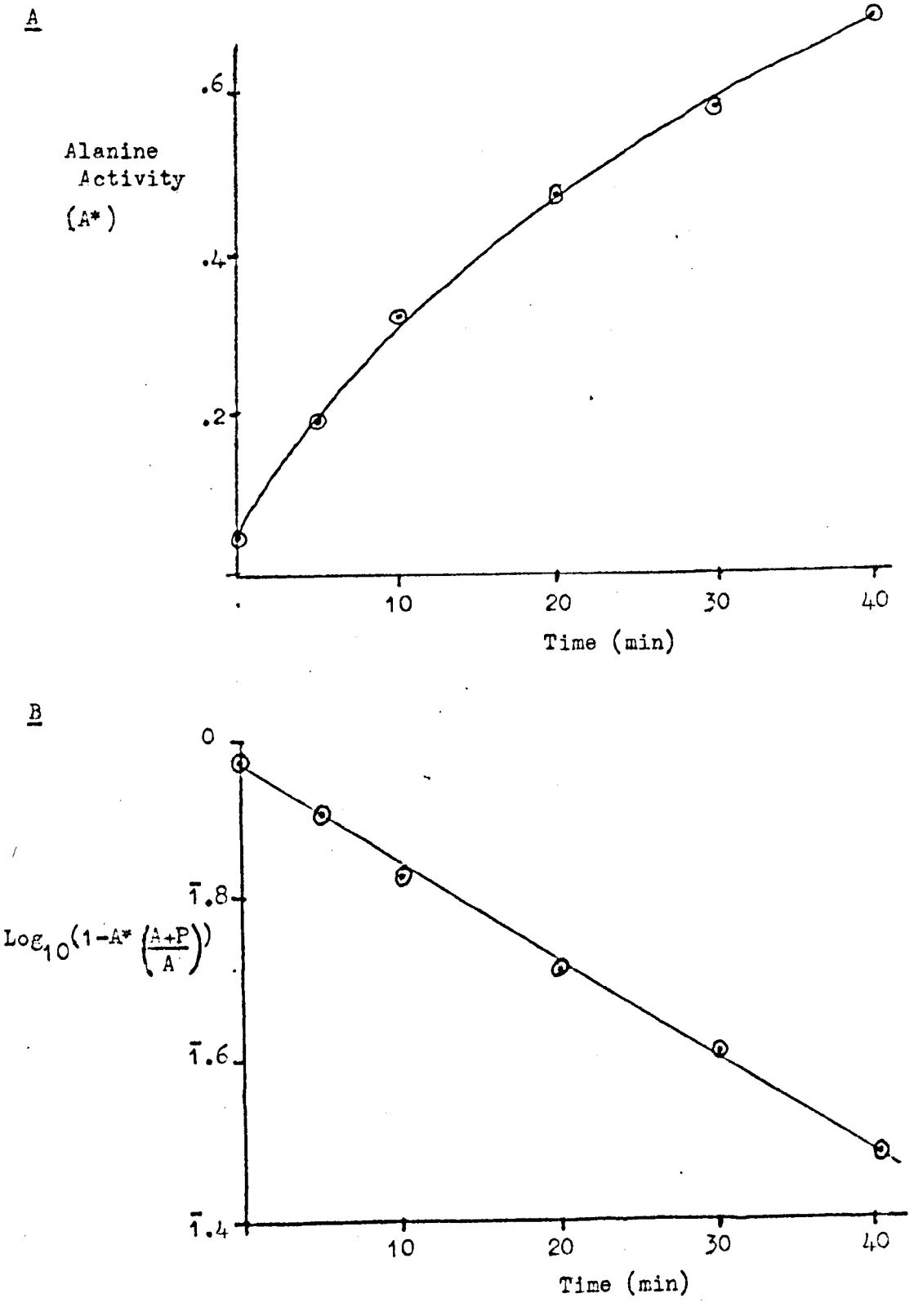
A
Alanine Activity (A*)
.6
.4
.2
10
20
30
40
Time (min)
B
0
$\bar{1}$.8
$\bar{1}$.6
$\bar{1}$.4
$\text{Log}_{10}(1-A^*\left(\frac{A+P}{A}\right))$
10
20
30
40
Time (min)

FIGURE 3.2.

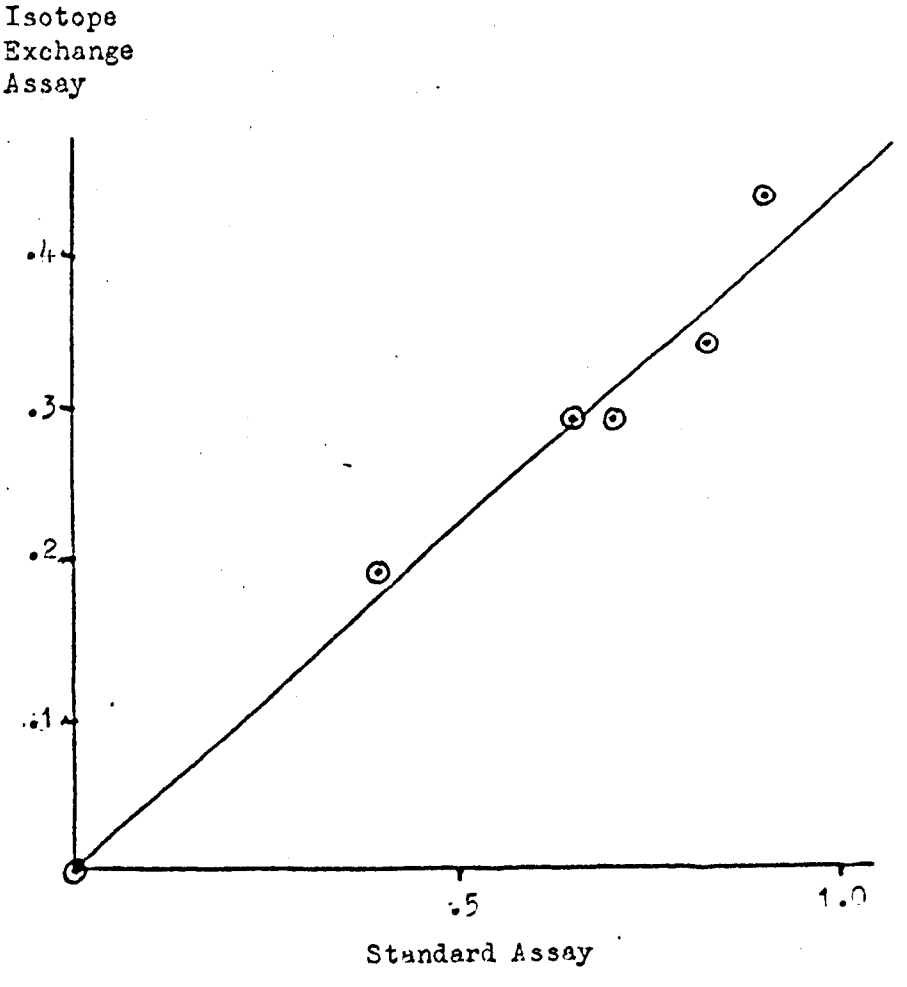

CHAPTER 4

PURIFICATION AND SOME PROPERTIES OF ALANINE AMINOTRANSFERASE FROM PIG HEART

4.1 INTRODUCTION

4.1(a) Earlier Preparation Procedures

The first ala AT purification was that of Green, Leloir and Nocito, in 1945 (69). The major steps in their procedure were these. The pigs hearts were homogenised and filtered. Ammonium sulphate, (AS), was added to the filtrate, to a concentration of 300 g/l. The precipitate was removed, redissolved and subjected to a heat step (60°C), followed by repeated AS fractions. The overall purification was fiftyfold.

More recently, procedures have been devised, using pig heart (70, 156, 170, 195), beef heart (29), rat liver (67, 174), and Cheepewa seed (46). The highest purification achieved with each mammalian source is discussed below.

In 1965, Bulos and Handler purified beef heart ala AT 2 240 fold, (to 123 units/mg). The hearts were homogenised. The supernatant was removed and purified, using an ASstep, heat, a second AS step, a DEAE cellulose column and a hydroxyapatite column (29).

In 1967, Gatehouse and coworkers (67) obtained an electrophoretically pure preparation of rat liver ala AT at 309 units/ mg. The livers were homogenised; the supernatant was separated and purified using a heat step, an AS step, a DEAE

cellulose column, a calcium phosphate gel, a second AS step and a DEAE Sephadex column.

In 1967, Saier and Jenkins (170) purified pig heart ala AT 380 fold to 340 units/mg, giving a preparation that was homogeneous by ultracentrifugation, but not by electrophoresis. Their detailed procedure is given here.

80 lb of pig heart ventricle were ground and dispersed in an equal volume of 5 mM EDTA in 100 mM pH 3.8 acetate buffer. This was heated to 60°C, maintained at that temperature for 15 minutes and filtered through cheesecloth. AS was added to the 30 l of supernatant, to a final concentration of 250 g/l. The precipitate was removed by centrifugation, (10 000 rev/min for 5 minutes), and dissolved in 100 mM pH 3.8 acetate with 10mM α ketogluterate - giving a volume of 500 ml.

This was dialysed twice against 20 l of the buffer and calcium phosphate gel was added to a final concentration of 50 g/l. The mixture was centrifuged, (12 000 rev/ min for 20 minutes), and the precipitate was stirred into 1 l of 50 mM pH 6.8 phosphate buffer. It was removed, and washed two of three times with this buffer. AS was added to the combined washings giving a final concentration of 400 g/l. The precipitate was removed by centrifugation, (10 000 rev/min for 5 minutes), and washed with 1.4 M AS. It was recentrifuged, dissolved in buffer A and dialysed against buffer A. Buffer A was 20 mM pH 7 tris chloride, 5 mM EDTA and 10 mM β mercaptoethanol, (ME).

A 4×40 cm DEAE Sephadex column was equilibrated with buffer A. The sample was applied and eluted with A until the A_{280} was below 0.1. The enzyme was eluted by 1 l of A with a linear gradient of potassium chloride from 0 to 0.13M. 5 ml fractions

TABLE 4.1

The procedure of Saier and Jenkins (170) for the purification of ala AT from pig heart.

The volume, protein content, ala AT activity, and ala AT specific activity are given for each stage.

TABLE 4.2

The procedure used for the work in this thesis, for the purification of ala AT from pig heart.

The volume, protein content, ala AT activity, and ala AT specific activity are given for each stage.

TABLE 4.1.

Step	Volume (ml)	Total Activity ($\times 10^3$)	Total Protein (gm)	Specific Activity (unit/gm)
Heat and filtration	30 000	125	140	0.9
First A.S. step	1 000	100	40	2.5
Calcium phosphate gel	2 500	63	12	5.2
Second A.S. step	400	63	7	9
DEAE Sephadex	50	45	1.0	40
CM Sephadex	5	27	0.17	160
Sephadex G 100		19	0.056	340

TABLE 4.2.

Step	Volume (ml)	Total Activity	Total Protein (gm)	Specific Activity (unit/gm)
Initial supernatant	15 000	57 000	174 Biuret	0.35
First A.S. step	3 000	45 000	55 Biuret	0.82
Heat step	2 600	39 000	29 Biuret	1.34
Second A.S. step	300	36 000	7.5 Biuret	4.8
A.S. fractionation and dialysis	53	27 700	2.1 A_{280}	13.3
DEAE Cellulose	300	18 000	0.20 A_{280}	90
First Sephadex G 200	65	10 700	0.043 A_{280}	250
Second Sephadex G 200	40	5 400	0.012 Folin	450

were collected, precipitated by AS, (400 g/l), dissolved in B and dialysed twice against B. Buffer B was 60 mM pH 5.5 acetate buffer, with 5 mM EDTA and 10 mM ME.

A 2×15 cm CM Sephadex column was equilibrated with B. The sample was applied and eluted with B. 2 ml fractions were collected, precipitated by AS, (400 g/l), dissolved in 5 ml of C, and dialysed against C. Buffer C was 100 mM pH 8.0 tris chloride with 5 mM EDTA and 10 mM ME.

A 1.5×110 cm Sephadex G100 column was equilibrated with C. The sample was applied, and eluted with C: 5 ml fractions were collected.

The progress of this purification is recorded in table 4.1.

4.1(b) Stability

A thiol protector, cysteine, was first used in an ala AT preparation in 1964 (195). Saier and Jenkins, in 1967, (170) showed that the long term stability is enhanced by three factors: a neutral pH; EDTA; and ME. They suspected that prolonged incubation with ME affected the absorption spectrum. Gatehouse et al., in 1967, (67) showed that in the absence of ME or another thiol reagent rat liver ala AT aggregates slowly.

Ala AT is said to be stable at 60°C from pH 4 to 8. However this is not true for the rat liver enzyme and the results of chapter 9 suggest that it is advisable to add EDTA.

4.2 PURIFICATION OF ALA AT FROM PIG HEART

This preparation differed considerably from that of Saier and Jenkins. The initial steps were carried out in a way similar to that of Bulos and Handler (29) - to increase the yield, and for

convenience. The calcium phosphate gel was not used as the purification was low. The detailed AS fractionation of Green and coworkers (69) was reintroduced. This lowered the purification of the CM Sephadex step, which was dropped. As the impurities at this stage had a high molecular weight (MW), Sephadex G200 was used in the final stages.

4.2(a) Purification of the Initial Solution

At all stages the enzyme was maintained at about 4°C unless otherwise stated.

5 to 6 kg of fresh pig heart were cleaned of fat and blood, chopped up, mixed and homogenised with ice-cold water in a Waring blendor, (for 45 seconds at medium speed). The 18 l of homogenate were left for one hour or more and centrifuged at 2 000 g for 15 minutes. The sediment was stirred with an equal volume of ice-cold water, left for an hour and centrifuged again at 2 000g for 15 minutes. The supernatants were pooled.

4.2(b) First Ammonium Sulphate Fractionation

AS was added slowly with stirring, to give a final concentration of 300 g/l. The preparation, (about 22 l), was left overnight, then centrifuged at 2 000 g for 2 hours. The precipitate was dissolved in 3 l of 1 mM EDTA and pH was adjusted to about 6.5 by adding 0.1 N sodium hydroxide, slowly with stirring.

4.2(c) Heat Treatment

The preparation was heated to 60°C in a hot water bath - this took up to 20 minutes. The temperature was held at 60°C ± 1° for ten minutes. It was then cooled, (in a salt-ice mixture), for

40 minutes, (at -5°C).

4.2(d) Second Ammonium Sulphate Fractionation

AS was stirred slowly into the supernatant, to a final concentration of 150 g/l. This was left overnight and centrifuged at 10 000 g for 20 minutes. This AS treatment was repeated on the supernatant until the activity had fallen to below 10%. For the preparation given in table 2.2. the fractions were taken at 110, 125, 131, 138 and 143 g AS/ l.

Precipitates were dissolved in small volumes of water and dialysed overnight, (in seperate sacs), against 10 l of 1 mM EDTA, 1 mM ME at pH 8. They were centrifuged at 20 000 g for 30 minutes andassayed for ala AT, and the A_{280} was measured. Samples of high specific activity were pooled and pH 7.5 phosphate buffer was added to a concentration of 5 mM.

4.2(e) Chromatography on DEAE Cellulose

A 4 × 30 cm DEAE cellulose, (DE 23) column was equilibrated with 5 mM pH 7.5 phosphate buffer, with 3 mM ME and 3 mM EDTA. The enzyme sample was applied and eluted by 400ml of 10 mM pH 7.5 phosphate, 3 mM ME and 3 mM EDTA - running at about 1.4 ml/min. This was followed by 600 ml of 3 mM ME and 3 mM EDTA, with a linear gradient of 10 to 100 mM pH 7.5 phosphate buffer running at 0.8 ml/ min.

10 ml fractions were collected and those with a high specific activity were pooled. AS was added, to a final concentration of 400 g/l. The preparation was left for four hours and centrifuged for 40 minutes at 10 000 g. The precipitate was dissolved in about 12 ml of buffer X and dialysed overnight against 1 l of X.

FIGURE 4.1

The ala AT purification - the ammonium sulphate fractionation

The protein content (from A_{280}), ala AT activity and ala AT specific activity are shown for each fraction.

FIGURE 4.2

The ala AT purification - DEAE cellulose column.

The elution profile is shown for

1) Ala AT activity
2) Protein concentration (from A_{280})
3) Ala AT specific activity

FIGURE 4.3

The ala AT purification - the Sephadex G200 columns.

The elution profile is shown for

1) Ala AT activity
2) Protein concentration (4.3.A from A_{280}) and (4.3.B from Folin-Ciocalteau estimation)
3) Ala AT specific activity

Figure 4.3.A is from the first Sephadex column

Figure 4.3.B is from the second Sephadex column

FIGURE 4.4

The protein profile on polyacrylamide gel electrophoresis, using partially purified ala AT, (A_{600} after amido black staining).

A After the DEAE cellulose column step.

B After the first Sephadex G200 column.

C After the second Sephadex G200 column.

FIGURE 4.1.

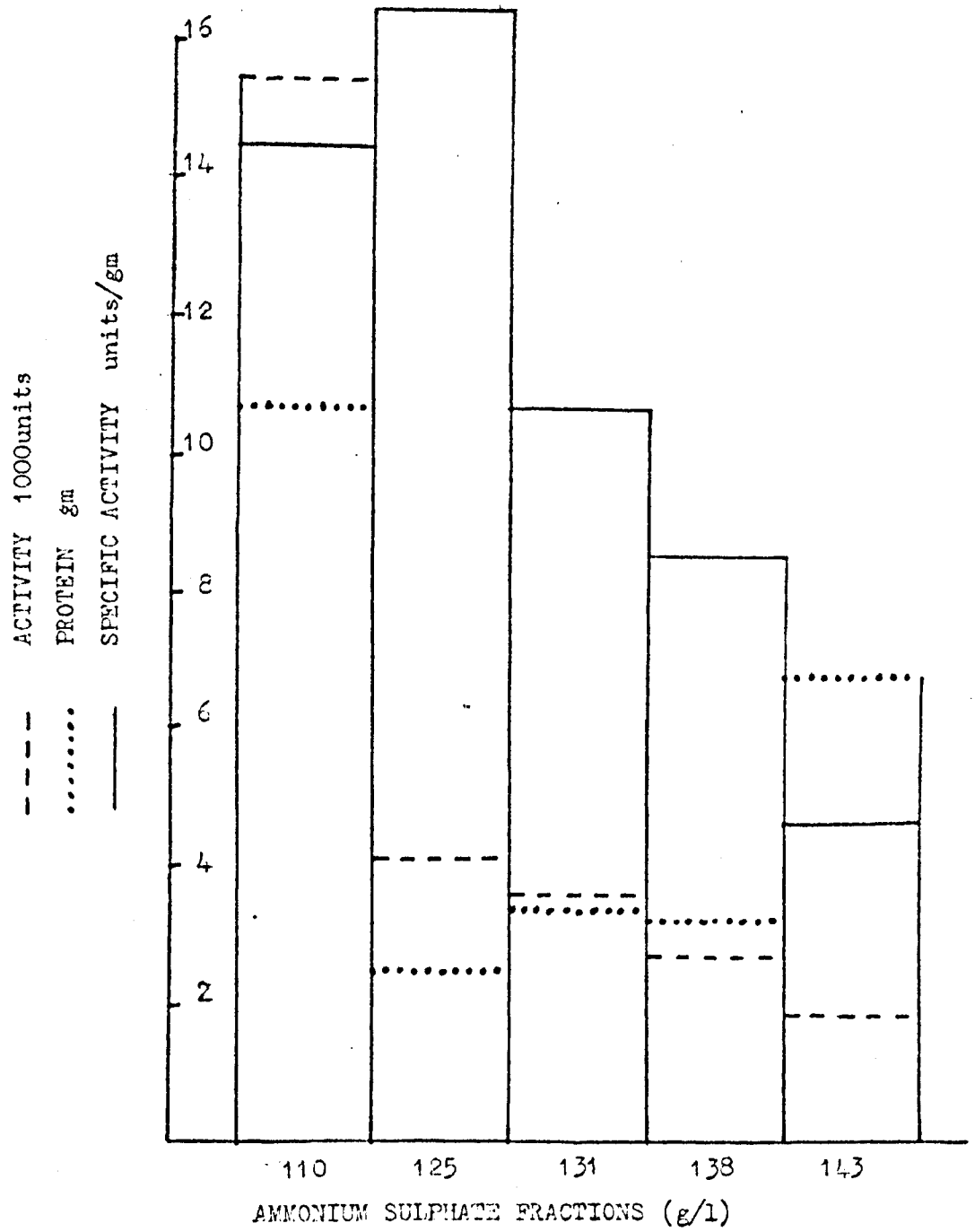
ACTIVITY 1000units
PROTEIN gm
SPECIFIC ACTIVITY units/gm
16
14
12
10
8
6
4
2
110
125
131
138
143
AMMONIUM SULPHATE FRACTIONS (g/l)

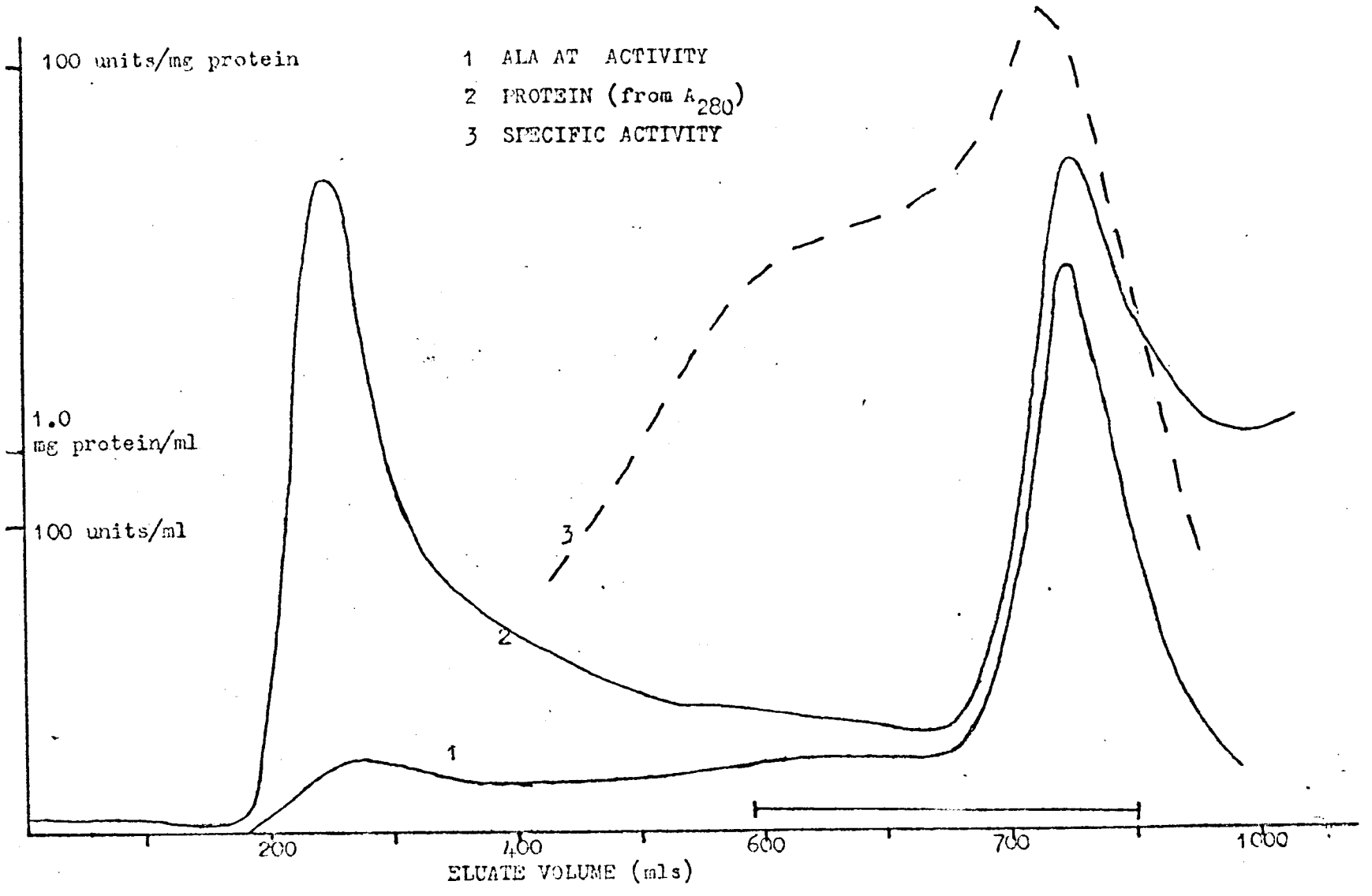
100 units/mg protein
1 ALA AT ACTIVITY
2 PROTEIN (from A_{280})
3 SPECIFIC ACTIVITY
1.0
mg protein/ml
100 units/ml
1
2
3
200
400
600
700
1000
ELUATE VOLUME (mls)

FIGURE 4.2.

FIGURE 4.3.

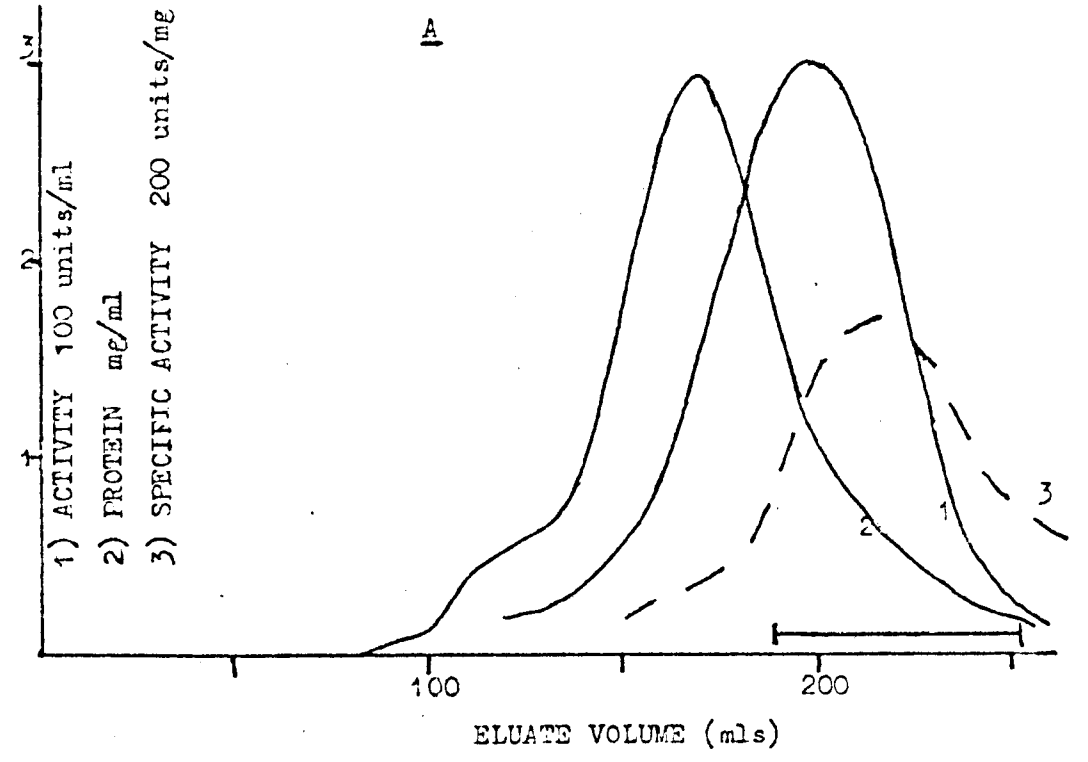
A
1) ACTIVITY 100 units/ml
2) PROTEIN mg/ml
3) SPECIFIC ACTIVITY 200 units/mg
100
200
ELUATE VOLUME (mls)

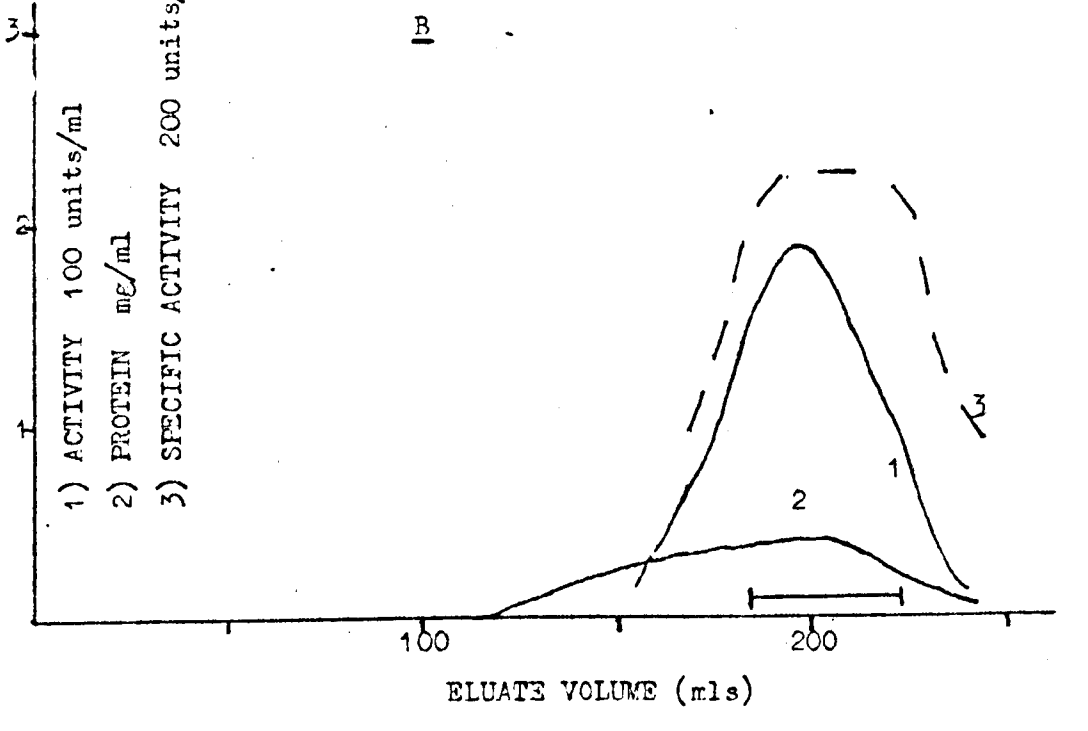
B
1) ACTIVITY 100 units/ml
2) PROTEIN mg/ml
3) SPECIFIC ACTIVITY 200 units/mg
100
200
ELUATE VOLUME (mls)

FIGURE 4.4.

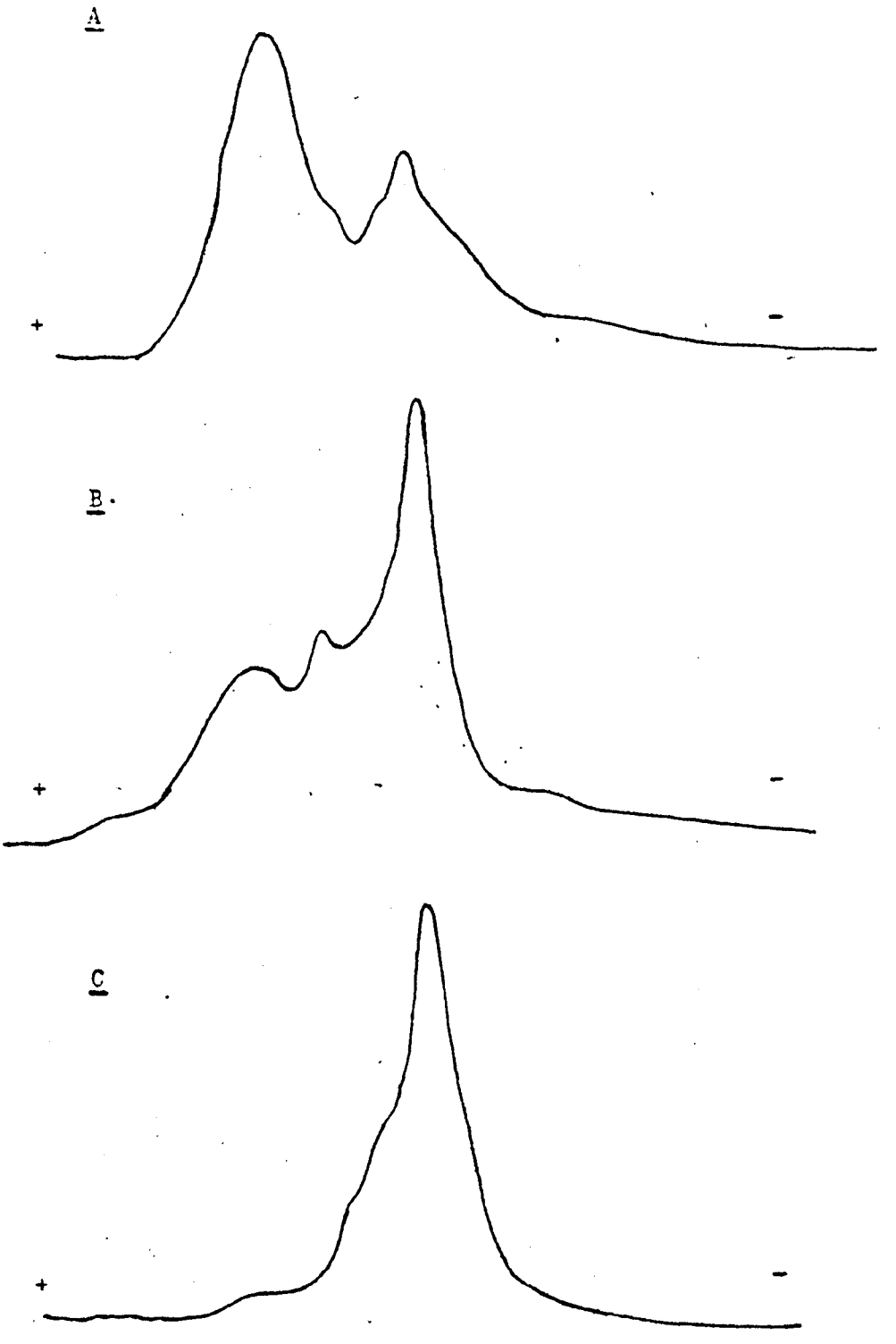

Buffer X was 20 mM pH 7.5 phosphate buffer with 5 mM ME and 5 mM EDTA.

4.2(f) Chromatography on Sephadex

A 2.5 × 90 cm Sephadex G200 column was equilibrated with buffer X. The sample was applied and eluted with X - at about 0.2 ml/ min.

5 ml fractions were collected and those with a high specific activity were pooled and concentrated to a volume of 5 ml using Aquacide III.

The sample was run down the Sephadex column in exactly the same way as before. Fractions were pooled and concentrated with Aquacide, to the desired concentration.

The details of the most successful preparation are given in table 4.2.. Yields were generally about 70% of this. The elution profiles for each column are given in figures 4.1., 4.2. and 4.3. Samples from various stages, (but from a different preparation) were subjected to electrophoresis. The gels were stained and scanned giving the results of figure 4.4.

4.3 SPECIFIC ACTIVITY

The specific activity of the purified enzyme was 450 units/mg where the units of activity are μmoles of pyruvate/min in the standard assay, (see chapter 3), and the protein was determined by the Folin - Ciocalteau method.

A sample of purified enzyme was assayed in four different ways - with duplicates. The following results were obtained.

A) the standard assey of chapter 3 .358 moles/min

B) the assay of Bulos and Handler, 1965 (29)
3 ml containing 45 mM pH 8.0 glycine + 12.5 mM L alanine + 15 mM ∝ketoglutarate at 25°C .147 moles/min

C) the assay of Wroblewski and LaDue, 1956, as used by Saier and Jenkins, 1967 (170, 211)
3 ml containing 33 mM pH 7.4 phosphate + 33 mM L alanine + 6.7 mM ∝ketoglutarate at 25.5°C 460 "units"/min

D) the assay of Segal, Beattie and Hopper, 1962 (174)
3 ml containing 100 mM pH 8.0 tris chloride + 100 mM L alanine + 7 mM ∝ketoglutarate at 30°C .434 moles/min

N.B. In this paper is given a conversion factor from this to a second assay used by Gatehouse et al. (67). It is 0.55.

Using these results and the published specific activities, the specific activities of the different preparations have been expressed in terms of the standard assay - table 4.3. It should be bornein mind that comparison between enzymes from different sources are only truly valid for those conditions under which they were both assayed.

It can be seen that the specific activity of this preparation was as high as for any preparation.

4.4 ELECTROPHORESIS ON POLYACRYLAMIDE

Polyacrylamide gel electrophoresis was carried out as described in chapter 2. The protein and activity profiles, (figure 4.5.), coincided and showed one symmetrical peak. There was a slight protein contamination moving behind the ala AT peak but it seems to be less than 5% of the total protein.

4.5 MOLECULAR WEIGHT DETERMINATION

There have been three estimates of the MW of pig heart ala AT 82 000 (9), 91 000 (195), and 115 000 (170). The first determination (on Sephadex G200) assigned MWs to some of the standards, that are considerably lower than those now accepted. The mean of the other two results is 102 000.

Electrophoresis in sodium dodecyl sulphate was carried out as described in chapter 2. The protein profiles obtained are shown in figure 4.6. The graph of the distance moved by a peak against the logarithm to the base 10 of the MW, (figure 4.7.), was linear. The position of the ala AT peak indicated that:

the molecular weight was 52 000.

This is quite different from the MW of the native enzyme. It seems certain that pig heart alaAT has a subunit structure, like the rat liver enzyme (67). The simplest explanation of the results is that there are two similar subunits, MW 52 000.

4.6 COENZYME CONTENT

The protein concentration of an enzyme sample was measured by

FIGURE 4.5

Polyacrylamide gel electrophoresis of purified pig heart ala AT.

A The protein profile from A_{600} after staining with amido-black.

B The ala AT activity profile.

FIGURE 4.6

The estimation of the subunit molecular weight of pig heart ala AT, by gel electrophoresis in sodium dodecyl sulphate.

A The protein profile, from A_{600} after staining with Coomassie blue.

B A graph of the $\log_{10}$ of the subunit molecular weight, against the distance moved by a protein peak from the top of the gel.

FIGURE 4.7

The difference between the spectrum in acid and the spectrum in alkaline solution, for two samples of pyridoxal 5' phosphate.

⊙ standard PLP solution, (at 2.0×10^{-5} M)

△ PLP prepared from purified ala AT (diluted to 0.76 mg/ml).

FIGURE 4.5.

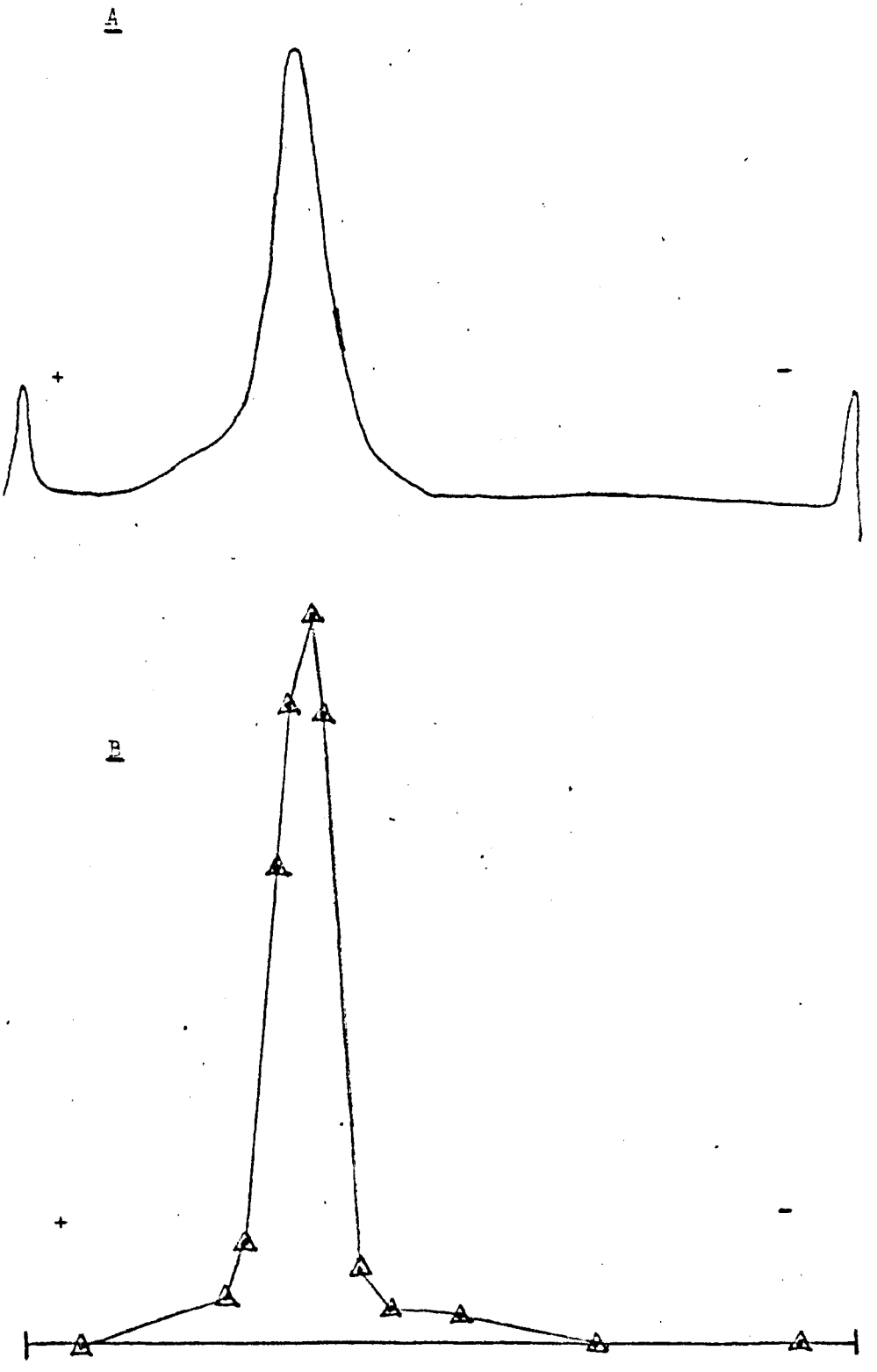

FIGURE 4.6.

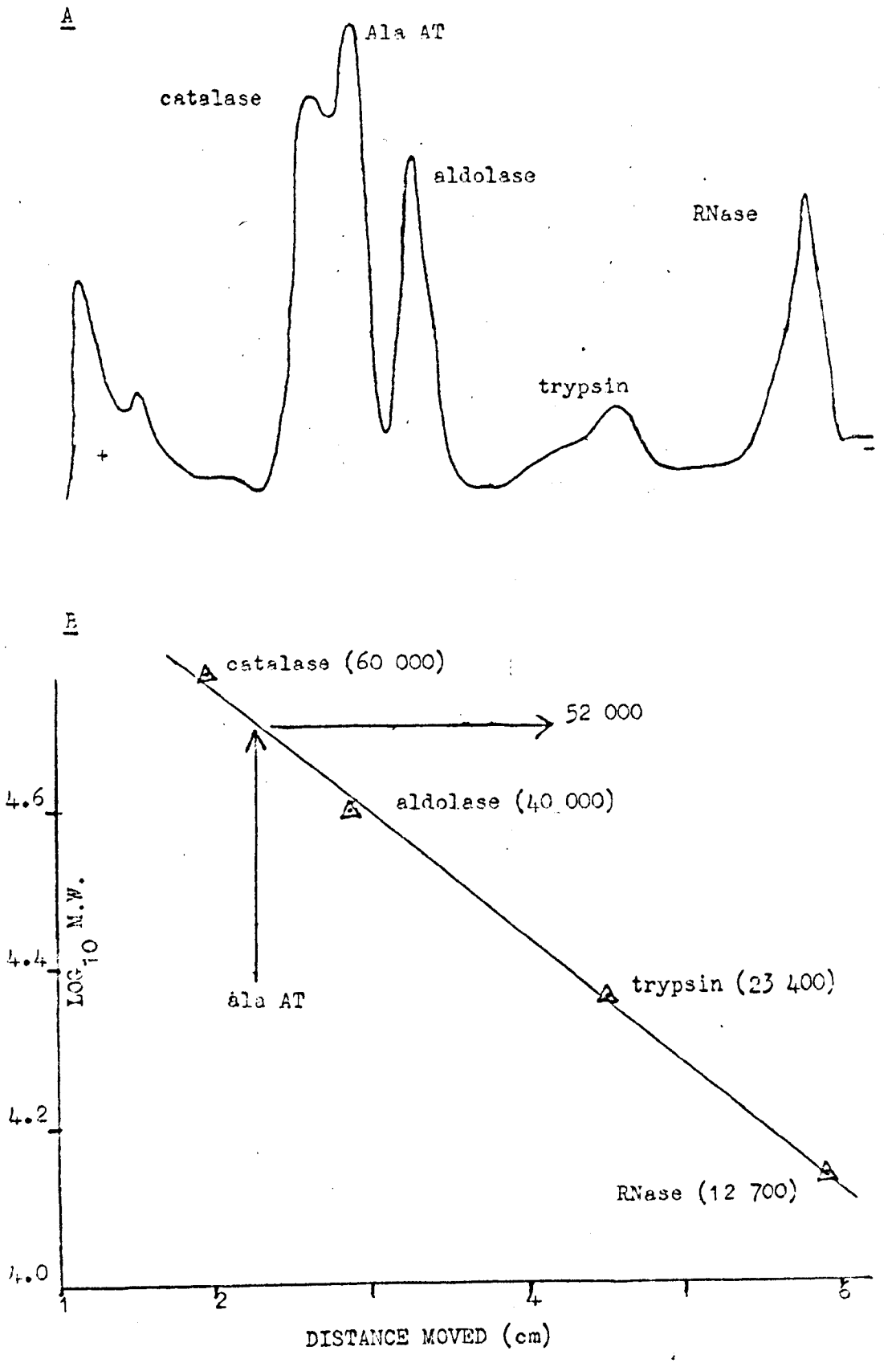
A
Ala AT
catalase
aldolase
RNase
trypsin
+
−
B
catalase (60 000)
52 000
aldolase (40 000)
trypsin (23 400)
RNase (12 700)
ala AT
4.6
4.4
4.2
4.0
LOG10 M.W.
1
2
4
6
DISTANCE MOVED (cm)

FIGURE 4.7.

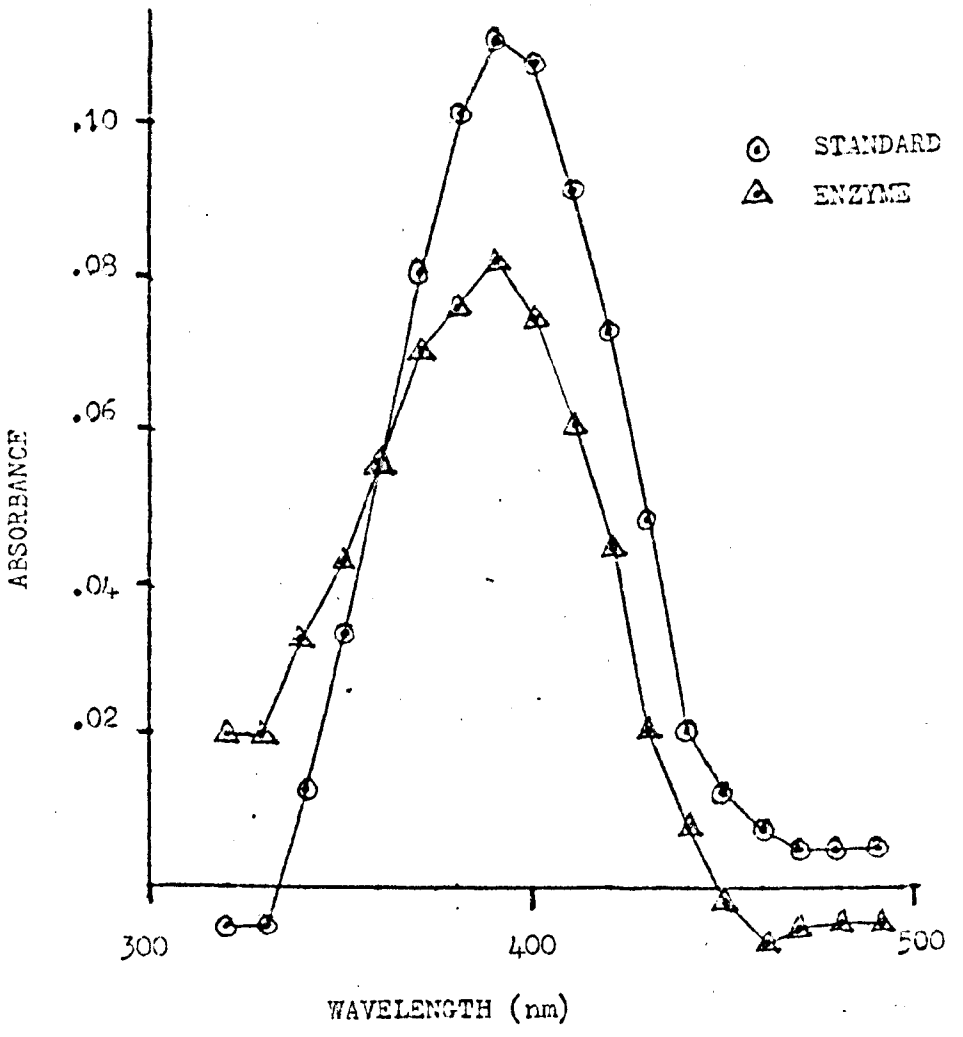
.10
.08
.06
.04
.02
ABSORBANCE
300
400
500
WAVELENGTH (nm)
STANDARD
ENZYME

the Folin - Ciocalteau method. It was 0.95 mg/ml.

The pyridoxal 5' phosphate , (PLP), content was estimated by the method of chapter 2. The two spectra, (for the enzyme and standard PLP) are given in figure 4.7. Their shapes are not identical, although both have peaks at about 390 nm. The discrepency is easily explained by assuming a very slight error in the concentrations of ME or trichloracetate, or assuming that a small part of the protein did not precipitate. The calculations of appendix6 are made on this basis. They give an enzyme PLP concentration of 1.75×10^{-5}M..

Hence, the PLP concentration is :

1 mole. PLP/54 000g protein

This is the highest value obtained with pig heart ala AT. It is very similar to the estimate of the subunit MW.

4.7 SUMMARY

The specific activity, electrophoresis and PLP estimation, all indicate that this is the highest purity achieved with pig heart ala AT. The electrophoresis showed no significant impurities. The closeness of the two subunit weight calculations also indicates that it is fairly pure. It seems likely that the enzyme is composed of two very similar subunits. The turnover number per mole of coenzyme was 375 sec^{-1}.

CHAPTER 5

ACTIVITY KINETICS AT PH 8.0

5.1 METHODS OF ANALYSIS

Ala AT activity fits the Dalziel rate equation (41).

$$v^{-1} = \phi_0 + \phi_1 S_1^{-1} + \phi_2 S_2^{-1} \qquad \text{(see chapter 1)}$$

When v^{-1} is plotted against S_1^{-1} at constant S_2, the gradient is ϕ_1 and is independent of S_2. The intercept, (y_1), on the v^{-1} axis fits the equation $y_1 = \phi_0 + \phi_2 S_2^{-1}$.

When y_1 is plotted against S_2^{-1}, the gradient is ϕ_2, the intercept on the y_1 axis is ϕ_0 (119).

The same constants can be obtained in the analogous way, beginning with a graph of v^{-1} against S_2^{-1}.

If one substrate, S_1, is a competitive inhibitor for the other substrate, S_2, the following steadystate equation holds.

$$v^{-1} = \phi_0 + \phi_1 S_1^{-1} + \phi_2(1 + S_1/K) S_2^{-1} \quad .$$

This is a particular case that can be derived from the general equation for inhibition.

A graph of v^{-1} against S_1^{-1}, at constant S_2 is non-linear.

A graph of v^{-1} against S_2^{-1}, at constant S_1, is linear. The intercepts on v^{-1}, (y_2), fit the equation $y_2 = \phi_0 + \phi_1 S_1^{-1}$. ϕ_0 and ϕ_1 can be calculated as before.

The gradient is $\phi_2(1 + S_1/K)$: when the gradient is plotted against S_1, the intercept on the ordinate is ϕ_2 and the intercept

on S_1 is $-K$.

If both substrates inhibit, then neither plot is linear and analysis becomes more complex. If a substrate inhibits by altering the ϕ_0 term, the same is true. However, neither case was observed at the concentrations used.

$$v^{-1} = \phi_0 + \phi_1(1 + I/K_1)\, S_1^{-1} + \phi_2(1 + I/K_2)\, S_2^{-1}$$

is the equation obtained in appendix 3(a), that relates v^{-1} to I, the inhibitor concentration when the inhibitor binds only to the free enzyme.

At constant S_2, constant I, when v^{-1} is plotted against S^{-1}, the gradient, g_1, is $\phi_1(1 + I/K_1)$.

At constant S_2, when g_1 is plotted against I, the intercept on I is $-K_1$. $-K_2$ is obtained in the analogous way.

According to this equation ϕ_0 is independent of I.

If ϕ_0 depends on I, it can be analysed according to the equation of appendix 3(b):

$$v^{-1} = \phi_0(1 + I/K_0) + \phi_1(1 + I/K_1)\, S_1^{-1} + \phi_2(1 + I/K_2)\, S_2^{-1}$$

The derivation of this equation required some unjustifiable assumptions, that limit its general application, however, the parameter, K_0, can be considered as a semi-quantitative measure of the dissociation constant.

K_1 and K_2 are obtained as before. There is no simple procedure for obtaining K_0. The one used was to plot v^{-1} against S_1^{-1}. The intercept on v^{-1} is $\phi_0(1 + I/K_0) + \phi_2(1 + I/K_2)\, S_2^{-1}$. S_2 is known and $\phi_2(1 + I/K_2)$ is the gradient of the graph of v^{-1} against S_2^{-1}. Hence $\phi_0(1 + I/K_0)$ is calculated and plotted against

I. The intercept on I is $-K_0$.

The commonest units for v are those of specific activity, (e.g. moles/ min/ mg enzyme). The kinetic experiments involved enzyme samples from different preparations. Some samples were too dilute for protein or PLP assays. Hence it was easiest and theoretically most sound to measure the ala AT in terms of an assay and not by the protein or coenzyme content.

v is given as moles/min/(moles/min in the standard assay)

i.e. V_A is $\frac{\text{rate under condition A}}{\text{rate in the standard assay}}$

5.2 EXPERIMENTS

The reaction velocity was measured by the forward, reverse, AB, and KB assays at varying substrate concentrations. The results were analysed in figures 5.1. to 5.7. as described earlier.

In the reverse and KB assays, extra points are shown at double the normal aspartate concentration to show up any aspartate inhibition.

The forward assay was repeated with 0.4 M formate. The S_1/S_2 ratio was held constant. The Dalziel equation then takes the form $v^{-1} = \phi_0 + x\, S_1^{-1}$. v^{-1} was plotted against S_1^{-1}. The intercept on v^{-1} was ϕ_0, (see figure 5.8.).

The kinetic constants are dependent on the buffer concentration. The results at different buffer concentrations were analysed according to the equation for a stoichiometric inhibitor, (figures 5.9. and 5.10.).

FIGURE 5.1

The forward assay in 50 mM pH 8.0 tris buffer, at 25°C.

A Lineweaver-Burk plot, with ∝ketoglutarate as substrate.

⊙ △ where L alanine concentration is 6.7 mM, 10 mM 23 mM or 100 mM.

■ using the intercepts on the v^{-1} axis, from figure 5.2.; i.e. at a theoretical alanine concentration of infinity.

FIGURE 5.2

The forward assay in 50 mM pH 8.0 tris buffer, at 25°C.

A Lineweaver-Burk plot, with L alanine as substrate.

⊙ △ where the ∝ketoglutarate concentration is .27 mM, .40 mM, .66 mM, 1.33 mM or 10.0 mM.

■ using the intercepts on the v^{-1} axis, from figure 5.1; i.e. the predicted values of v^{-1}, at saturation with ∝ketoglutarate.

FIGURE 5.3

The reverse assay in 50 mM pH 8.0 tris buffer, at 25°C.

A Lineweaver-Burk plot, with L glutamate as substrate.

⊙ △ where the pyruvate concentration is 10 mM, .67 mM, .40 mM or .27 mM.

■ using the intercepts on v^{-1} from figure 5.4.; i.e. the predicted values of v^{-1}, at saturation with pyruvate.

⊹ The result at .27 mM pyruvate, 5 mM L glutamate, is repeated, at twice the normal L aspartate concentration.

FIGURE 5.1.

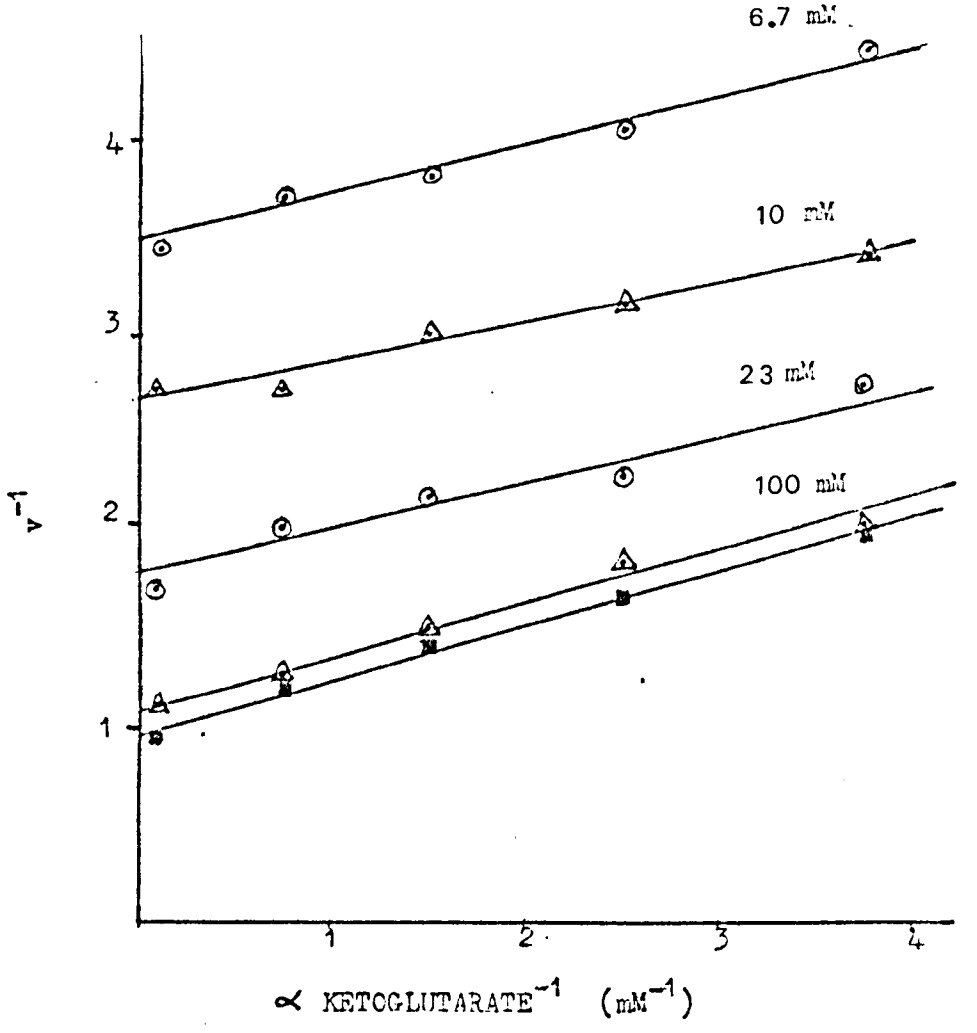

FIGURE 5.2.

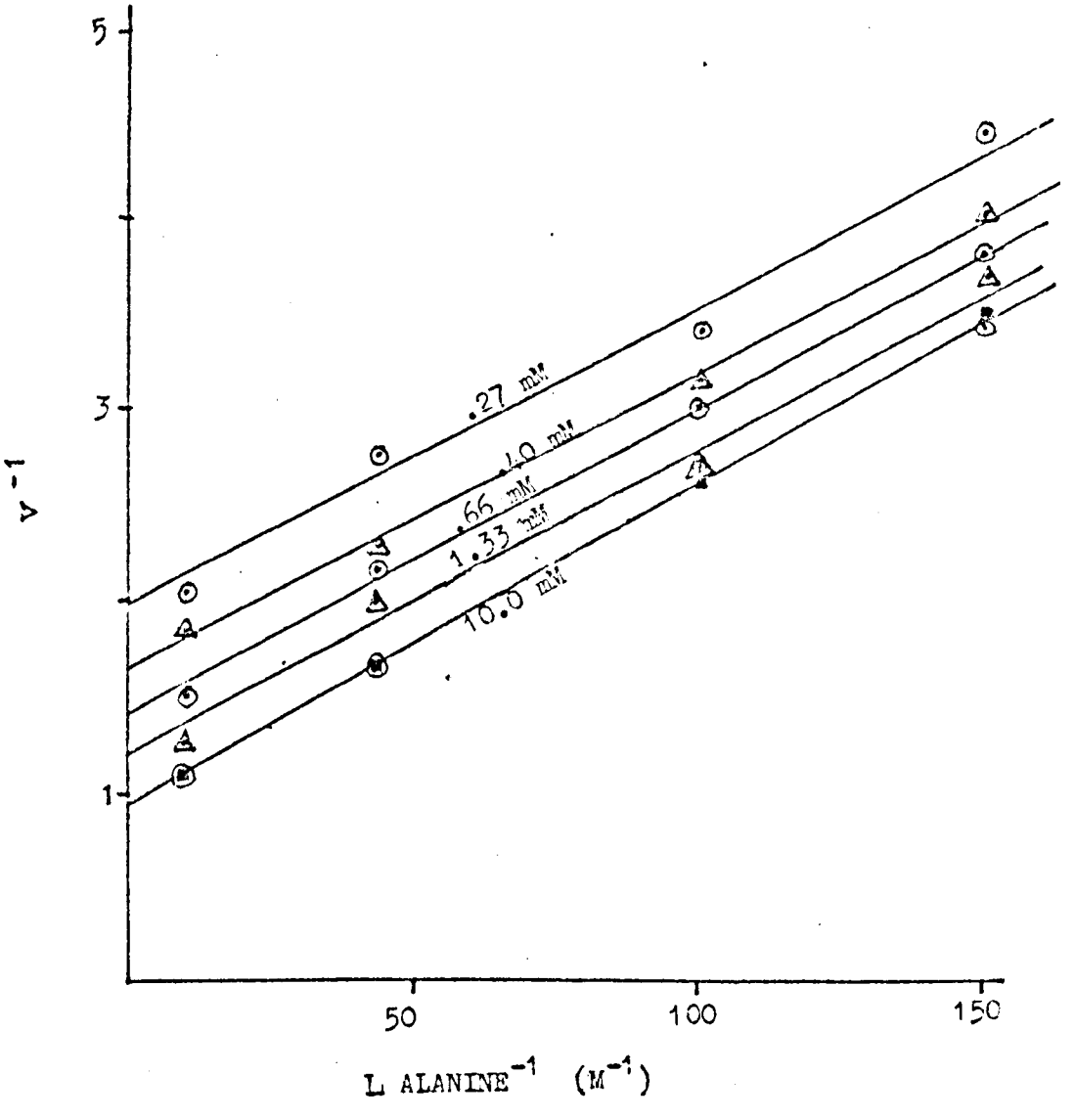

FIGURE 5.3.

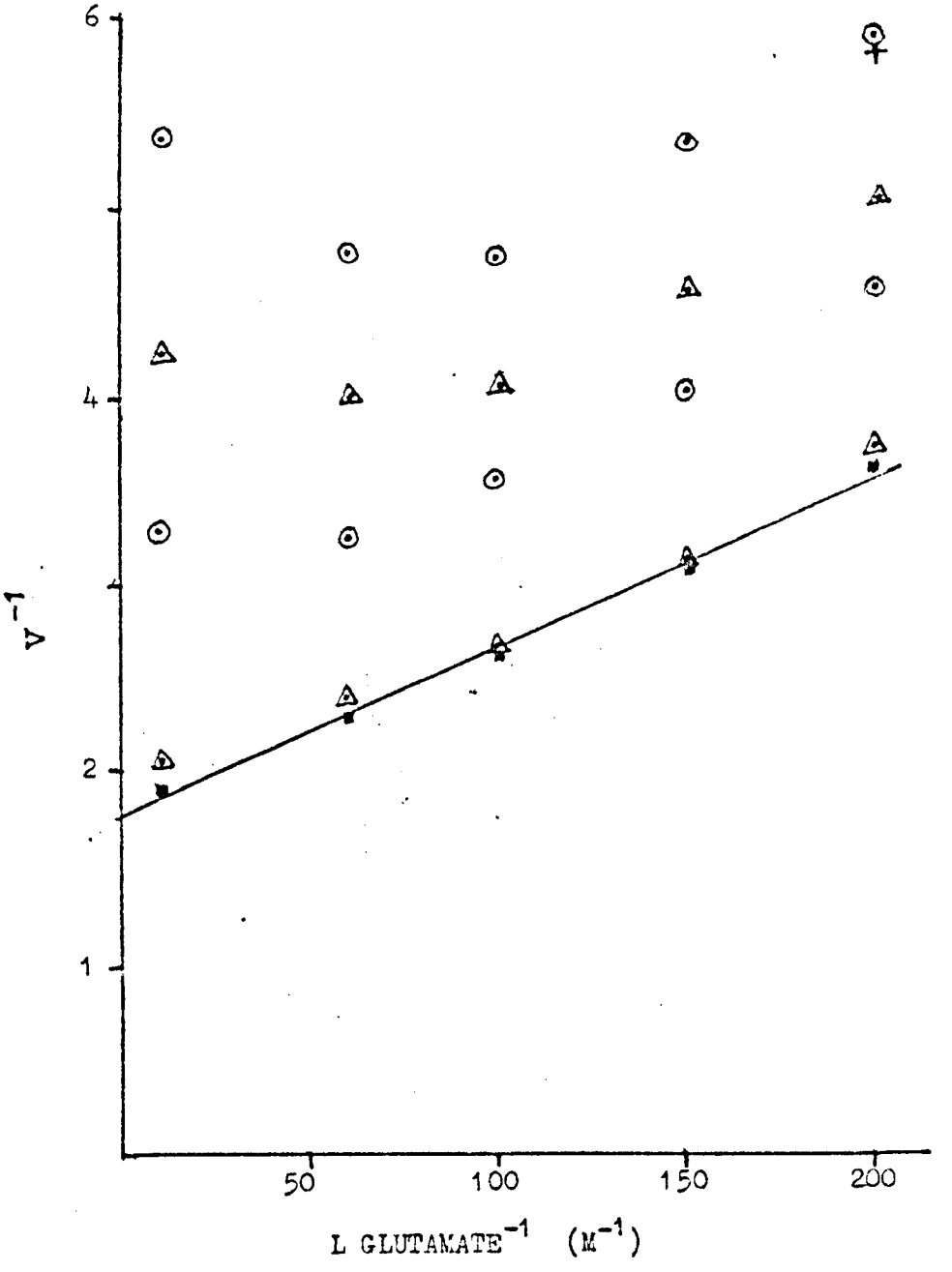

FIGURE 5.4

The reverse assay in 50 mM pH 8.0 tris buffer, at 25°C.

A Lineweaver-Burk plot, with pyruvate as substrate.

L glutamate concentration is 5 mM, 6.7 mM, 10 mM, 16.7 mM or 100 mM.

FIGURE 5.5

The reverse assay in 50 mM pH 8.0 tris buffer, at 25°C.

A graph of the gradient from figure 5.4, (i.e. the apparent value of ϕ_{pyr}), against L glutamate.concentration.

FIGURE 5.6

The aminobutyrate assay in 50 mM pH 8.0 tris buffer, at 25°C.

A Lineweaver-Burk plot, with ∝aminobutyrate as substrate.

⊙ with 2.0 mM ∝ketoglutarate

+ with .04 mM ∝ketoglutarate

FIGURE 5.7

The ketobutyrate assay in 50 mM pH 8.0 tris buffer, at 25°C.

A Lineweaver-Burk plot with ∝ketobutyrate as substrate.

⊙ with 10 mM L glutamate

+ with 3 mM L glutamate

FIGURE 5.4.

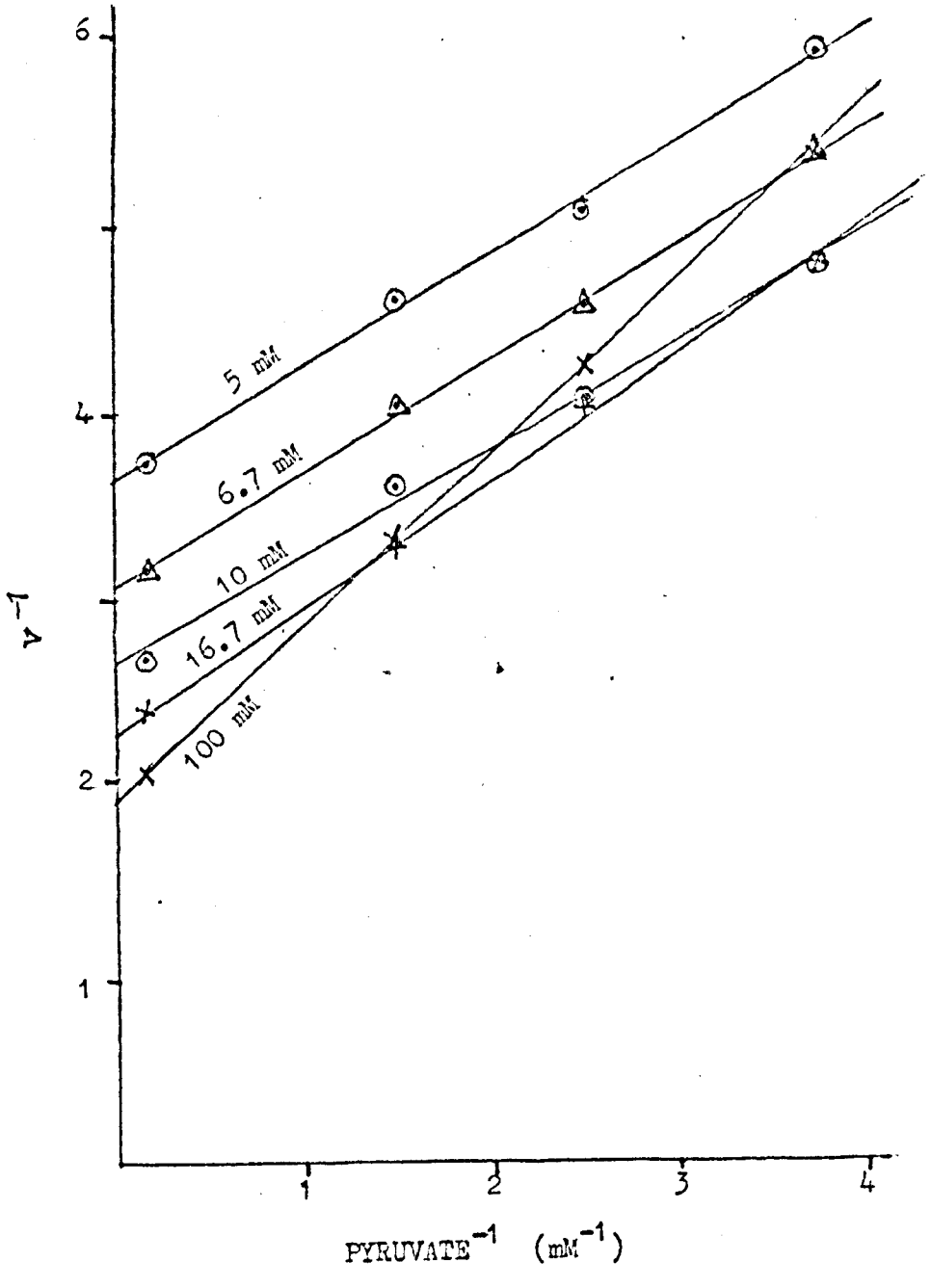

FIGURE 5.5.

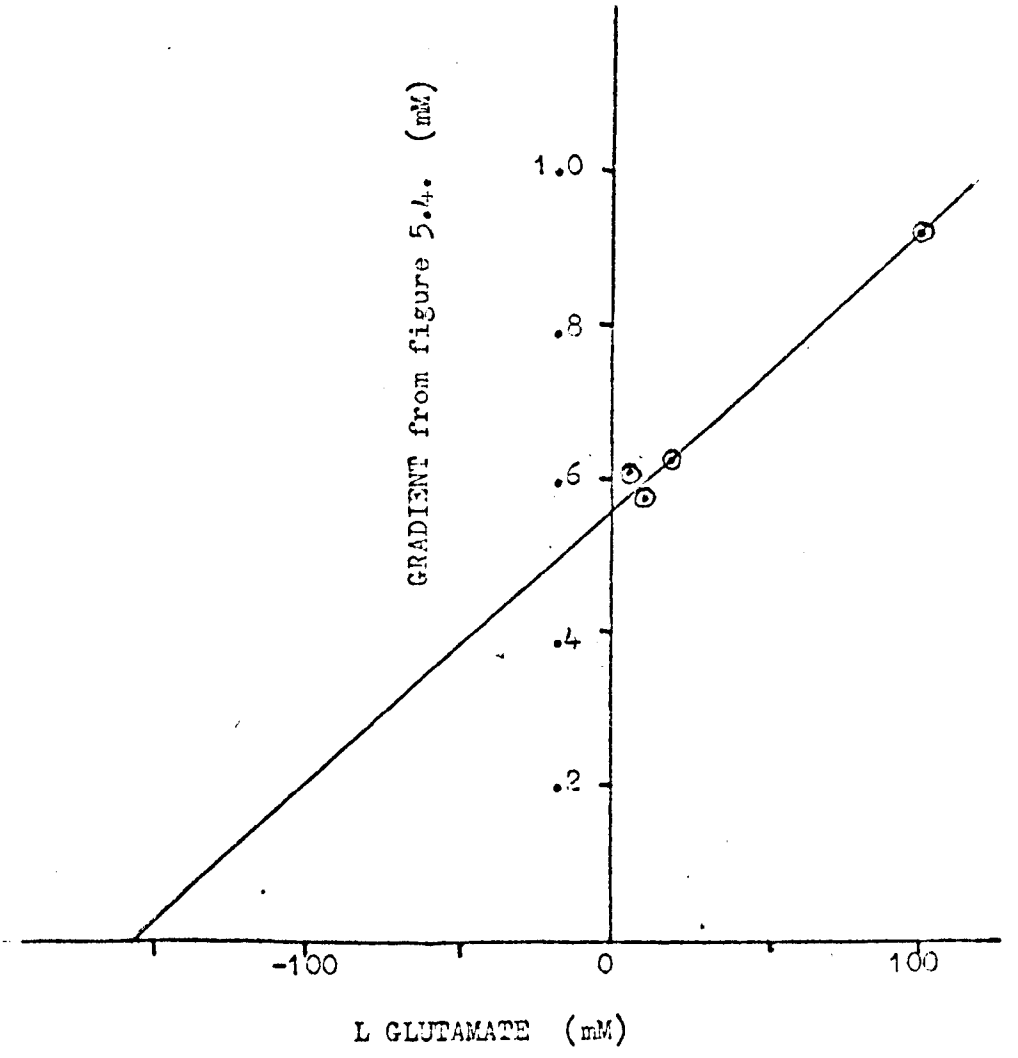

FIGURE 5.5.

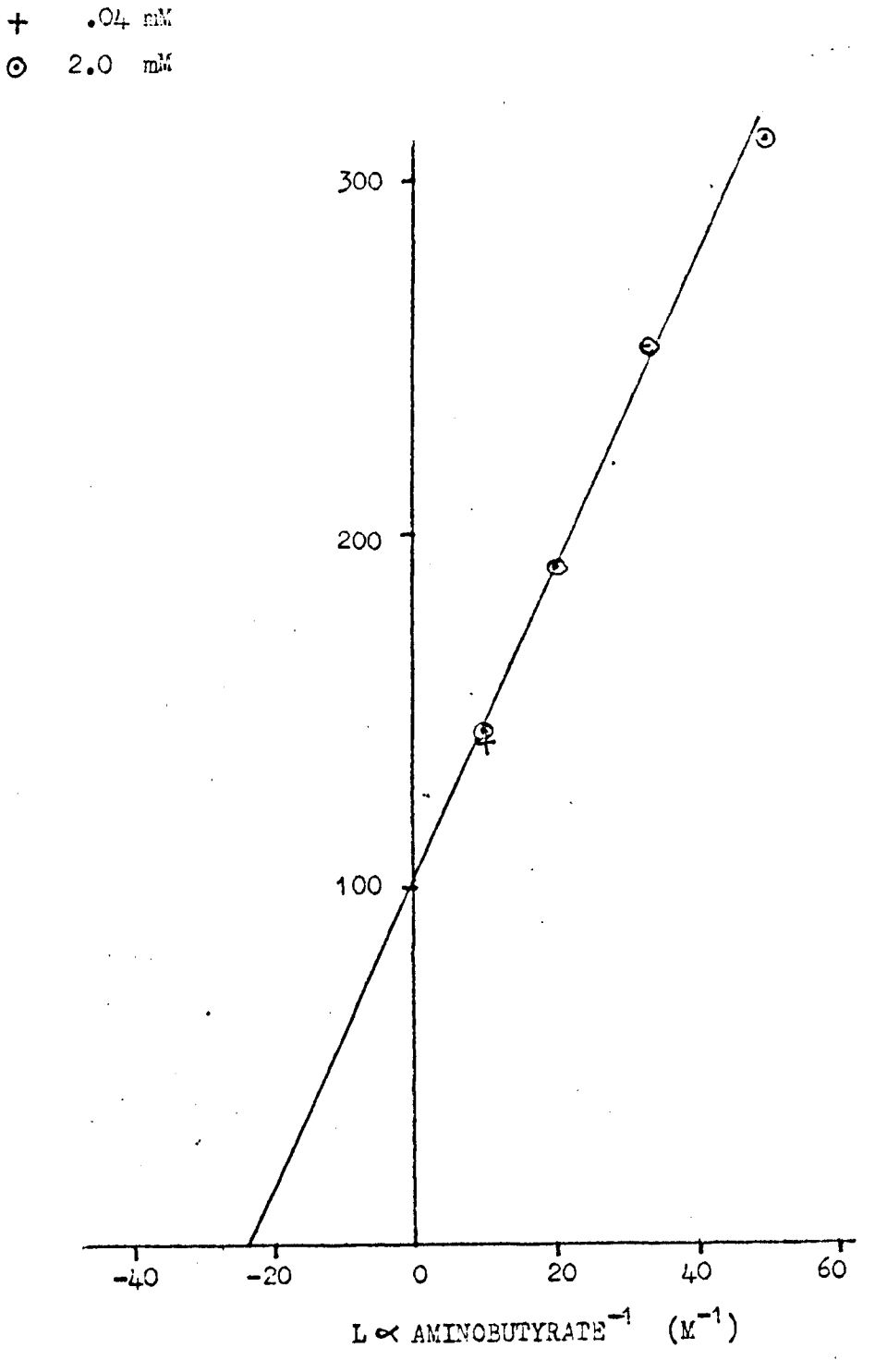

FIGURE 5.7.

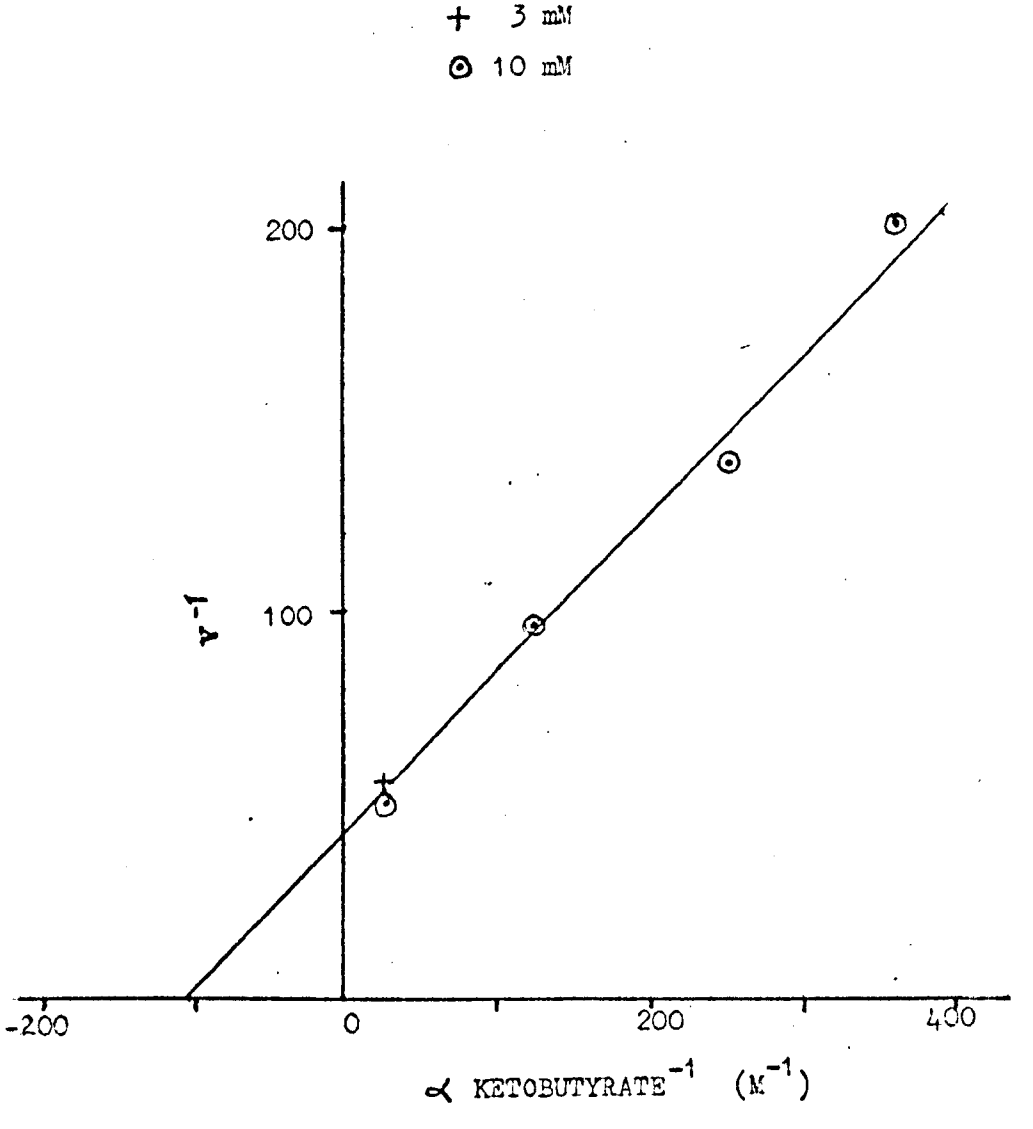

FIGURE 5.8

The forward assay in 50 mM pH 8.0 tris buffer, at 25°C, and with 0.4 M formate. For each assay,

L alanine concentration : ∝ketoglutarate concentration = 40

The Lineweaver-Burk plot with L alanine as substrate is given.

FIGURE 5.9

The forward assay, in pH 8.0 tris buffer, at 25°C. The buffer concentration is 100 mM or 200 mM, as indicated.

A A Lineweaver-Burk plot, with L alanine as substrate, at 2.7 mM ∝ketoglutarate.

B A Lineweaver-Burk plot, with ∝ketoglutarate as substrate, at 100 mM L alanine.

FIGURE 5.10

The forward assay in pH 8.0 tris buffer, at 25°C.

A A graph of the apparent $\emptyset_0$ against buffer concentration.

B A graph of the apparent value of $\emptyset_{ala}$, (i.e. the gradient from figure 5.9.A), against buffer concentration.

C A graph of the apparent value of $\emptyset_{KG}$, (i.e. the gradient from figure 5.9.B), against buffer concentration.

FIGURE 5.8.

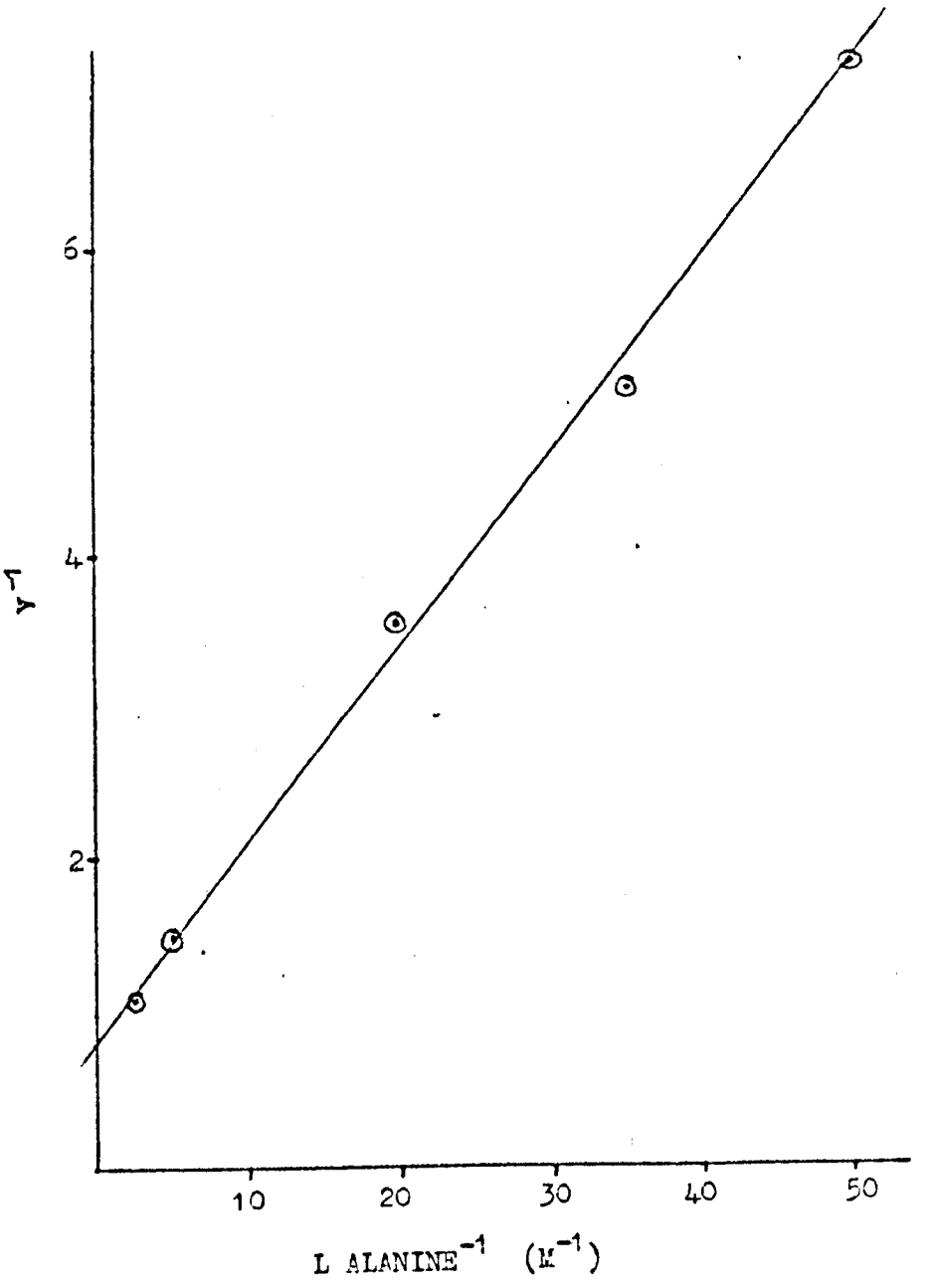

FIGURE 5.9.

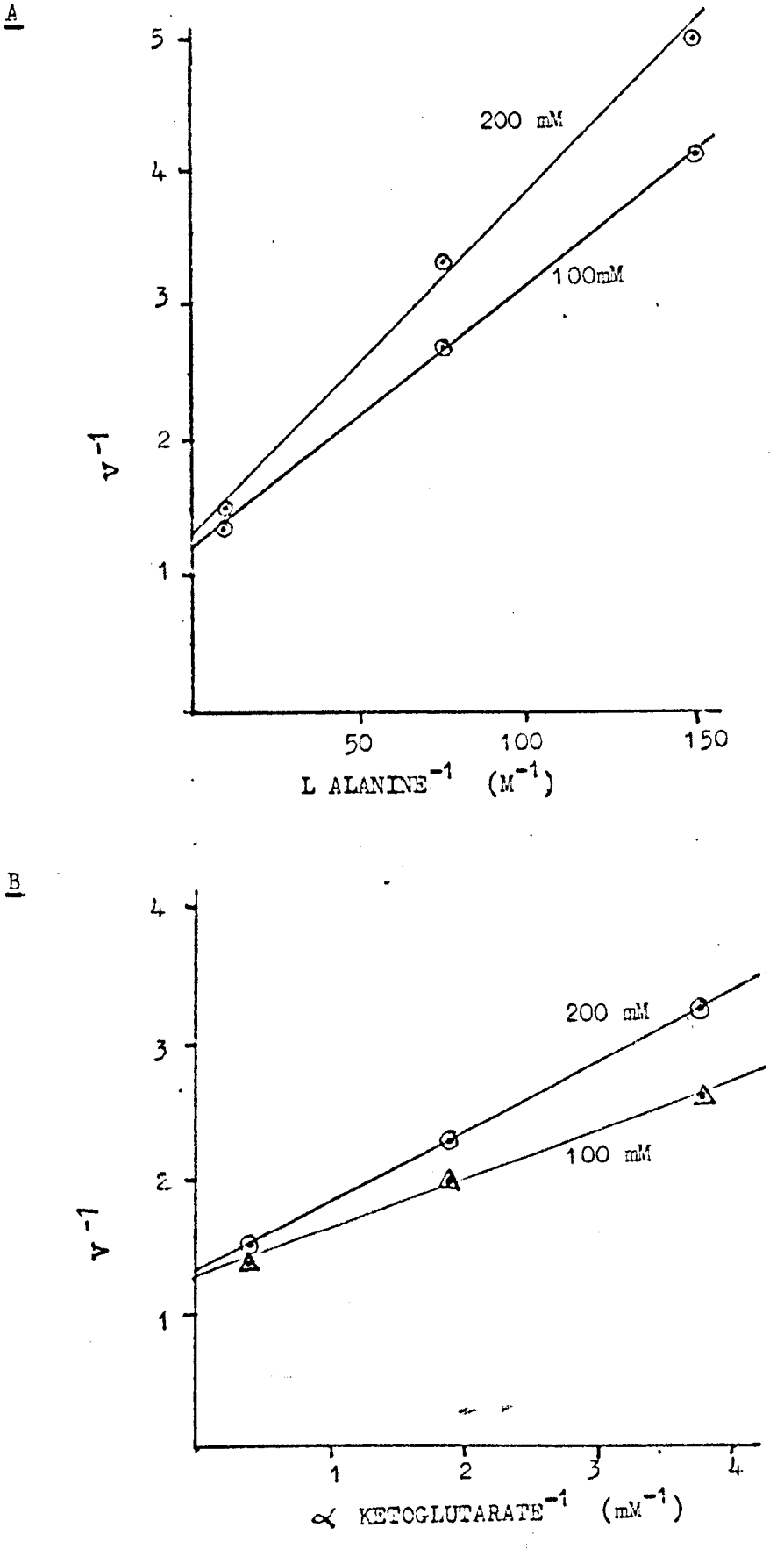
A
5
4
3
2
1
200 mM
100mM
v^{-1}
50
100
150
L ALANINE^{-1} (M^{-1})
B
4
3
2
1
200 mM
100 mM
v^{-1}
1
2
3
4
α KETOGLUTARATE^{-1} (mM^{-1})

FIGURE 5.10.

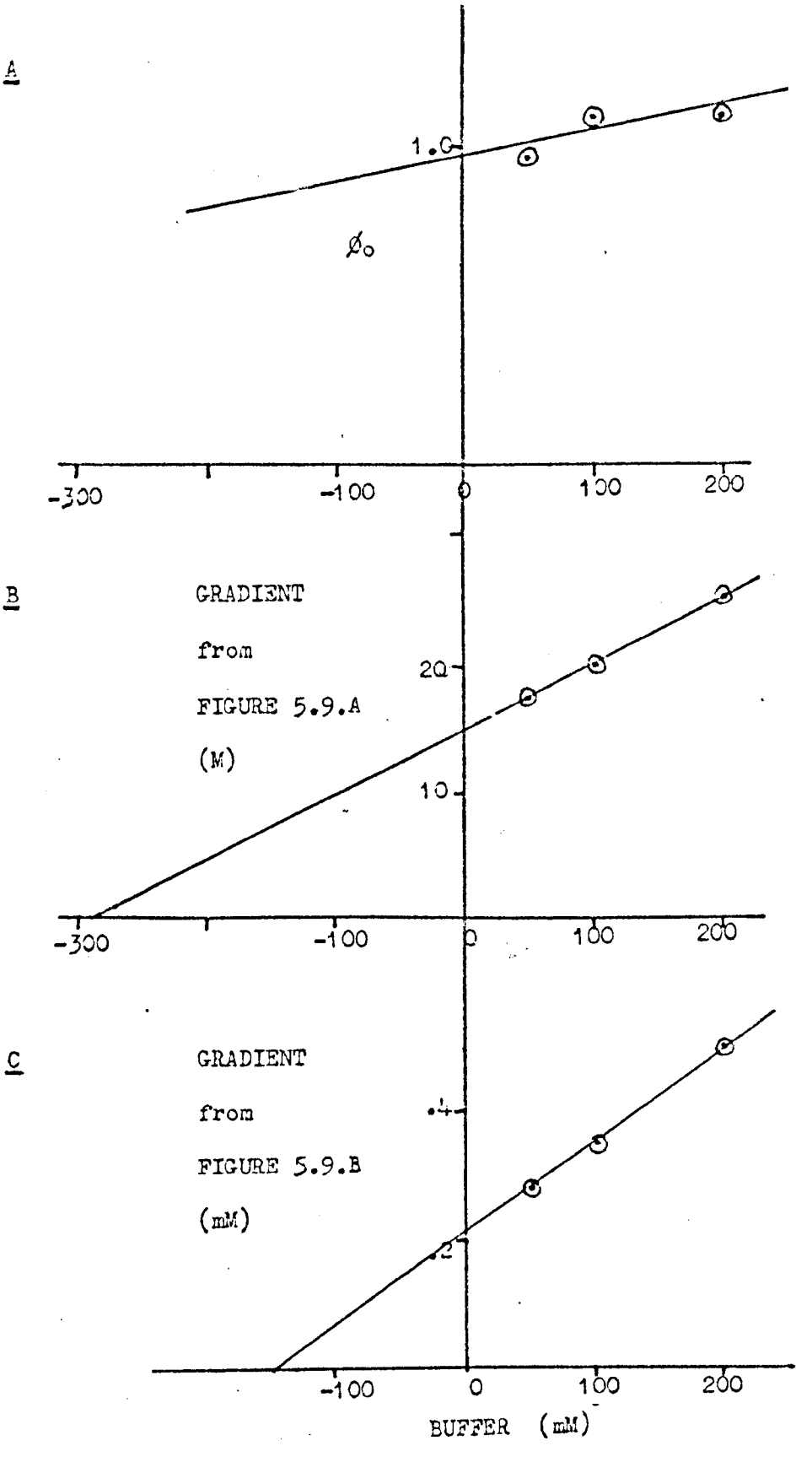
A
1.0
ϕ_o
-300
-100
0
100
200
B
GRADIENT
from
FIGURE 5.9.A
(M)
20
10
-300
-100
0
100
200
C
GRADIENT
from
FIGURE 5.9.B
(mM)
.4
.2
-100
0
100
200
BUFFER (mM)

FIGURE 5.11

The forward assay, in 50 mM pH 8.0 tris buffer, at 25°C, with 33 mM or 67 mM DL ∝ aminobutyrate, as indicated.

A A Lineweaver-Burk plot, with ∝ ketoglutarate as substrate, at 100 mM L alanine.

B A Lineweaver-Burk plot, with L alanine as substrate, at 2.7 mM ∝ ketoglutarate.

FIGURE 5.12

The forward assay, in 50 mM pH 8.0 tris buffer, at 25°C.

A A graph of the apparent $\emptyset_0$ against DL ∝ aminobutyrate concentration.

B A graph of the apparent $\emptyset_{ala}$, (i.e. the gradient from figure 5.11.B), against DL ∝ aminobutyrate concentration.

C A graph of the apparent $\emptyset_{KG}$, (i.e. the gradient from figure 5.11A), against DL ∝ aminobutyrate concentration.

FIGURE 5.13

The reverse assay, in 50 mM pH 8.0 tris buffer, at 25°C, with 2 mM or 4 mM ∝ ketobutyrate, as indicated.

A A Lineweaver-Burk plot, with L glutamate as substrate, at 5 mM pyruvate.

B A Lineweaver-Burk plot, with pyruvate as substrate, at 10 mM L glutamate.

FIGURE 5.11.

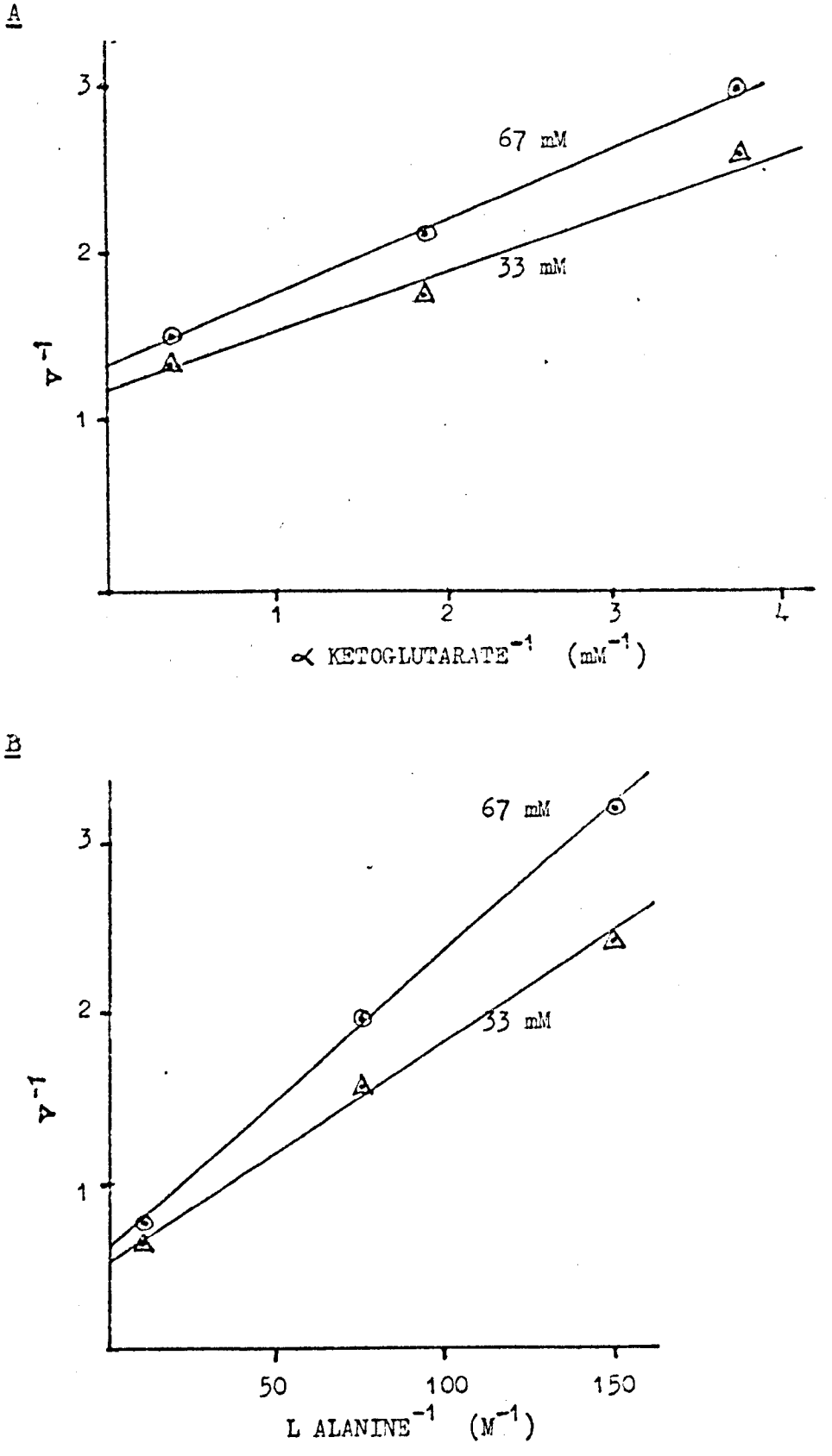
A
67 mM
33 mM
v^{-1}
1
2
3
4
∝ KETOGLUTARATE^{-1} (mM^{-1})
B
67 mM
33 mM
v^{-1}
1
2
3
50
100
150
L ALANINE^{-1} (M^{-1})

FIGURE 5.12.

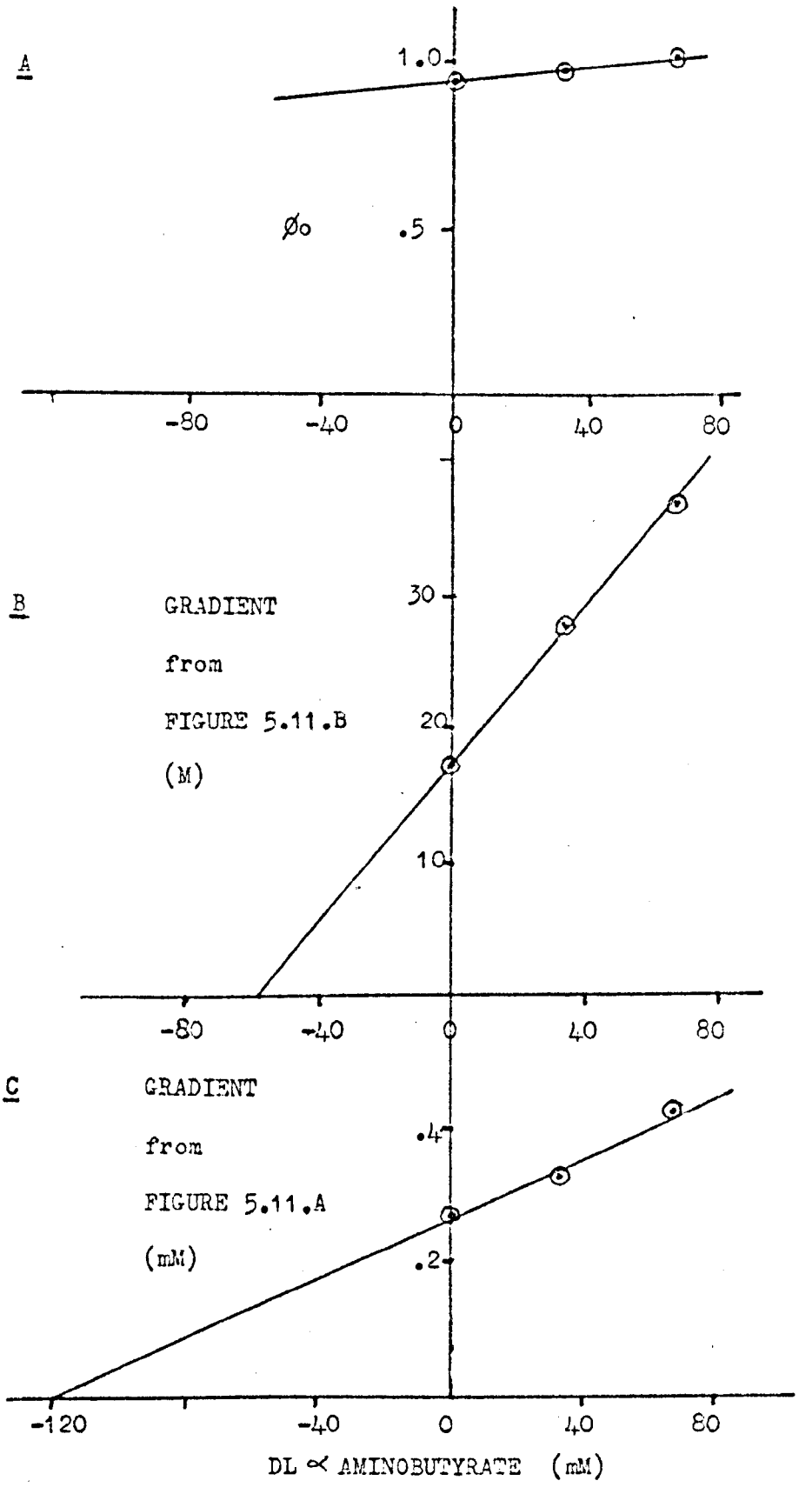
A
1.0
Øo
.5
-80
-40
0
40
80
B
GRADIENT
from
FIGURE 5.11.B
(M)
30
20
10
-80
-40
0
40
80
C
GRADIENT
from
FIGURE 5.11.A
(mM)
.4
.2
-120
-40
0
40
80
DL ∝ AMINOBUTYRATE (mM)

FIGURE 5.13.

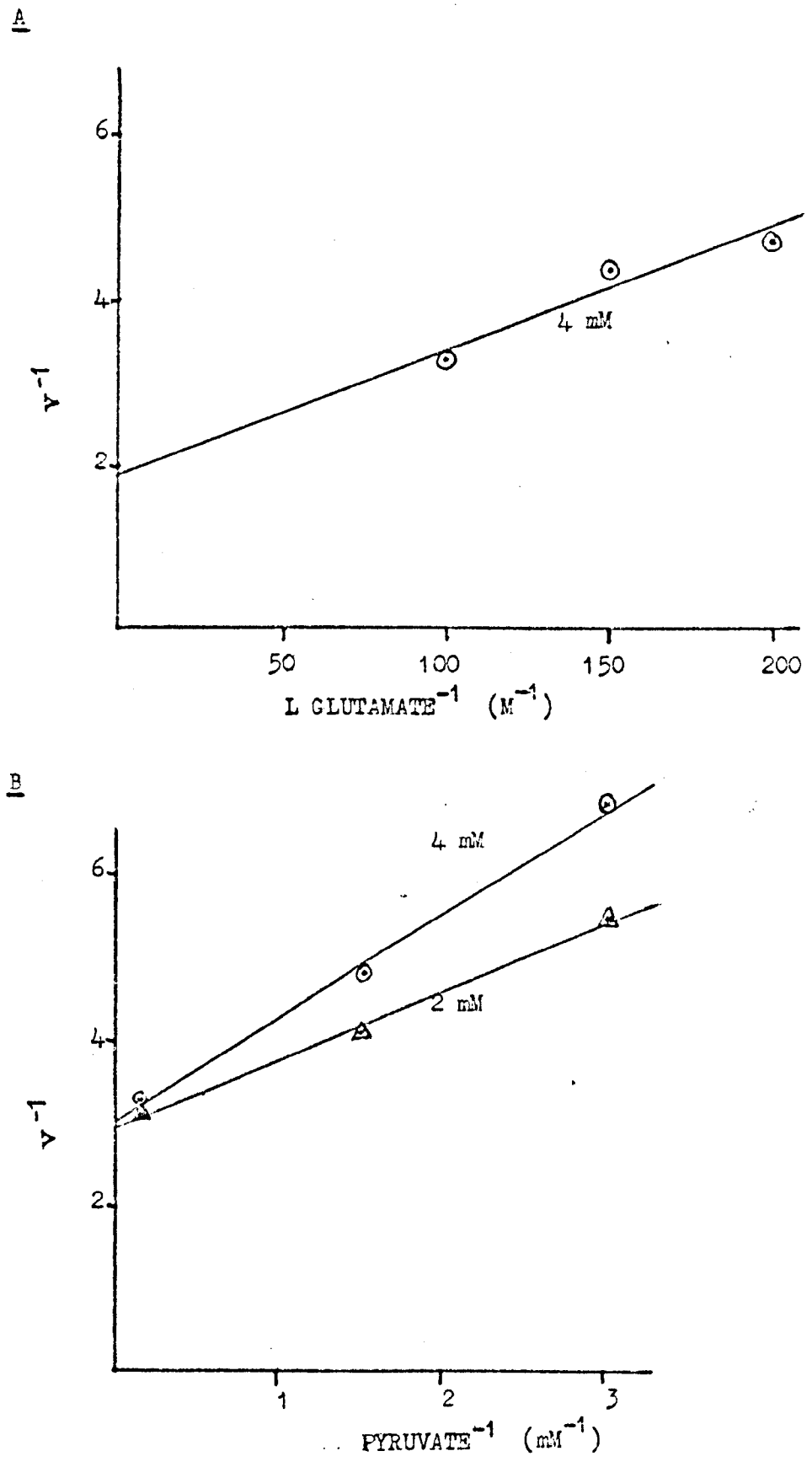
A
6
4
2
v^{-1}
4 mM
50
100
150
200
L GLUTAMATE^{-1} (M^{-1})
B
6
4
2
v^{-1}
4 mM
2 mM
1
2
3
PYRUVATE^{-1} (mM^{-1})

FIGURE 5.14

The reverse assay, in 50 mM pH 8.0 tris buffer, at 25°C.

A A graph of the apparent $\emptyset_0$ against ∝ ketobutyrate concentration.

B A graph of the apparent value of $\emptyset_{glu}$, (i.e. the gradient from figure 5.13.A), against ∝ ketobutyrate concentration.

C A graph of the apparent value of $\emptyset_{pyr}$, (i.e. the gradient from figure 5.13.B), against ∝ ketobutyrate concentration.

FIGURE 5.15

The forward assay, in 50 mM pH 8.0 tris buffer, at 25°C, with 8.3 mM or 16.7 mM fumarate, as indicated.

A A Lineweaver-Burk plot, with ∝ ketoglutarate as substrate, at 100 mM L alanine.

B A Lineweaver-Burk plot, with L alanine as substrate, at 2.7 mM ∝ ketoglutarate.

FIGURE 5.16

The forward assay, in 50 mM pH 8.0 tris buffer, at 25°C.

A A graph of the apparent $\emptyset_0$ against fumarate concentration.

B A graph of the apparent $\emptyset_{ala}$,(i.e. the gradient from figure 5.15.B), against fumarate concentration.

C A graph of the apparent $\emptyset_{KG}$, (i.e. the gradient from figure 5.15.A), against fumarate concentration.

FIGURE 5.14.

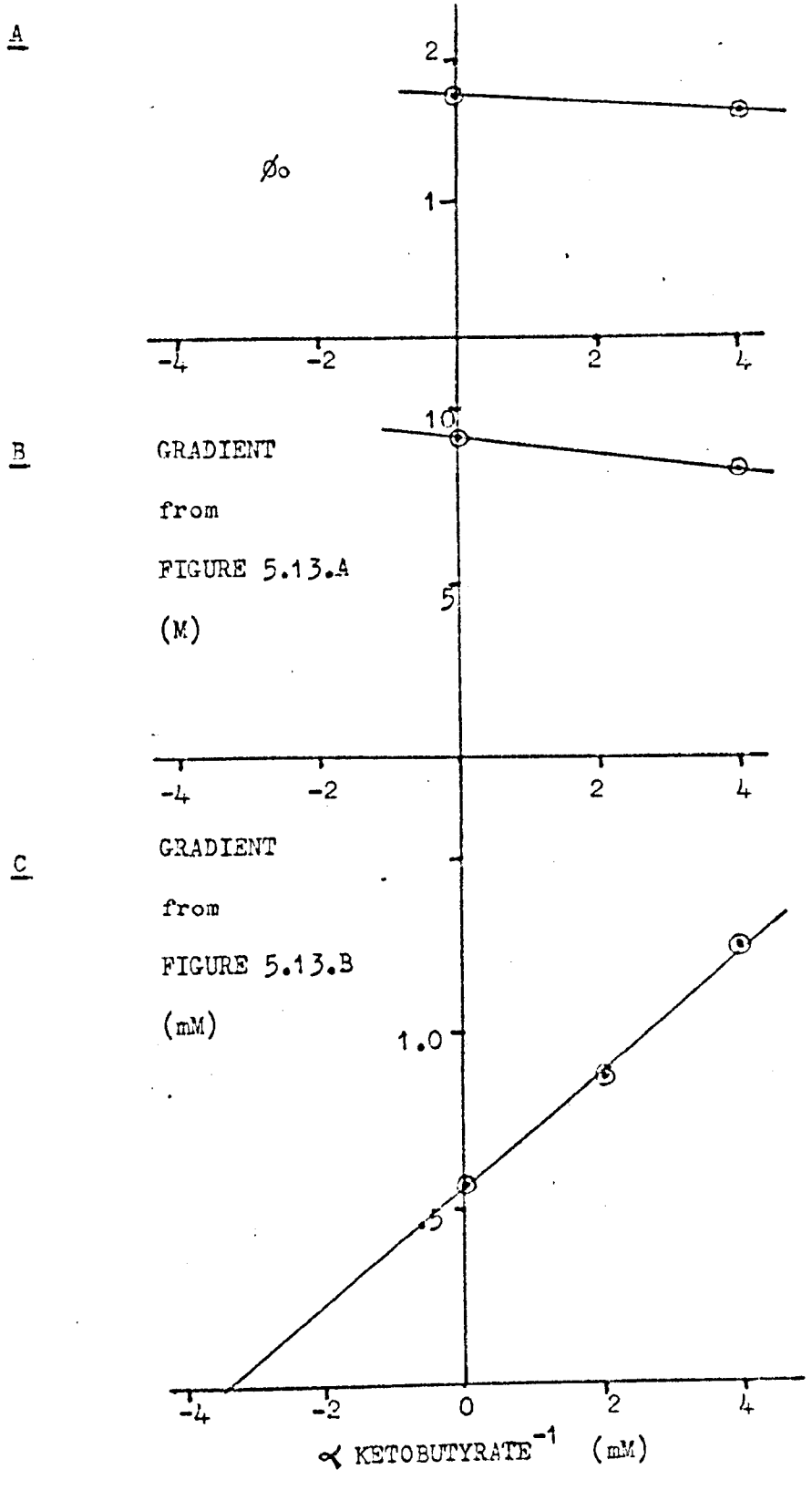
A
2
ϕ_o
1
-4
-2
2
4
B
10
GRADIENT
from
FIGURE 5.13.A
(M)
5
-4
-2
2
4
C
GRADIENT
from
FIGURE 5.13.B
(mM)
1.0
.5
-4
-2
0
2
4
α KETOBUTYRATE^{-1} (mM)

FIGURE 5.15.

A

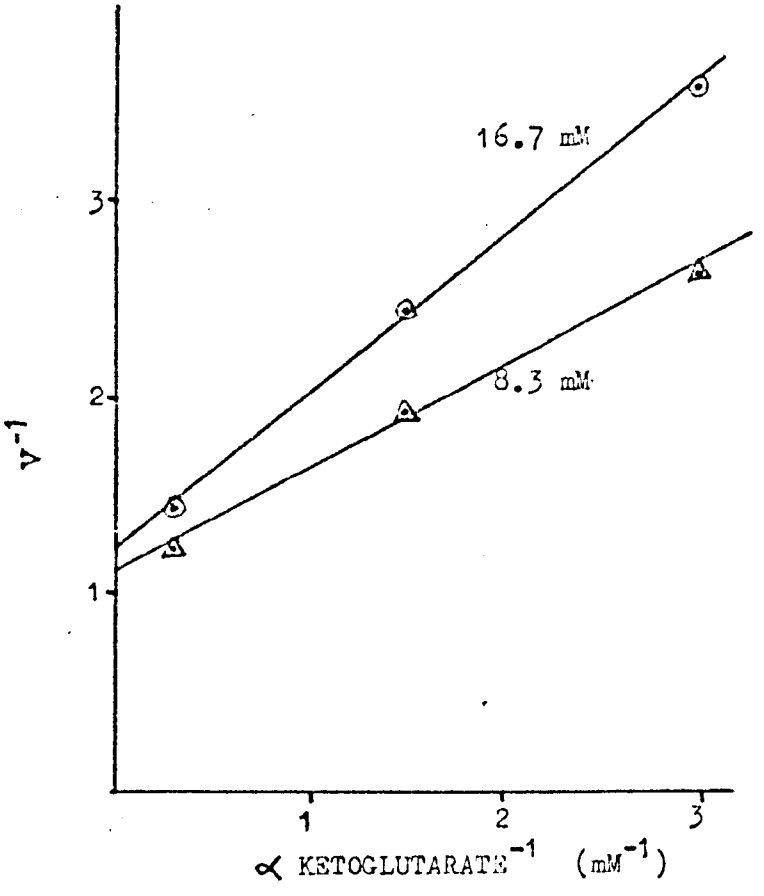

B

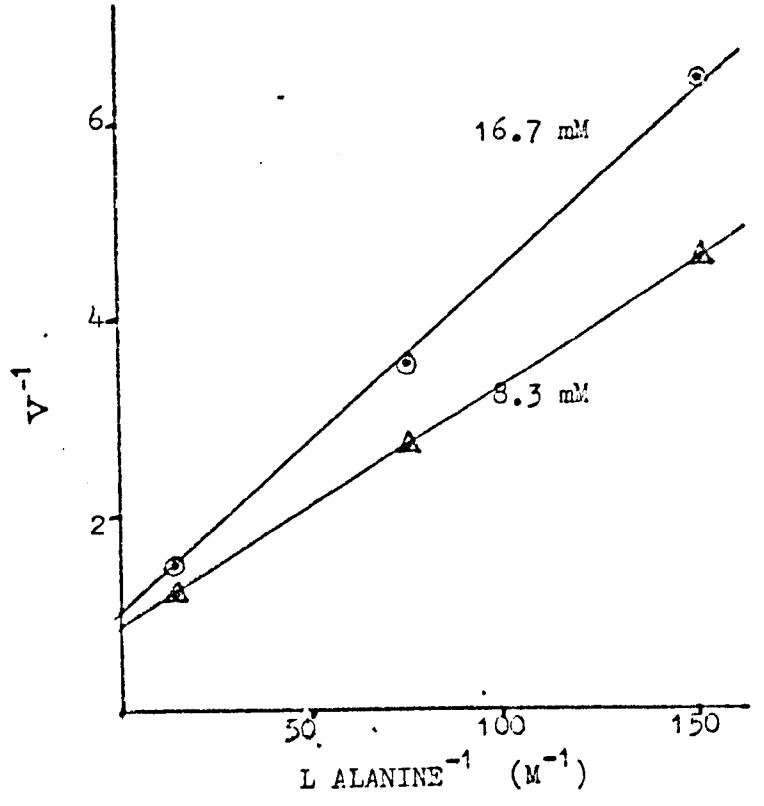

FIGURE 5.16.

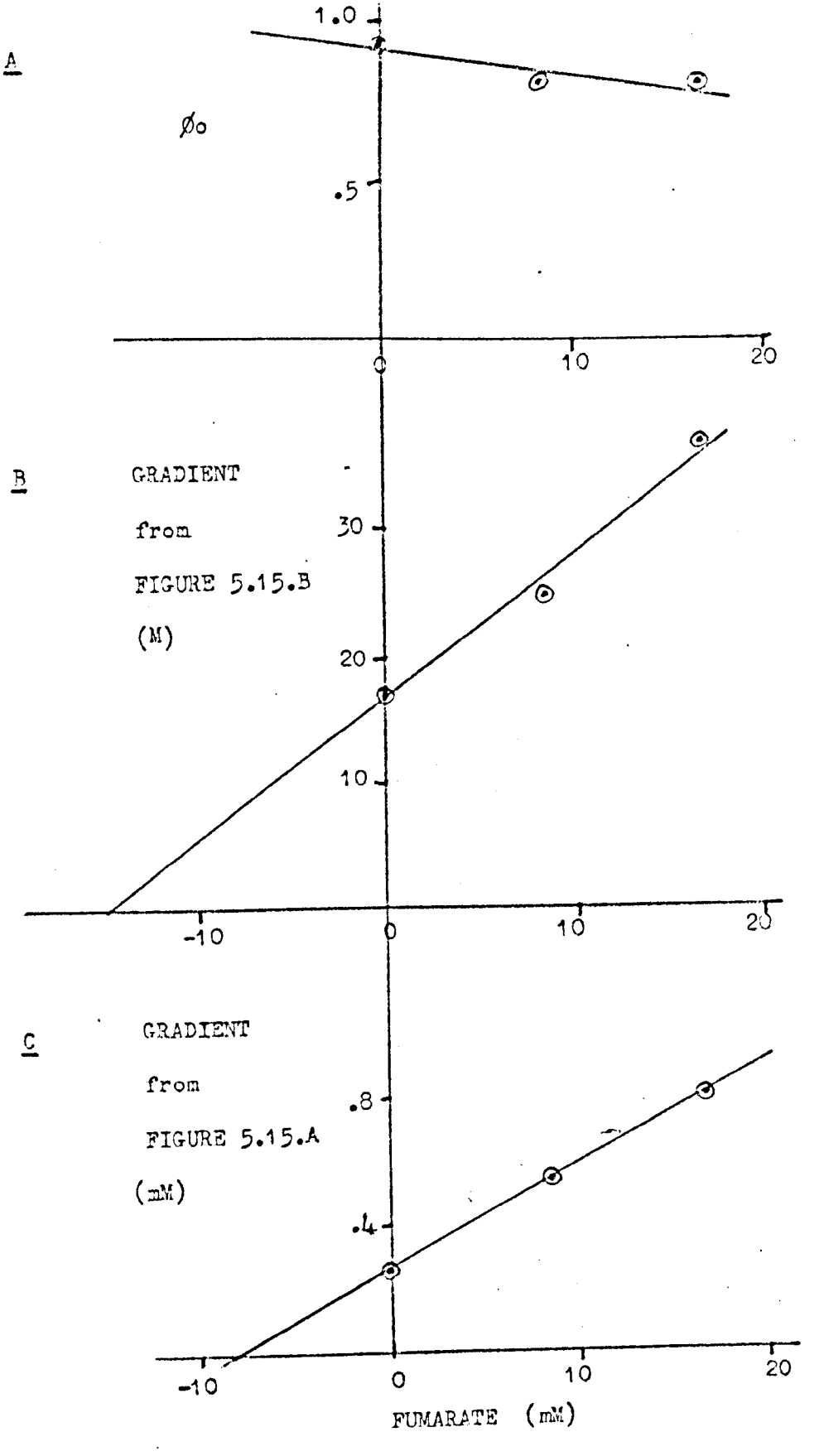
A
1.0
Øo
.5
0
10
20
B
GRADIENT
from
FIGURE 5.15.B
(M)
30
20
10
-10
0
10
20
C
GRADIENT
from
FIGURE 5.15.A
(mM)
.8
.4
-10
0
10
20
FUMARATE (mM)

FIGURE 5.17

The forward assay, in 50 mM pH 8.0 tris buffer, at 25°C, with 167 mM or 333 mM acetate, as indicated.

A Lineweaver-Burk plot, with L alanine as substrate, at 2.7 mM ∝ ketoglutarate.

B A Lineweaver-Burk plot, with ∝ ketoglutarate as substrate, at 100 mM L alanine.

FIGURE 5.18

The forward assay, in 50 mM pH 8.0 tris buffer, at 25°C.

A A graph of the apparent $\emptyset_0$ against acetate concentration.

B A graph of the apparent $\emptyset_{ala}$, (i.e. the gradient from figure 5.17.A), against acetate concentration.

C A graph of the apparent $\emptyset_{KG}$, (i.e. the gradient from figure 5.17.B), against acetate concentration.

FIGURE 5.19

The forward assay, in 50 mM pH 8.0 tris buffer, at 25°C, with 1 mM or 2 mM thiosemicarbazide, as indicated.

A A Lineweaver-Burk plot, with L alanine as substrate, at 2.7 mM ∝ ketoglutarate.

B A Lineweaver-Burk plot, with ∝ ketoglutarate as substrate, at 100 mM L alanine.

FIGURE 5.17.

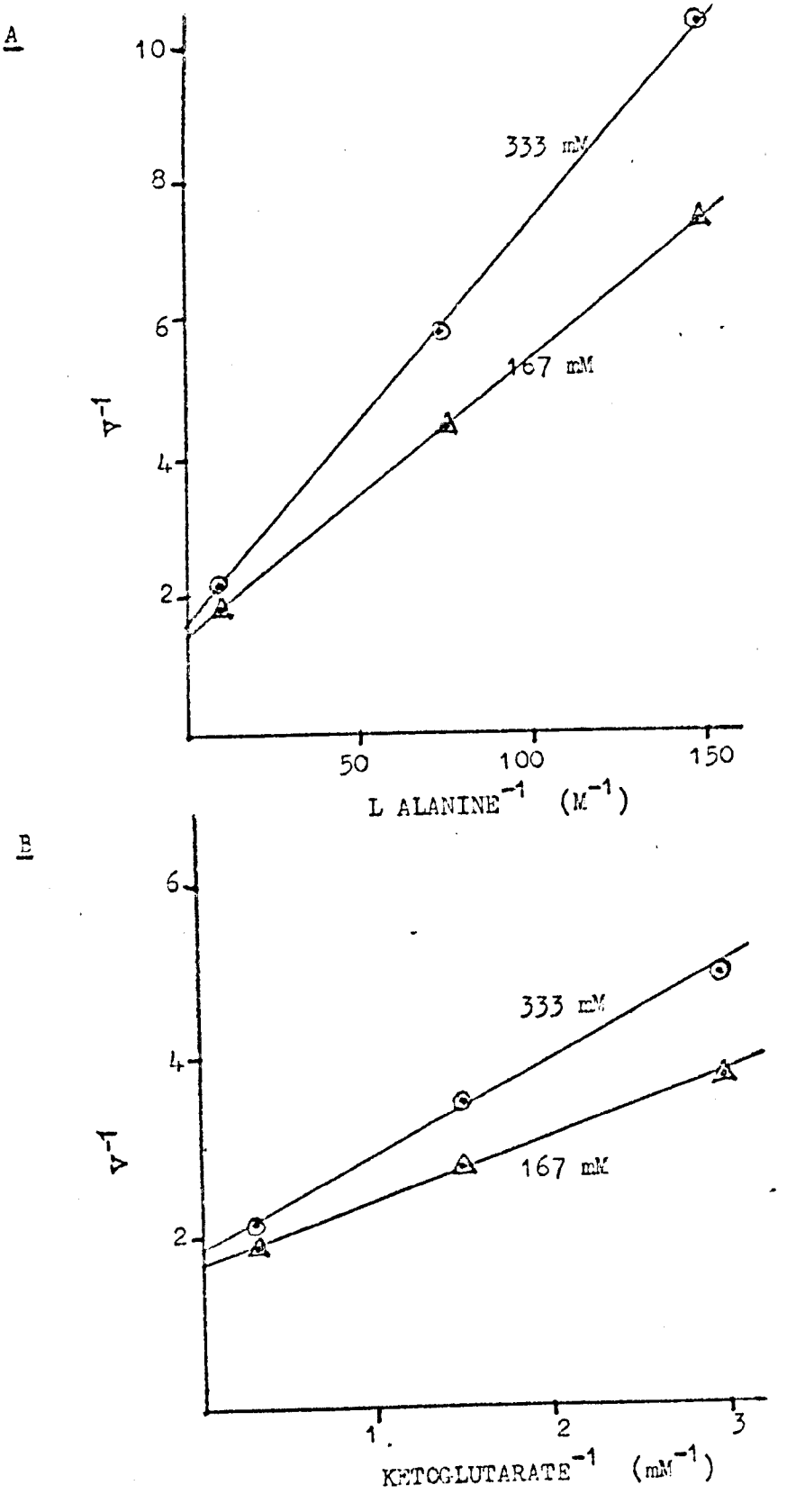
A
10
8
6
4
2
v^{-1}
333 mM
167 mM
50
100
150
L ALANINE^{-1} (M^{-1})
B
6
4
2
v^{-1}
333 mM
167 mM
1
2
3
KETOGLUTARATE^{-1} (mM^{-1})

FIGURE 5.18.

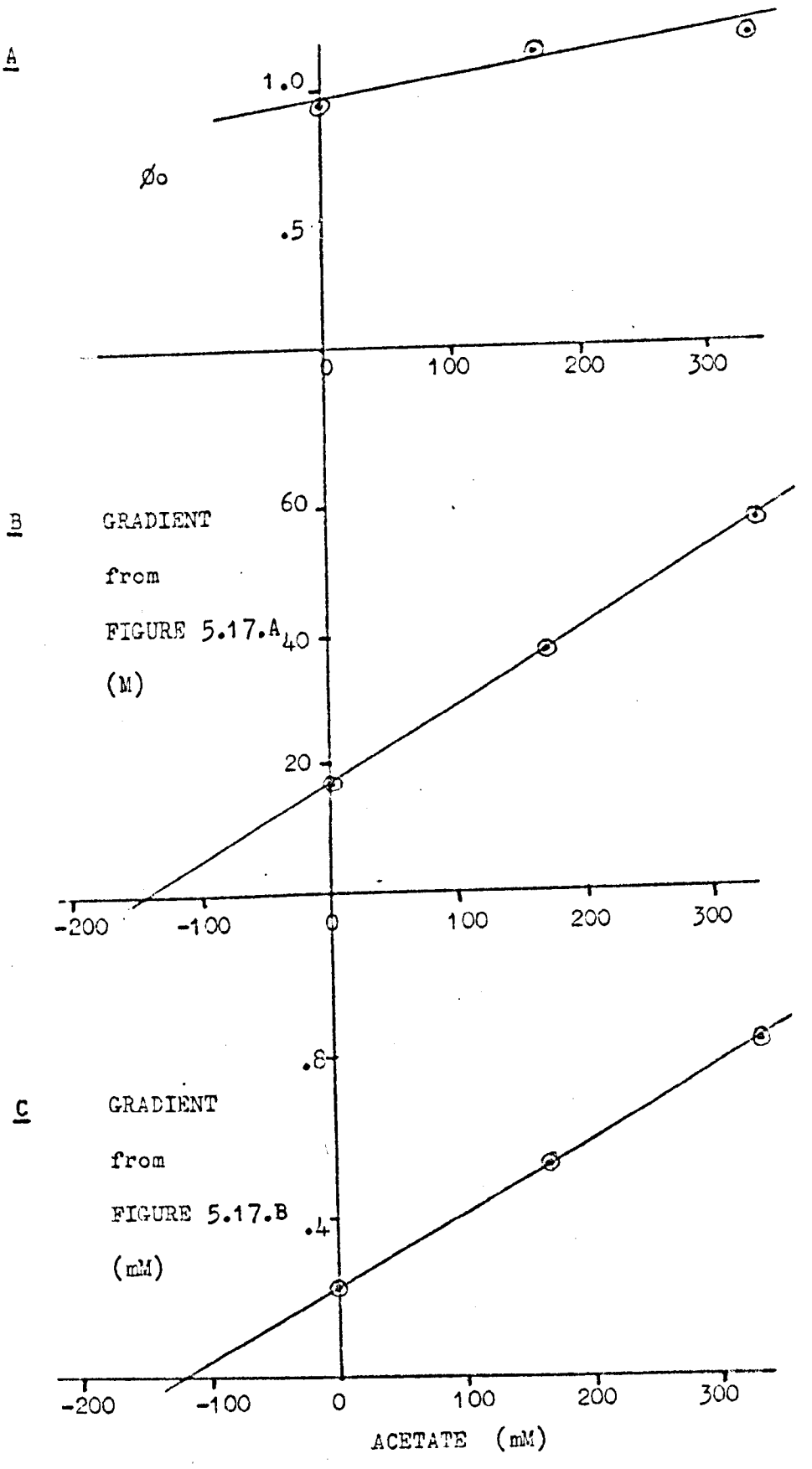
A
1.0
Øo
.5
0
100
200
300
B
GRADIENT
from
FIGURE 5.17.A
(M)
60
40
20
-200
-100
0
100
200
300
C
GRADIENT
from
FIGURE 5.17.B
(mM)
.8
.4
-200
-100
0
100
200
300
ACETATE (mM)

FIGURE 5.19.

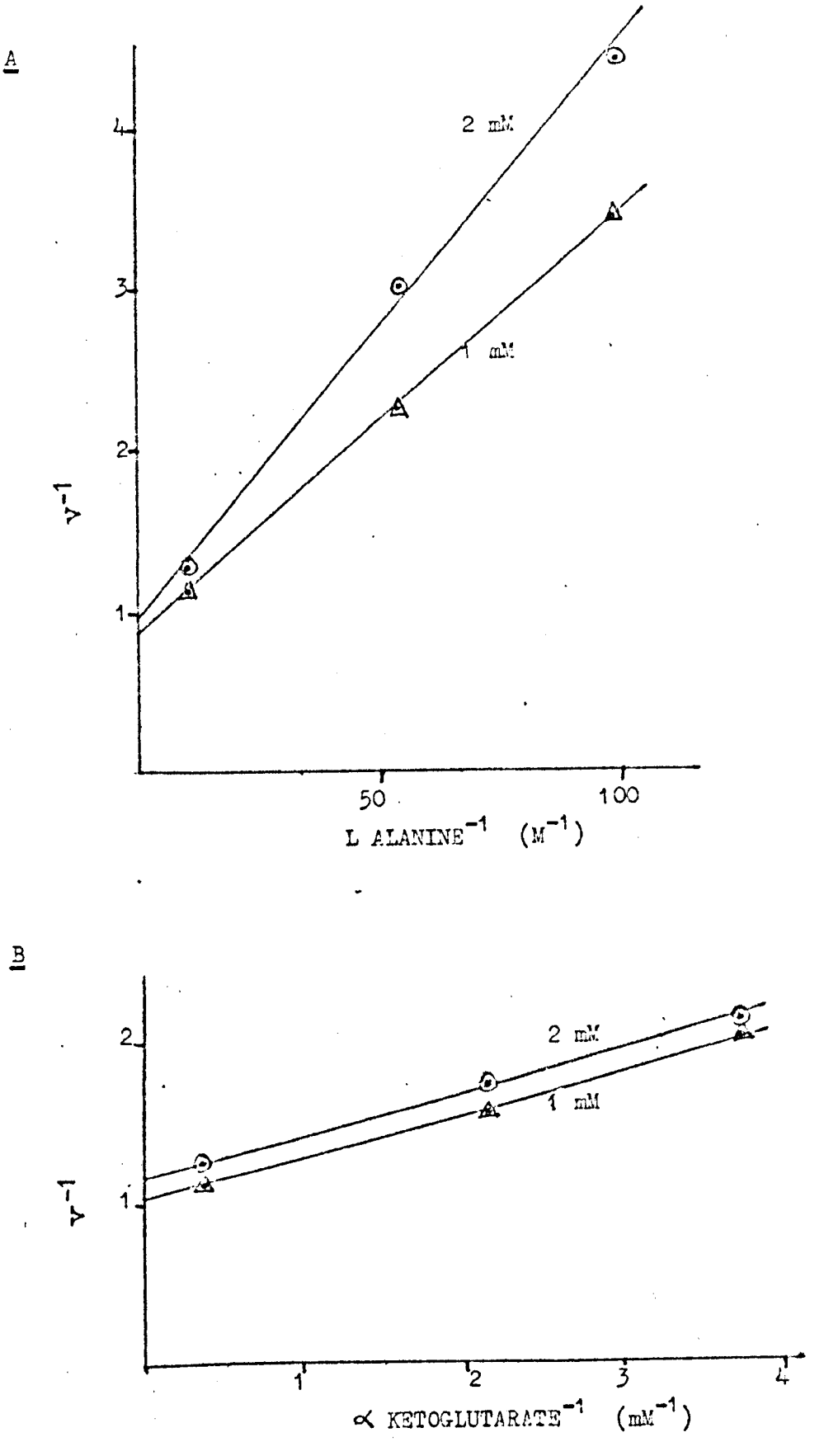
A
2 mM
1 mM
4
3
2
1
v^{-1}
50
100
L ALANINE^{-1} (M^{-1})
B
2 mM
1 mM
2
1
v^{-1}
1
2
3
4
∝ KETOGLUTARATE^{-1} (mM^{-1})

FIGURE 5.20

The forward assay, in 50 mM pH 8.0 tris buffer, at 25°C.

A A graph of the apparent ϕ_O against TSC concentration.

B A graph of the apparent ϕ_{ala}, (i.e. the gradient from figure 5.19.A), against TSC concentration.

C A graph of the apparent ϕ_{KG}, (i.e. the gradient from figure 5.19.B), against TSC concentration.

FIGURE 5.20.

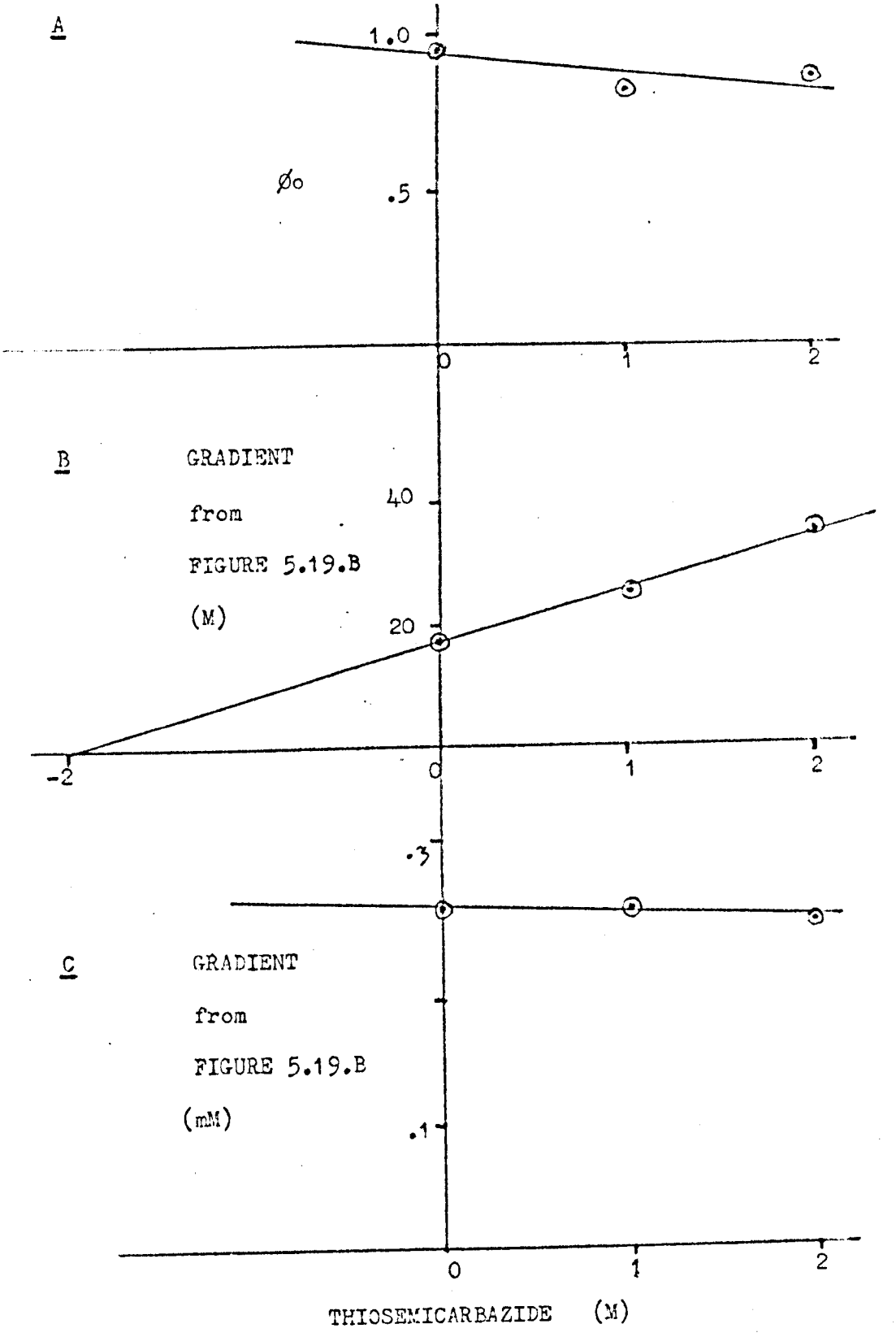
A
1.0
Øo
.5
0
1
2
B
GRADIENT
from
FIGURE 5.19.B
(M)
40
20
-2
0
1
2
.3
C
GRADIENT
from
FIGURE 5.19.B
(mM)
.1
0
1
2
THIOSEMICARBAZIDE (M)

It might be considered that the buffer acts not as a specific inhibitor but through an ion-cloud effect, as described in the Debye- Hückel theory. In the next chapter, the reasons are given for supposing that this is not the case.

The inhibition constants for a number of inhibitors were obtained. ∝Ketobutyrate was used with the reverse assay; the other inhibitors with the forward assay, (figure 5.11. to 5.20.).

5.3 ' RESULTS

The kinetic constants for each assay, in 50 mM pH 8.0 tris chloride, at 25°C are given in table 5.1: they are similar to those at 37°C.

The $\emptyset_0$ for the forward and reverse assays were similar, but were two orders higher for the AB and KB assays. The three amino-acids had similar K_ms; the K_m for ∝ketobutyrate was an order higher than for pyruvate and ∝ketoglutarate.

Formate inhibited substrate binding but also reduced $\emptyset_0$(forward assay) by an amount that was just significant.

The inhibitor constants in 50 mM pH 8.0 tris chloride are given in table 5.2.

Because the inhibitor constants for the buffer were very high, the calculated values have a large error. The inhibition by buffer at 50 mM was small and the effect on $\emptyset_0$ was negligible.

Except for butyrate the other inhibitors showed no binding to the enzyme- substrate complex.

The results with the amino- acids fit well with the results of Saier and Jenkins (171), in table 1.1. The ∝ carboxyl group

TABLE 5.1

Kinetic parameters obtained at 25°C, in 50 mM pH 8.0 tris buffer.

The $\emptyset$ constants are expressed as the ratio of the absolute value of $\emptyset_i$ to the absolute rate of the standard assay, (see text).

$\emptyset_1$, $\emptyset_2$ and K_M parameters are expressed in mM.

TABLE 5.2

The calculated dissociation constants for some ala AT inhibitors, with different forms of the enzyme. These were obtained at 25°C, in 50 mM tris buffer.

TABLE 5.1

ASSAY	ϕ_o	ϕ_1	ϕ_2	K_M
FORWARD	ϕ_o 0.96	ϕ_{ala} 17.2	ϕ_{KG} 0.27	
REVERSE	ϕ_o 1.78	ϕ_{glu} 9.3	ϕ_{pyr} 0.57	
AMINOBUTYRATE	ϕ_o 105	ϕ_{AB} 5040		$K_{M\ AB}$ 48
KETOBUTYRATE	ϕ_o 42		ϕ_{KB} 147	$K_{M\ KB}$ 3.5

TABLE 5.2.

INHIBITOR	assay	PL-ala-AT (mM)	ES complex (mM)	PM-ala-AT (mM)
DL ∝ Aminobutyrate	forward	58	high	120
L Norleucine	forward	13	high	80
L Aspartate	forward	96	high	51
L Serine	forward	180	high	265
Glycine	forward	high	high	high
L Glutamate	reverse			160
D Alanine	forward	high	high	270
L∝Methylglutamate	forward	18	high	12
ɣ Aminobutyrate	forward	480	high	350
Hydroxylamine	forward	.008	high	high
Thiosemicarbazide	forward	2.0	high	high
Propylamine	forward	high	high	high
∝Ketobutyrate	reverse	high	high	3.5
Acetate	forward	135	high	117
Butyrate	forward	69	200	21
Malonate	forward	47	high	20
Succinate	forward	69	high	27
Glutarate	forward	170	high	37
Maleate	forward	82	high	12
Fumarate	forward	15	high	8.0
Buffer	forward	295	high	148
Buffer	reverse	325	high	220

is important; the amino-group should be in the α position and L configuration. The nature of the side group is important - it seems likely that in all the substrates, the side group is bound to the enzyme. Certain amino-acids bind better to the PM form than to the PL form. This is the opposite of the case with substrate amino- acids. Hence L aspartate, D alanine, γaminobutyrate and DLαmethyl glutamate are poor substrate analogues.

Hydroxylamine and thiosemicarbazide, (TSC), are much more nucleophilic than amino-acids at pH 8 and they bound better to the PL form, though at an observably slow rate; the spectrophotometer record was not linear until after 3 minutes. They did not bind well to the PM form, confirming that they bound to the internal aldimine.

Of the carboxylic acids all but acetate bound better to the PM form. The sequence malonate, succinate, and glutarate, showed that increased chain length had an adverse effect on binding - probably because of the restricted motion of the bound inhibitor. Thus the introduction of a double bond into succinate reduced the dissociation constant, for fumarate and maleate. Fumarate bound better than maleate.

CHAPTER 6

ACTIVITY KINETICS AT VARIOUS PH S

6.1 EXPERIMENTS

Some kinetic parameters were measured at pHs other than 8.0 These were obtained from:

1) the forward, reverse, aminobutyrate and ketobutyrate assays
2) the buffer effect on the forward and reverse assays
3) α aminobutyrate and α ketobutyrate inhibition
4) fumarate, acetate and TSC inhibition

For these last three inhibitors the experiment was carried out at three different buffer concentrations. To limit the amount of work, fewer points were used for these. At each constant inhibitor and buffer concentration, three points were used for fumarate. With TSC and acetate only one point was used at α ketoglutarate $> 3.5\ \phi_{KG}$ and L alanine $< .05\ \phi_{ala}$; so that

$$v^{-1} = \phi_{ala}(1 + I/K_i)\ ala^{-1}$$

In this case only ϕ_{ala} was obtained.

6.2 BUFFER EFFECT

Often when the effect of pH on kinetic constants is being studied, any effects produced by the buffers are ignored. For ala AT the effects of buffer were too considerable and varied too greatly with pH, for them to be ignored. The buffer effect was calculated and buffer independent constants were obtained. (63, 118, 133).

The buffer might act by a non-specific ion-cloud effect as postulated in the Debye-Huckel theory and would fit an equation $\log \phi \propto \mu^{\frac{1}{2}}$ (where μ is the ionic strength). This seems to be the case for many urease inhibitors (115, 116)

Alternatively the buffer may act by a limitted and specific binding, in which case it is acting as a normal inhibitor and fits the equation $\phi \propto I$.

The kinetic constants at varying buffer concentrations are given in table 6.1. The results at four different pHs, employing four different species of buffer, are given. The graphs of $\log_{10} \phi$ against $\mu^{\frac{1}{2}}$ and of ϕ against buffer concentration are both linear within experimental error in each case, with different values at $\mu =$ (buffer) = 0. With asp AT and phosphate buffer, a complicated relation between activity and buffer concentration existed(25).

However, the Debye-Huckel equation depends on the ionic strength and not on the nature of the ions. To prove that it does not explain buffer inhibition, it is only necessary to show that any one inhibitor gives a considerably lower ϕ at the same ionic strength. Figures 6.1. and 6.2. show ϕ_{ala} at varying buffer and inhibitor concentrations. These results demonstrate that the effect of acetate, tris chloride and glycine buffers is quite inexplicable by the Debye-Huckel theory.

With phosphate buffers, although some inhibitors gave considerably greater inhibition than phosphate at the same ionic strength, none gave less. Acetate, (figure 6.13.), fitted in very well with the phosphate results at pH 7.0. Acetate acts as a specific inhibitor: i.e. its ionic strength effect is a minor component in acetate inhibition. It, therefore, seems unlikely that the phosphate inhibition is mainly due to an ionic

TABLE 6.1

The value of various kinetic parameters at 25°C, at different buffer concentrations. Results are given for pH 5.0 acetate, pH 7.0 phosphate, pH 8.0 tris chloride, and pH 10.0 glycine buffers

FIGURE 6.1

Graphs of $\log_{10}$(apparent ϕ_{ala}) against (ionic strength)$^{.5}$.

According to the Debye-Huckel interpretation, a straight line should be obtained, that is independent of the nature of the ionic species.

A At pH 5.0

+ With sodium acetate buffer

⊙ with sodium acetate buffer and disodium fumarate

B At pH 7.0

+ with potassium phosphate buffer

⊙ with potassium phosphate buffer and sodium acetate

FIGURE 6.2

Graphs of $\log_{10}$(apparent ϕ_{ala}) against (ionic strength)$^{.5}$.

According to the Debye-Huckel interpretation, a straight line should be obtained, that is independent of the nature of the ionic species.

A At pH 8.0

+ with tris chloride buffer

⊙ with tris chloride buffer and disodium glutarate.

B At pH 10.0

+ with sodium glycinate buffer

⊙ with sodium glycinate and disodium fumarate

TABLE 6.1.

pH buffer	[buffer] mM	$\phi o_{Forward}$	$\phi o_{Reverse}$	ϕ_{ala}	ϕ_{glu}	ϕ_{pyr}	ϕ_{KG}
pH 5.0 Acetate	50	2.7	9.8	1580	920	4.9	1.3
	150	3.2	8.2	2590	1670	4.8	.98
	250	3.2	8.3	3600	2230	5.2	.97
pH 7.0 Phosphate	50	.87	1.78	47	42	1.45	.76
	100	.87	1.75	61	45	2.24	1.25
	150	1.04	1.5	74	56	2.76	1.74
pH 8.0 Tris chloride	50	.96	1.8	17.2	10.3	.49	.27
	100	1.07	2.0	19.8	11.3	.57	.35
	150		1.8		13.0	.67	
	200	1.09		25.0			.51
pH 10.0 Glycine	50	2.1	2.4	7.3	10.2	2.65	1.88
	100	2.5	2.0	13.0	15.6	4.15	2.76
	150	2.6	2.2	16.6	20.0	5.92	3.50

FIGURE 6.1.

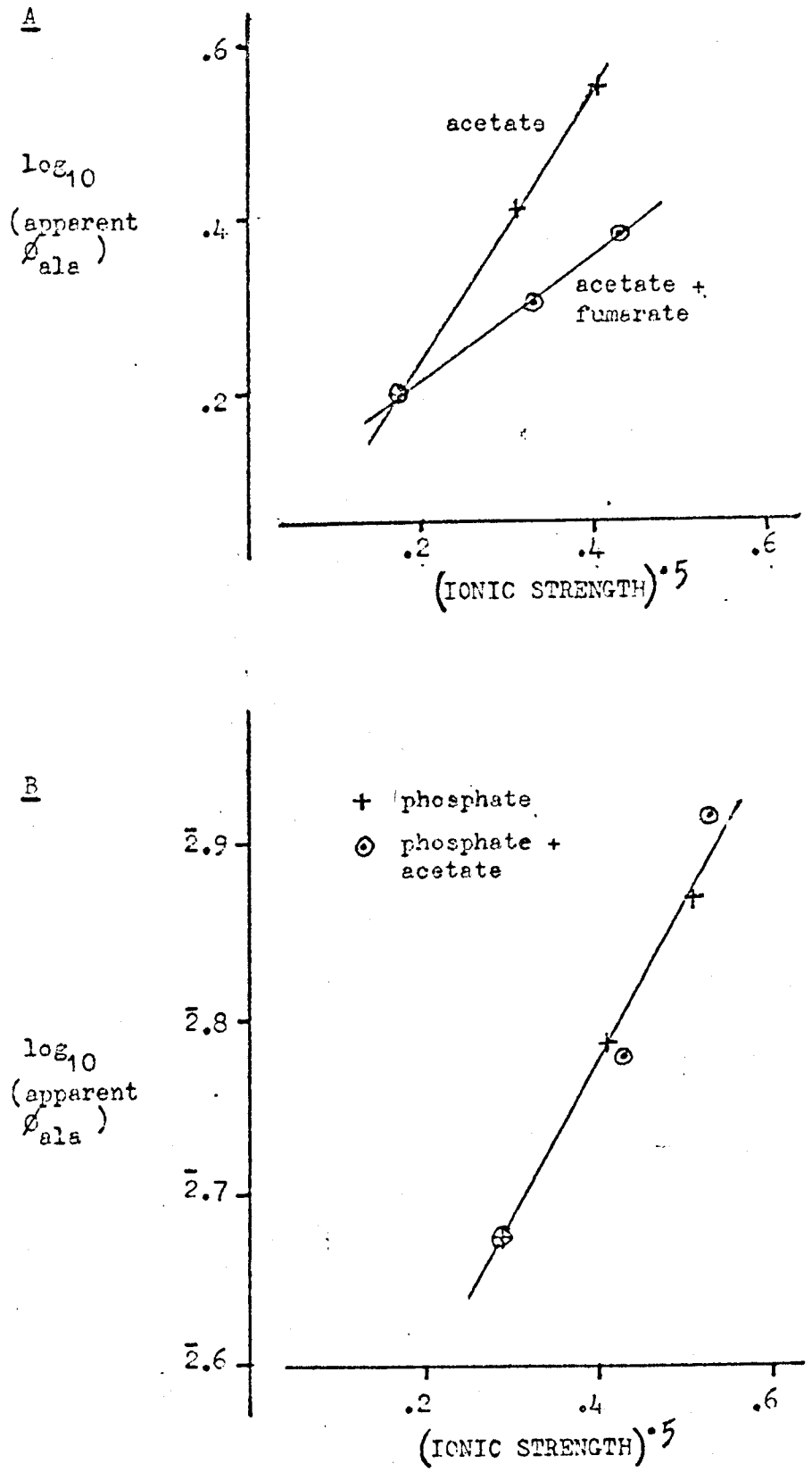
A
$\log_{10}$ (apparent ϕ_{ala})
.6
.4
.2
acetate
acetate + fumarate
.2
.4
.6
(IONIC STRENGTH)$^{.5}$
B
$\log_{10}$ (apparent ϕ_{ala})
$\bar{2}.9$
$\bar{2}.8$
$\bar{2}.7$
$\bar{2}.6$
+ phosphate
⊙ phosphate + acetate
.2
.4
.6
(IONIC STRENGTH)$^{.5}$

FIGURE 6.2.

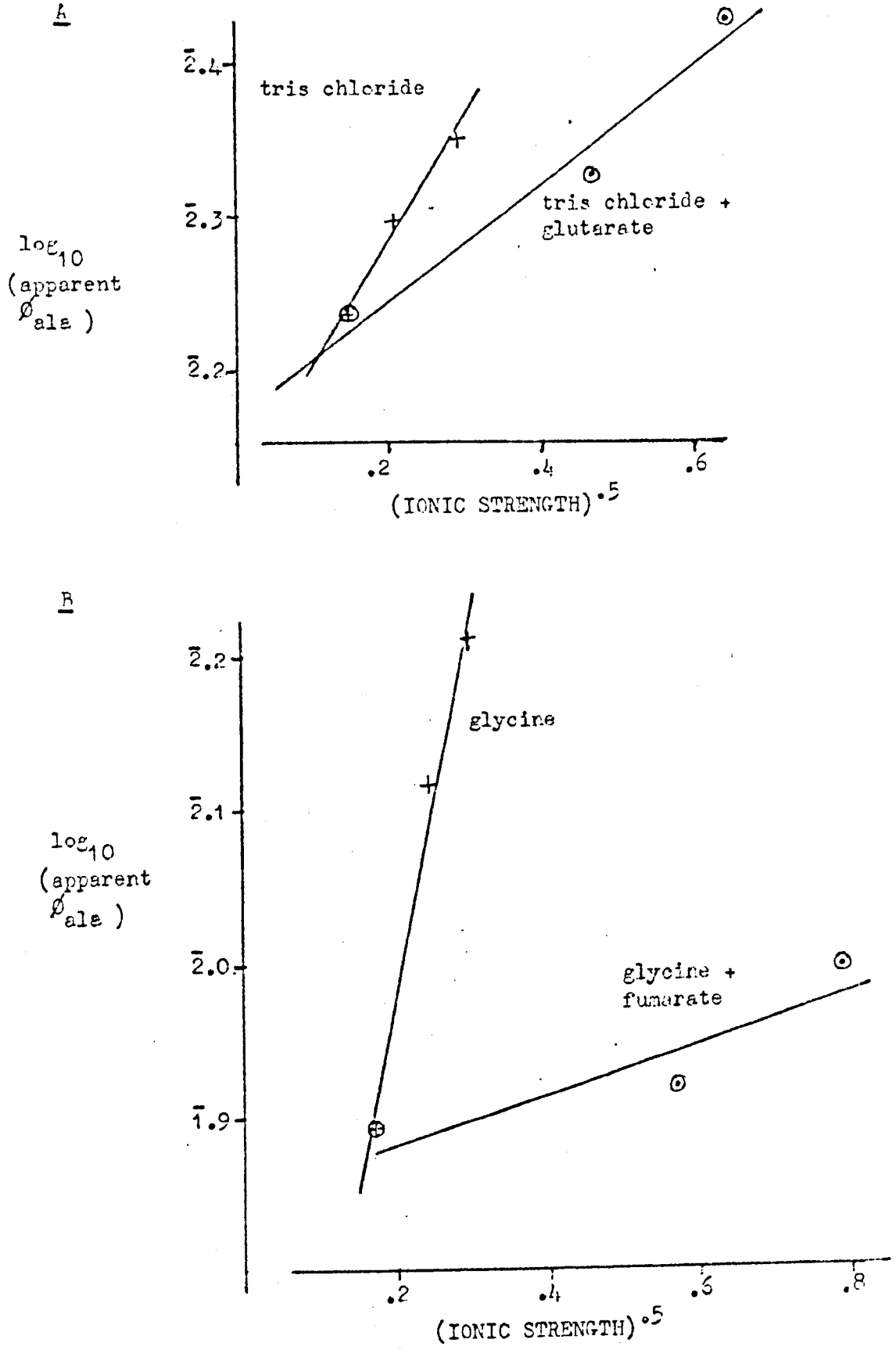
A
$\bar{2}.4$
$\bar{2}.3$
$\bar{2}.2$
tris chloride
tris chloride + glutarate
$\log_{10}$ (apparent ϕ_{ala})
.2
.4
.6
(IONIC STRENGTH)$^{.5}$
B
$\bar{2}.2$
$\bar{2}.1$
$\bar{2}.0$
$\bar{1}.9$
glycine
glycine + fumarate
$\log_{10}$ (apparent ϕ_{ala})
.2
.4
.6
.8
(IONIC STRENGTH)$^{.5}$

FIGURE 6.3

A graph of ϕ_0 against buffer concentration, for the forward and reverse assays.

A with pH 7.0 phosphate buffer

B with pH 5.0 acetate buffer

FIGURE 6.4

Graphs of ϕ_0 against buffer concentration, for the forward and reverse assays.

A with pH 10.0 glycine buffer

B with pH 8.0 tris chloride buffer

FIGURE 6.3.

A

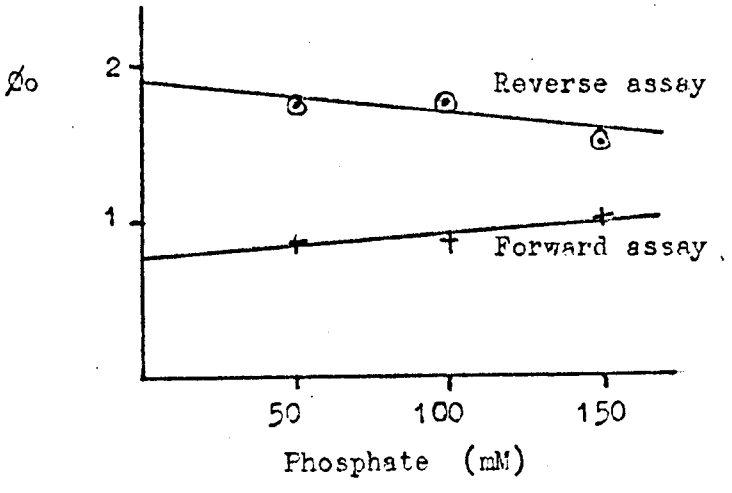
Øo
2
1
Reverse assay
Forward assay
50
100
150
Phosphate (mM)

B

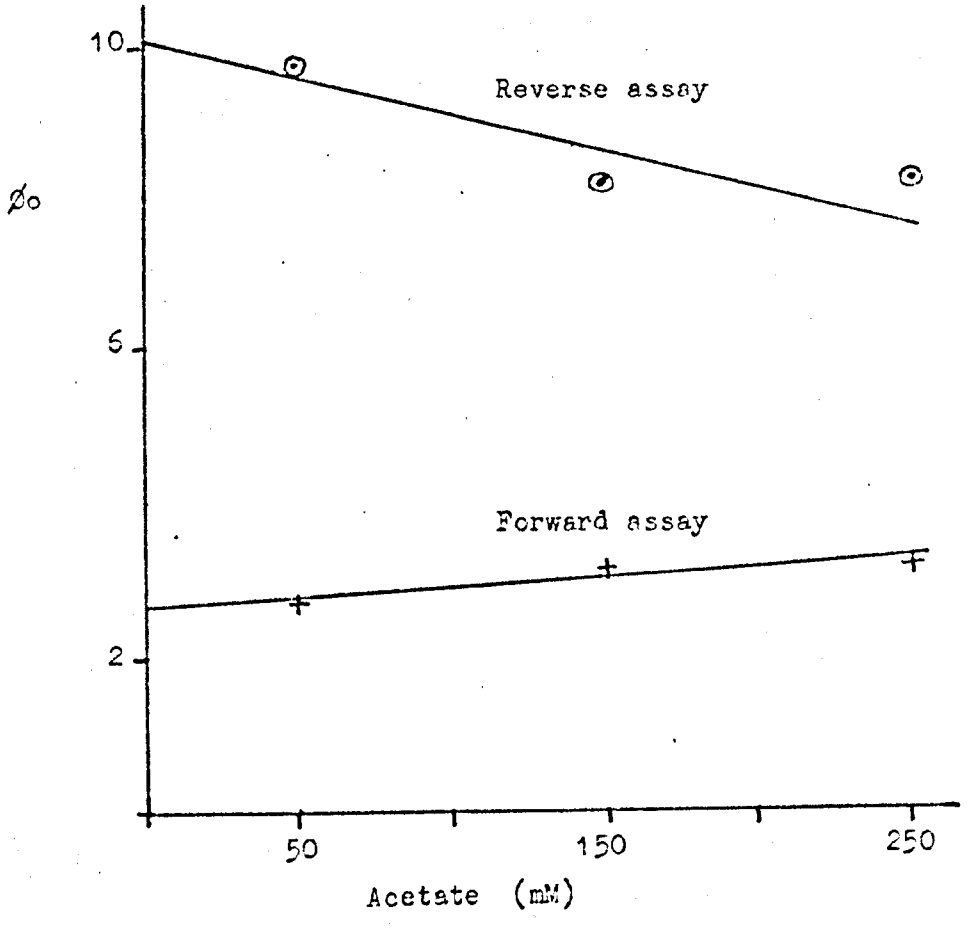
10
6
2
Øo
Reverse assay
Forward assay
50
150
250
Acetate (mM)

FIGURE 6.4.

A

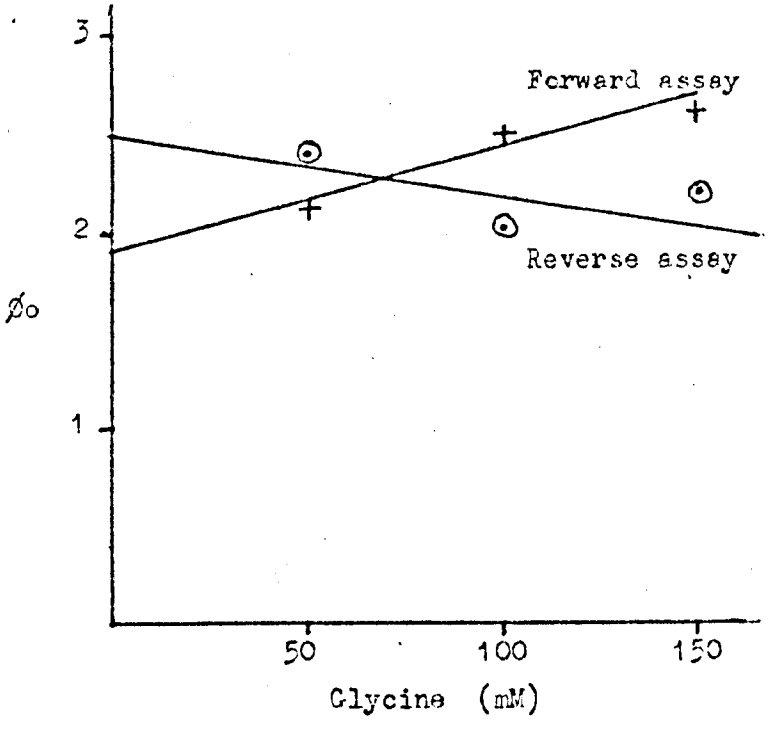
3
2
1
Øo
Forward assay
Reverse assay
50
100
150
Glycine (mM)

B

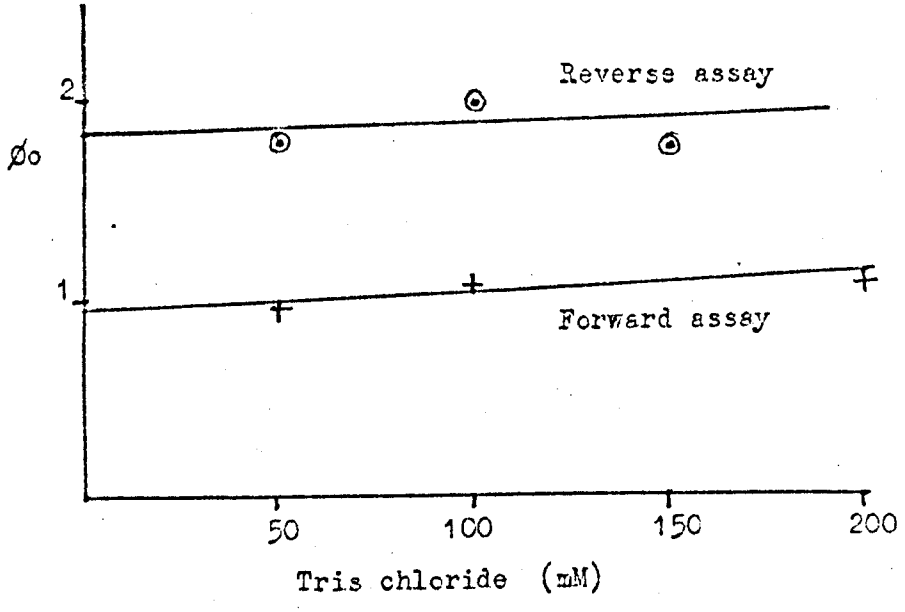
2
1
Øo
Reverse assay
Forward assay
50
100
150
200
Tris chloride (mM)

strength effect.

It is assumed that all buffers acted as specific stoichiometric inhibitors: i.e. $\emptyset \propto I$.

The graphs of $\emptyset_0$ against buffer concentration, (figure 6.3. and 6.4.), gave $\emptyset_0$ at buffer = 0 within 10% of $\emptyset_0$ at buffer = 50 mM, in each case. As can be seen, this correction for buffer effect had a high probable error, hence the parameter used was $\emptyset_0$ at 50 mM buffer.

In some cases it was not feasible to study the substrate and buffer inhibition separately. The following simultaneous equations were used:

$$K_a' = K_a(1 + b/K_b)$$

where K_a' is the apparent inhibition constant for inhibitor A; the concentration of B is b.

Similarly, $K_b' = K_b(1 + a/Ka)$

K_a and K_b are the true inhibition constants.

For the α aminobutyrate and α ketobutyrate parameters, the buffer inhibition constants obtained with L alanine and pyruvate were used.

The fumarate, acetate and TSC results were treated by the method of appendix 4, to give buffer independent inhibition constants.

6.3 RESULTS

These are given in tables 6.2. and 6.3.

TABLE 6.2

The following kinetic constants are given at several pHs, 25°C, $\emptyset_{O(\text{forward assay})}$, $\emptyset_{O(\text{reverse assay})}$, $\emptyset_{O(\text{AB assay})}$, $\emptyset_{O(\text{KB assay})}$, $\emptyset_{ala}$, $\emptyset_{glu}$, $\emptyset_{AB}$, $\emptyset_{pyr}$, $\emptyset_{KG}$, $\emptyset_{KB}$, Km AB, and Km KB.

$\emptyset_{substrate}$ and Km s are expressed in M.

All constants were measured in 50 mM buffer. They are adjusted to give the value at zero buffer concentration, (see text)

The $\log_{10}$ of the adjusted constant is given.

TABLE 6.3

The following kinetic constants, at 25°C in 50 mM buffer, are given for several pHs: the inhibition constants for DL α amino-butyrate, fumarate, acetate, and thiosemicarbazide, using the apparent $\emptyset_{ala}$; the inhibition constant for α ketobutyrate, using the apparent $\emptyset_{pyr}$; and the inhibition constant for fumarate, using the apparent $\emptyset_{KG}$.

The K_i are expressed in M.

These values are adjusted for substrate and buffer inhibition to give the K_i at zero substrate and buffer concentration, (see text).

The $\log_{10}$ of the adjusted K_i are given.

TABLE 6.2.

pH	5.0	5.5	6.0	6.5	7.0	7.5
Øo Forward $\log_{10}$	2.7 .43	1.28 .106	.87 $\bar{1}$.939	.81 $\bar{1}$.908	.87 $\bar{1}$.939	.86 $\bar{1}$.934
Øo Reverse $\log_{10}$	9.8 .99	4.5 .653	2.04 .309		1.78 .250	1.54 .170
Øo AB assay $\log_{10}$	204 2.310	137 2.136	115 2.060	98 1.992		
Øo KB assay $\log_{10}$	167 2.230	74 1.870	43 1.678			
Øala Ki (buffer) corrected $\log_{10}$	1.56 .110 1.07 0.106	.667 .105 .450 $\bar{1}$.652	.110 .165 .086 $\bar{2}$.935	.0975 .137 .071 $\bar{2}$.850	.048 .125 .034 $\bar{2}$.531	.0232 .080 .014 $\bar{2}$.146
Øglu Ki(buffer) corrected $\log_{10}$	.890 .100 .595 $\bar{1}$.774	.610 .080 .370 $\bar{1}$.568	.089 .165 .068 $\bar{2}$.832		.0424 .250 .035 2.534	.018 .068 .0104 $\bar{2}$.013
ØAB Ki (buffer) corrected $\log_{10}$	190 .100 127 2.104	104 .105 70 1.844	30.6 .165 23.5 1.389	25.0 .137 18.3 1.262		
Øpyr Ki (buffer) corrected $\log_{10}$	.0039 high .0039 $\bar{3}$.590	.00318 .171 .00245 $\bar{3}$.389	.0014 .110 .00096 $\bar{4}$.982		.00145 .060 .00079 $\bar{4}$.888	.00050 .034 .00020 $\bar{4}$.300
ØKG Ki (buffer) corrected $\log_{10}$	.0013 high .0013 $\bar{3}$.113	.00076 high .00076 $\bar{4}$.880	.00083 .100 .00055 $\bar{4}$.740	.00089 .0392 .00039 4.590	.00070 .035 .00029 $\bar{4}$.462	.00035 .045 .00015 $\bar{4}$.176
ØKB Ki (buffer) corrected $\log_{10}$	1.60 high 1.60 .204	.98 .171 .76 $\bar{1}$.881	.60 .110 .41 $\bar{1}$.613			
Km AB Ki (buffer) corrected $\log_{10}$	.930 .100 .680 $\bar{1}$.832	.760 .105 .500 $\bar{1}$.700	.266 .165 .204 $\bar{1}$.310	.256 .137 .188 $\bar{1}$.274		
Km KB Ki (buffer) corrected $\log_{10}$	.0096 high .0096 $\bar{3}$.982	.0132 .171 .0102 $\bar{2}$.007	.0125 .110 .0086 $\bar{3}$.934			

TABLE 6.2.(cont)

pH	8.0	8.5	9.0	9.5	10.0	10.5
Øo Forward $\log_{10}$	.96 1.982	.94 1.974	1.30 .113	1.45 .161	2.1 .322	
Øo Reverse $\log_{10}$	1.78 .250		1.60 .203	1.57 .196	2.5 .398	2.4 .380
Øo AB assay $\log_{10}$	105. 2.022	105 2.022	127 2.103	189 2.276	217 2.338	
Øo KB assay $\log_{10}$	42 1.620				40 1.601	39 1.591
Øala Ki (buffer) corrected $\log_{10}$	.0172 .295 .0147 $\bar{2}$.166	.0265 high .026 $\bar{2}$.414	.0374 .334 .033 $\bar{2}$.518	.036 .117 .025 $\bar{2}$.397	.078 .061 .043 $\bar{2}$.632	
Øglu Ki (buffer) corrected $\log_{10}$	.0092 .325 .0080 $\bar{3}$.900		.0126 .330 .0111 $\bar{2}$.045	.0155 .125 .0110 $\bar{2}$.045	.0102 .065 .0059 $\bar{3}$.771	.0147 .140 .0108 $\bar{2}$.032
ØAB Ki (buffer) corrected $\log_{10}$	5.05 .295 4.32 .634	6.60 high 6.60 .820	9.11 .334 7.9 .900	8.3 .117 5.8 .762	9.55 .061 5.3 .722	
Øpyr Ki (buffer) corrected $\log_{10}$	.00057 .220 .00047 $\bar{4}$.671		.00106 .085 .00067 $\bar{4}$.826	.00125 .115 .00086 $\bar{4}$.936	.00265 .031 .00102 $\bar{3}$.008	.0037 .086 .00235 $\bar{3}$.372
ØKC Ki (buffer) corrected $\log_{10}$	.00026 .148 .00019 4.288	.00030 .120 .00021 $\bar{4}$.322	.00033 .117 .00023 $\bar{4}$.361	.00050 .076 .00030 $\bar{4}$.478	.00151 .0334 .00060 $\bar{4}$.778	
ØKB Ki (buffer) corrected $\log_{10}$	.176 .220 .143 1.155				.656 .035 .27 1.432	.78 .086 .49 1.690
Km AB Ki (Buffer) corrected $\log_{10}$	.048 .295 .041 $\bar{2}$.614	.063 high .063 $\bar{2}$.799	.072 .334 .063 $\bar{2}$.799	.044 .117 .031 $\bar{2}$.491	.044 .061 .024 $\bar{2}$.380	
Km KB Ki (buffer) corrected $\log_{10}$	.0042 .220 .0034 $\bar{3}$.534				.0164 .035 .00675 $\bar{3}$.829	.020 .086 .0127 $\bar{2}$.102

TABLE 6.3.

pH	5.0	5.5	6.0	6.5	7.0	7.5
∝AB						
Ki v. ala	high	high	.250	.315	.120	.070
Ki (buffer)			.165	.137	.125	.080
corrected	high	high	.192	.230	.086	.043
$\log_{10}$			$\bar{1}$.283	$\bar{1}$.361	$\bar{2}$.934	$\bar{2}$.634
∝KB						
Ki v. pyr	.0164	.030	.018		.0073	.0060
[glu]	.083	.167	.025			.025
Ki (glu)	.410	.135	.092		high	.073
Ki (buffer)	high	.171	.110		.068	.034
corrected	.0135	.0119	.0099		.0042	.0021
$\log_{10}$	$\bar{2}$.130	$\bar{2}$.075	$\bar{3}$.986		$\bar{3}$.622	$\bar{3}$.322
Fumarate						
Ki v. ala	.103	.073	.038	.042	.0295	.021
corrected	.072	.053	.036	.042	.020	.013
$\log_{10}$	$\bar{2}$.856	$\bar{2}$.724	$\bar{2}$.556	$\bar{2}$.623	$\bar{2}$.301	$\bar{2}$.114
Ki v. KG	.046	.036	.026	.025	.0152	.013
corrected	.046	.035	.024	.020	.013	.0065
$\log_{10}$	$\bar{2}$.663	$\bar{2}$.544	$\bar{2}$.380	$\bar{2}$.301	$\bar{2}$.114	$\bar{3}$.812
Acetate						
Ki v. ala	.082	.077		.173	.268	.130
corrected	.082	.077		.073	.087	.108
$\log_{10}$	$\bar{2}$.914	$\bar{2}$.886		$\bar{2}$.864	$\bar{2}$.940	$\bar{1}$.033
TSC						
Ki v. ala	.00080		.00107		.00097	.00150
corrected	.00080		.00098		.00097	.00145
$\log_{10}$	$\bar{4}$.904		$\bar{4}$.992		$\bar{4}$.986	$\bar{3}$.161

TABLE 6.3. (cont)

pH	8.0	8.5	9.0	9.5	10.0
∝AB					
Ki v. ala	.055	.090	.094	.047	.040
Ki (buffer)	.295	high	.334	.117	.061
corrected	.047	.090	.082	.033	.022
$\log_{10}$	$\bar{2}$.672	$\bar{2}$.952	$\bar{2}$.914	$\bar{2}$.518	$\bar{2}$.342
∝KB					
Ki v. KG	.0035		.0064	.0051	.016
[glu]	.010				
Ki (glu)	.137		high	high	high
Ki (buffer)	.220		.085	.115	.035
corrected	.0027		.0040	.0038	.066
$\log_{10}$	$\bar{3}$.430		$\bar{3}$.602	$\bar{3}$.580	$\bar{2}$.821
Fumarate					
Ki v. ala	.0183	.040	.076	.116	.490
corrected	.017	.040	.066	.090	.200
$\log_{10}$	$\bar{2}$.230	$\bar{2}$.602	$\bar{2}$.820	$\bar{2}$.954	$\bar{1}$.301
Ki v. KG	.0083	.0115	.026	.022	.118
corrected	.0080	.0105	.0128	.0155	.036
$\log_{10}$	$\bar{3}$.903	$\bar{2}$.021	$\bar{2}$.118	$\bar{2}$.190	$\bar{2}$.556
Acetate					
Ki v. ala	.160	.223	.322	.378	1.0
corrected	.134	.204	.254	.233	.5
$\log_{10}$	$\bar{1}$.126	$\bar{1}$.310	$\bar{1}$.404	$\bar{1}$.367	$\bar{1}$.70
TSC					
Ki v. ala	.00277		.00277		.00355
corrected	.00217		.00260		.0029
$\log_{10}$	$\bar{3}$.336		$\bar{3}$.415		$\bar{3}$.462

6.4 THEORY

$$\log K = \log K_0 + \log(1 + H/K_i) - \log(1 + H/K_j)$$

where K is a dissociation constant for a complex

and K_i is a dissociation constant for a proton on the dissociated species

and K_j is a disscciation constant for a proton on the complex

The curve of $\log_{10} K$ against pH can be analysed by the Dixon method (2, 44, 45).

$$\log k = \log\left(\frac{a_i H + B_i K_i}{K_i + H}\right)$$

where k is a rate constant. K_i is the dissociation constant for a proton. This, too is susceptible to a Dixon analysis.

6.5 $\emptyset_0$

$$\emptyset_0 = \emptyset_0^{AA} + \emptyset_0^{KA}$$

where $\emptyset_0^{AA}$ is the constant for the reaction, amino-acid → keto-acid and $\emptyset_0^{KA}$ is the constant for the reaction, keto-acid → amino-acid

Hence $\emptyset_0^{KG} < \emptyset_0$(forward assay)

And $\emptyset_0^{AB} = \emptyset_0$(AB assay) $- \emptyset_0^{KG}$

$$\therefore \quad \emptyset_0(\text{AB assay}) > \emptyset_0^{AB} > \emptyset_0(\text{AB assay}) - \emptyset_0(\text{Forward assay})$$

As the first and last terms are almost equal at every pH,

$$\emptyset_0(\text{AB assay}) \doteq \emptyset_0^{AB}$$

Similarly, $\emptyset_0(\text{KB assay}) \doteq \emptyset_0^{KB}$

Figure 6.5. shows that the $\emptyset_0$ for the forward and reverse assays could be obtained by combining two $\emptyset_0$ curves of the same shapes as those seen in the ketobutyrate and aminobutyrate assays. Hence it is reasonable to suppose that the pH dependence of $\emptyset_0^{AB}$ is

FIGURE 6.5

Graphs of $\emptyset_0$ against pH for four different assays.

A forward assay

B reverse assay

C aminobutyrate assay

D ketobutyrate assay

FIGURE 6.6

Graphs of $\log_{10} \emptyset_0$ against pH. The straight lines are those used in the Dixon analysis of the pKs.

⊙ from the aminobutyrate assay

+ from the ketobutyrate assay

FIGURE 6.7

Graphs of $\log_{10} \emptyset_{\text{amino-acid}}$ against pH. The straight lines are those used in the Dixon analysis of the pKs.

+ $\emptyset_{AB}$

⊕ $\emptyset_{AB}$ calculated from $K_{i\ AB}$

$\emptyset_{ala}$

$\emptyset_{glu}$

FIGURE 6.5.

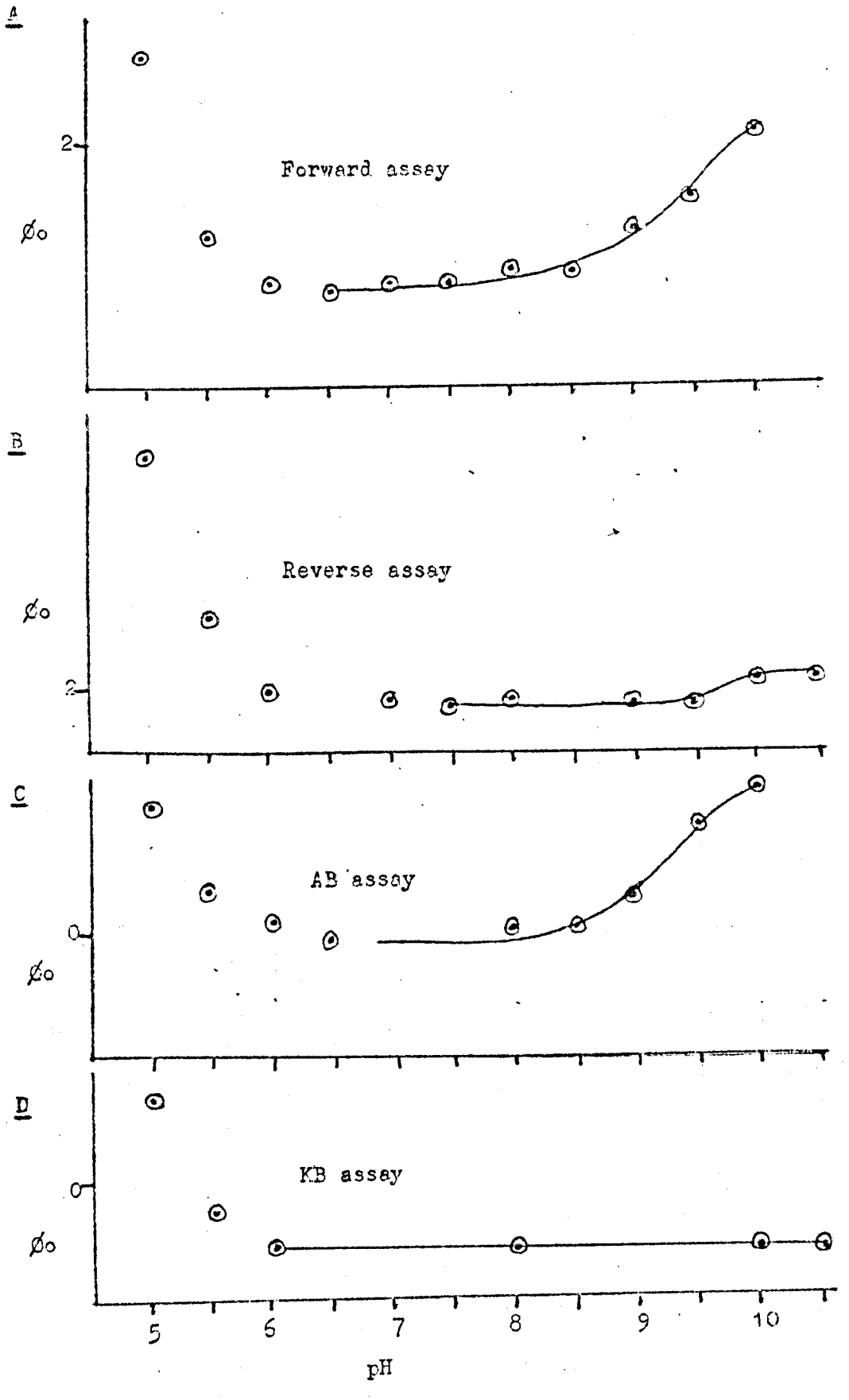
A
2
Forward assay
Øo
B
Reverse assay
Øo
2
C
AB assay
0
Øo
D
KB assay
0
Øo
5
6
7
8
9
10
pH

FIGURE 6.6.

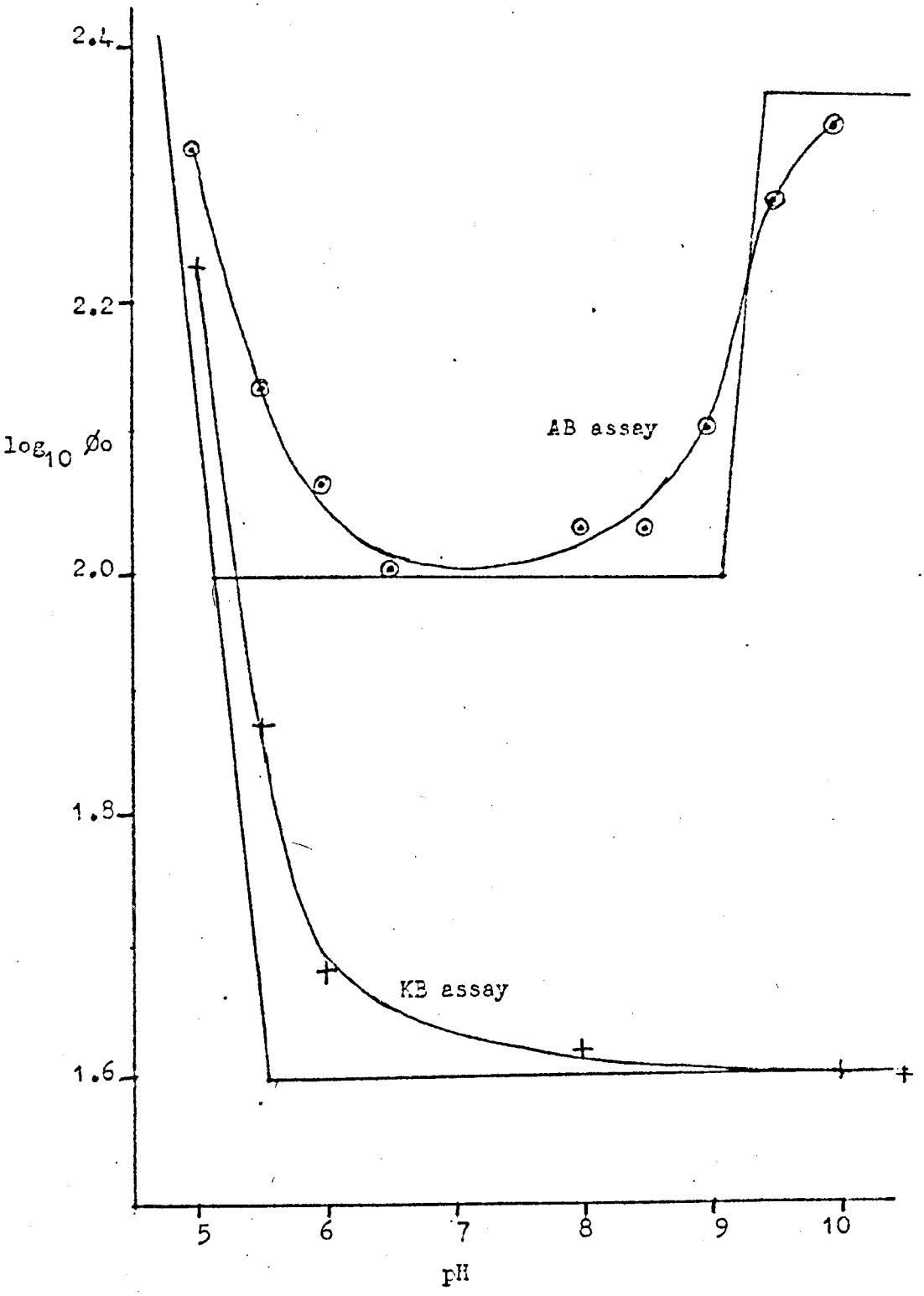

FIGURE 6.7.

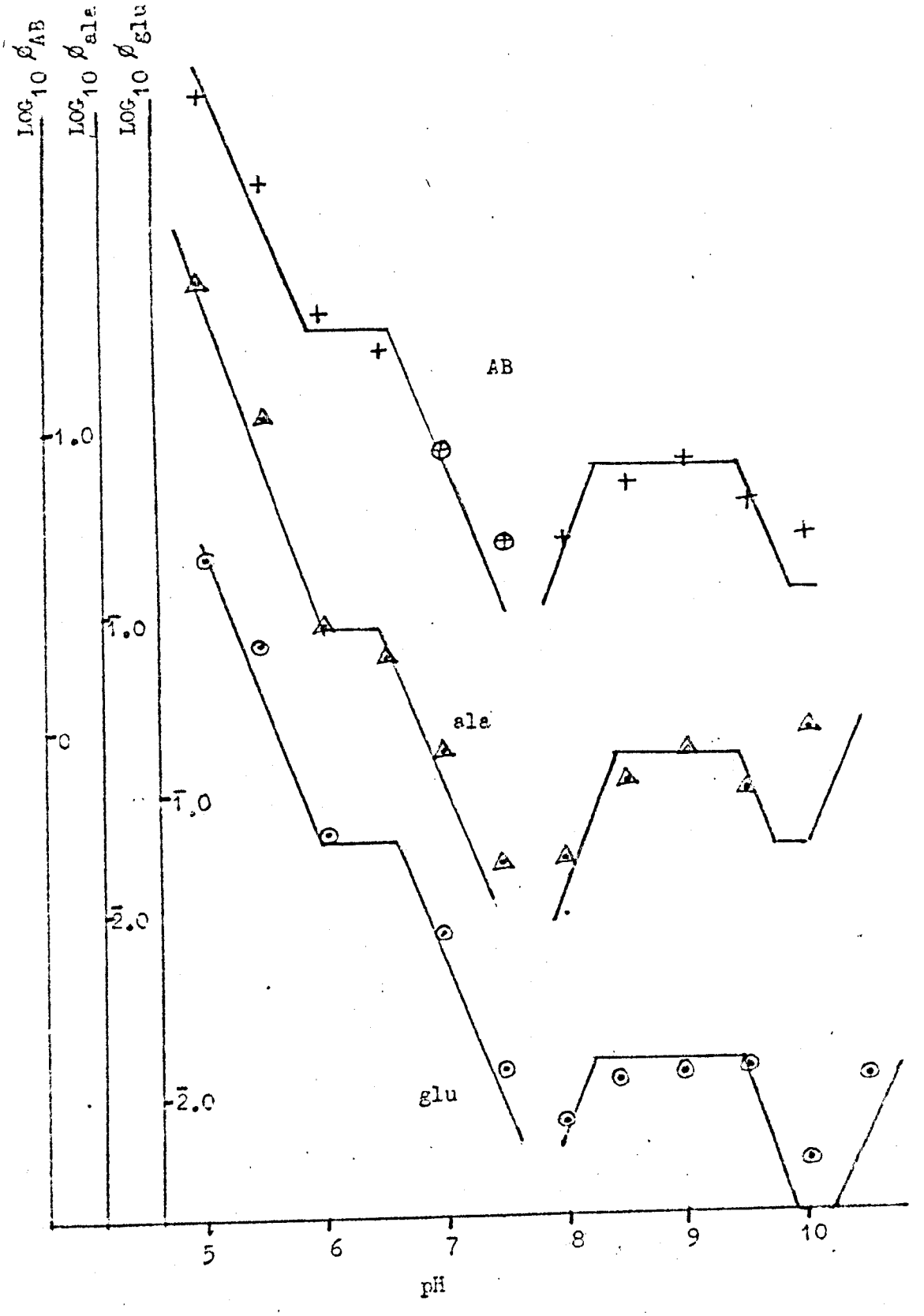
$\log_{10} \phi_{AB}$
$\log_{10} \phi_{ala}$
$\log_{10} \phi_{glu}$
1.0
0
$\bar{1}.0$
$\bar{1}.0$
$\bar{2}.0$
$\bar{2}.0$
AB
ala
glu
5
6
7
8
9
10
pH

FIGURE 6.8

Graphs of $\log_{10} \phi_{\text{keto-acid}}$ against pH. The straight lines are those used in the Dixon analysis of the pKs.

+ ϕ_{KB}

⊕ ϕ_{KB} calculated from $K_{i\ KB}$, assuming that $\phi_{O(KB\ assay)}$ is pH independent above pH 7.0.

△ ϕ_{pyr}

⊙ ϕ_{KG}

FIGURE 6.9

A graph of $\log_{10} K_{AB}$ against pH. The straight lines are those used in the Dixon analysis.

⊙ K is the Michaelis constant for ∝ aminobutyrate

△ K is the inhibition constant for ∝ aminobutyrate, (against L alanine).

FIGURE 6.10

A graph of $\log_{10} K_{KB}$ against pH. The straight lines are those used in the Dixon analysis.

⊙ K is the Michaelis constant for ∝ ketobutyrate

△ K is the inhibition constant for ∝ ketobutyrate, (against pyruvate).

FIGURE 6.8.

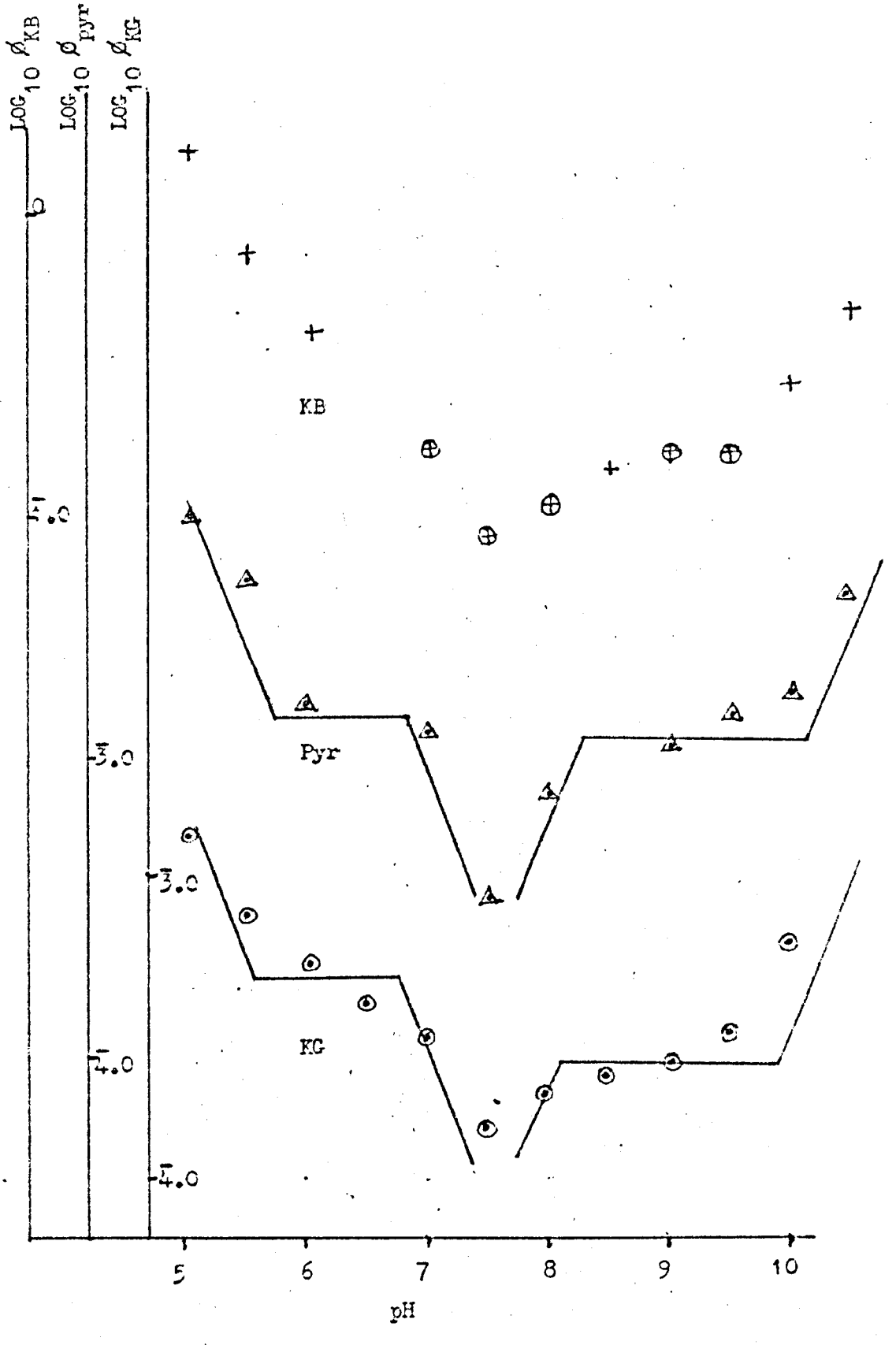
$LOG_{10}\ \phi_{KB}$
$LOG_{10}\ \phi_{pyr}$
$LOG_{10}\ \phi_{KG}$
KB
Pyr
KG
-3.0
-3.0
-4.0
-4.0
5
6
7
8
9
10
pH

FIGURE 6.9.

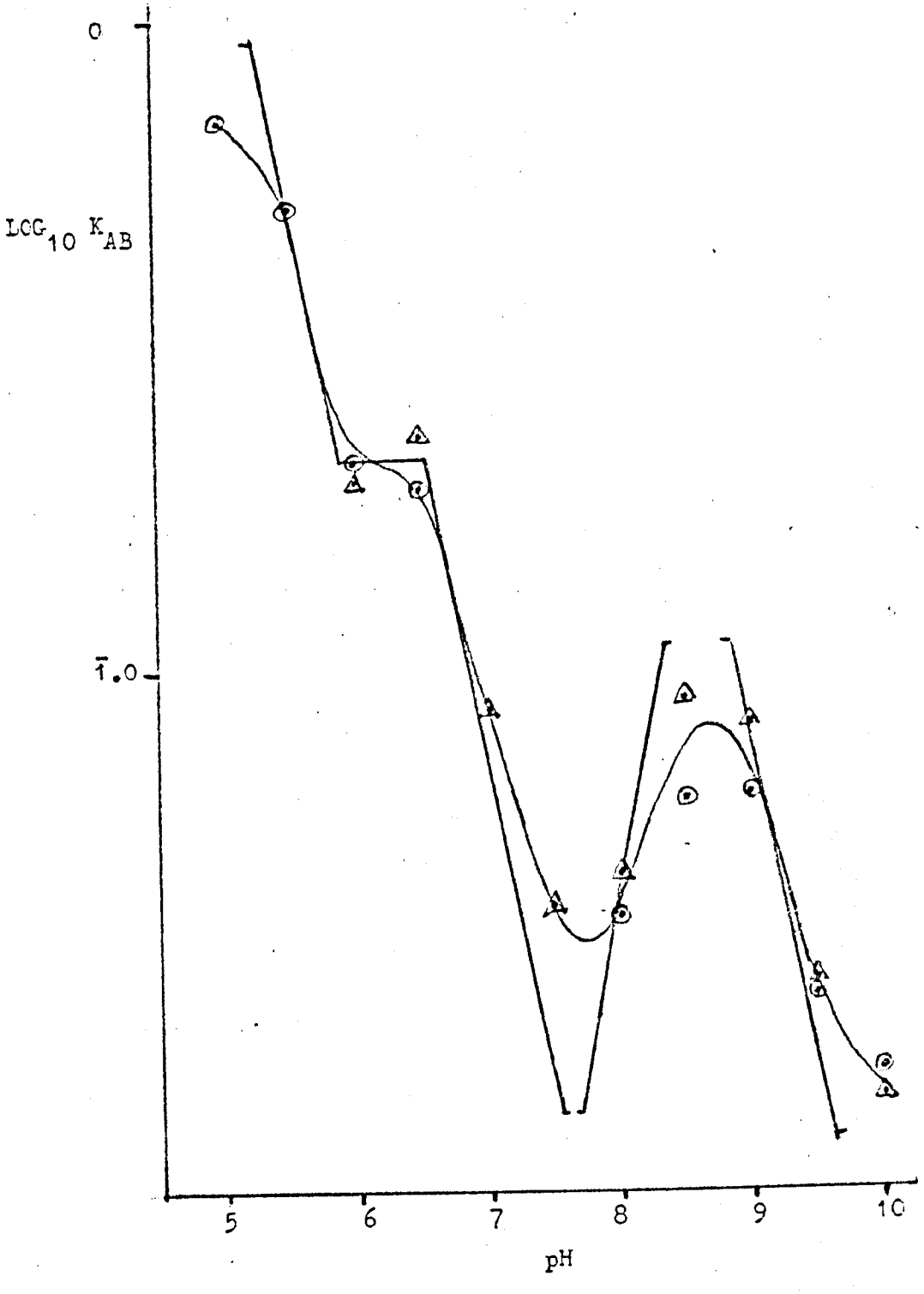

FIGURE 6.10.

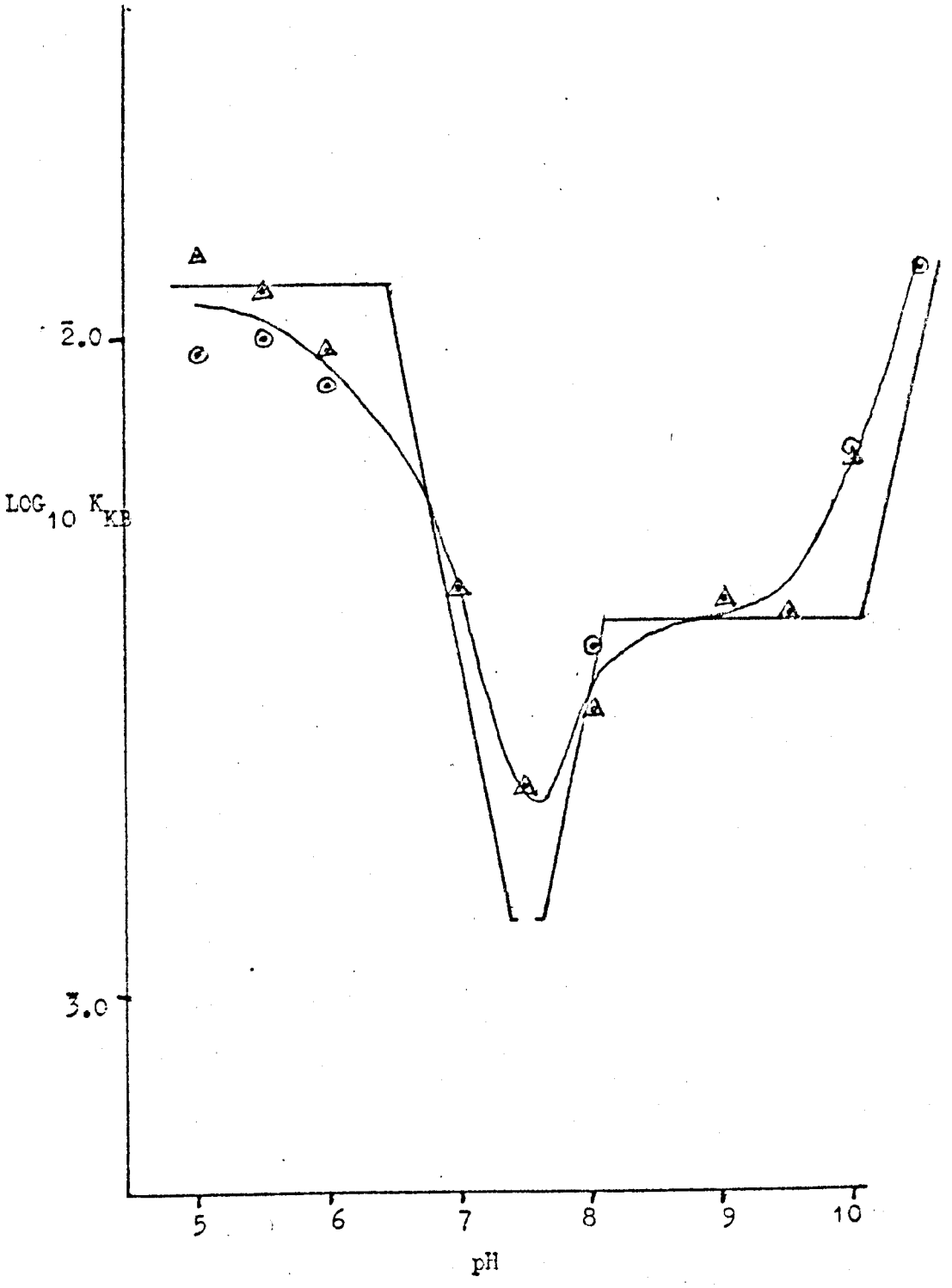

representative of ϕ_0^{AA} and ϕ_0^{KB} is representative of ϕ_0^{KA}.

Figure 6.6. indicates that ϕ_0^{KB} has one kinetically significant pK at a low pH; that ϕ_0^{AB} shows one pK at a low pH and one at a high pH. The low pK can be analysed by the method of Dixon: it was at pH 5.6 for ϕ_0^{KB}, and pH 5.2 for ϕ_0^{AB}.

The high pK was at about pH 9.2.

6.6 SUBSTRATE BINDING

Figures 6.7. and 6.8. show the variation of log ϕ_1 and log ϕ_2 with pH. The ∝ aminobutyrate and ∝ ketobutyrate results are similar to those for the normal substrates.

Figure 6.9. gives the Dixon analysis of the K_m and K_i of ∝ aminobutyrate. These parameters are comparable at every pH tested; i.e. $K_m = K_i$. This shows that when it inhibits, ∝ aminobutyrate binds in the same way as it does for transamination (and D ∝ aminobutyrate contributes little to inhibition). Also, the K_m equals the binding constant. This is the quasi-equilibrium situation.

The analysis shows at least four pKs in PL-ala AT, with ∝ aminobutyrate, (pH ~5.9, ~7.5, ~7.5 and ~10), and at least four in the enzyme-substrate complex, (pH ~5.4, ~6.5, ~8, and ~9). Where one form of the enzyme has two pKs within one pH unit of each other, analysis is imprecise.

Figure 6.10. gives the Dixon anelysis of K_m and K_i for ∝ ketobutyrate. The two parameters are very similar at all pHs. Hence, $K_m = K_i$, and K_m is the binding constant for ∝ ketobutyrate.

Analysis shows at least three pKs in PM-ala AT with ∝ ketobutyrate, (pH ~7.5, ~7.5, and ~10), and at least two in the enzyme-substrate complex, (pH ~6.5, and ~8).

FIGURE 6.11

Graphs of $\log_{10}$(inhibition constant) against pH, for fumarate The straight lines are those used for the Dixon analysis of pKs.

△ from inhibition of L alanine binding

⊙ from inhibition of ∝ ketoglutarate binding

FIGURE 6.12

A graph of $\log_{10}$(inhibition constant) against pH, for acetate inhibition of L alanine binding. The straight lines are those used for the Dixon analysis of pKs.

FIGURE 6.13

A graph of $\log_{10}$(inhibition constant) against pH, for TSC inhibition of L alanine binding. The straight lines are those used for the Dixon analysis of pKs.

TABLE 6.4

Each pK observed in the free enzymes is close to pH 5.8, pH 7.5, or pH 10.0. Each pK observed in the enzyme-substrate and enzyme-inhibitor complexes is close to pH 5.3, pH 6.6, pH 8.3, pH 9.0, or is greater than pH 10.0.

The table records, for each inhibitor, which categories of pK are seen to affect the binding of that inhibitor to ala AT.

FIGURE 6.11.

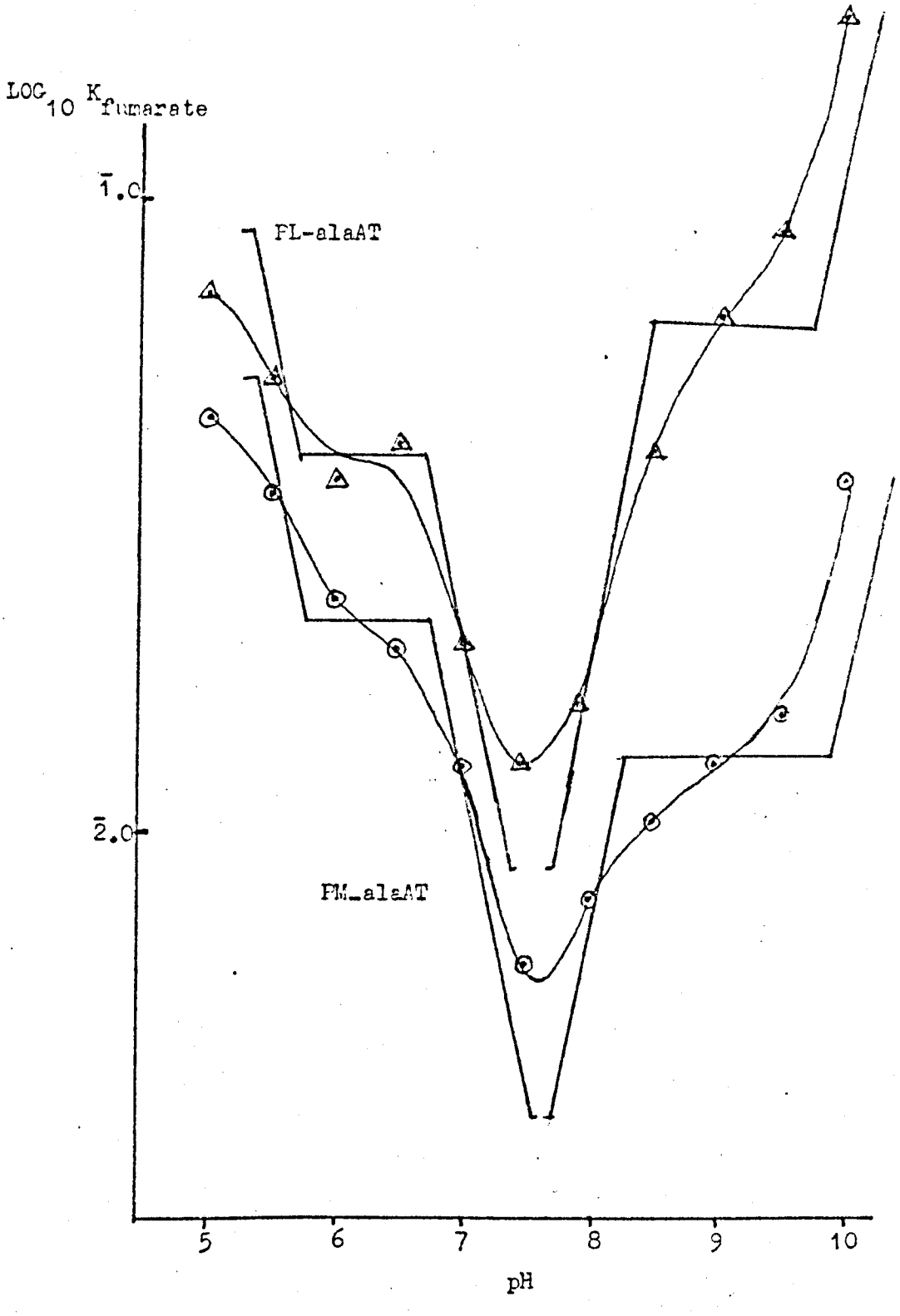

FIGURE 6.12.

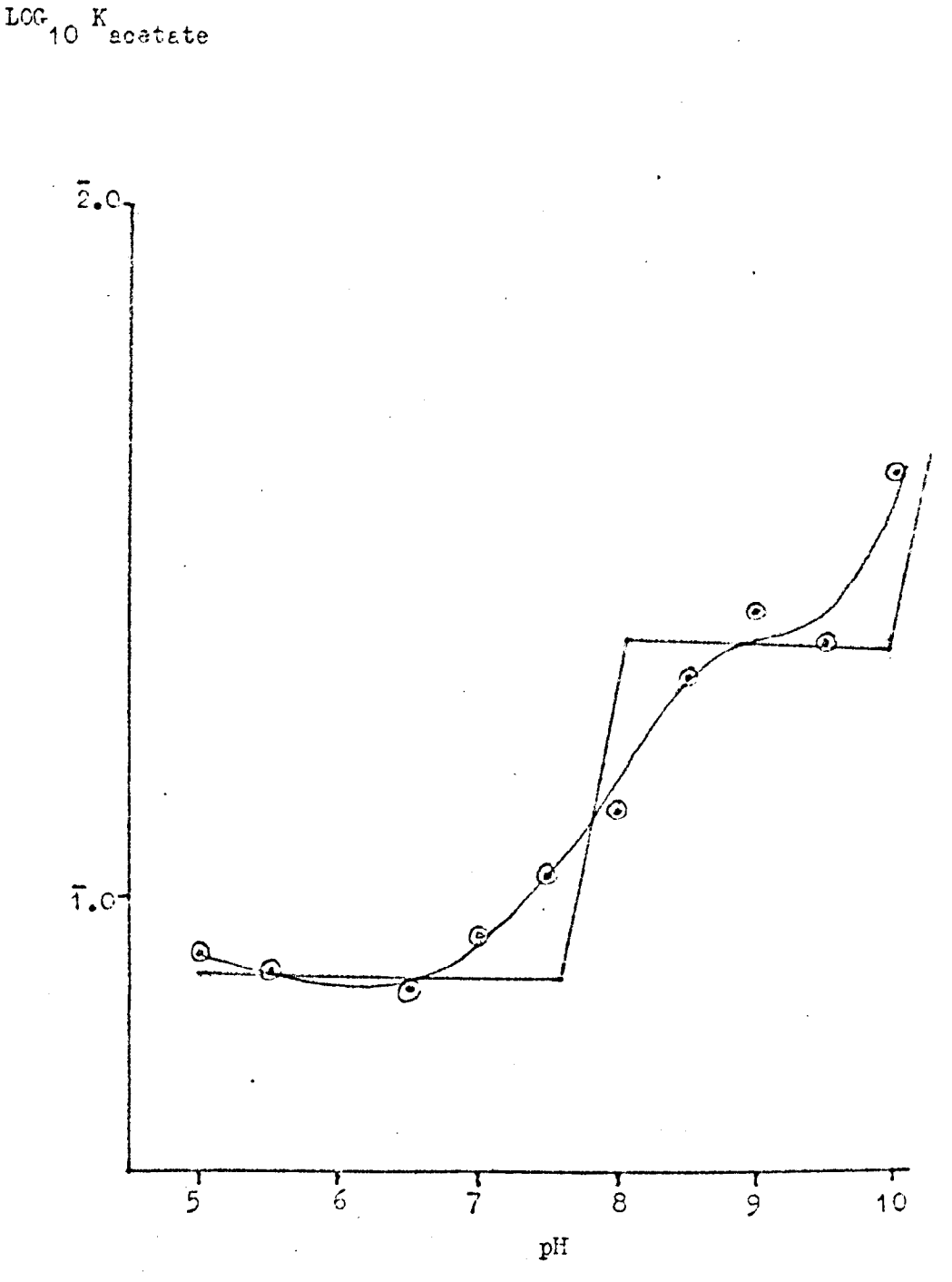

FIGURE 6.13.

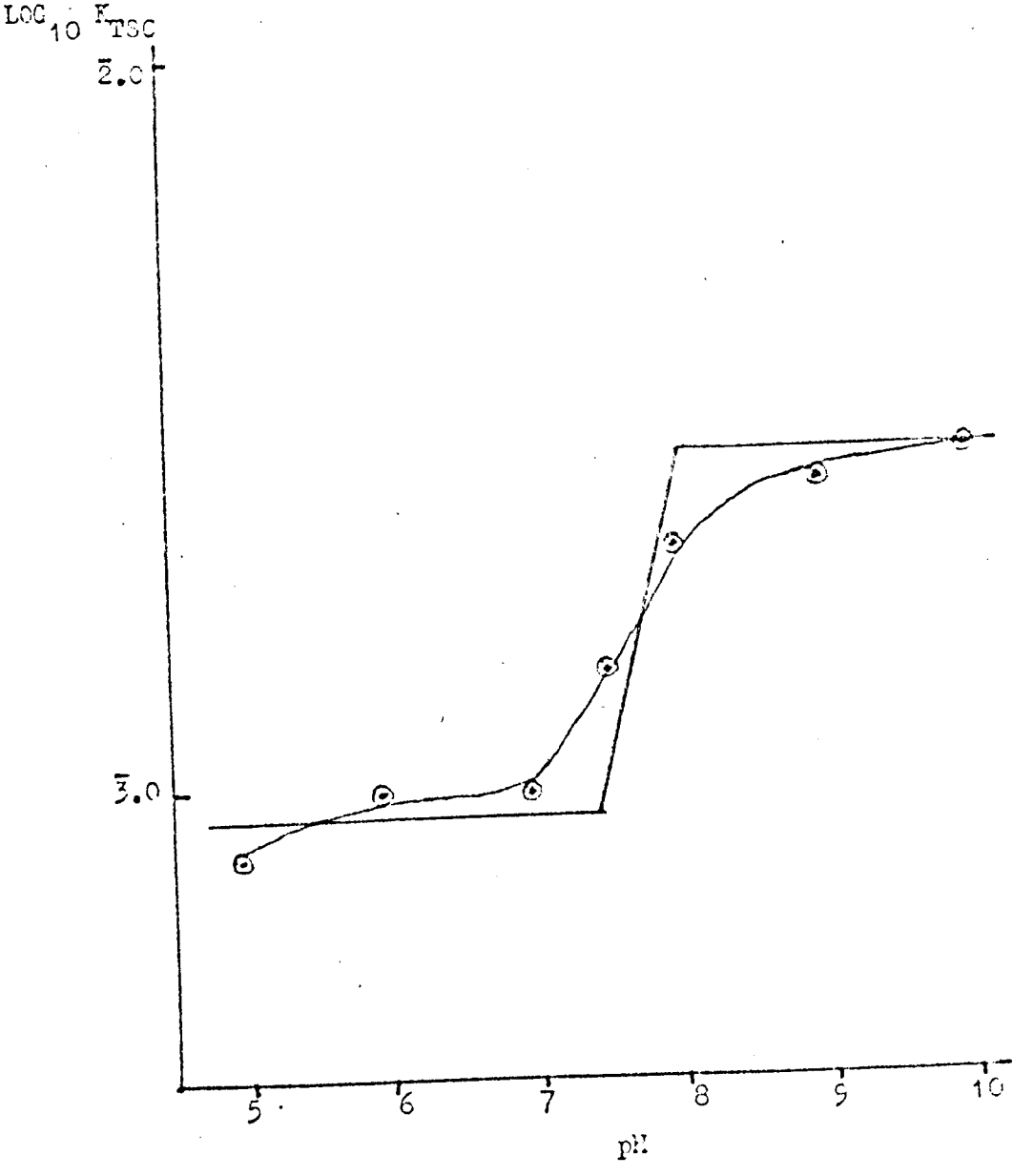

TABLE 6.4.

	pK (free alaAT)				pK (complex)				
Inhibitor	5.8	~7.5	~7.5	10.0	5.3	6.6	8.3	~9	>10
∝ Aminobutyrate	✓	✓	✓	✓	✓	✓	✓	✓	
∝ Ketobutyrate		✓	✓	✓		✓	✓		✓
Fumarate (PL form)	✓	✓	✓	✓	✓	✓	✓		✓
Fumarate (FM form)	✓	✓	✓	✓	✓	✓	✓		✓
Acetate		✓		✓			✓		✓
Thiosemicarbazide		✓					✓		

6.7 INHIBITOR BINDING

Figure 6.11. gives the Dixon analysis for fumarate inhibition The PL-ala AT shows at least four pKs, (pH ~5.7, ~7.5, ~7.5 and 10). The enzyme-inhibitor complex shows at least three pKs, (pH ~5.3, ~6.7 and ~8.5). The PM-ala AT shows at least four pKs, at (pH ~5.8, ~7.5, ~7.5, and ~10). The PM-ala AT-fumarate complex shows at least three pKs, (pH ~5.4, ~6.7, and ~8).

Figure 6.12. gives the analysis of acetate inhibition. PL-ala AT shows at least two pKs, (pH 7.6, and ~10). The enzyme-acetate complex shows at least one pK, (pH 8.1).

Figure 6.13. gives the analysis of TSC inhibition. The PL-ala AT shows at least one pK, (pH 7.5).

6.8 AN INITIAL INTERPRETATION

The most striking result is the similarity of the two fumarate pH profiles, indicating that there is not a great deal of difference between the active sites of the PM and PL forms.

The simplest rationalisation assumes that similar pKs belong to similar groups: only four different ionisable groups are strictly necessary to fit the kinetic data of table 6.4., giving five different effects.

	Enzyme		Complex
1)	pK 5.6 - 5.9	⟶	pK 5.2 - 5.4
2)	pK ~ 7.5	⟶	pK 6.5 - 6.7
3)	pK ~ 7.5	⟶	pK 8.1 - 8.5
4)	pK 9.8 - 10.2	⟶	pK $\rangle$ 10
5)	pK ~ 9.8	⟶	pK ~ 9

The results of this chapter are discussed fully in chapter 8.

CHAPTER 7

VISIBLE SPECTRA AT PH 8.0

7.1 EXPERIMENTS

The visible absorption spectra obtained with ala AT are given in figure 7.1.

TSC, fumarate and acetate were each titrated against PL-ala-AT.

L alanine was titrated against ala AT, at high pyruvate concentration.

L glutamate was titrated against ala AT at a high ∝ketoglutarate concentration.

DL ∝aminobutyrate was titrated against ala AT at a high ∝ketobutyrate concentration.

In each case, the spectra were adjusted for changes in volume and the binding constant was determined from a double reciprocal plot, as described in appendix 5. It is simplest to use the absorbance at a particular wavelength; however, any linear combination of absorbances is equally valid. The parameter introduced in appendix 2 is insensitive to slight shifts in the spectral base-line, which did occur. The parameter used was $2 \times A_{430} - A_{470} - A_{390}$, (called p_{430}). The binding constant was used to obtain the absorbance at any wavelength, for the complex.

7.2 RESULTS

The PM-alaAT spectrum showed a peak at about 330 nm. The

FIGURE 7.1

The absorption spectrum of ala AT, (.90)mg/ml), in 5 mM ME, 5 mM EDTA and 50 mM pH 8.0 trisbuffer. The enzyme is in the pyridoxamine or pyridoxal form, as indicated.

FIGURE 7.2

A The absorption spectra of ala AT, (.90 mg/ml), in 5 mM ME, 5 mM EDTA and 50 mM pH 8.0 tris buffer. The enzyme is in the pyridoxal form; for one spectrum, 5.95 mM TSC has been added.

B The TSC titration with PL-ala AT.
A graph of $(\Delta A_{390})^{-1}$ against $(TSC)^{-1}$.

FIGURE 7.3

A The absorption spectra of ala AT, (.90 mg/ml), in 5 mM ME 5 mM EDTA and 50 mM pH 8.0 tris buffer. The enzyme is in the pyridoxal form; for one spectrum, 192 mM acetate has been added.

B The TSC titration with PL-ala AT.
A graph of $(\Delta p_{430})^{-1}$ against $(acetate)^{-1}$.

FIGURE 7.4

A The absorption spectra of ala AT, (.90 mg/ml), in 5 mM ME, 5 mM EDTA and 50 mM pH 8.0 tris buffer. The enzyme is in the pyridoxal form; for one spectrum, 62.5 mM fumarate has been added.

B The fumarate titration with PL-ala AT.
A graph of $(\Delta p_{430})^{-1}$ against $(fumarate)^{-1}$.

FIGURE 7.1.

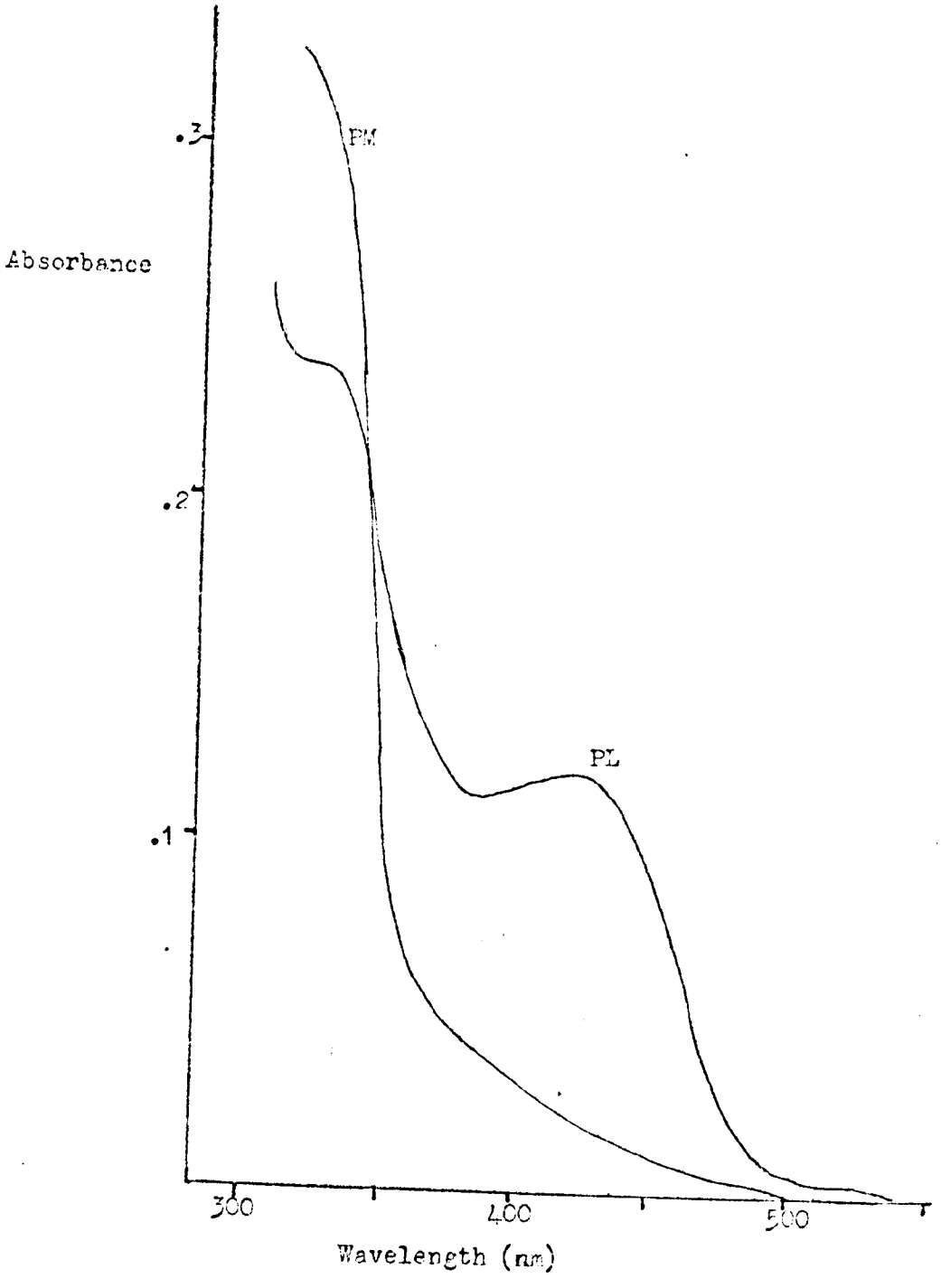

FIGURE 7.2.

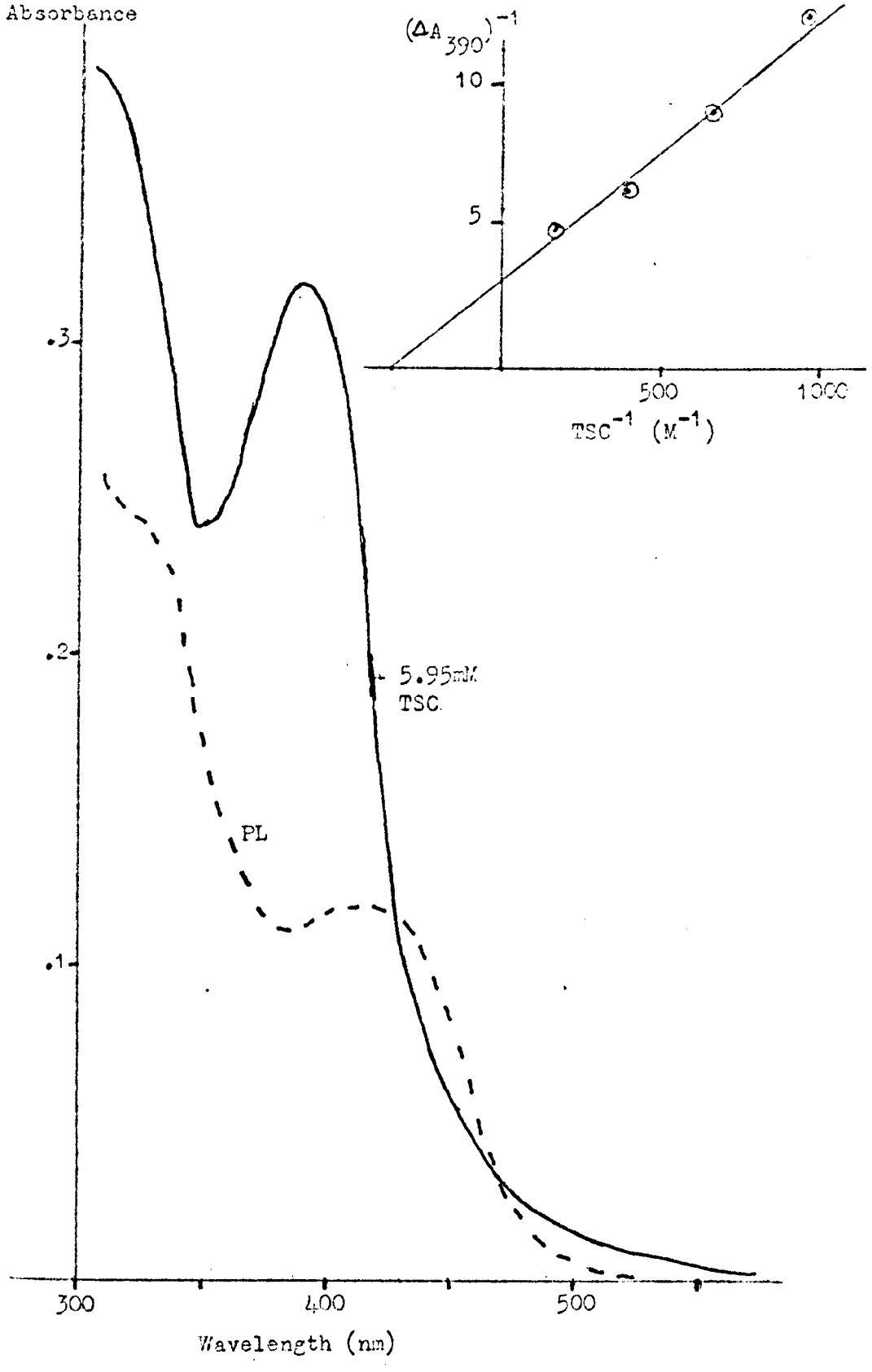
Absorbance
.3
.2
.1
300
400
500
Wavelength (nm)
5.95mM
TSC
PL
$(\Delta A_{390})^{-1}$
10
5
500
1000
TSC^{-1} (M^{-1})

FIGURE 7.3.

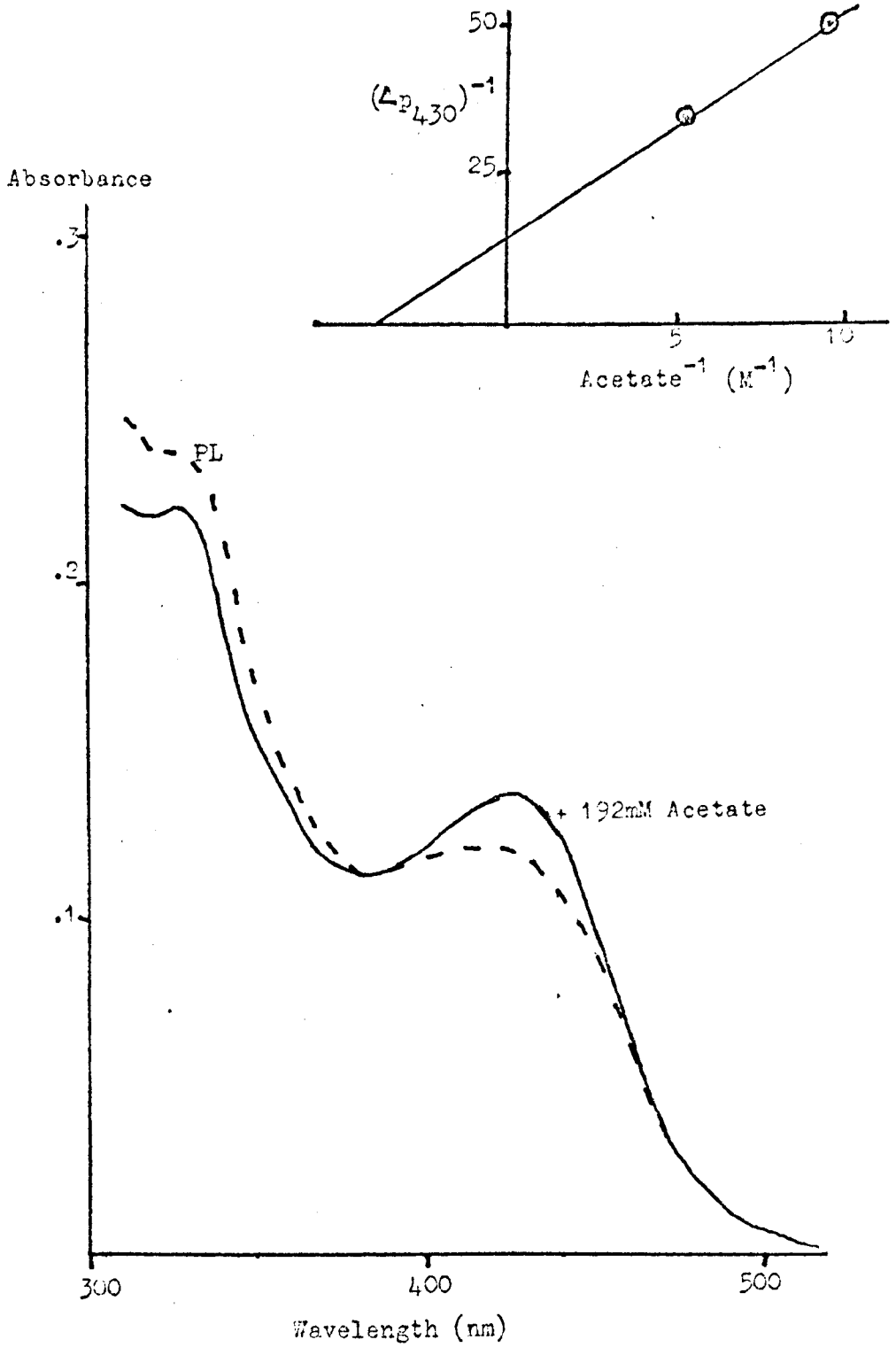
50
$(\Delta P_{430})^{-1}$
25
5
10
Acetate^{-1} (M^{-1})
Absorbance
.3
.2
.1
PL
+ 192mM Acetate
300
400
500
Wavelength (nm)

FIGURE 7.4.

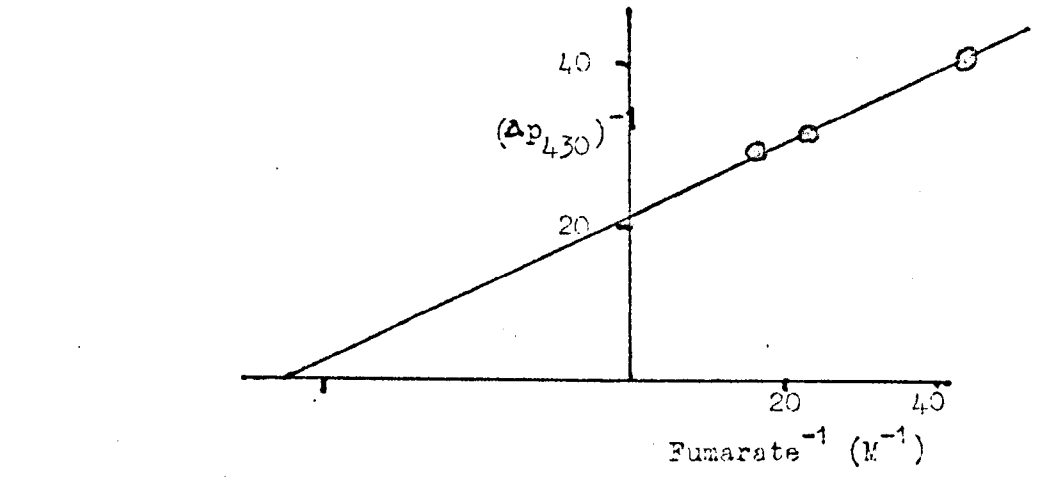
40
$(\Delta p_{430})^{-1}$
20
20
40
Fumarate^{-1} (M^{-1})

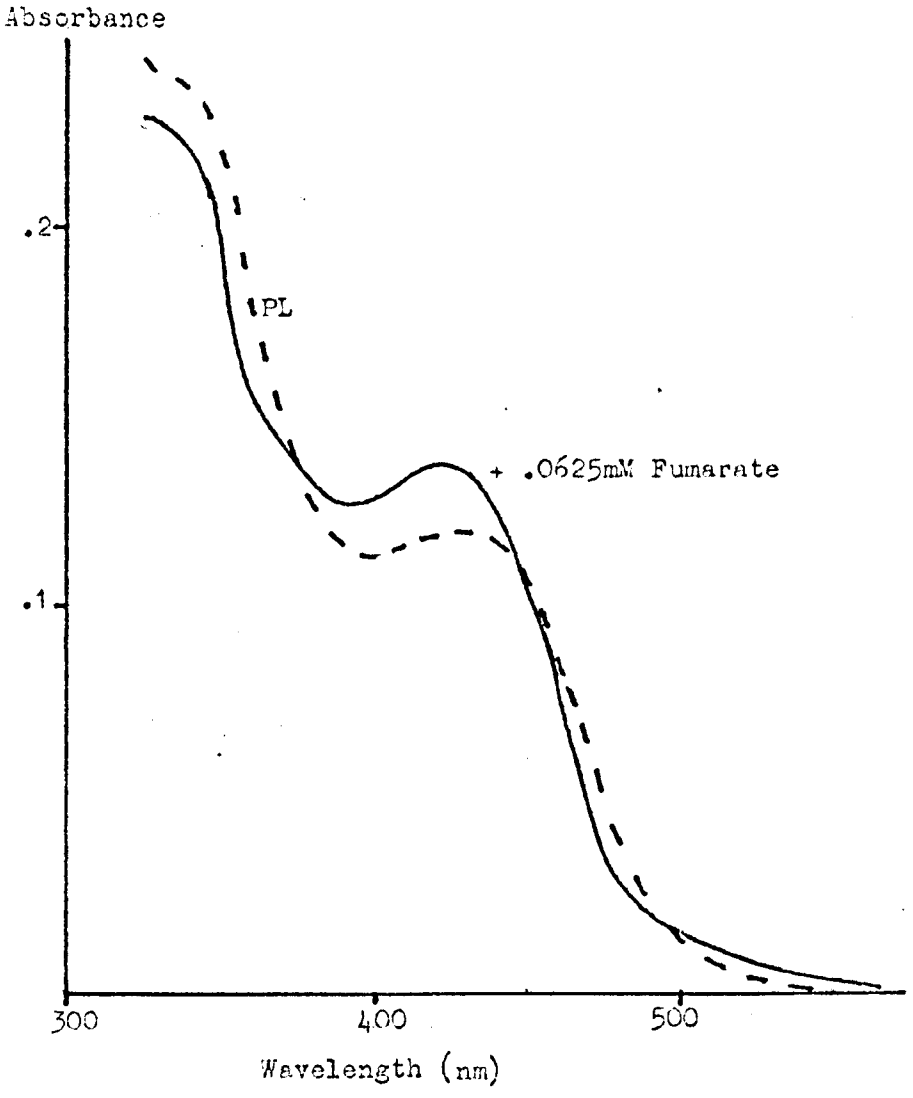
Absorbance
.2
.1
PL
+ .0625mM Fumarate
300
400
500
Wavelength (nm)

FIGURE 7.5

A The absorption spectra of ala AT, (.90 mg/ml), in 5 mM ME, 5 mM EDTA and 50 mM pH 8.0 tris buffer and 5 mM pyruvate. For one spectrum, 65 mM L alanine has been added.

B The L alanine titration with ala AT plus pyruvate.

A graph of $(\Delta A_{490})^{-1}$ against (L alanine)$^{-1}$. N.B. The intercept on the (L alanine)$^{-1}$ axis, was first determined from the graph of $(p_{430})^{-1}$ against (L alanine)$^{-1}$, as shown.

FIGURE 7.6

A The absorption spectra of ala AT, (.90 mg/ml), in 5 mM ME, 5 mM EDTA and 50 mM pH 8.0 tris buffer and 12.5 mM ∝ ketoglutarate. For one spectrum, 86 mM L glutamate has been added.

B The L glutamate titration with ala AT, plus ∝ ketoglutarate.

A graph of $(\Delta A_{490})^{-1}$ against (L glutamate)$^{-1}$. N.B. The intercept on the (L glutamate)$^{-1}$ axis, was first determined from the graph of $(p_{430})^{-1}$ against (L alanine)$^{-1}$, as shown.

FIGURE 7.7

A The absorption spectra of ala AT, (.90 mg/ml), in 5 mM ME, 5 mM EDTA and 50 mM pH 8.0 tris buffer and 11 mM ∝ ketobutyrate. For one spectrum, 250 mM DL ∝ aminobutyrate has been added.

B The DL ∝ aminobutyrate titration, with ala AT, plus ∝ ketobutyrate.

A graph of $(\Delta p_{430})^{-1}$ against (DL ∝ aminobutyrate)$^{-1}$.

FIGURE 7.5.

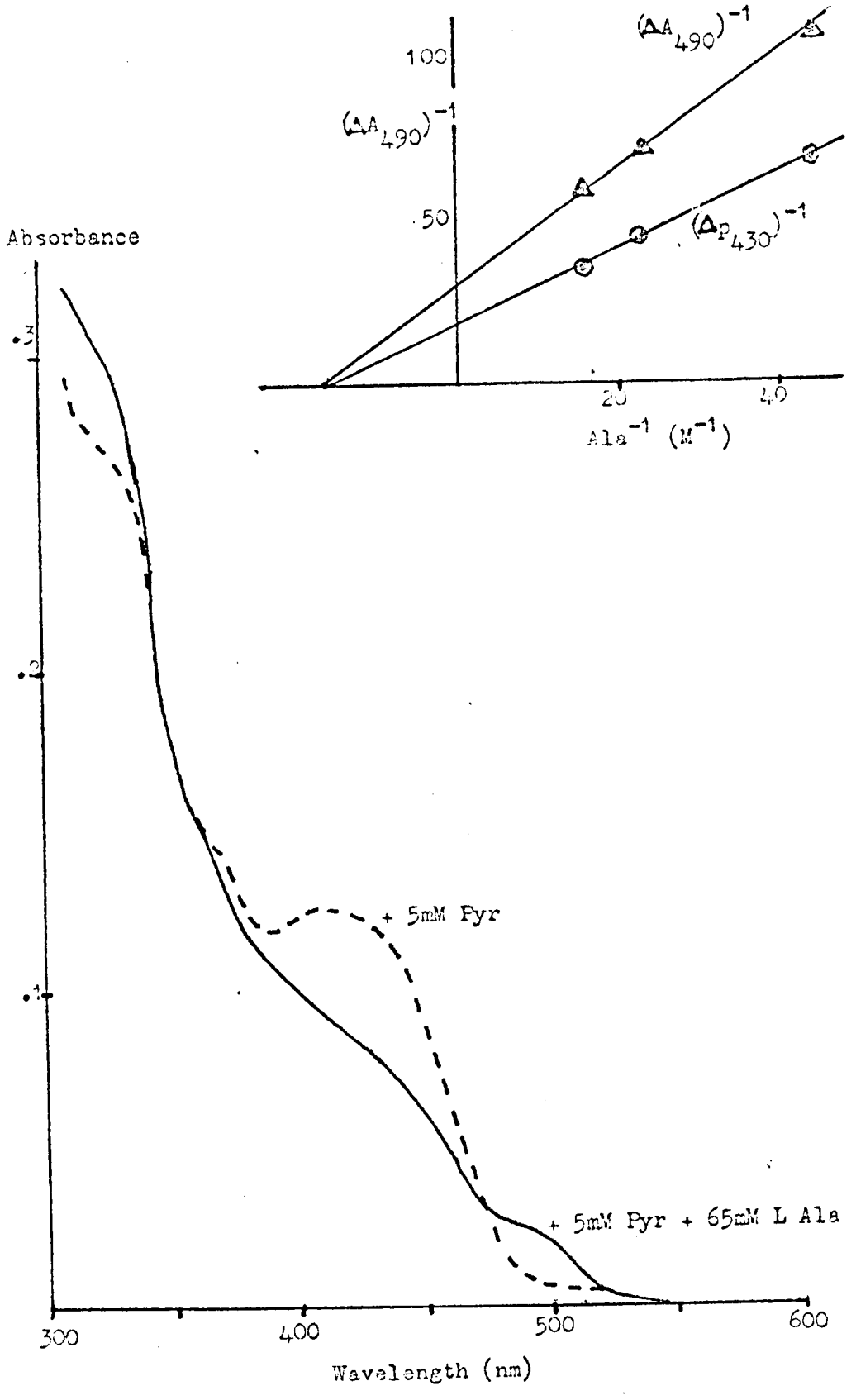
100
$(\Delta A_{490})^{-1}$
$(\Delta A_{490})^{-1}$
50
$(\Delta P_{430})^{-1}$
20
40
Ala^{-1} (M^{-1})
Absorbance
.3
.2
.1
+ 5mM Pyr
+ 5mM Pyr + 65mM L Ala
300
400
500
600
Wavelength (nm)

FIGURE 7.6.

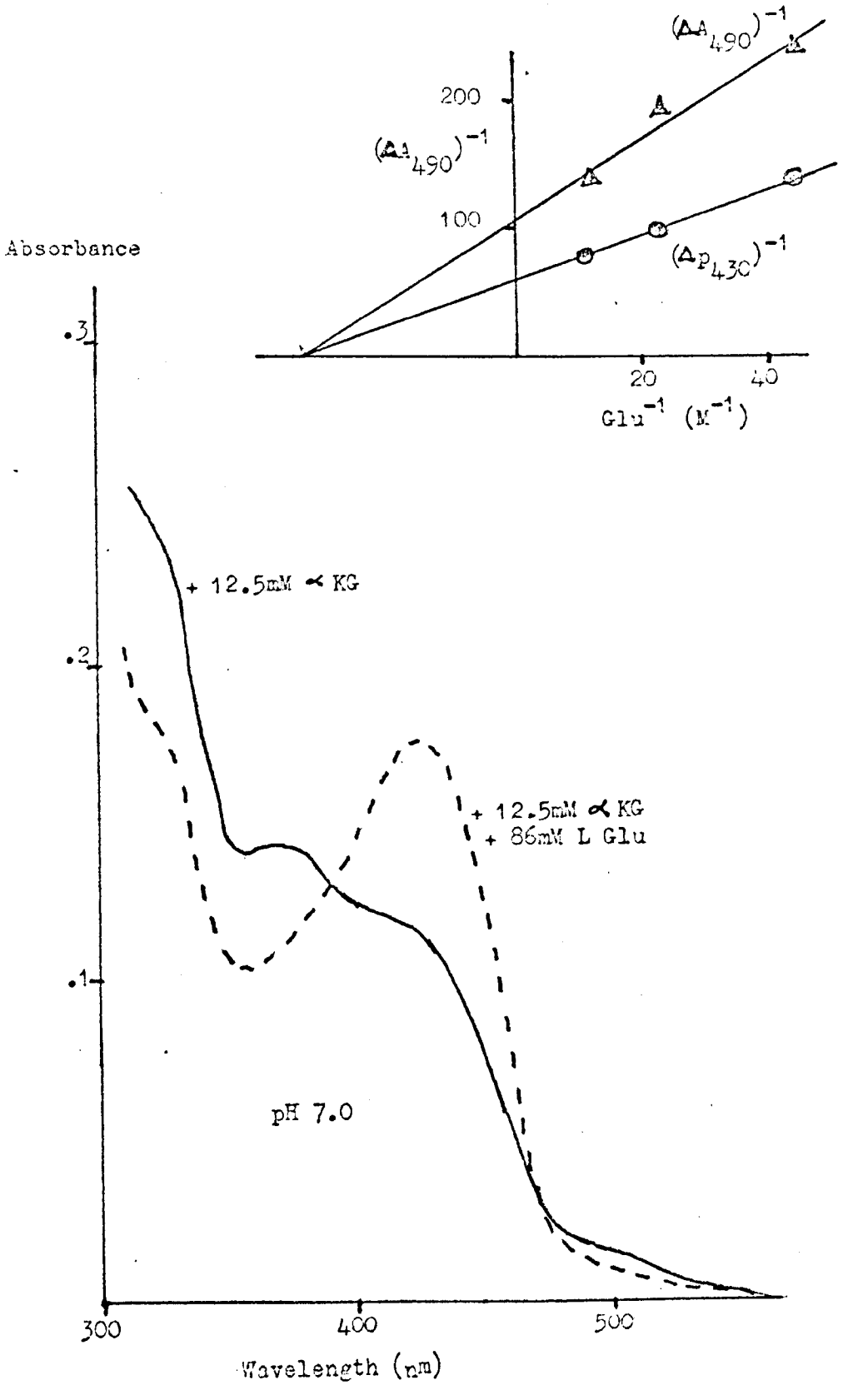
$(\Delta A_{490})^{-1}$
200
$(\Delta A_{490})^{-1}$
100
$(\Delta P_{430})^{-1}$
20
40
Glu^{-1} (M^{-1})
Absorbance
.3
.2
.1
+ 12.5mM ∝ KG
+ 12.5mM ∝ KG
+ 86mM L Glu
pH 7.0
300
400
500
Wavelength (nm)

FIGURE 7.7.

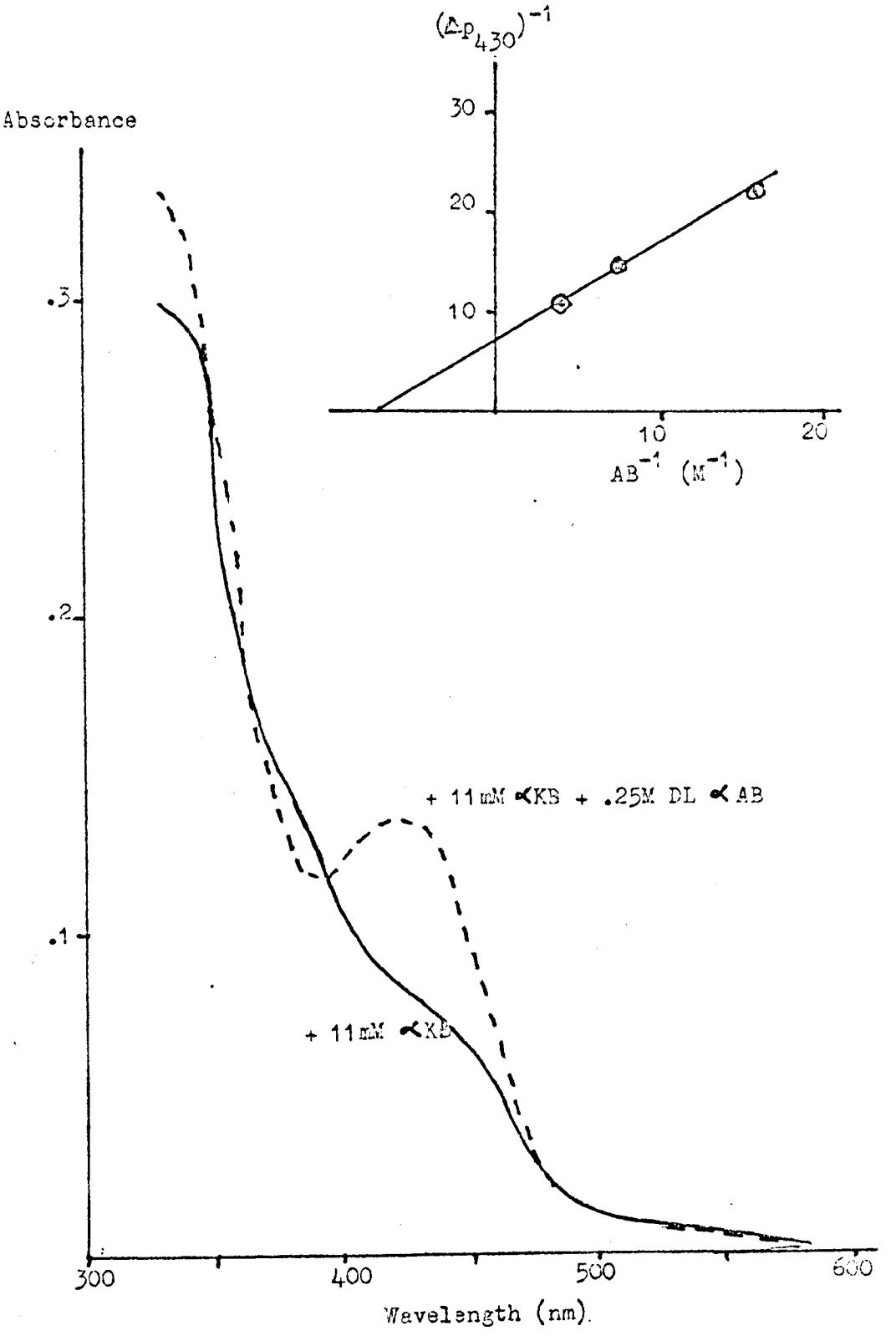
$(\Delta P_{430})^{-1}$
30
20
10
10
20
AB^{-1} (M^{-1})
Absorbance
.3
.2
.1
+ 11 mM ∝KB + .25M DL ∝AB
+ 11 mM ∝KB
300
400
500
600
Wavelength (nm).

PL-ala AT spectrum showed peaks at 330 and 430 nm, (see figure 7.1). Both gave the same spectrum at 25 mM and 50 mM buffer.

On the addition of TSC to PL-ala AT, (see figure 7.2.), the peak moved to 390 nm which is the λ_{max} of the TSC complex in asp AT and is close to the 380 nm peak obtained with other carbonyl reagents in rat liver ala AT. The spectral dissociation constant was 2.8 mM, equal to the inhibition constant.

The addition of fumarate or acetate increased the absorbance of the 430 nm peak, (see figure 7.3 and 7.4). The significance of this and the binding constants are discussed in chapter 8.

Addition of L alanine to PM-ala AT gave no detectable change in the spectrum.

Addition of 10 mM pyruvate to PL-ala AT gave a small increase in the absorbance at wavelengths below 400 nm, (figure 7.5).

When L alanine was added to ala AT with 5 or 10 mM pyruvate, the 330 nm peak increased slightly, the 430 nm peak largely disappeared and a new peak at 490 nm appeared, (figure 7.5). This can be explained in part by a decrease in the aldimine and an increase in the ketimine content of the enzyme. Jenkins, who first observed the peak at 490 nm (99, 100) considered that it was probably due to a deprotonated ,reaction intermediate. These changes are not due to the formation of a PM- ala AT-L alanine complex, or a PL-ala AT-pyruvate complex.

L glutamate plus α ketoglutarate gave a similar result, with a smaller 490 nm peak, (figure 7.6). With α aminobutyrate plus α ketobutyrate the 490 nm peak was small or absent, (figure 7.7).

The long wavelength of the 490 nm peak suggests strongly that it is due to an intermediate with a more extensive conjugated

system than is found in pyridoxamine or pyridoxal imines. If the αcarbon of the aldimine were deprotonated, the resulting compound would be a highly conjugated system (154, 163). The N methyl derivative of this compound has been prepared by Schirch and Slotter (173) and has a λ_{max} at 490 nm. This makes it almost certain that the species absorbing at 490 nm is a deprotonated form. N.B. A similar peak has been observed with serine transhydroxymethylase (169).

Figure 7.8 is the bare outline of a mechanism in which the five distinct forms of the enzyme, (PM form, PL form, substrate aldimine, substrate ketimine, and A_{490} species), are shown with their probable structures. The tautomerisation step has been studied in non-enzymic systems (7, 8, 12, 27, 28, 134, 173, 187) and catalysis by imidazole has been observed (8, 27, 28, 187).

The high resonance energy of the fully conjugated structure, (10 kcals greater than in the aldimine) (154), makes it certain that any deprotonated form will show this extensive conjugation and will absorb at long wavelengths. As will be shown in the next chapter, only one distinct peak is seen at long wavelengths, at any pH - so A_{490} is a measure of the total concentration of deprotonated forms.

FIGURE 7.8

A simple four-step model of alanine aminotransferase, activity, showing some of the chemical changes that occur during catalysis.

FIGURE 7.8.

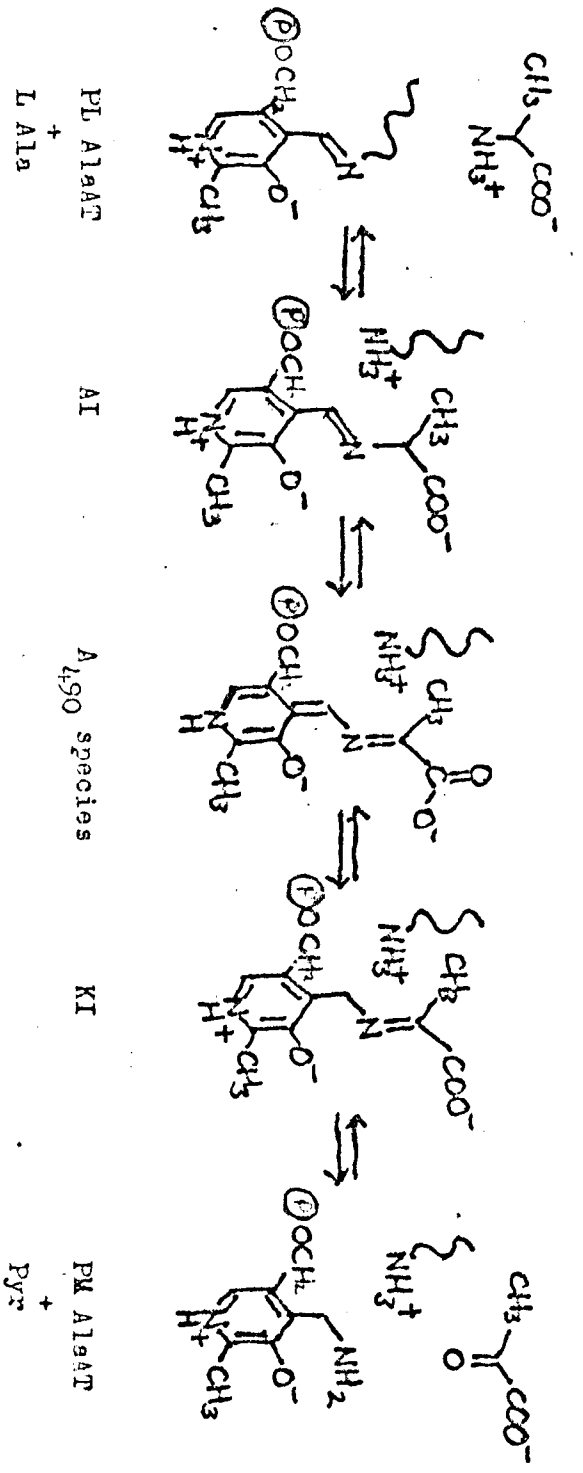

CHAPTER 8

ABSORPTION SPECTRA AT VARIOUS PH S AND DISCUSSION ON THE PH DEPENDENCE OF SPECTRAL AND KINETIC PARAMETERS

SPECTRA

8.1 EXPERIMENT

About half of the experiments of chapter 7 were repeated at other pHs. They were the PL-ala AT spectrum, alone and with fumarate or acetate; and the ala AT spectrum plus pyruvate and L alanine.

8.2 RESULTS

8.2(a) PL-Ala AT

The PL-ala AT spectrum was pH dependent. There were two forms, (figure 8.1), with a simple pK at pH 7.6, (see figure 8.2), as compared to a pK of 7.4 obtained by Saier and Jenkins (170).

At each pH, the spectrum was the same in 25 mM and 50 mM buffer. The spectrum at pH 7.5 was the same in 50 mM phosphate or 50 mM tris chloride. The spectrum in tris chloride was repeated in 25 mM, 100 mM and 150 mM buffer. There was no significant change in the spectrum.

The difference between the pK given here and that of Saier and Jenkins may be due to the very high ionic strength of the buffer, (0.4 M phosphate), that they used. For asp AT, the

FIGURE 8.1

The absorption spectrum of PL-ala AT, (.90 mg/ml), in 5 mM ME, 5 mM EDTA and 50 mM buffer. The buffer is pH 5.5 acetate or pH 10 .0 glycine, as indicated.

FIGURE 8.2

The absorption spectrum of PL-ala AT, (.90 mg/ml), in 5 mM ME, 5 mM EDTA and 50 mM buffer.

A graph of p_{430}, $(2\,A_{430} - A_{390} - A_{470})$, against pH.

FIGURE 8.3

The absorption spectrum of PL-ala AT, (.90 mg/ml), in 5 mM ME, 5 mM EDTA and 50 mM buffer.

A graph of p_{430}, (i.e. $2\,A_{430} - A_{390} - A_{470}$), against pH.

— PL-ala AT

△ PL-ala AT - fumarate complex

⊙ PL-ala AT - acetate complex

TABLE 8.1

The table compares the inhibition constant (for L alanine binding), with the spectral dissociation constant, at various pHs.

Results are given for fumarate or acetate with PL ala AT, at 25°C, in 50 mM buffer.

FIGURE 8.1.

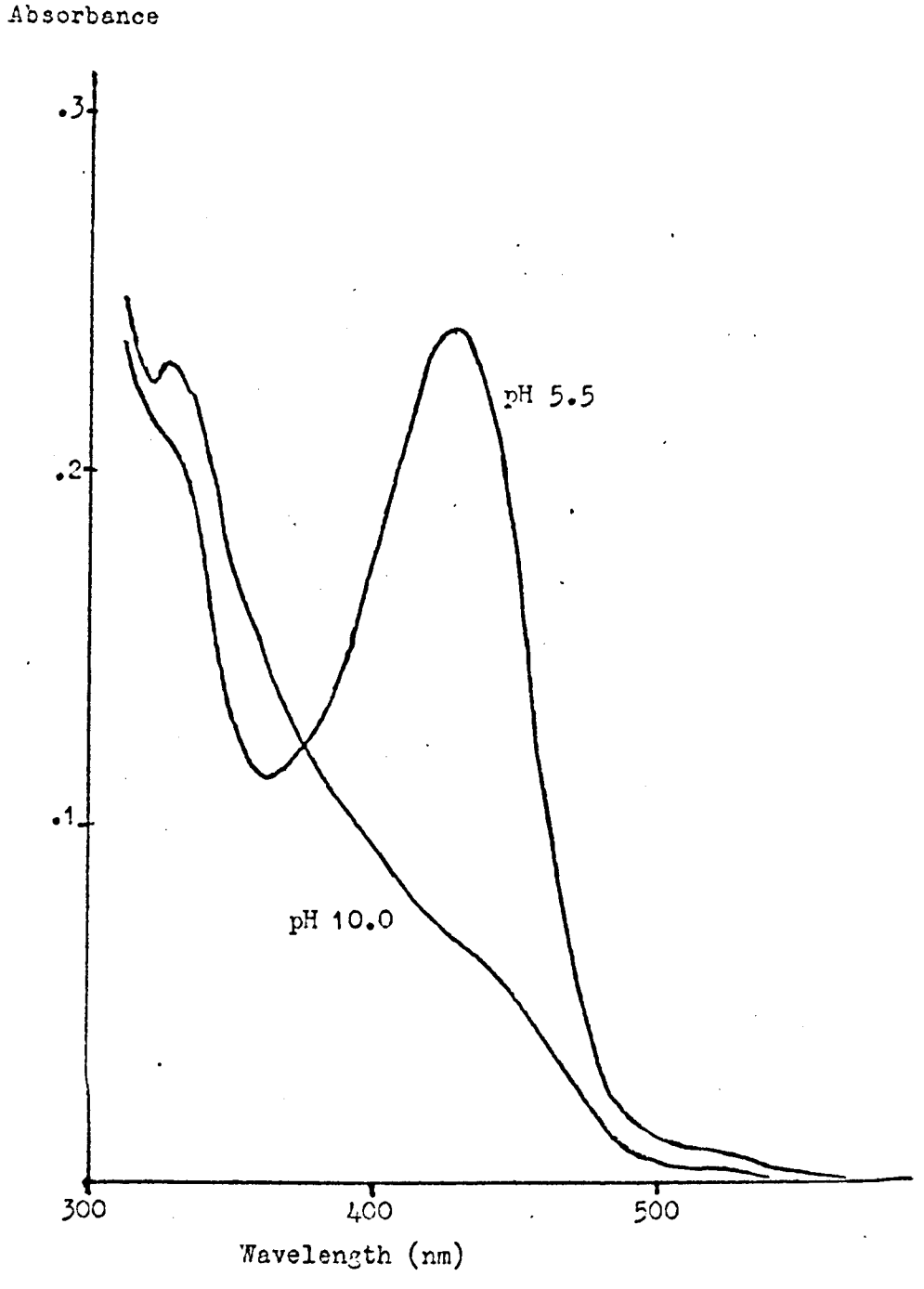

FIGURE 8.2.

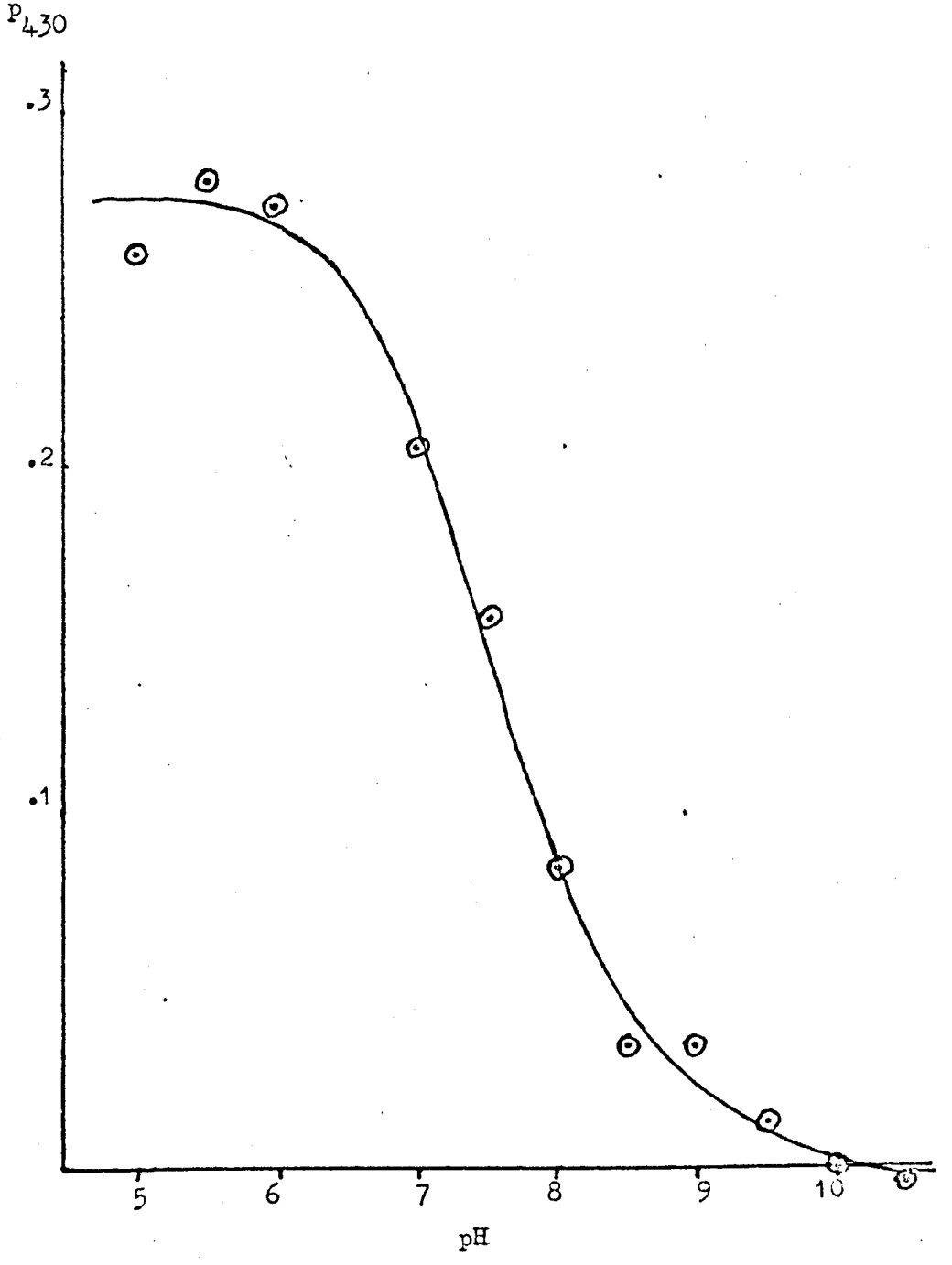

FIGURE 8.3.

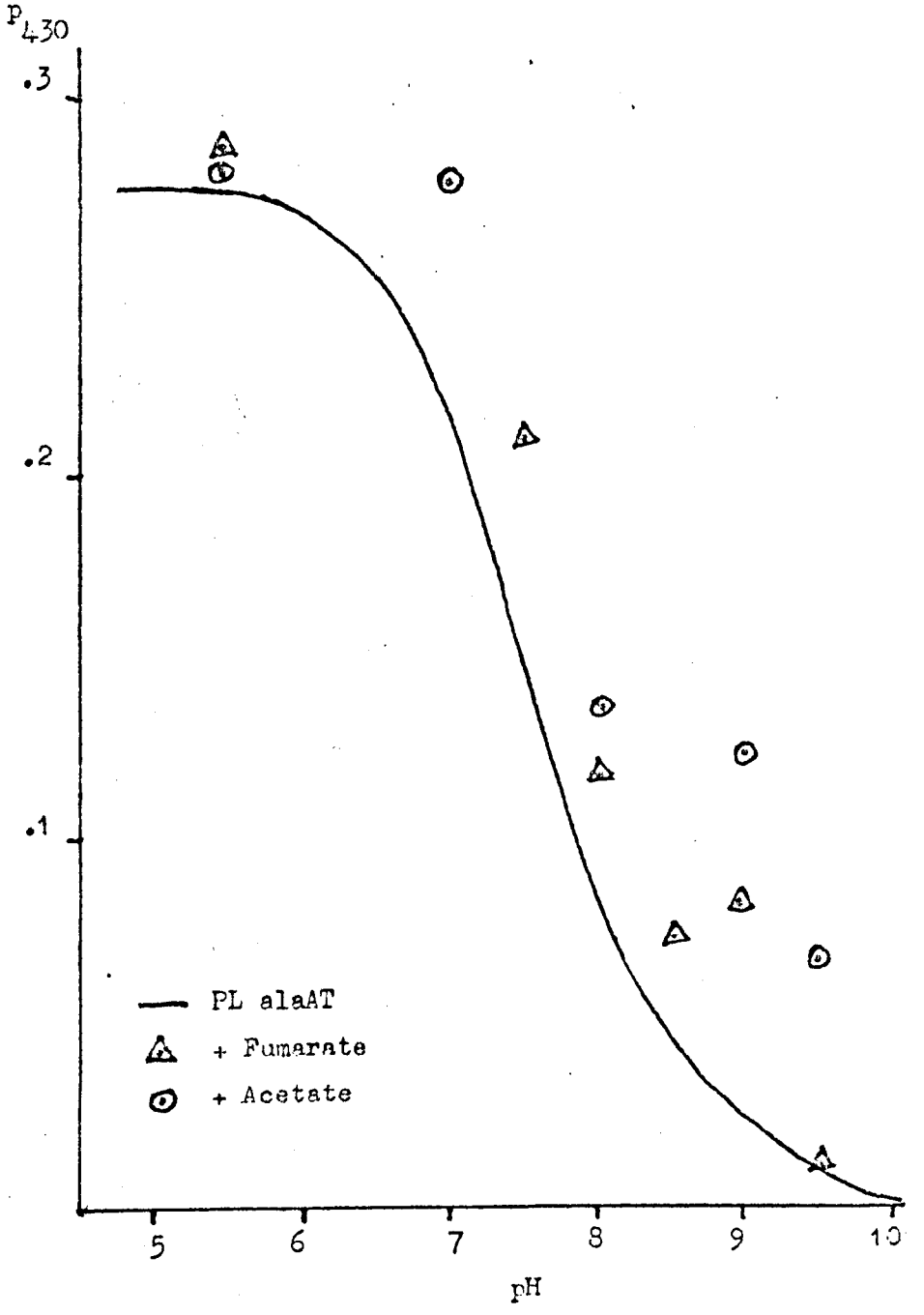

TABLE 8.1.

pH		7.0	7.5	8.0	8.5	9.0	9.5
FUMARATE	K_i v. ala		.021	.018	.040	.076	
	$K_{spectral}$		.032	.022	.087	.087	
ACETATE	K_i v. ala	.27		.16		.32	.38
	$K_{spectral}$	.26		.25		.33	.4

spectral pK is very sensitive to the nature of the buffer (30).

8.2(b) Fumarate

Figure 8.3 shows that the rise in A_{430}, when fumarate binds to PL-ala AT, is due simply to the spectral pK being raised to about pH 8.0. The dissociation constants were only obtainable at pH 7 - 9. They are significantly greater then those obtained from inhibition experiments, but show the same pH dependence, (table 8.1). It seems that most, but not all of the fumarate inhibition, is due to that type of binding which raises the spectral pK.

8.2(c) Acetate

Acetate had the same effect on the PL-ala AT spectrum as did fumarate, (figure 8.3). The dissociation constants were high and were obtained with only two points - however, they agreed quite well with those obtained in the inhibition studies, (table 8.1).

8.2(d) Pyruvate and L Alanine

The theory and calculation of the spectrum of the equilibrium enzyme complex with pyruvate and L alanine is given in appendix 5. These spectra, (at pH 5.5, 7.0, 9.0 and 10.5), are given in figures 8.4 to 8.7. Some significant parameters are given in table 8.2 and are plotted in figures 8.8. and 8.9.

At each pH, the pyruvate concentration was many times greater than $\emptyset_{pyr}$. At each pH, two different pyruvate concentrations were used, but the differences in A_{490} and p_{490} were small. The pyruvate was in excess.

FIGURE 8.4

The absorption spectrum of .90 mg/ml of the equilibrium ala AT-substrate complex, in 50 mM pH 5.5 acetate buffer.

The substrates were L alanine and pyruvate, at 25°C, in 5 mM ME and 5 mM EDTA.

△ using 13 mM pyruvate

⊙ using 40 mM pyruvate

FIGURE 8.5

The absorption spectrum of .90 mg/ml of the equilibrium ala AT-substrate complex, in 50 mM pH 7.0 phosphate buffer.

The substrates were L alanine and pyruvate, at 25°C, in 5 mM ME and 5 mM EDTA.

△ using 7 mM pyruvate

⊙ using 20 mM pyruvate

FIGURE 8.6

The absorption spectrum of .90 mg/ml of the equilibrium ala AT-substrate complex, in 50 mM pH 9.0 glycine buffer.

The substrates were L alanine and pyruvate, at 25°C, in 5 mM ME and 5 mM EDTA.

⊙ using 7 mM pyruvate

△ using 20 mM pyruvate

FIGURE 8.4.

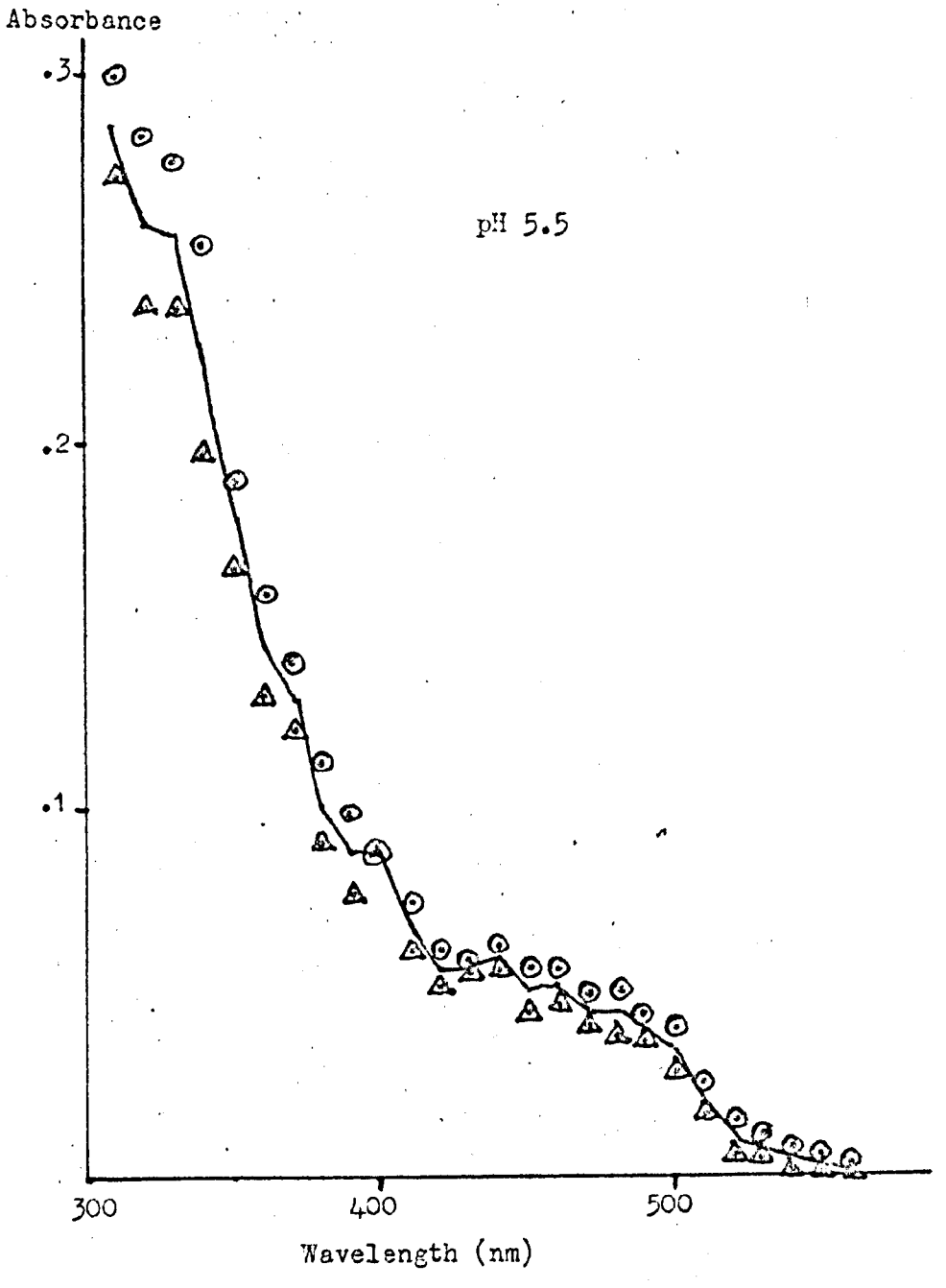

FIGURE 8.5.

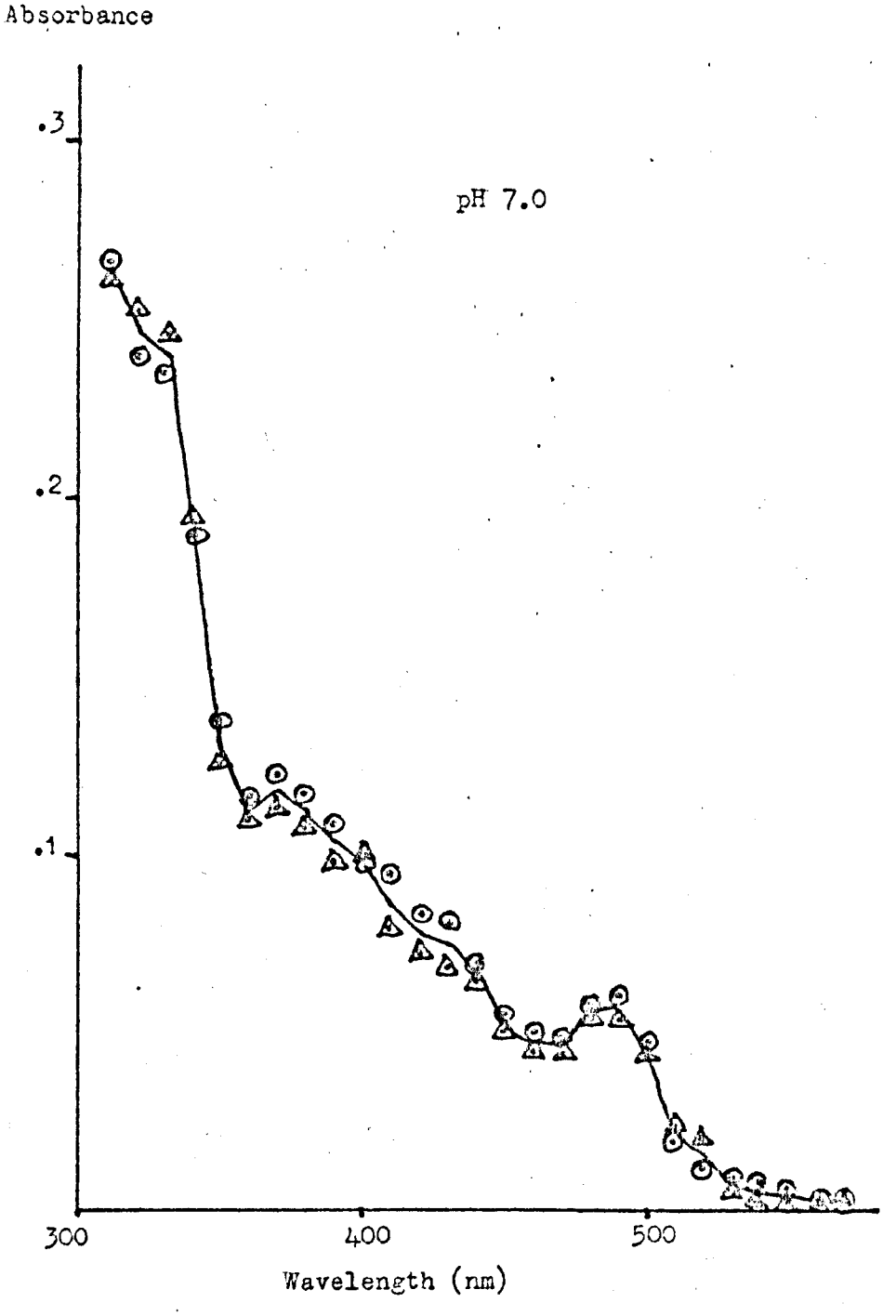

FIGURE 8.6.

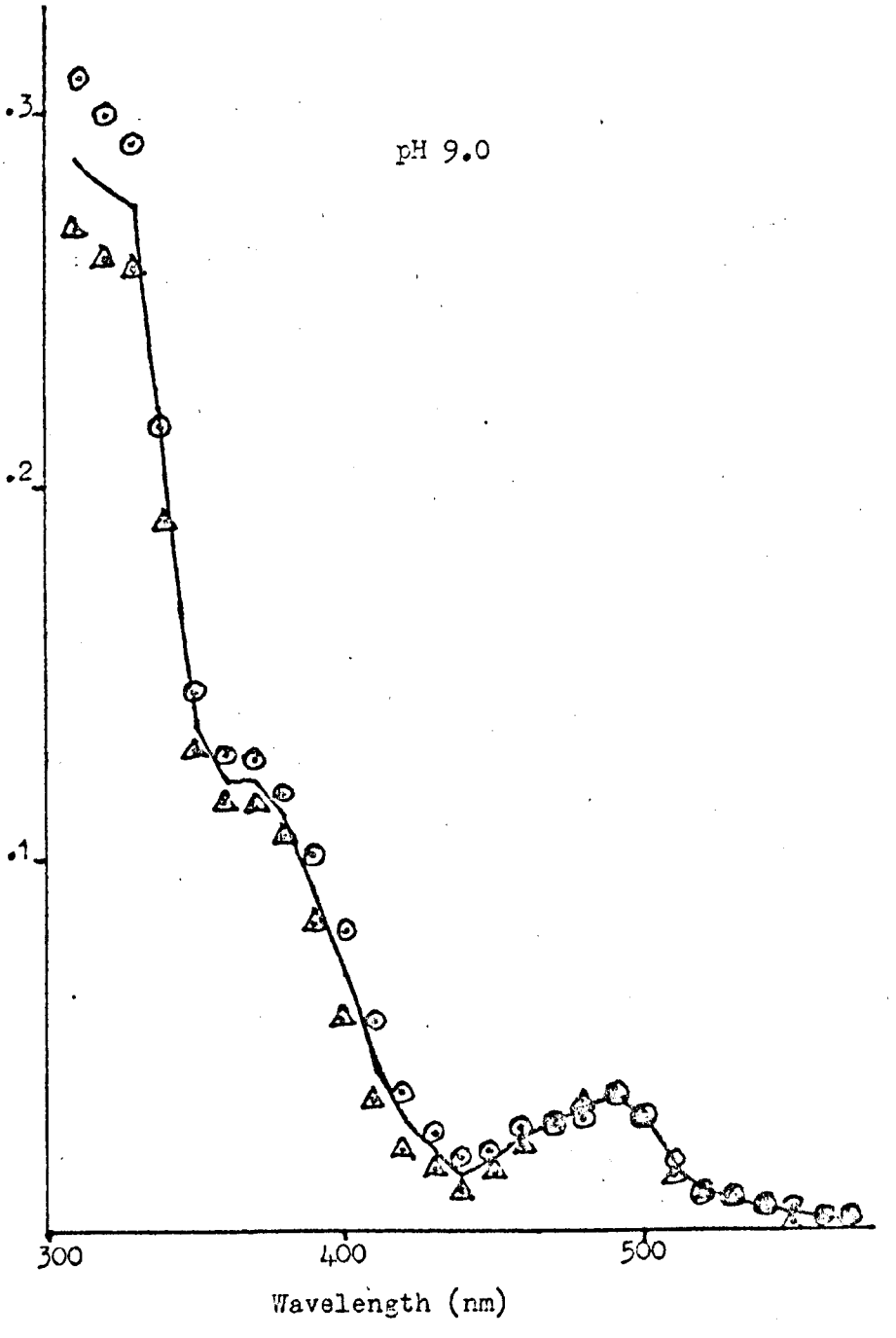

FIGURE 8.7

The absorption spectrum of .90 mg/ml of the equilibrium ala AT-substrate complex, in 50 mM pH 10.5 glycine buffer.

The substrates were L alanine and pyruvate, at 25°C, in 5 mM ME and 5 mM EDTA.

△ using 20 mM pyruvate

○ using 40 mM pyruvate

TABLE 8.2

The table shows the value of five spectral parameters of the equilibrium ala AT-substrate complex where L alanine and pyruvate are the substrates.

The results were obtained with .90 mg/ml enzyme at seven different pHs; at each pH, results were obtained using two different pyruvate concentrations. The parameters are given in .001 absorbance units.

FIGURE 8.8

The spectral parameters, obtained for the equilibrium ala AT-substrate complex, with L alanine and pyruvate, (from table 8.2).

A A graph of A_{430} against pH.

B A graph of P_{430}, (i.e. $2A_{430} - A_{410} - A_{450}$), against pH.

FIGURE 8.7.

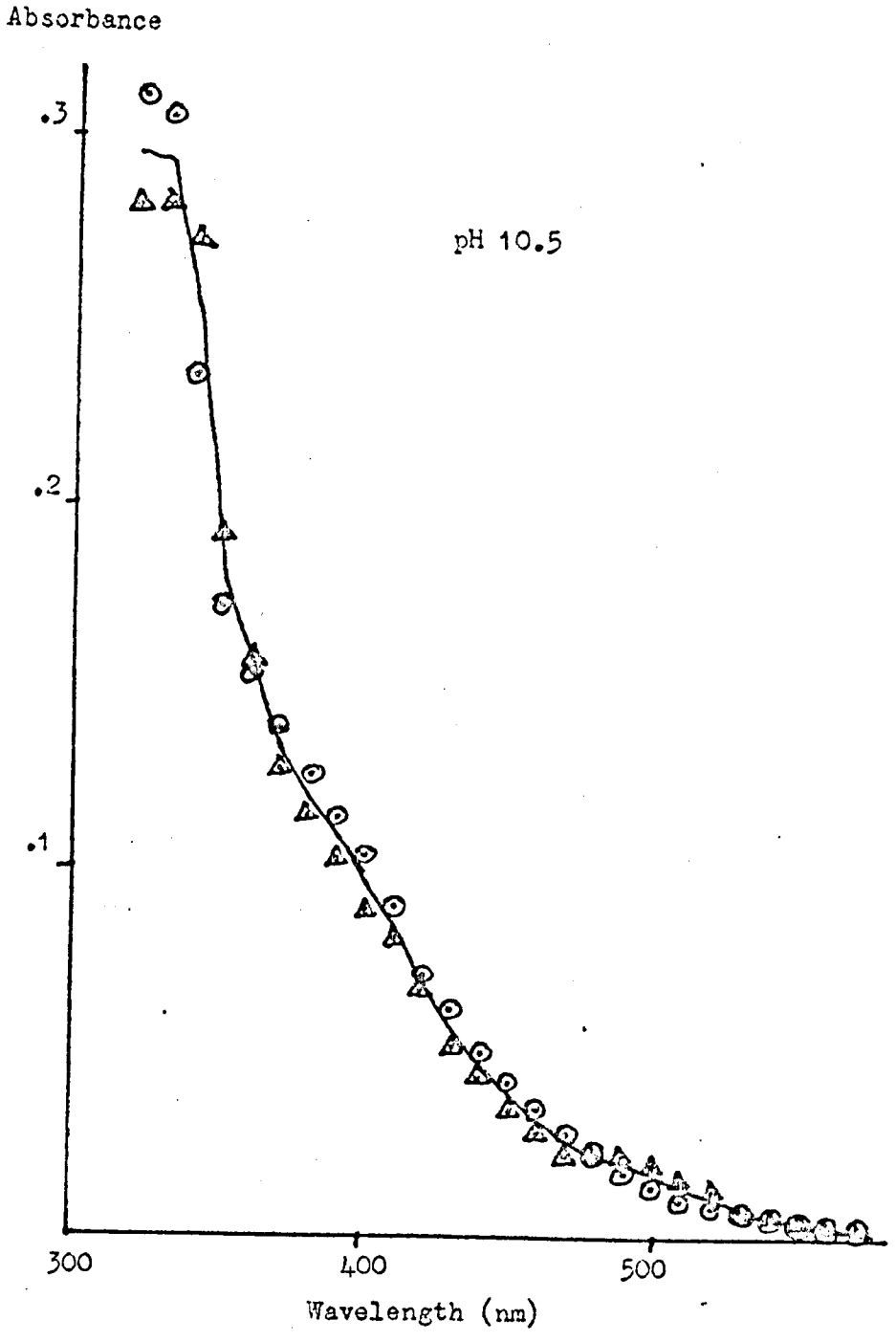

TABLE 8.2.

pH	5.5		6.0		7.0		8.0		9.0		10.0		10.5	
Pyr(mM)	13	40	10	30	7	20	5	15	7	20	10	20	20	40
P_{430}	-14	-15	5	-5	-2	-7	-34	-40	-65	-77	-25	-30	-23	-18
A_{430}	57	63	59	83	65	82	41	50	26	13	40	48	53	62
A_{490}	37	34	43	54	49	63	37	43	32	35	18	23	21	20
P_{430}	-25	-12	8	-13	5	10	-17	-8	-19	-15	-13	-13	-9	-8
P_{490}	17	15	38	28	39	37	27	31	20	24	2	-1	0	-3

FIGURE 8.8.

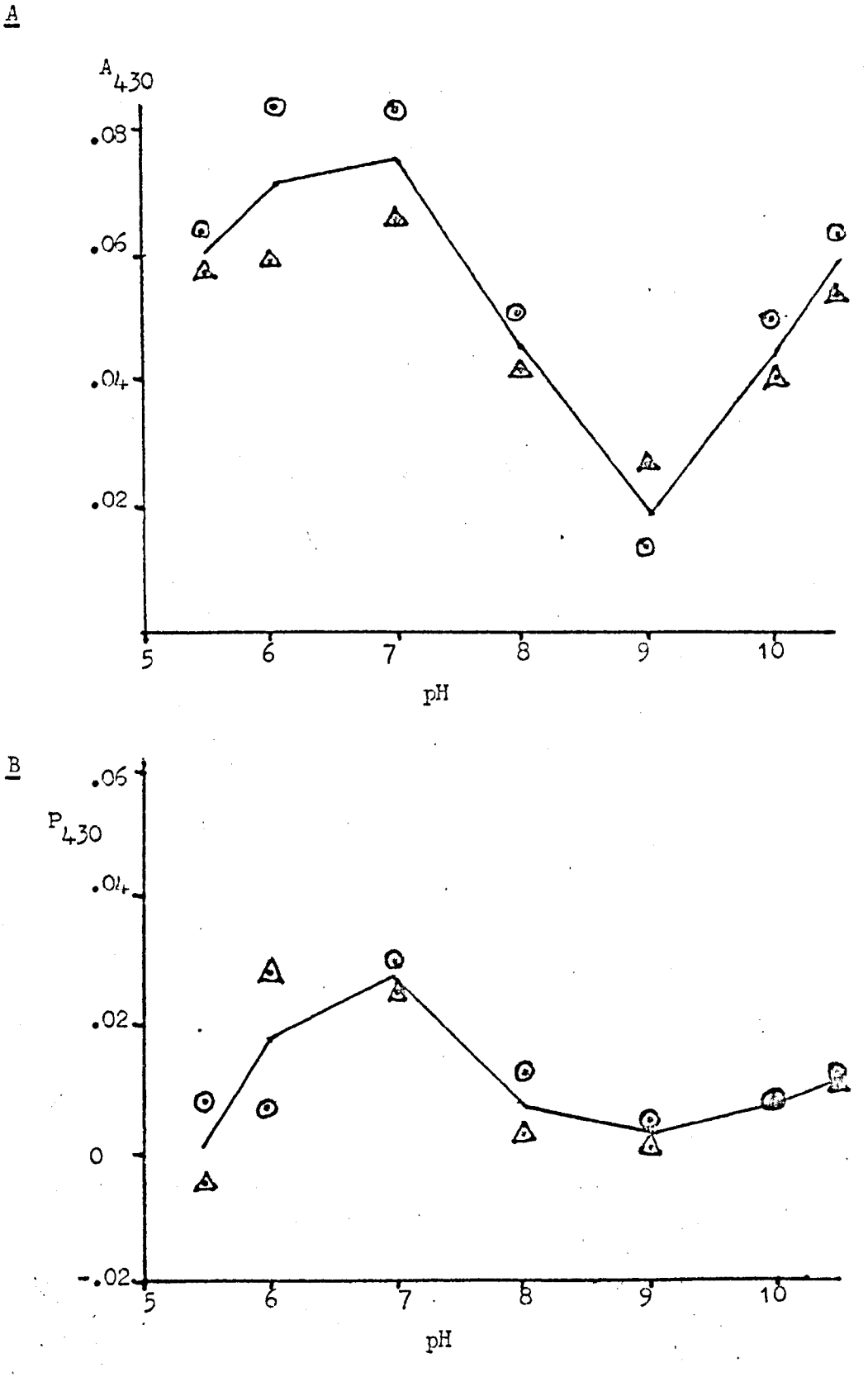

FIGURE 8.9

The spectral parameters, obtained for the equilibrium ala AT-substrate complex, with L alanine and pyruvate, (from table 8.2).

A A graph of A_{490} against pH.

B A graph of P_{490}, (i.e. $2\,A_{490} - A_{470} - A_{510}$), against pH.

FIGURE 8.9.

A

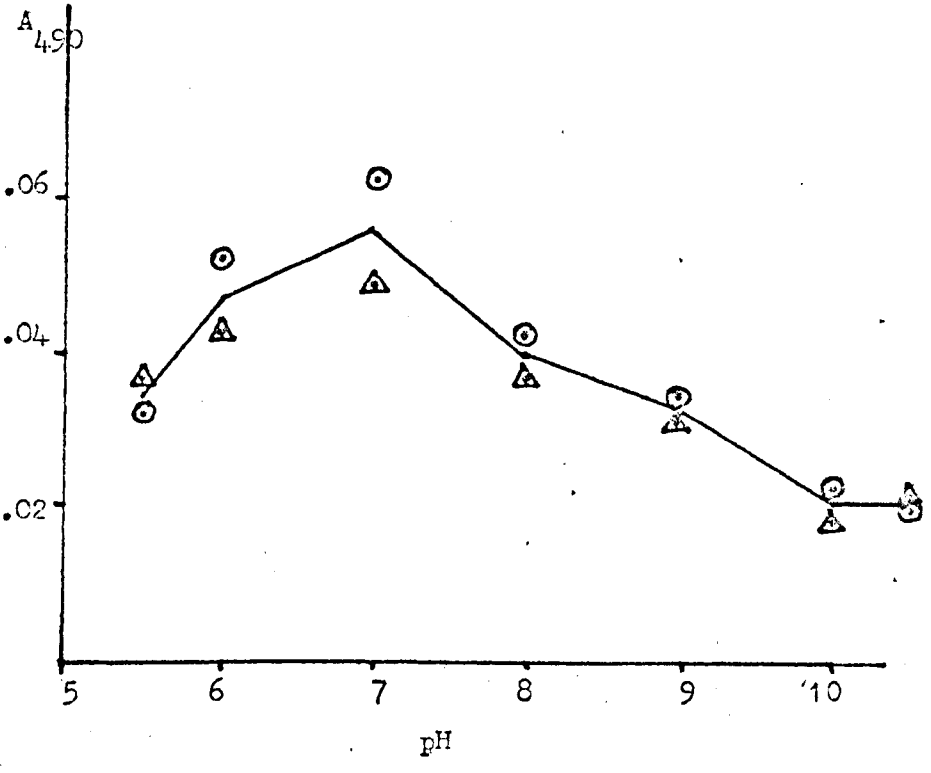

B

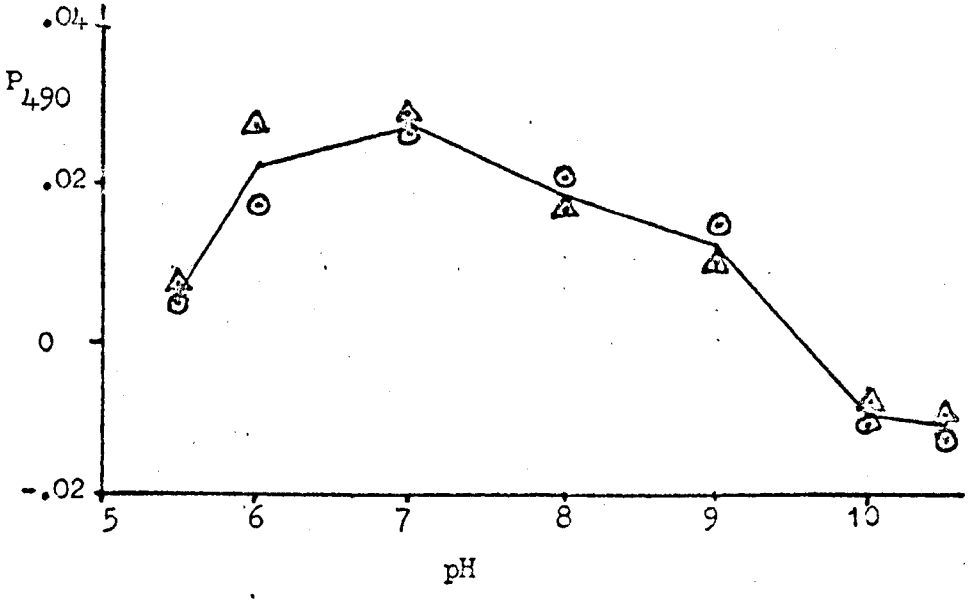

For half the results, (at the higher pyruvate concentration), five different L alanine concentrations were used, (giving four point graphs).

The variation of A_{430} and A_{490} are not completely independent because a form with its λ_{max} at one wavelength will still absorb at a second wavelength. A useful function is a measure of the convexity of the spectrum at wavelength λ. It is

$$P = 2A_{(\lambda)} - A_{(\lambda + a)} - A_{(\lambda - a)}$$

This is the function used in the estimation of PLP, (see appendix 2), and it is relatively insensitive to the absorbance of forms with a peak more than "a"nm from λ.

The results show that A_{430} and P_{430} (that is $2A_{430} - A_{410} - A_{450}$) show similar pH dependence; A_{490} and P_{490} (that is $2A_{490} - A_{470} - A_{510}$) show similar pH dependence.

It is evident from figures 8.4 to 8.7 that the absolute error was greater at shorter wavelengths. Hence the results at below 350 nm were not accurate enough to be useful.

It is difficult to assign accurate pKs to these results. There are three pH regions showing considerable and distinct spectral changes at pH <6, pH 7 -9, and pH 9 -10. Each shows a change in both the 490 nm and 430 nm terms.

DISCUSSION

8.3 SUBSTRATE BINDING

The five categories of pK shifts, produced by substrate binding, are:

pH ~5.8→~5.3

pH ~7.5→~6.6

pH ~7.5→~8.2

pH ~9.7→~9

pH $\sim 10 \rightarrow > 10$

Fumarate binding reveals a pK at pH $\sim$5.7, in both the PL and PM forms of ala AT.

When αaminobutyrate binds to PL-ala AT, it lowers a pK at pH 5.9 to pH 5.3. This pK 5.3 is presumably the same as the pK 5.2 shown by ϕ_O^{AB}. If that is so, ϕ_{AB} should show just one pK below pH 6, (at pH 5.9). ϕ_{AB} does, and so do ϕ_{ala} and ϕ_{glu}.

When αketobutyrate binds to PM-ala AT, there is no change seen in any pK below pH 6. ϕ_{KB}, ϕ_{KG}, and ϕ_{pyr}, all reveal a pK at pH 5.7, but this must be the same in the PM-ala AT and the PM-ala AT -keto-acid complex.

PL and PM-ala AT seem to have slightly different pKs for the same group. When an amino-acid binds to PL-ala AT. the pK is lowered.

The pK shift, pH $\sim$7.5 $\rightarrow \sim$ 8.2, shown by activity kinetics, is identified with the spectral pK shift, pH 7.6 $\rightarrow \sim$ 8, shown by acetate and fumarate binding to PL-ala AT. These are the pKs of the aldimine nitrogen atom. The pK at pH $\sim$8.2, seen in the PM-ala AT-keto-acid complex, would then be that of the ketimine nitrogen.

In PM-ala AT, there is no imine and the pK at pH $\sim$7.5 is probably that of the PMP amino group and the pK $\sim$8.2 of the PM-ala AT-fumarate complex is probably that of the PMP amino group.

The pK shift of pH $\sim$10 $\rightarrow >$ 10 is produced when fumarate binds to the PL or to the PM form of ala AT. Therefore, it is not due to the ionisation of the lysine from the internal aldimine.

This pK shift is seen with acetate inhibition. The spectral

dissociation constant for acetate is greater than the inhibition constant. Hence the large rise in the inhibition constant at high pH implies a rise in the spectral dissociation constant at high pH, (although this could not be measured directly). Therefore, this pK at pH~10 affects that acetate binding which raises the aldimine pK

This pH effect could be due to a group that binds to the carboxyl group of the ligand. It could also be due to the large change in the total charge on the enzyme, which may occur in this pH region.

In the case of fumarate, the pK shift of pH~7.5→~6.6 can not be ascribed to the negative charge on the carboxyl groups, which would tend to raise any pK. Some spatial effect, such as steric hindrance or a conformational change must be invoked. N.B. Acetate does not show this effect.

∝Aminobutyrate has a pK~9.9, which could obviously affect binding. The lysine from the internal aldimine has a pK that should show up in K_{AB}. This might be the pK at pH~9, but that is very low for a lysyl residue: Dixon and Webb suggest that the normal range for lysine ε amino pKs in proteins is pH 9.4 - 10.6. The nature of this pK is discussed later in the chapter.

8.4 ENZYME-SUBSTRATE COMPLEX

A rough estimate of the relative stability of the three spectrally distinct enzyme-substrate complexes was attempted at pH 7.

Figure 8.10.A shows the relationship between A_{490} and A_{430}

for some free enzyme spectra. The ala-AT -substrate complex has an A_{430} = .074, corresponding to an A_{490} of .01. This was subtracted from the actual A_{490} of the complex, giving a figure of .04 for the estimate of the A_{490} that is due to the deprotonated species.

If the molar absorbance was 40 000 $M^{-1}cm^{-1}$, (as for the model system (173)), and the coenzyme concentration was 2 x 10^{-5}M, (using the equivalent weight from chapter 3), then, at pH 7, the deprotonated form constitutes about 5 % of the equilibrium complex - where L alanine and Pyruvate are used.

Figure 8.10.B shows the relationship between A_{430} and PL-ala AT concentration at pH 5.5, (using only two points - it is assumed to be linear). The A_{430} of the complex was .074, giving a figure of 25 % for the aldimine in the complex.

The difference between A_{430} of PL-ala AT at pH 5.5 and pH 10 is .17. The difference between A_{430} of the complex at pH 7 and pH 9 is .05, (figure 8.11), suggesting a figure of 30 % for the aldimine content in the complex.

The mean value for the estimates of aldimine is 27 %.

The deprotonated species constitutes about 5 %.

The ketimine , therefore, is 68 % of the complex.

These figures are very rough. It seems certain that the deprotonated species is only a minor component of the equilibrium complex at any pH.

The scheme from figure 7.8 is used here.

$$E_L \rightleftharpoons AI \rightleftharpoons A_{490} \rightleftharpoons KI \rightleftharpoons E_M$$

It is assumed that formation of a covalent enzyme-substrate complex is rapid, giving the quasi-equilibrium condition.

FIGURE 8.10

A A graph of A_{490} against A_{430}, for .90 mg/ml ala AT, in different forms, and at different pHs.

⊙ PL ala AT, at different pHs

△ PL ala AT-TSC complex, at pH 8.0

□ PM ala AT at pH 8.0.

B A graph of aldimine content against A_{430}, for .90 mg/ml ala AT at pH 5.5.

⊙ PL ala AT. i.e. 100 % aldimine

□ PM ala AT, i.e. 0 % aldimine

FIGURE 8.11

Difference spectra of .90 mg/ml ala AT, in 5 mM ME, 5 mM EDTA and 50 mM buffer, at 25°C.

△ The difference between the PL ala AT spectra at pH 5.5 and at pH 10.0.

⊙ The difference between the spectra of ala AT-substrate complex, with L alanine and pyruvate, at pH 7.0 and pH 9.0.

FIGURE 8.12

A graph of ϕ_0^{AB} against pH.

⊙ experimentally obtained results

— the values obtained in appendix 6

FIGURE 8.10.

A

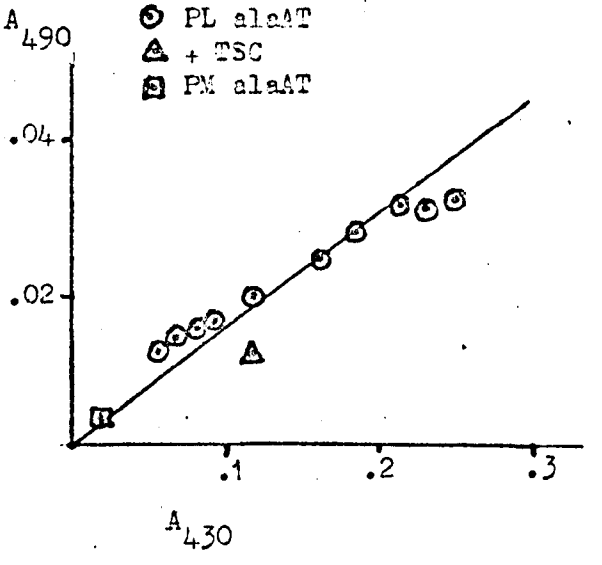

B

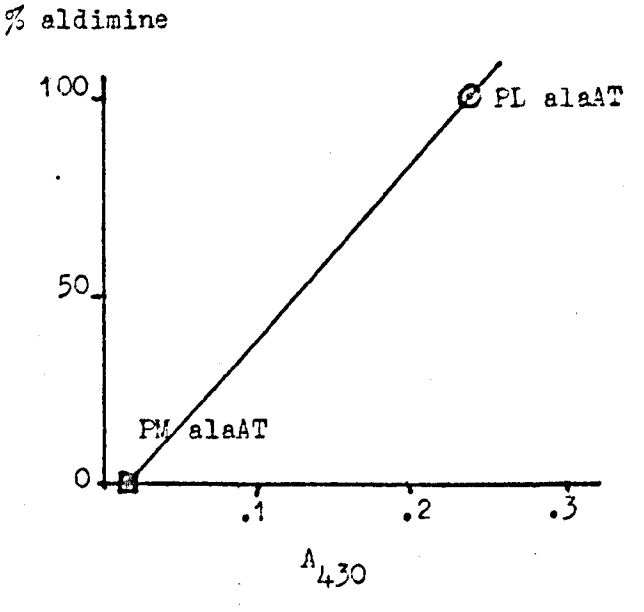

FIGURE 8.11.

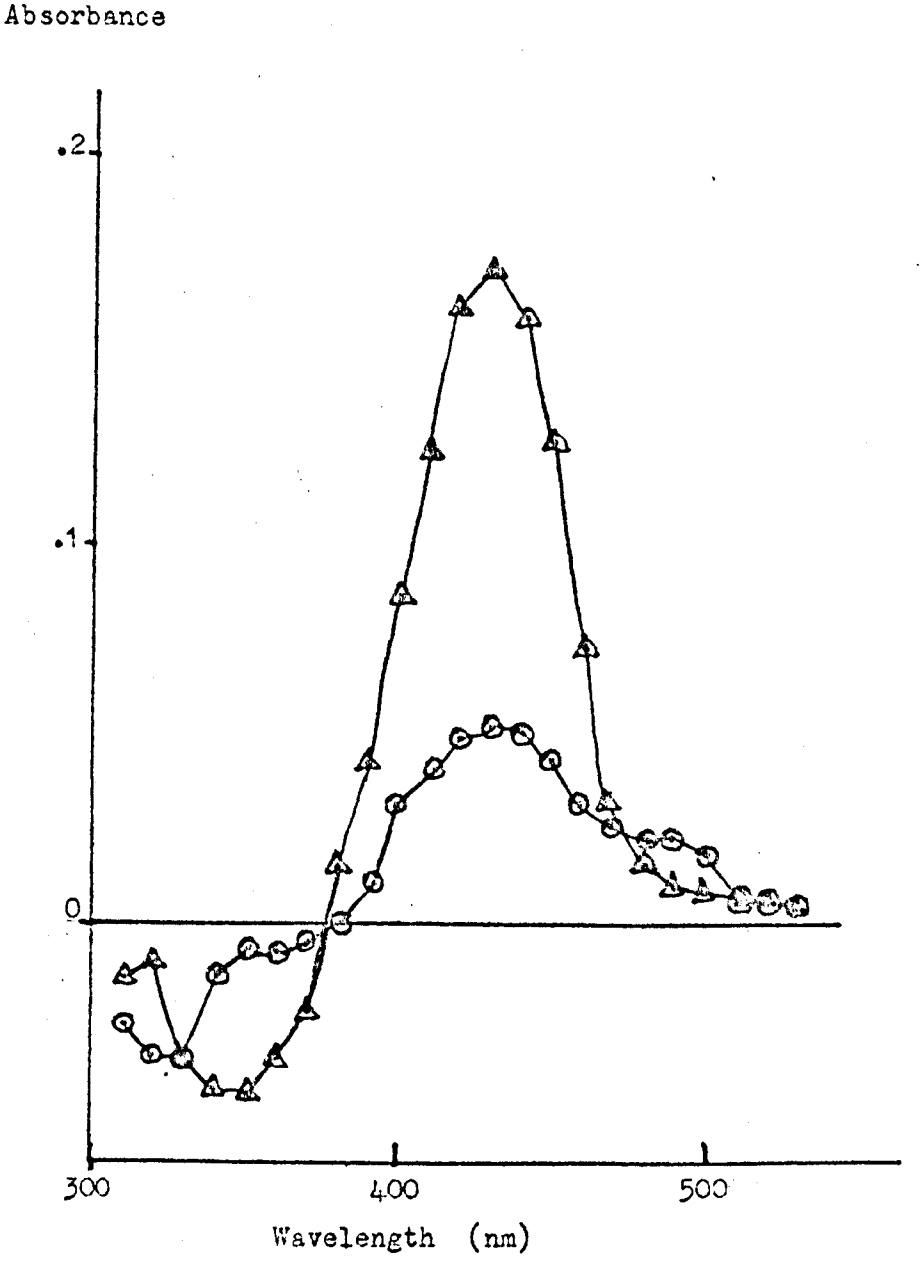

FIGURE 8.12.

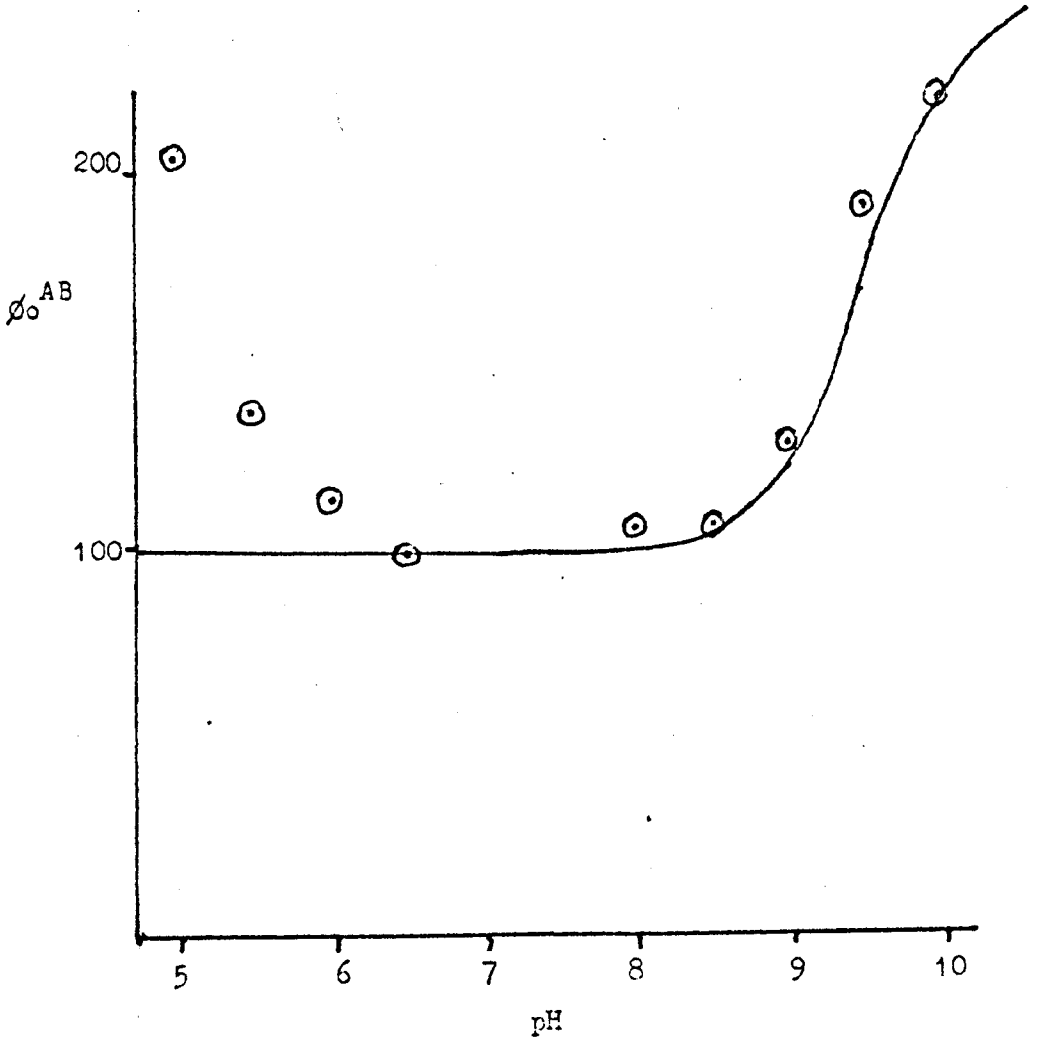

In chapter 6, it was shown that this was so for ∝ aminobutyrate and ∝ ketobutyrate. It is apparent that for both these substrates this rapid binding was covalent. ∝ Ketobutyrate binds much better to the PM form and binds much better than butyrate. ∝ Aminobutyrate binds much better to the PL form and binds better than butyrate. So for these two substrates, ϕ_0 measures the rate of the step between the aldimine and ketimine complexes.

It has already been stated that the ϕ_0s of the other substrates have a similar pH dependence and that they show no pKs attributable to the free enzyme. Hence it is reasonable to suppose that with pyruvate and L alanine the tautomerisation is the slow step.

The pK ~ 8 seen in the spectral results has been attributed to the aldimine pK.

The ϕ_0^{AB} and ϕ_0^{KB} change little in this region, suggesting that the AI : KI ratio does not change drastically, so that the large fall in A_{430} of the enzyme-substrate complex, as the pH increases, cannot be ascribed to a fall in the concentration of AI.

The difference between the pH 7 and pH 9 spectra is shown in figure 8.11: there is a peak at 430 nm (and at 490 nm).

The ∝ aminobutyrate K_m (and ϕ_{ala}) show a pK at about pH 8 in the PL-ala AT-amino-acid complex and this has already been ascribed to the aldimine pK. The ketimine pK has a similar value.

A_{490} falls as the pH is raised: this would be expected. The fall is small, showing that the ionisation state of the imine nitrogen has only a small effect on the stability of the deprotonated form - as is shown by quantum mechanical calculations (163).

The change in ϕ_0 is small or absent.

The pK at pH ~9.5 affected both ϕ_0^{AB} and the spectrum of the equilibrium enzyme-substrate complex, but not ϕ_0^{KB}.

As the pH rises, the A_{490}:AI ratio falls. This could be due to (A) a change in the composition of the A_{490} species, (but that should not effect the AI : KI ratio).

(B) a change in the composition of AI.

(C) a difference between the A_{490} and AI pKs.

This third explanation would require there to be a group with a pK ~9 in the AI and a pK ~9.5 in the KI and A_{490} species; which would fit the K_{AB} results. A chemical explanation would be possible, but not easy.

The second explanation supposes that there are two forms of the aldimine: the internal aldimine with an amino-acid bound non-covalently and the substrate aldimine with a free lysyl residue.

In appendix 6 a simple model is presented in which the equilibrium between these two forms is pH dependent while the other parameters contributing to ϕ_0 are not. The imine pKs for both these complexes are considered to be equal. The amino group pK of the bound substrate is set at pH 8.0; this is the mean of the value suggested by Ivanov and Karpeisky (90), pH 7.8, and the pK of triglycine, a good model compound, at pH 8.1. The lysine pK would then be about pH 9.6. The actual and calculated values for ϕ_0^{AB} are given in figure 8.12. The fit is quite good. At physiological pH nearly all the AI would be in the substrate aldimine form. At high pH the equilibrium concentrations of the

two aldimines would be similar.

The binding constant would no longer be a simple parameter, but $\phi_{\text{amino-acid}}$ would be. We have already made the rate constant in the tautomerisation reaction pH independent at high pH, for this model. This is very reasonable considering the pH independence of ϕ_0^{KE} at high pH. Consequently, the pH dependence of $\phi_{\text{amino-acid}}$ is the pH dependence of the PL-ala AT - substrate aldimine equilibrium. In figure 6.7, the lysine pK seems to fit best at about pH 9.5.

It was not possible to fit the ϕ_{ala} and ϕ_{glu} results to this simple scheme without introducing a further pK at pH ~10.0 for L alanine and at pH~10.3 for L glutamate. A pK~10 $\longrightarrow$ >10 effect has been seen with inhibitor binding and has already been discussed.

This explanation, (B), is in no way proved, but is to be preferred for three reasons. It gives the lysine group a realistic pK. At high pH, the binding constants of covalently and non-covalently bound amino-acids are not very different: at pH 10, $K_{ala} \doteq \phi_{ala}$ and ϕ_{ala} = 43 mM, while the inhibition constant for L alanine (against αketoglutarate) is 65 mM and the inhibition constant of glycine (against L alanine) is 61 mM. The explanation (C) requires an ad hoc chemical explanation, while for explanation (B) the existence of two different aldimine complexes is independently deduced, in chapter 13.

Binding studies showed that the pK 5.3 in the AI and the pK 5.7 in the KI belong to the same group.

The spectral results down to pH 5.5 will only show up the consequences of the pK 5.7. ϕ_0^{AE} is fairly pH independent from

pH 5.5 to 9.0.

As the pH falls, the A_{490} : KI ratio falls. This could be due to (A) a change in the composition of the A_{490} species, (but that does not explain the fall in the AI : KI ratio).

(B) a change in the composition of the KI forms, (but K_{KB} shows no change in this pH region).

(C) a difference in the pKs of the A_{490} and KI species.

Consider the scheme

$$AI \underset{k_2}{\overset{k_1}{\rightleftharpoons}} A_{490} \underset{k_4}{\overset{k_3}{\rightleftharpoons}} KI$$

When A_{490} : KI falls, either k_3 rises or k_4 falls. As the pH falls below pH 6, ϕ_0^{KB} rises, suggesting that it is k_4 that falls. If the quasi-equilibrium assumption holds, ϕ_0^{AB} depends on k_1, k_2, and k_3, but not on k_4 and ϕ_0^{AB} changes little between pH 5.5 and 9.0. We conclude that the pK 5.7 affects only k_4 to a significant extent.

Now the effect of a group that stabilises the A_{490} species by its electron-accepting properties should be to increase k_4 at low pHs. An acidic group that donates a proton for the protonation step should have little effect on k_4. The only remaining type of interfering group is a basic group that accepts a proton in the deprotonation step, and the pK 5.7 is the pK of such a group.

The spectral results were not obtained at so low a pH that the same conclusions could be reached for the pK at pH 5.2, but it seems likely that this group acts as a catalytic base in both directions.

At pH 7 the net charge on the three enzyme-substrate complex

forms seems to be the same. Now as the A_{490} species has been deprotonated in one position, it must be protonated in a second position, where the AI and KI forms at pH 7 are not. Hence the pK of this group is pH$>$7 in the A_{490} species and pH$<$7 in the imines. It is possible that this group is the catalytic base, the pyridine nitrogen of the coenzyme or structural water.

CHAPTER 9

NON-SPECIFIC INACTIVATION

9.1 HEAT

Ala AT was incubated at 65°C in 50 mM pH 7.5 phosphate, in the presence of various reagents. Samples were removed and assayed by the standard assay.

Figure 9.1.A shows the normal time course for heat inactivation. Figure 9.1.B shows the log plot. This was not a simple first order reaction: it can be analysed into two reactions of which one is rapid and gives a partial inactivation while the second is slower, giving a fairly complete inactivation. The distinct nature of the fast reaction was still more obvious at 40°C

Table 9.1. shows the effect of adding ME and EDTA. Probably ME prevents oxidation, while EDTA removes metal ions. N.B. 4μM copper(II) sulphate gave a very rapid, though incomplete, inactivation at 50°C. EDTA and ME enhance the long term stability of ala AT at 4°C (170).

In all subsequent experiments, 5 mM EDTA was present and only the rate of the slow reaction was measured.

9.1(a) Substrate and Inhibitor Protection

Table 9.2 shows the effect of various substrates and inhibitors on ala AT stability.

The PL and PM forms did not differ. The amino-acid or keto-acid alone, gave little protection so that most or all of the

FIGURE 9.1

Inactivation of PL-ala AT at 65°C, in 50 mM pH 7.5 phosphate.

A A graph of activity aginst time.

B A graph of $\log_{10}$ activity against time.

TABLE 9.1

Inactivation of PL-ala AT at 65°C, in 50 mM pH 7.5 phosphate.

The rate constant for inactivation is given in the presence or absence of 5 mM ME and 5 mM EDTA.

TABLE 9.2

Inactivation of ala AT at 65°C, in 50 mM pH 7.5 phosphate, 5 mM ME and 5 mM EDTA.

The rate constants for inactivation are given, in the presence of some substrates and inhibitors.

FIGURE 9.1.

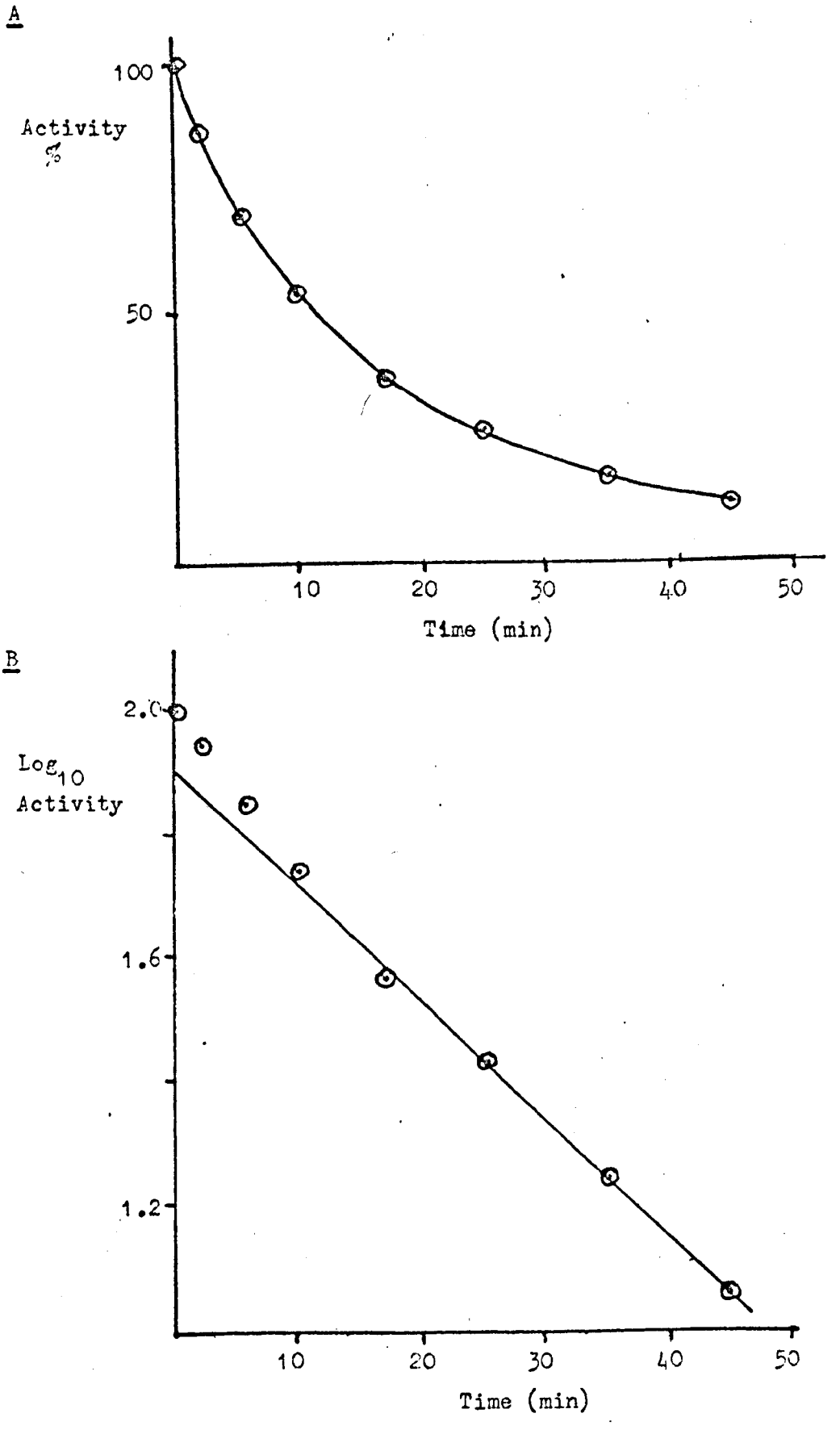
A
100
Activity
%
50
10
20
30
40
50
Time (min)
B
2.0
Log10
Activity
1.6
1.2
10
20
30
40
50
Time (min)

TABLE 9.1.

Additions		RATE (min^{-1})
ME (5mM)	EDTA (5mM)	
–	–	.052
✓	–	.033
–	✓	.028
✓	✓	.028
✓	✓	.029

TABLE 9.2.

Additions	Rate	
	($10^{-2}min^{-1}$)	%
PL alaAT	2.85	100
PM alaAT	2.9	
100mM L glu + 2mM ∝ KG	1.1	38
100mM L ala + 2mM pyr	1.8	63
100mM L ala + 2mM pyr + 200mM formate	1.1	38
200mM formate (PL alaAT)	2.0	70
50mM fumarate (PL alaAT)	1.1	38
50mM fumarate (PM alaAT)	1.0	35
100mM L glu	2.5	88
100mM L ala	2.6	91

protection with two substrates was due to the increased stability of the enzyme-substrate complex.

L alanine and pyruvate protected less than L glutamate and ∝ ketoglutarate, except when formate was present, when the rate fell to 38 %. If pyruvate plus L alanine and formate acted independently, together they should have given a rate of .70 × .63 = .44 : they are substantially independent.

Fumarate,(which does not bind covalently to ala AT), gave as good protection as L glutamate plus ∝ketoglutarate.

9.2 UREA

Ala AT was incubated at 25°C with 5.6 M urea in the presence of various reagents. Samples were removed and assayed by the standard assay.

Figure 9.2 shows the normal time course for urea inactivation The log plot shows that it was first order to below 10% initial activity.

9.2(a) pH and Coenzyme Effect

Table 9.3 gives the rate of inactivation under different conditions. Figure 9.4 shows the rate constants in the absence of substrate or inhibitors.

Between pH 5.5 and 9.5 the PM form is more stable than the PL form: both showed the same pH dependence. Some experiments were repeated in 150 mM buffer. The rate fell but only slightly and did not affect the interpretation of the results.

The fall in stability at extreme pHs, (with pKs at pH$<$5.5 and pH$>$9.5), was expected. The low pK was too low to be identified with the pK in that region, obtained in the activity experiments.

FIGURE 9.2

Inactivation of PL-ala AT, at 25°C, in 5.6 M urea, with 50 mM pH 7.0 phosphate buffer.

A A graph of enzyme activity against time

B A graph of $\log_{10}$ activity against time.

TABLE 9.3

Inactivation of PL-ala AT, at 25°C, in 5.6 M urea. The buffer concentration is 50 mM unless otherwise stated.

The rate constants for inactivation are given, at different pHs and in the presence of some substrates and inhibitors.

FIGURE 9.3

Inactivation of ala AT, at 25°C, in 5.6 M urea.

A graph of the rate of inactivation against pH.

⊙ for PL-ala AT in 50 mM buffer

△ for PL-ala AT in 150 mM buffer

\+ for PM-ala AT in 50 mM buffer

FIGURE 9.2.

A

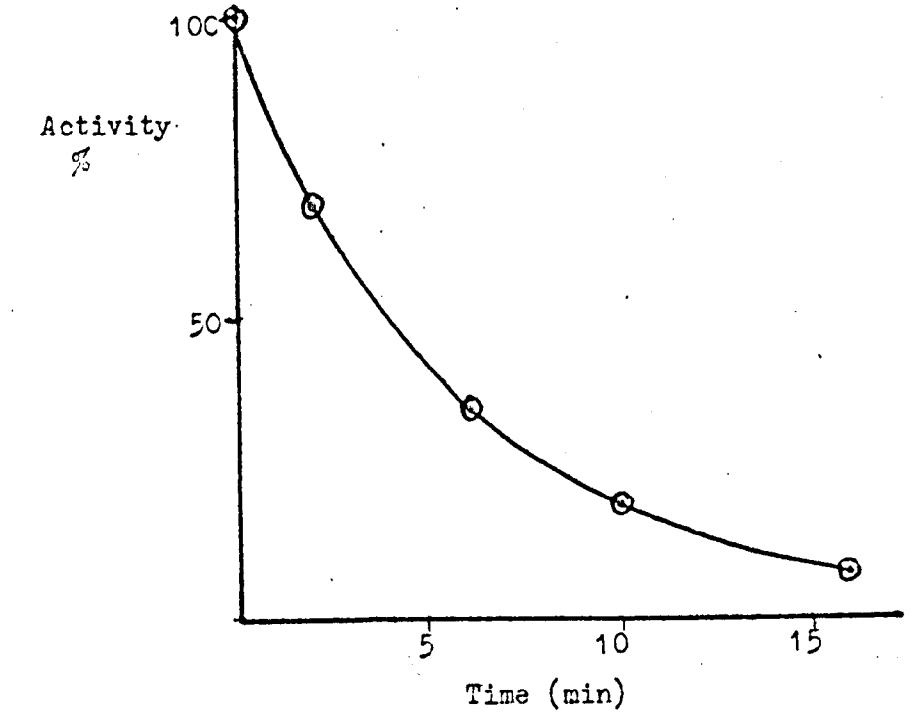
100
Activity
%
50
5
10
15
Time (min)

B

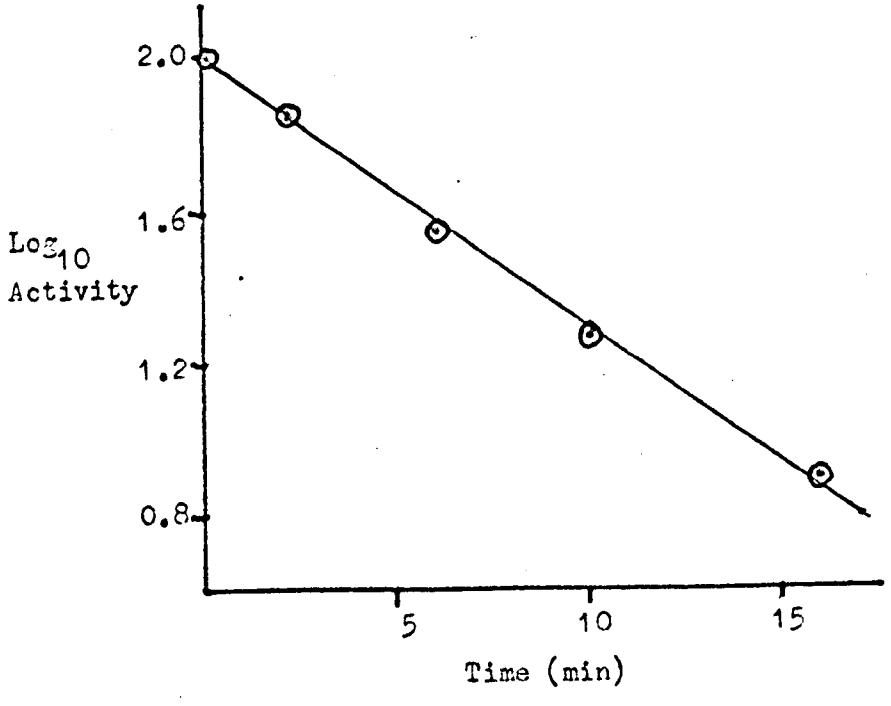
2.0
1.6
1.2
0.8
Log10
Activity
5
10
15
Time (min)

TABLE 9.3.

pH	5.0	5.5	6.0	6.5	7.0	7.5	8.0	9.0	9.5	10.0
PL alaAT	4.8	3.1	1.7	1.6 1.8	1.7	2.3	2.3 2.3	2.4	2.7	4.3 5.5
PM alaAT	4.3 4.6	2.0		.71 .80		1.3	1.2 1.3	1.7		4.9
100mM L ala + 10mM pyr				1.5 1.6			1.6 1.6			
100mM L ala							2.0			
80mM L glu + 10mM αKG							.46 .54			
80mM L glu							1.8			
200mM formate (PL alaAT)							.92 .92			
200mM formate (PM alaAT)				.23 .32			.41 .46			
100mM fumarate (PL alaAT)							.67 .71			
100mM fumarate (PM alaAT)				.69 .82			.67 .78	.78		
150mM buffer (PL alaAT)		2.4		1.2			1.95		2.1	

FIGURE 9.3.

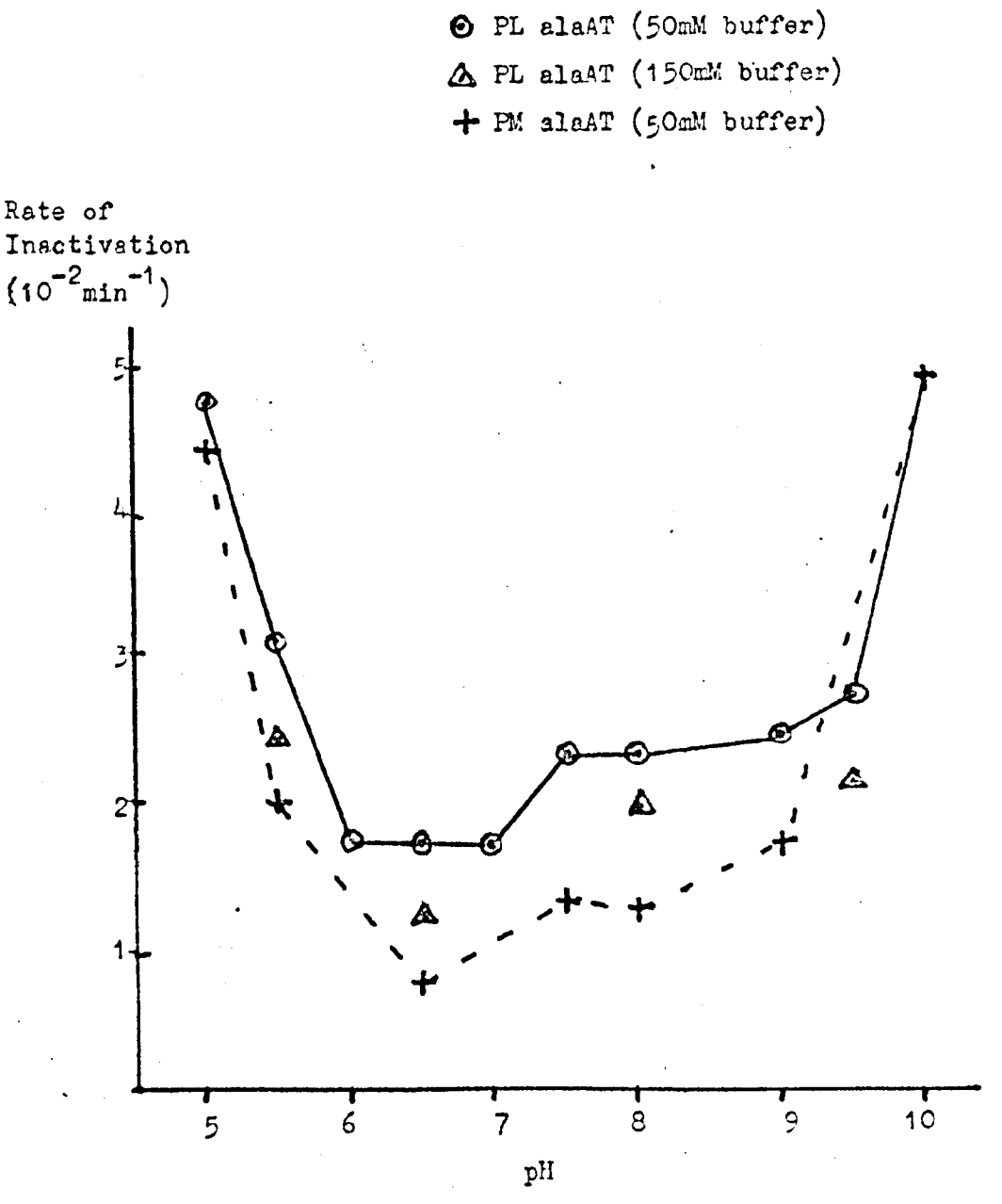
PL alaAT (50mM buffer)
PL alaAT (150mM buffer)
PM alaAT (50mM buffer)
Rate of Inactivation (10^{-2} min^{-1})
5
4
3
2
1
5
6
7
8
9
10
pH

There was one pK in the neutral region, at about pH 7.3 .

9.2(b) Substrate and Inhibitor Effect

With pyruvate plus L alanine, the pK 7.3 was no longer seen - similarly with L glutamate plus ∝ ketoglutarate and with fumarate, but not with formate..

Fumarate-PM-ala AT and fumarate-PL-ala AT complexes showed the same inactivation rates at pH 8.0.

With formate the rate was 40 % that of the free enzyme, in every case.

The rate of inactivation was lower with L glutamate plus ∝ ketoglutarate than it was with L alanine plys pyruvate.

9.3 DISCUSSION

It has been suggested by Saier and Jenkins (171) that formate activation is due to the formate binding at the site on the enzyme which binds the γ carboxyl group of L glutamate or ∝ ketoglutarate.

Let us assume that this is so; then protection against heat or urea inactivation can be ascribed to two kinds of binding. One is binding at the γ carboxyl site. The other is shown by fumarate and substrates but not by formate.

The heat results fit this theory well. Suppose that binding at the γ carboxyl site gives 66 % of the inactivation rate of the free enzyme; that the second kind of binding gives a rate of 59 %; and hence with both types of binding, a rate of 39 %. The results in table 9.1 fit this interpretation very well.

The urea inactivation was more complicated. The degree of protection was dependent on pH and the state of the coenzyme, too. If binding at the γ carboxyl site reduced the rate of inactivation

to 40 % and binding at the second site produced the rate of inactivation that the PL form would give at pH 6: i.e. there was no pK 7.3, then the following results would be obtained for the rate constants under different conditions.

+ L alanine + pyruvate	1.6 (pH 6.5)	1.6 (pH 8)	
+ L glutamate + ketoglutarate		.65 (pH 8)	
PL ala AT + formate	.92 (pH 8)		
PM ala AT + formate	.32 (pH 6.5)	.46 (pH 8)	
PM ala AT + fumarate	.65 (pH 8)		
PM ala AT + fumarate	.65 (pH 6.5)	.65 (pH 8)	.65 (pH9)

This corresponds well with the results of table 9.3. The greatest error is where L glutamate and ∝ ketoglutarate are present: the measured value was 0.77 times the projected value.

In both the urea and heat experiments, the substrates and inhibitors were at saturation concentrations, at 25°C and in the absence of urea. It was hoped that this was also true for the conditions of the experiments.

CHAPTER 10

PHOTO-OXIDATION

10.1 INTRODUCTION

Photosensitised modification of proteins has been studied using a number of different dyes (203, 204, 205, 206, 207).

Weil and his coworkers studied the photo-oxidation of a number of different proteins in the presence of methylene blue. They observed that of the free amino-acids only tryptophan, tyrosine, histidine, methionine and cysteine could be oxidised (203). In experiments on lysozyme and β lactoglobulin, the rate of modification of the different types of residue, at pH 8, was found to be hist $\rangle$ trp $\rangle$ tyr $\rangle$ cys $\rangle$ met = 0 . Changes in viscosity and solubility were observed (204, 205).

Photo-inactivation, using methylene blue, has been achieved with chymotrypsin (206), RNase (207), enolase(22), phosphofructokinase (1), asp AT (127, 129, 130) and glutamate dehydrogenase (85).

Westhead introduced a new dye, rose bengal, which is an anion and might be expected to show a greater affinity for the active sites which bind anionic substrates, than methylene blue does. With enolase (208, 209), rose bengal gave a much faster inactivation, while modifying fewer residues and not affecting its sedimentation properties - unlike methylene blue (22). Aldolase (85) and asp AT (127) have also been studied with rose bengal.

The mechanism of the reaction is generally held to be that

described by Oster, Bellin, Kimball and Schrader. Here, D is the dye; D^* and D' are excited states; S is the residue that is oxidised; and O_2 is molecular oxygen.

$$
\begin{array}{ccccc}
D + h\nu_1 & \longrightarrow & D^* & \longrightarrow & D + h\nu_2 \\
 & & \downarrow & & \\
D_2 & \xleftarrow{+D} & D' & \longrightarrow & D + h\nu_3 \\
 & & \downarrow & & \\
D_2 + O_2 & \xleftarrow{+D} & DO_2 & \longrightarrow & D + O_2 \\
 & & \downarrow & & \\
 & & D + SO_2 & &
\end{array}
$$

The dye is excited by radiation and then falls to a metastable triplet state, that combines with oxygen to give a strong oxidising agent, DO_2, which oxidises a protein residue. The absorbed energy may be lost by a number of alternative reactions - as shown.

10.1(a) Aspartate Aminotransferase

Martinez- Carrion and his coworkers photo-oxidised asp AT with rose bengal and with methylene blue. In each case there was a first-order inactivation. The rate was pH dependent, showing a pK at pH 6.5. There was no substrate protection and no change in the elution properties on Sephadex G200. The oxidised residue was shown to be a histidine, by amino- acid analysis (127).

They showed that the A_{430} fell, (while the loss of coenzyme was less than 10 %), and the A_{325} rose, (as it did in model histidine-containing peptides). The circular dichroic spectrum was altered, while the sedimentation and immunological properties were not (129).

Further spectral work showed that all normal substrates and inhibitors would still bind well to the photo-oxidised enzyme, but that erythro β hydroxy - aspartate and dihydroxy fumarate would no

longer form a complex absorbing at 490 nm (130).

They concluded that one histidyl residue was oxidised and that it was essential for the abstraction of a proton from the ketimine and aldimine forms of the enzyme-substrate complex.

The relatively unequivocal interpretation of these results suggested that photo-oxidation could usefully be carried out on the mechanistically similar ala AT.

10.2 RESULTS USING ROSE BENGAL

Figure 10.1 is a typical graph of activity against time for the rose bengal photo-oxidation of ala AT at 12°C, where the standard assay was used. This had previously been reported by Reis (212). The log plot was not linear, but the $\log(A_t - A_\infty)$ against time was linear, when appropriate values of A_∞ were used. A_t is the activity at time t. By trial, A_∞/A_o was found to be about 20%. This could be due to the residual activity of the modified enzyme, or less probably it could be a resistant fraction of the native enzyme.

The rate constant, (obtained for $A_\infty = 20\% A_o$), was substantially independent of the state of the ala AT coenzyme, the buffer concentration, or the pH, (table 10.1 and figure 10.2). The result at pH 4.6 has been adjusted to take account of a slow inactivation in the absence of light.

In pH 7.5 phosphate, partial protection was provided by formate, (alone or with L alanine plus pyruvate), and by L glutamate plus α ketoglutarate, but not by L alanine plus pyruvate, α aminobutyrate plus α ketoglutarate, L glutamate alone, or α ketoglutarate alone, (table 10.1). The protection was pH dependent.

FIGURE 10.1

Photo-inactivation of PL-ala AT, by .005 % rose bengal, with 50 mM pH 7.5 phosphate buffer, at 12°C.

A A graph of ala AT activity against time.

B A graph of $\log_{10}(A_t - A_\infty)$ against time. $A_\infty = 18$ gives the best straight line for these results.

TABLE 10.1

Photo-inactivation of PL-ala AT, by .005 % rose bengal, at 25°C.

The rate constant for inactivation is given, at different pHs, and buffer concentrations, and with different forms of the enzyme, and plus some substrates and inhibitors.

FIGURE 10.2

Photo-inactivation of PL-ala AT, by .005 % rose bengal, at 25°C, in 50 mM buffer.

A graph of the rate constant for inactivation against pH.

The point marked +, was corrected, to take account of a slow inactivation that occurred in the dark at pH 4.6.

FIGURE 10.3

The activity pH profile for ala AT; for the native enzyme and for enzyme, photo-oxidised by rose bengal.

⊙ Forward assay, with .25 M L alanine and .01 M ∝ ketoglutarate

Δ Reverse assay, with .4 M L glutamate and .006 M pyruvate

FIGURE 10.1

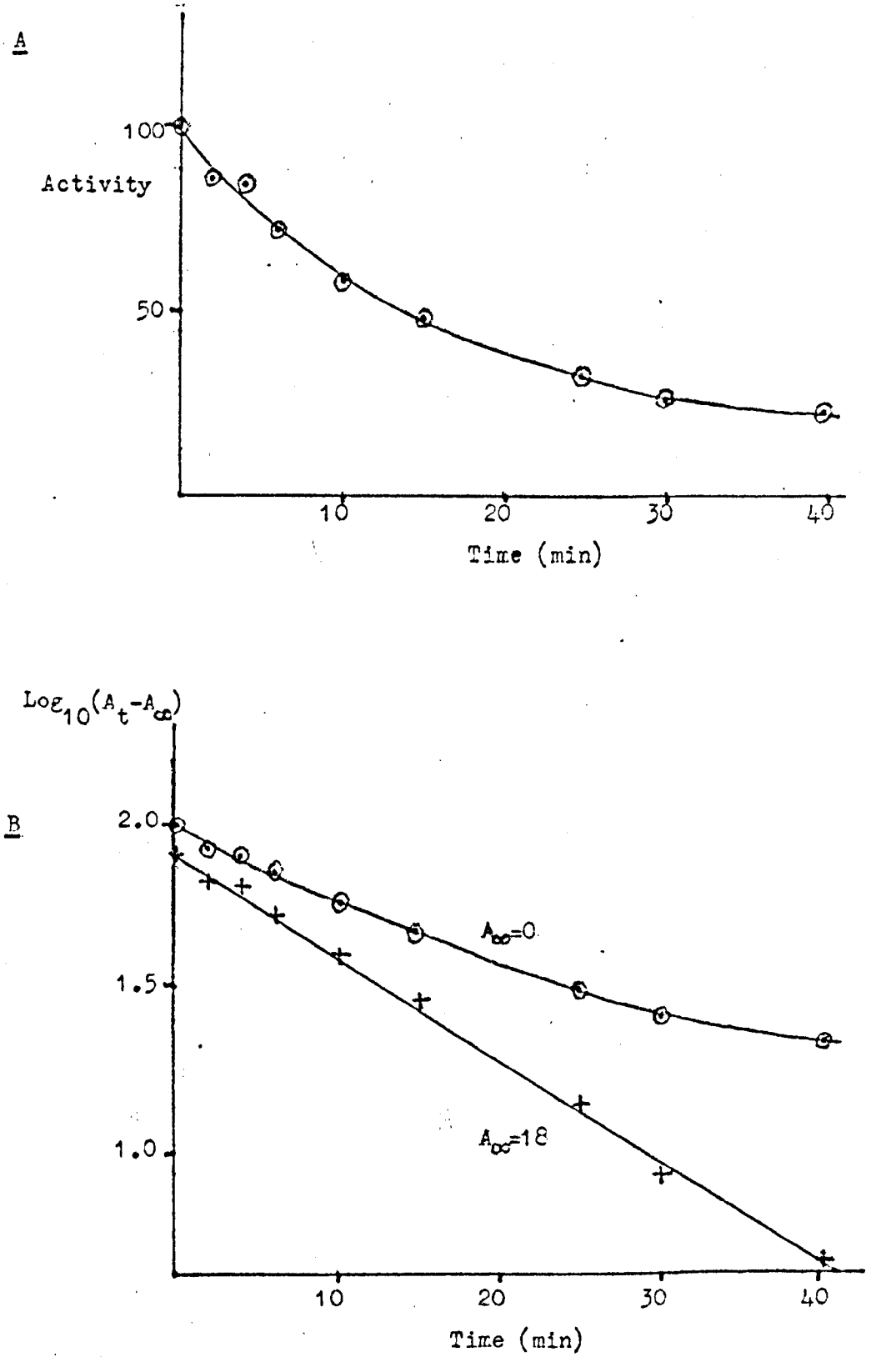
A
100
Activity
50
10
20
30
40
Time (min)
B
Log10(At-A∞)
2.0
1.5
1.0
A∞=0
A∞=18
10
20
30
40
Time (min)

TABLE 10.1.

Buffer	Buffer Concentration	Coenzyme	Additions	Rate (10^{-2} min^{-1})
pH 7.5 Phosphate	.033M	PM		7.7
pH 7.5 Phosphate	.433M	PM		8.2
pH 7.5 Phosphate	.033M	PL		8.7
pH 7.5 Phosphate	.433M	PL		7.7
pH 7.5 Phosphate	.050M	PL	.20M Formate	5.0
pH 7.5 Phosphate	.050M		.133M L Ala .0017M Pyr	7.7
pH 7.5 Phosphate	.050M		.133M L Ala .0017M Pyr .20M Formate	5.0
pH 7.5 Phosphate	.050M		.133M DL∝AB .0030M Pyr	7.9
pH 7.5 Phosphate	.050M		.133M L Glu .0017M ∝KG	5.6
pH 7.5 Phosphate	.050M	PM	.133M L Glu	8.7
pH 7.5 Phosphate	.050M	PL	.0017M ∝KG	8.2
pH 6.0 Phosphate	.050M		.133M L Glu .0017M ∝ KG	8.7
pH 7.0 Phosphate	.050M		.133M L Glu .0017M ∝ KG	8.0
pH 8.0 Tris	.050M		.133M L Glu .0017M ∝ KG	5.5
pH 9.0 Tris	.050M		.133M L Glu .0017M ∝ KG	6.8
pH 10.0 Glycine	.050M		.133M L Glu .0017M ∝ KG	7.4

FIGURE 10.2.

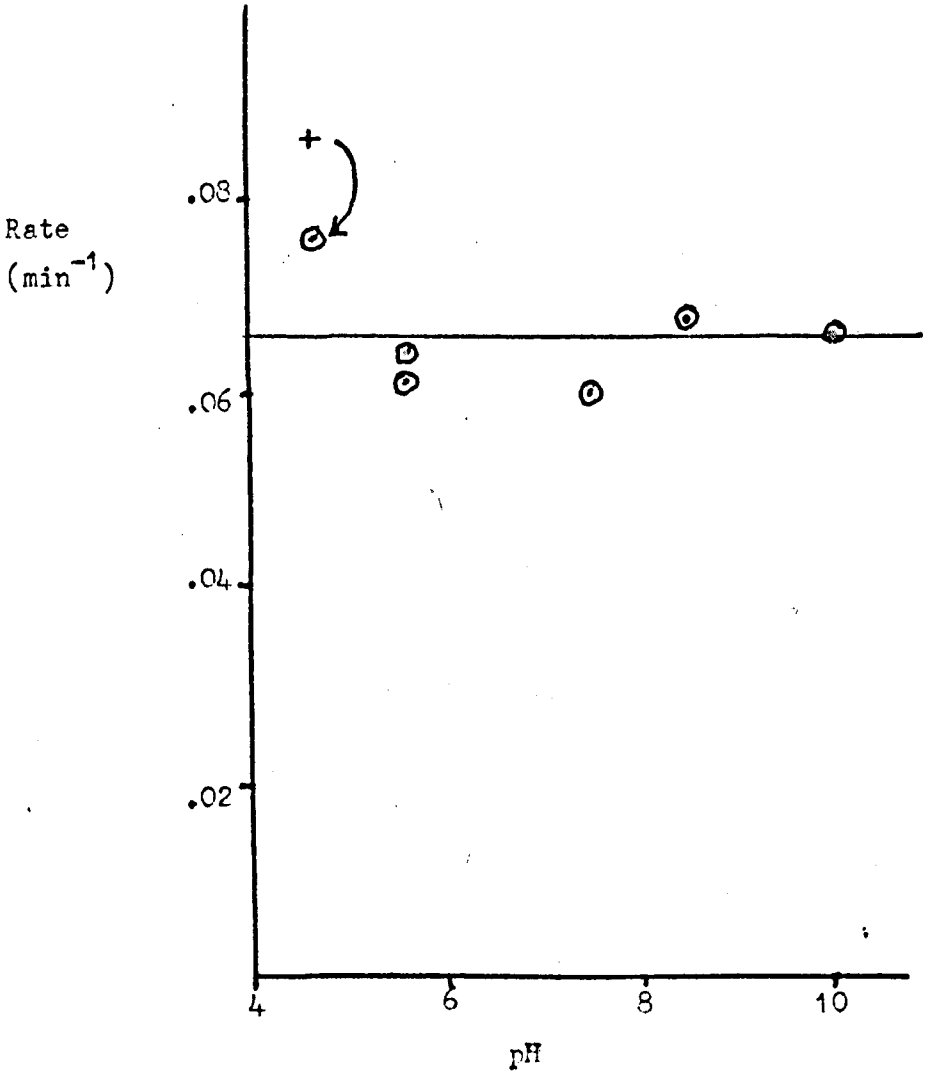

FIGURE 10.3.

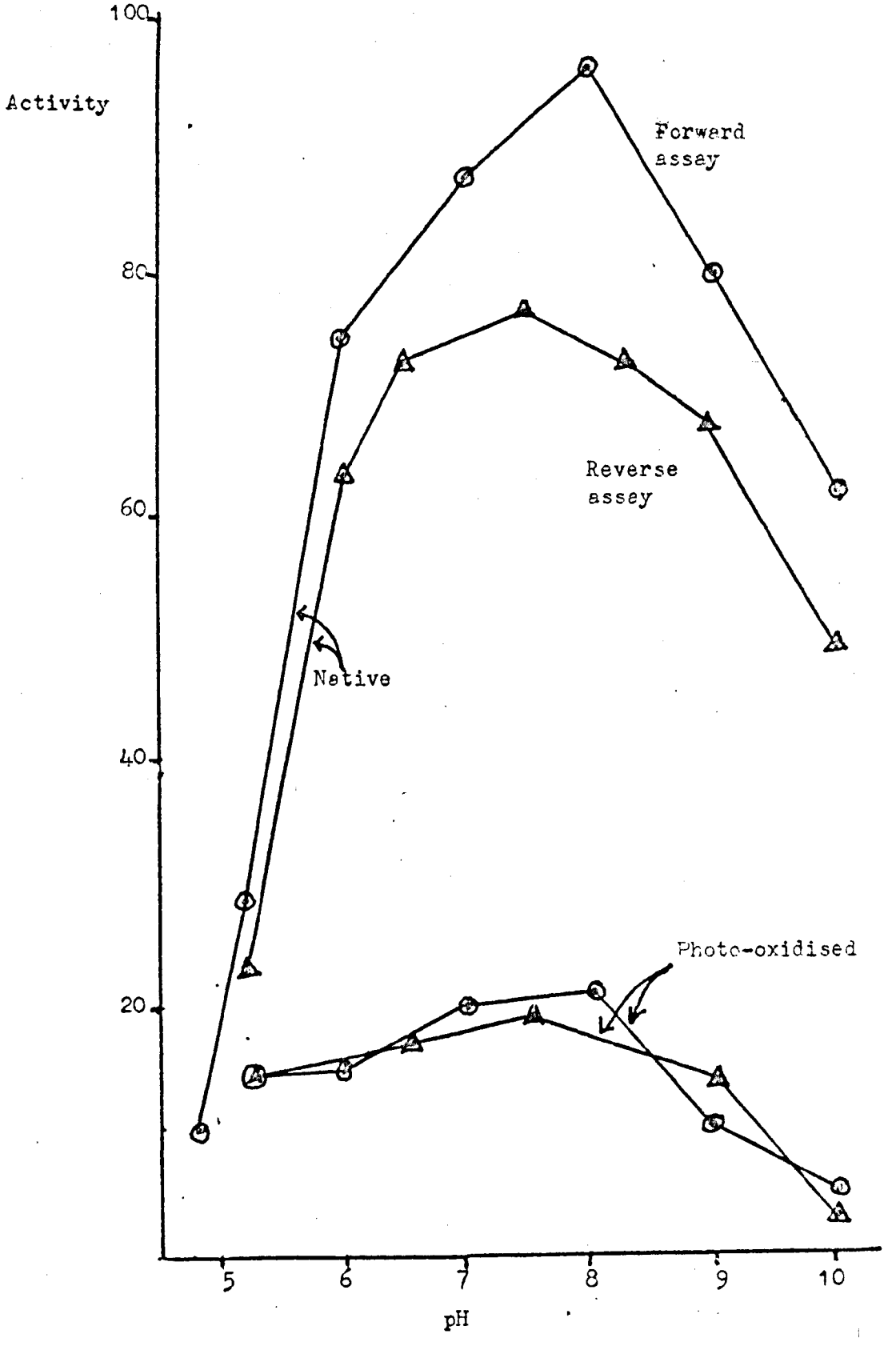
100
80
60
40
20
Activity
Forward assay
Reverse assay
Native
Photo-oxidised
5
6
7
8
9
10
pH

FIGURE 10.4

Photo-inactivation of PL-ala AT, by .005 % rose bengal, with 50 mM pH 7.5 phosphate buffer, at 12°C.

A A graph of ala AT activity against time.

⊙ the isotope exchange assay

△ the standard assay

B A graph of activity in the isotope exchange assay against activity in the standard assay.

TABLE 10.2

The table shows the proportion of the initial activity that remained after complete photo-oxidation by rose bengal of ala AT.

Results are given for the standard, reverse, aminobutyrate, ketobutyrate and isotope exchange assays at pH 7.5 and using high substrate concentrations, (see text).

FIGURE 10.4.

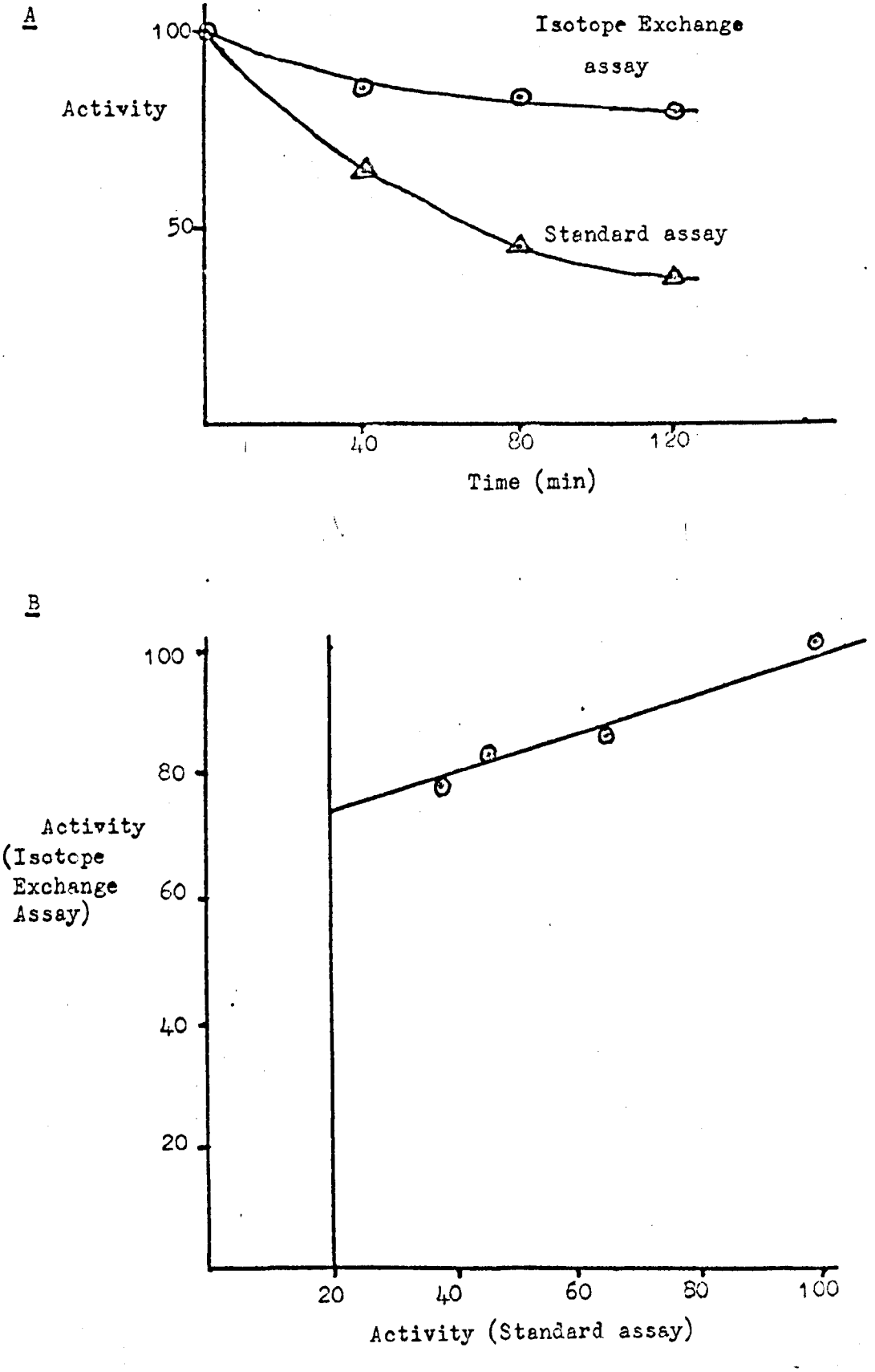
A
100
Activity
50
Isotope Exchange assay
Standard assay
40
80
120
Time (min)
B
100
80
Activity (Isotope Exchange Assay)
60
40
20
20
40
60
80
100
Activity (Standard assay)

TABLE 10.2.

Assay	Residual Activity / Initial Activity
Standard	20 %
Reverse	25 %
Aminobutyrate	100 %
Ketobutyrate	100 %
Isotope exchange	73 %

10.2(a) Kinetic Properties of Photo-oxidised Ala AT

The time course of photo-oxidation was followed with different assays, at different pHs: the forward assay (at 0.25 M L alanine and 10 mM ∝ketoglutarate), the reverse assay (at 0.4 M L glutamate and 6mM pyruvate), the aminobutyrate assay (at 0.4 M DL ∝ aminobutyrate and 1 mM ∝ ketoglutarate), and the ketobutyrate assay (at 40 mM L glutamate and 40 mM ∝ ketobutyrate)

The results for each assay were plotted against the standard assay, giving a linear plot. It was assumed that photo-oxidation was complete at $A_t = 20\ \% A_o$, for the standard assay. The final values for the other assays were taken from the intercepts on this line, (as in figure 10.4.B).

The aminobutyrate and ketobutyrate assays showed no change.

The forward and reverse assays gave similar pH profiles after photo-oxidation, but at a much reduced activity, (figure 10.3). The last assay at pH 7.5, (when the enzyme was more than 70 % photo-oxidised), was repeated with both substrate concentrations halved; it was no different. Hence for the forward and reverse assays, the measured fall in activity was due only to a rise in β_o.

The isotope exchange assay was carried out after varying periods of photo-oxidation. The results, (figure 10.4) indicated a residual activity of 73 %.

Table 10.2 shows the effect of photo-oxidation on five different assays at pH 7.5.

10.2(b) Stability of Photo-oxidised Alanine Aminotransferase

The photo-oxidised enzyme was unstable. After photo-oxidation to 33 % initial activity, the enzyme was dialysed against 10 mM ME, 5mM EDTA and 8 mg/l PLP.

TABLE 10.3

Photo-oxidation of PL-ala AT, by 0.005 % rose bengal, with 50 mM pH 7.5 phosphate buffer, at 12°C.

The changes in activity after partial photo-oxidation, and a subsequent dialysis, are shown for the standard assay and aminobutyrate assay.

FIGURE 10.5

Inactivation of PL-ala AT, at 50°C, in 5 mM ME, 5 mM EDTA and 50 mM pH 7.5 phosphate buffer.

A A graph of activity with time.

⊙ native ala AT

\+ after photo-oxidation with rose bengal

B A graph of $\log_{10}(A_t - A_\infty)$ with time, for ala AT that has been partially photo-oxidised by rose bengal. $A_\infty = 32$ gives the best straight line, (after 10 min).

TABLE 10.4

Inactivation of PL-ala AT, at 50 °C, in 5 mM ME, 5 mM EDTA and 50 mM pH 7.5 phosphate buffer.

The rate constant for the inactivation of the (rose bengal) photo-oxidised enzyme is given , in the presence of some substrates and inhibitors.

TABLE 10.3.

	Standard Assay %	AB Assay %
Native alaAT	100	100
Photo-Oxidised	30	97
after dialysis against buffer	0	0
after dialysis against buffer, ME, and EDTA	10	44
after dialysis against buffer, ME, EDTA, and PLP	14	60

FIGURE 10.5.

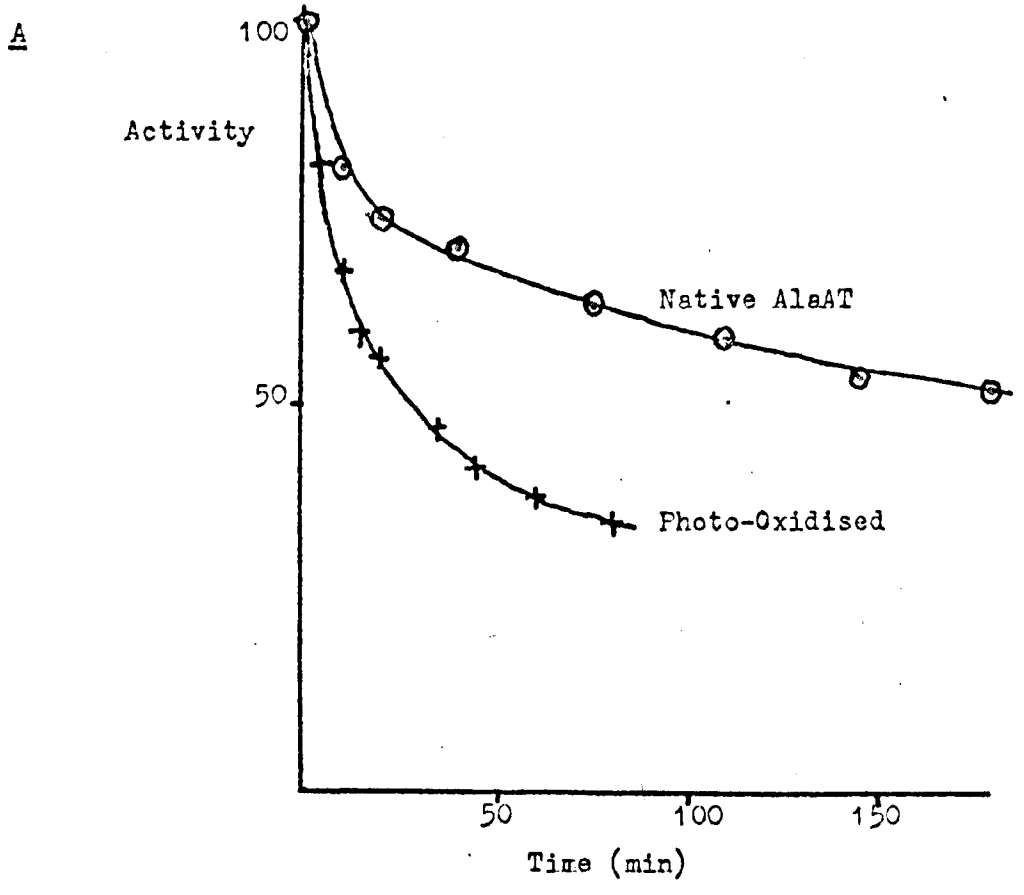
A
100
Activity
50
Native AlaAT
Photo-Oxidised
50
100
150
Time (min)

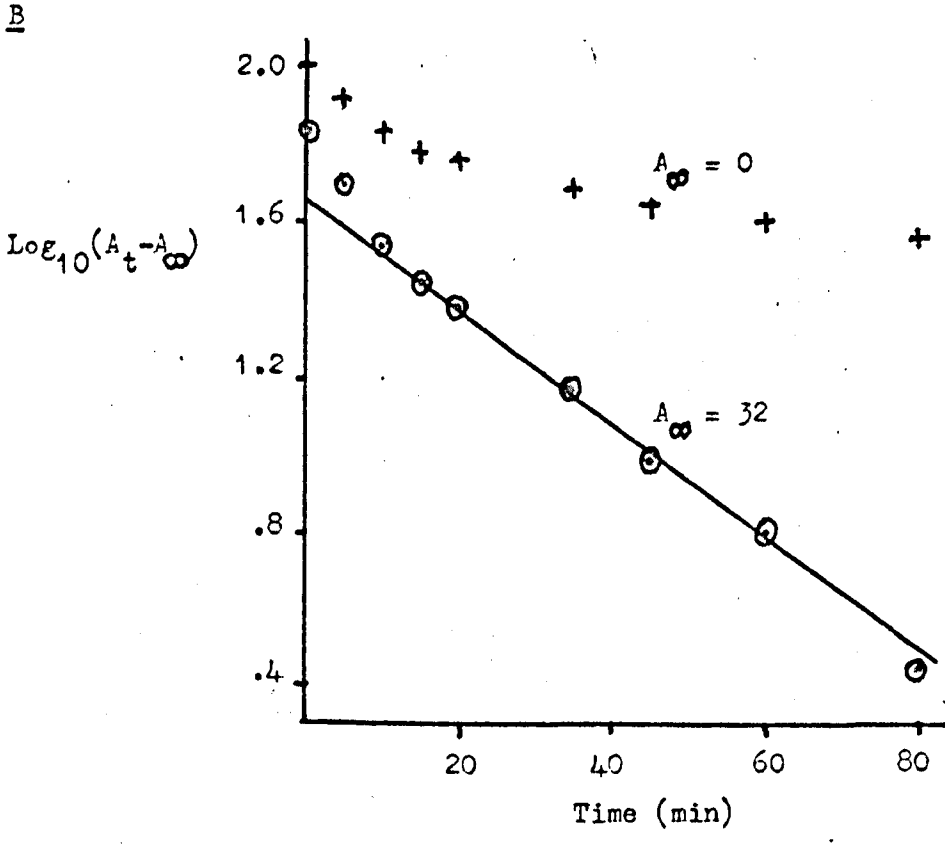
B
2.0
1.6
1.2
.8
.4
$Log_{10}(A_t - A_\infty)$
$A_\infty = 0$
$A_\infty = 32$
20
40
60
80
Time (min)

TABLE 10.4.

Additions	Rate (10^{-2} min^{-1})
—	4.1
100mM L Ala + 2mM Pyr	2.6
100mM L Glu + 2mM ∝KG	3.0
200mM Formate	3.8

The results, (table 10.3), showed an almost complete inactivation on dialysis. With ME plus EDTA, it was considerable, and with PLP as well, the protection was only slightly greater. N.B. Over half the residual activity was due to "unphoto-oxidised" enzyme.

The two assays, (forward and aminobutyrate), show similar inactivation on dialysis, and similar protection.

It seems very likely that the instability of the enzyme was due to a second photo-oxidation, quite distinct from the photo-inactivation.

The photo-oxidised enzyme was considerably more heat labile than the native enzyme. The heat inactivation experiment of chapter 9 was repeated at 50°C on the native and photo-oxidised enzyme, (figure 10.5). The slow inactivation was almost absent in the native enzyme. After partial photo-oxidation, it was considerable, but partial - after 10 min. it fitted the equation $\log(A_t - A_\infty) = kt$. A_∞ was found by trial. This equation assumes that, the native enzyme was completely stable at 50°C. All the same, both linear and reproducible results were obtained. The rate constants are given in table 10.5: they show substrate protection, but no significant effect attributable to a separate protection at the γ carboxyl site.

It has not been proved that the photo-inactivation and the increased heat lability are due to the oxidation of the same group.

10.2(c) Discussion

The identity of the K_i and K_m for α aminobutyrate shows that it binds to most of the enzyme and is transaminated by most of the enzyme. It is not possible to maintain that 20 % of the

enzyme is resistant to rose bengal photo-oxidation and that this 20 % carries all the aminobutyrate activity. Hence the residual activity is the activity of the photo-oxidised enzyme. The measured inactivation was due to a rise in ϕ_0 and was very dependent on the substrate.

The C_4 substrates showed no inactivation. The C_3 substrates showed a small drop in activity. The effect was much greater in the forward and reverse assays, when the C_5 substrates gave a large contribution to ϕ_0.

The γ carboxyl group is distinguished by three factors. Binding at the γ carboxyl site seems to give some protection against photo-inactivation. The protection afforded against heat inactivation, by the γ carboxyl group, is lost. The rise in ϕ_0 is greatest where the substrate has a γ carboxyl group.

The pH independence of the inactivation rate suggests only that the modified residue was not histidine, and therefore was tyrosine, cysteine or tryptophan.

10.3 RESULTS USING METHYLENE BLUE

Figure 10.6. shows activity against time at pH 8.0, (at 25°C, with methylene blue, and using the standard assay); it is first order. AT 12°C, at high pH a similar result was obtained. At low pH the reaction was not first order and seemed to give some residual activity. Because of this, results at all pHs were taken from 100 to 50 % activity and rate constants were taken from the simple first-order plots.

The variation of this rate constant with pH showed a simple pK at pH 7.6, (figure 10.7).

There was some evidence that methylene blue photo-oxidation

FIGURE 10.6

Photo-inactivation of PL-ala AT, by .0017 % methylene blue, with 50 mM pH 8.0 tris buffer, at 25°C.

A A graph of ala AT activity against time

B A graph of $\log_{10}$(activity) against time

FIGURE 10.7

Photo-inactivation of ala AT, by .0017 % methylene blue, in 50 mM buffer, at 12°C.

A graph of the rate constant for inactivation against pH.

⊙ for PM-ala AT or PL-ala AT

\+ with 133 mM L alanine and 1.33 mM pyruvate

× with 133 mM L glutamate and 1.33 mM ∝ ketoglutarate

FIGURE 10.8

Photo-inactivation of ala AT, by 0.0017 % methylene blue, in 50 mM buffer, at 25°C

A graph of the rate constant for inactivation against pH.

⊙ for PL-ala AT

△ for PM-ala AT

\+ with 670 mM DL ∝ aminobutyrate and 3 mM pyruvate

× with 670 mM DL ∝ aminobutyrate

FIGURE 10.6.

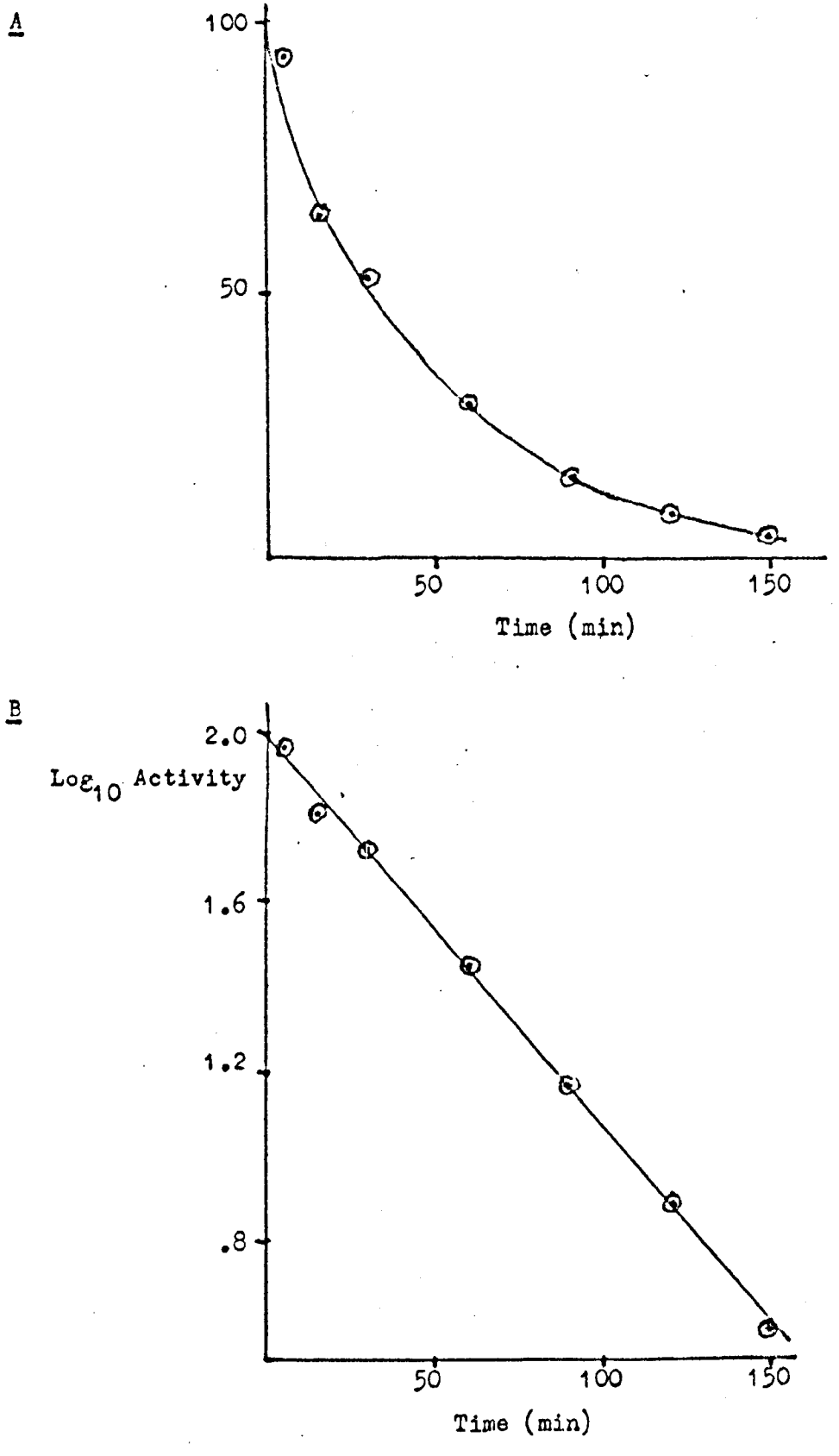
A
100
50
50
100
150
Time (min)
B
2.0
Log10 Activity
1.6
1.2
.8
50
100
150
Time (min)

FIGURE 10.7.

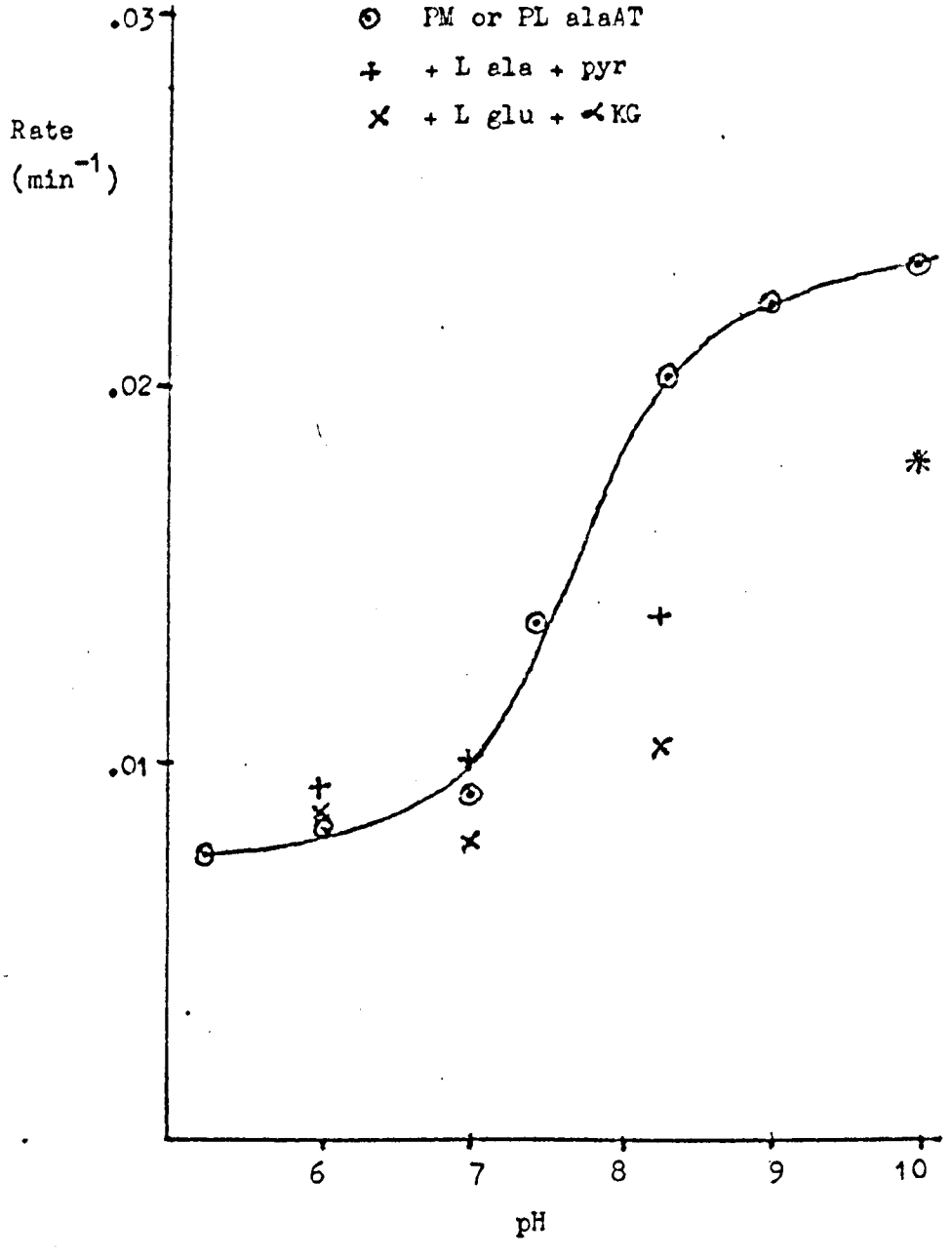

FIGURE 10.8.

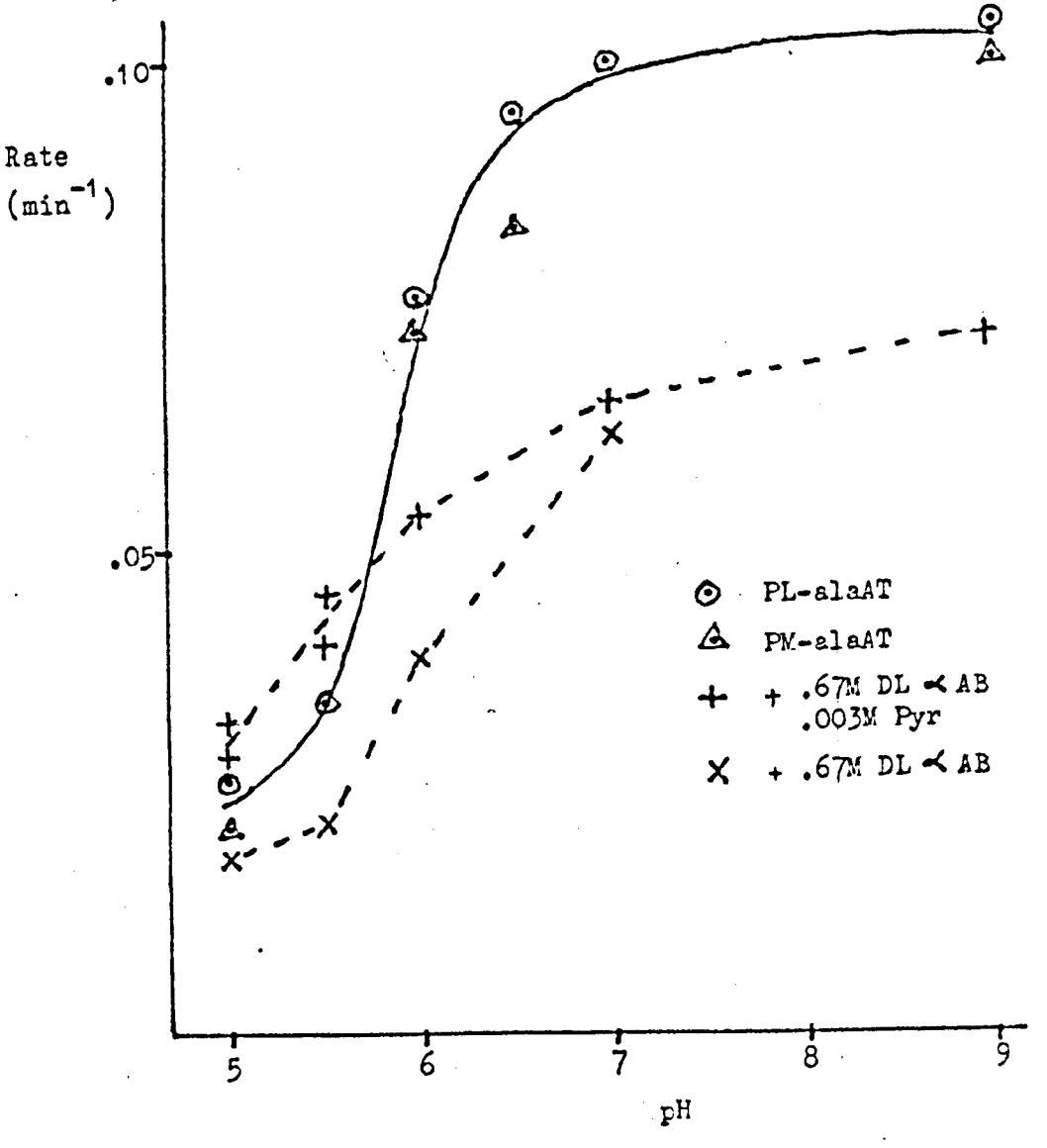
.10
.05
Rate
(min^{-1})
5
6
7
8
9
pH
PL-alaAT
PM-alaAT
+ .67M DL ∝ AB
.003M Pyr
+ .67M DL ∝ AB

at pH 5.2 was like rose bengal photo-oxidation.

(A) There was a residual activity.

(B) There was no loss of aminobutyrate activity at low pH, while at high pH the loss of aminobutyrate activity was slightly slower than the loss of standard activity.

(C) After photo-oxidation with methylene blue at pH 5.2 for five hours, the activity dropped to 28 %. This solution was then photo-oxidised with rose bengal (which involved a three-fold dilution). This second inactivation was very rapid, (and almost totally due to the rose bengal) and gave a calculated residual activity of 58 % of the activity at the start of the rose bengal photo-oxidation.

Suppose the two photo-oxidations involved the same residue. The final residual activity should be expressed in terms of the activity before either photo-oxidation, and would then be 28 % × 58 % which is 17 %; not far from 20 %.

Both L alanine plus pyruvate and L glutamate plus ∝ketoglutarate gave pH dependent, partial protection,(figure 10.7).

For comparison with other experiments, methylene blue photo-oxidation was repeated at 25°C.

At pH 7, the inactivation was first order to below 4 %, (figure 10.6). The results are given in figure 10.8.

There was no coenzyme effect or buffer effect. There was a pK at about pH 5.9. The protonated form was inactivated slowly.

∝Aminobutyrate protected PM-ala AT. ∝Aminobutyrate with pyruvate lowered the rate at high pH and raised it at low pH. Although some L alanine and ∝keto-butyrate were formed during the experiment,their concentrations were always low.

An attempt was made to predict the effect of saturating the enzyme with substrates,using the kinetic parameters of chapter 6.

TABLE 10.5

Photo-oxidation of ala AT, by .0017 % methylene blue, at 25°C, 50 mM buffer, at four pHs.

Rate constants for inactivation are given for ala AT plus 670 mM ∝ aminobutyrate and 3 mM pyruvate. Using the kinetic results of chapter 7, an attempt is made to predict the rate constants for the ala AT-∝aminobutyrate complex.

FIGURE 10.9

Photo-inactivation of ala AT, by 0.0017 % methylene blue, at 25°C, in 50 mM buffer.

A graph of the rateconstant for inactivation against pH, for the ala-AT-∝ aminobutyrate complex.

There are two graphs, calculated in two different ways. Points are shown with a 10 % error.

TABLE 10.5.

pH	5.0	5.5	6.0	7.0
K_{AB} (M)	.830	.900	.250	.120
AB-alaAT / total alaAT	.45	.43	.73	.85
mean rate + AB + Pyr (min^{-1})	.0295	.0427	.055	.065
rate, PL-alaAT (min^{-1})	.026	.0336	.076	.101
projected rate, AB-alaAT	.034	.055	.048	.058
rate, PM-alaAT + AB (min^{-1})	.0185	.022	.039	.062
projected rate, AB-alaAT (min^{-1})	.043	.070	.061	.065

FIGURE 10.9.

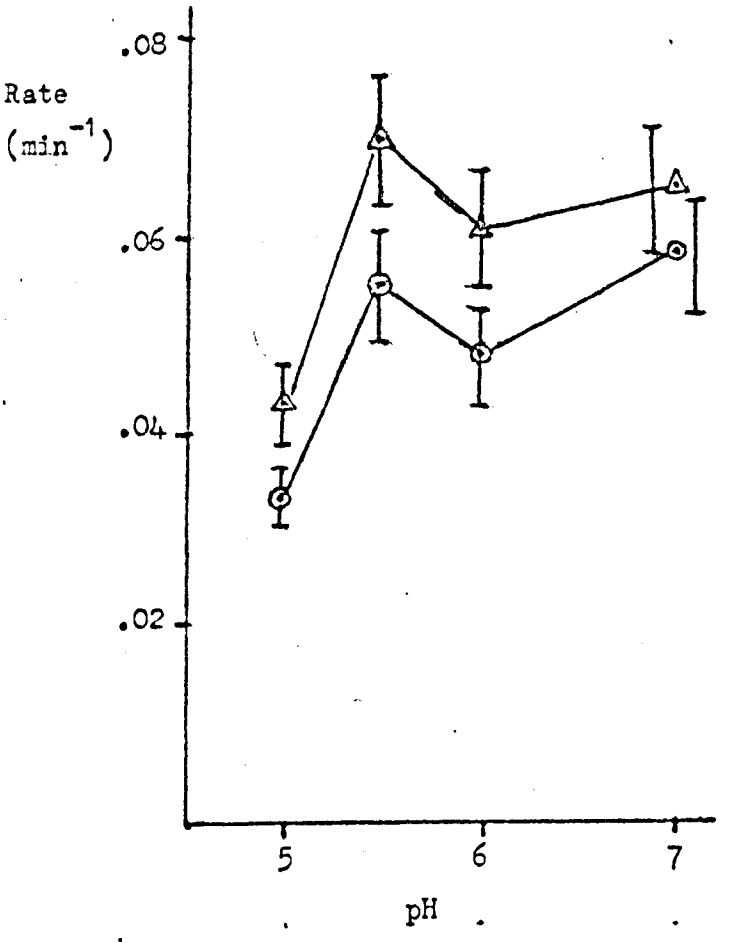

The calculation is shown in table 10.5 and the predicted values in figure 10.9. The calculation assumes either; (A)that the protection of the PM form by ∝aminobutyrate was due to binding at the active site, or; (B)that this protection was due to some other effect,(such as association with the dye), that affects the PM and PL forms equally.

Both calculations indicate that the pK in the ∝ aminobutyrate-PL-ala AT complex had been shifted from pH 5.9 to below pH 5.5.

10.3(a) Discussion

The pK for photo-oxidation is generally close to,but not identical with,the pK of the group under attack (14). The group is likely to be a histidyl residue, as this is the only labile group with a pK between pH 5 and 9 (209).

The change in pK between 10°C and 25°C was enormous and not easily explained.

The pK at 25°C was close to that shown by the kinetics, for the PL and PM forms. As in the kinetic results, this pK was lowered in the ∝ aminobutyrate-PL-alaAT complex.

CHAPTER 11

AMINO-GROUP REAGENTS

11.1 INTRODUCTION

In ala AT, lysine is the residue that forms the internal aldimine with the PLP. It has been suggested that a second lysine might bind the α carboxyl group of the substrates (160). Experiments were undertaken with amino-group reagents, to investigate the role of lysine.

11.2 ACID ANHYDRIDES

After one hour's incubation with 5 mM succinic anhydride or acetic anhydride, at pH 8 and 25°C, there was no fall in the activity of the PL or PM form of ala AT. Under these conditions, reaction with free amino-groups should have been complete (74, 197).

11.3 ALDEHYDES

No inhibition at pH 8 and 25°C, was observed in the presence of 0.1 M propionaldehyde or 0.1 M salicaldehyde. Formaldehyde gave considerable inhibition. At pH 7, the following values of the formaldehyde K_i were obtained, (see figure 11.1).

from ϕ_0 (i.e. binding to the enzyme-substrate complex)	1.0 mM
from ϕ_{ala} (i.e. binding to the PL-ala AT)	high
from ϕ_{KG} (i.e. binding to the PM-ala AT)	0.75 mM

However, formaldehyde gave a slow irreversible inactivation, which would make extensive investigations of reversible inhibition risky.

FIGURE 11.1

The forward assay, in 50 mM pH 7.0 phosphate buffer, at 25°C.

A A Lineweaver-Burk plot, with L alanine as substrate, at 2.7 mM ∝ ketoglutarate, and 0 mM, 1 mM, or 2 mM formaldehyde.

B A Lineweaver-Burk plot, with ∝ ketoglutarate as substrate, at 100 mM L alanine, and 0 mM, 1 mM, or 2 mM formaldehyde.

C ⊙ A graph of apparent ϕ_{KG} against formaldehyde concentration.

× A graph of apparent ϕ_{0} against formaldehyde concentration.

FIGURE 11.2

Inactivation of PM-ala AT, by 50 mM formaldehyde, in 50 mM pH 7.0 phosphate buffer, at 25°C.

A A graph of ala AT activity against time.

B A graph of $\log_{10}$(activity) against time.

TABLE 11.1

Inactivation of ala AT, by formaldehyde, at 25°C.

Rate constants of inactivation are given at different pHs, buffer concentrations and formaldehyde concentrations, for different forms of the enzyme, and in the presence of some substrates and inhibitors.

Results are expressed in $10^{-3}min^{-1}$.

FIGURE 11.1.

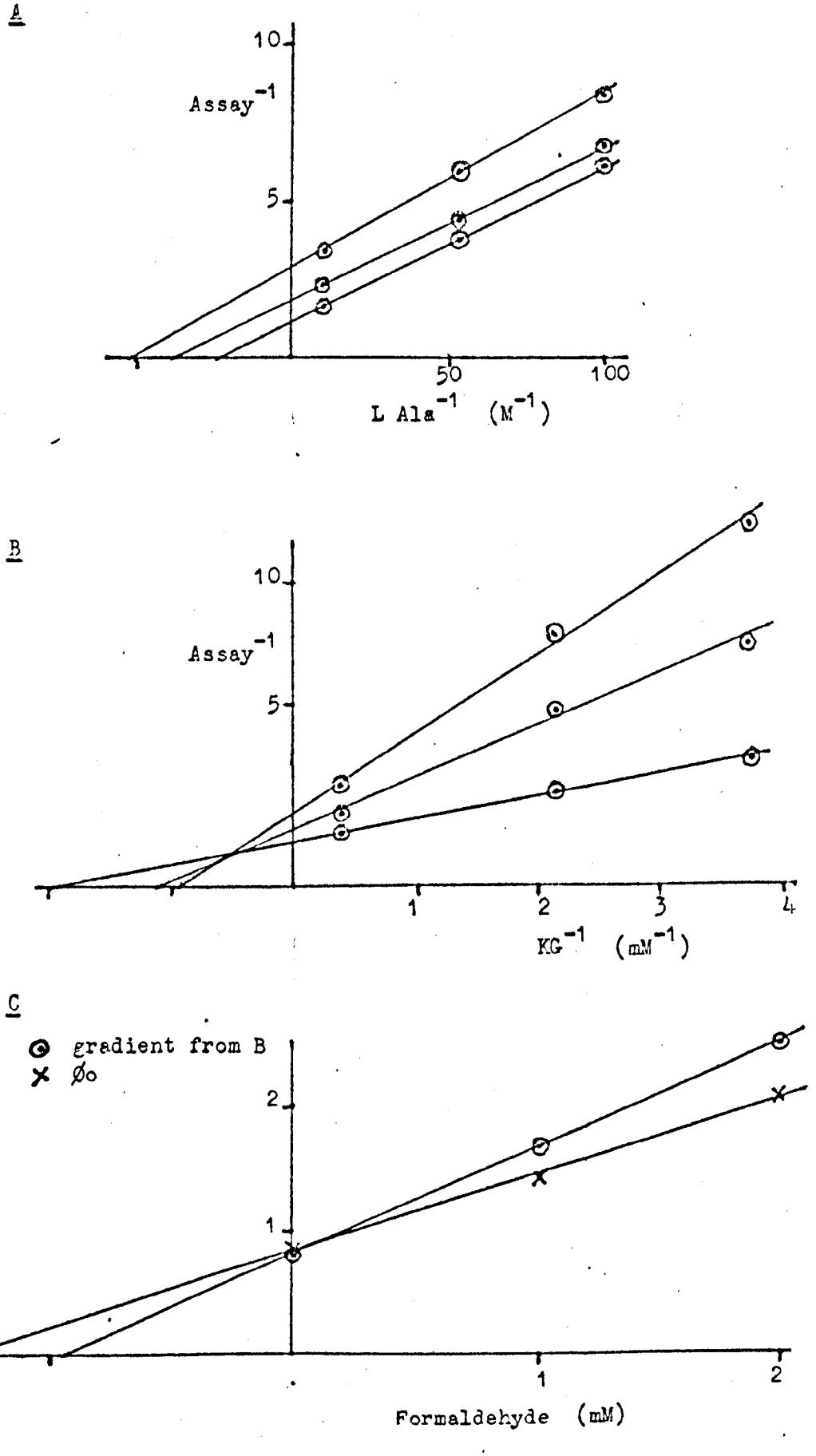
A
10
Assay^{-1}
5
50
100
L Ala^{-1} (M^{-1})
B
10
Assay^{-1}
5
1
2
3
4
KG^{-1} (mM^{-1})
C
gradient from B
Øo
2
1
1
2
Formaldehyde (mM)

FIGURE 11.2.

A

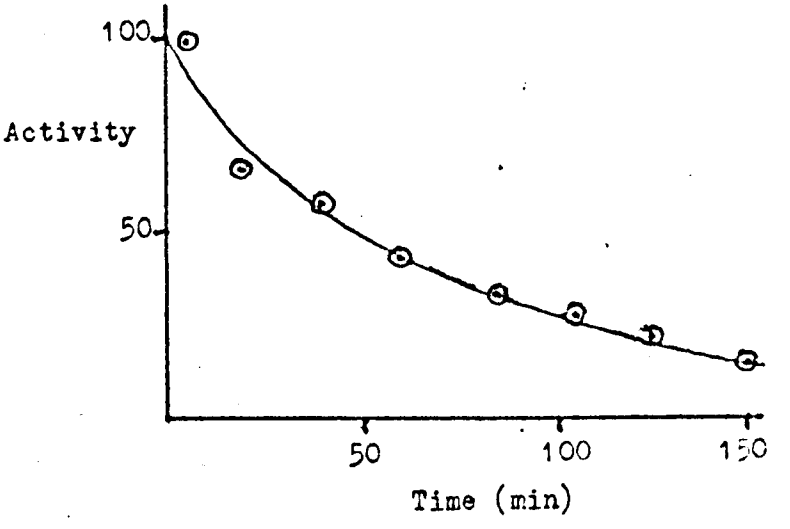

B

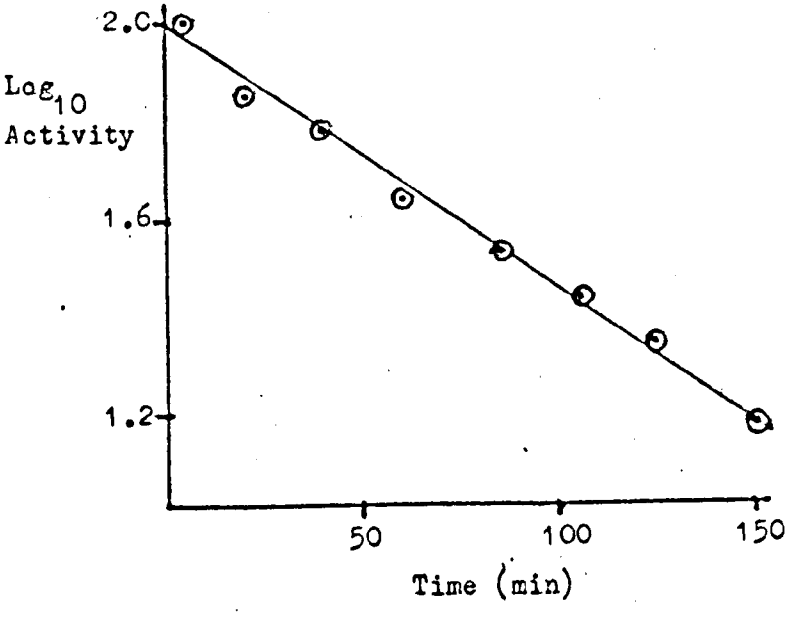

TABLE 11.1

Addition	Formaldehyde (mM)	pH								
		5.0	5.5	6.0	6.5	7.0	7.5	8.0	9.0	10.0
PL	20			0				1.7	12.5	13.1
	50			0		4.0			35	
.10OM Fumarate	20								11.7	
.20OM L Aspartate	50					5.0				
.10OM ∝ Methyl Glu	50					6.3				
PM	20			6.9		12.5		1.9	88	122
	50	7.8	17.3	16.6	28	27	14.6	4.8	186	
.02OM Buffer	50							5.9		
.15OM Buffer	20								100	13.4
	50	9.0	13.9	10.4	20.3	25	14.6	0		
.10OM Fumarate	20								132	
	50			17.2		24.6		13.4		
.10OM Maleate	50							3.2		
.3OM L Ala .008M Pyr	50					22.4		22.6		
.3OM ∝ AB .008M Pyr	50					22.4				

11.4 FORMALDEHYDE

11.4(a) Introduction

In 1944, Neuberger (150) showed that formaldehyde attacks histidine. It binds rapidly and reversibly to the amino group and to the imidazole nitrogens. There is a slow irreversible reaction, giving a product in which the formaldehyde links the amino nitrogen to an imidazole carbon atom and the ring is broken. The rate constants shows a pK at pH 6.5.

Fraenkel-Conrat and Olcott (60, 61) showed that formaldehyde reacts with polyamines to give aminomethylol which can react irreversibly, fixing indoles, guanidine, primary amides and imidazole. Formaldehyde reacts irreversibly with proteins. The total moles of formaldehyde bound never exceeded the number of amino groups in the free enzyme, or the sum of the histidyl and tryptophanyl residues.

It is now generally accepted that the irreversible reaction of formaldehyde with protein is due to the formation of a bridge between an amino group and an imidazole or indole (45). This means that it can show the spatial proximity of two such groups.

11.4(b) Inactivation

Figure 11.2 shows the change in activity with time, when PM-ala AT was incubated with 50 mM formaldehyde at pH 7 and 25°C. The inactivation was first order to below 16 %.

Table 11.1 and figure 11.3 show the variation of rate with pH, buffer concentration, formaldehyde concentration and the state of the coenzyme. It was not possible to measure rapid rates of inactivation accurately. The results at pH 9 and 10 should be treated as semi-quantitative.

FIGURE 11.3

Inactivation of PM-ala AT, by 50 mM formaldehyde, at 25°C.

A graph of the rate constant of inactivation aginst pH.

+ Results at 50 mM buffer

⊙ Results at 0 mM buffer. These were calculated by assuming that the dependence of the rate constant on buffer concentration was linear.

FIGURE 11.4

A PM-ala AT sample was resolved, and the apoenzyme was removed (as described in chapter 2). The absorption spectrum was obtained for equal quantities of native ala AT and ala AT, partially, (77 %) inactivated by formaldehyde.

⊙ native ala AT

+ after formaldehyde treatment

FIGURE 11.5

Titration of TSC against PL-ala AT, in 50 mM pH 7.0 phosphate

One sample was native ala AT. One sample had been 62 % inactivated by formaldehyde, (see text).

A graph of $(\Delta A_{390})^{-1}$ against $(TSC)^{-1}$.

⊙ native ala AT

△ after formaldehyde treatment.

FIGURE 11.3.

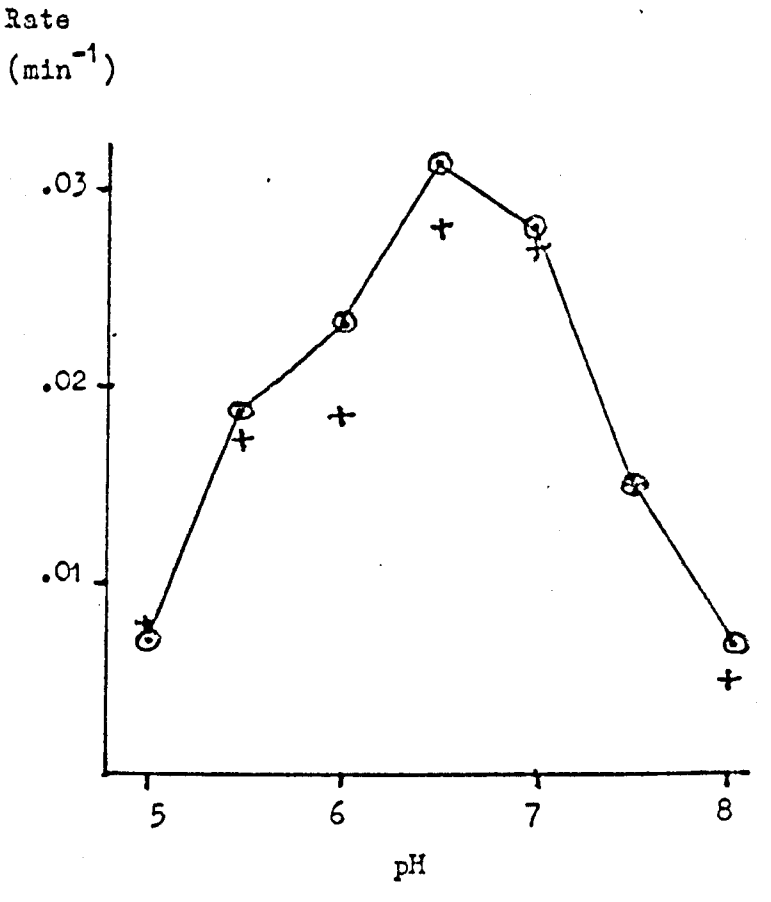

FIGURE 11.4.

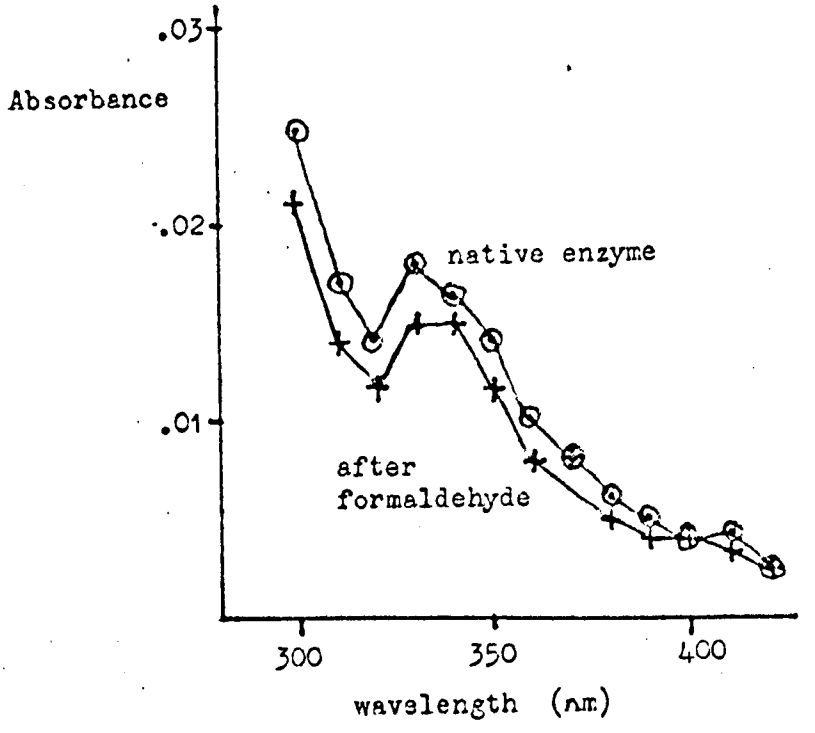
.03
Absorbance
.02
.01
native enzyme
after
formaldehyde
300
350
400
wavelength (nm)

FIGURE 11.5.

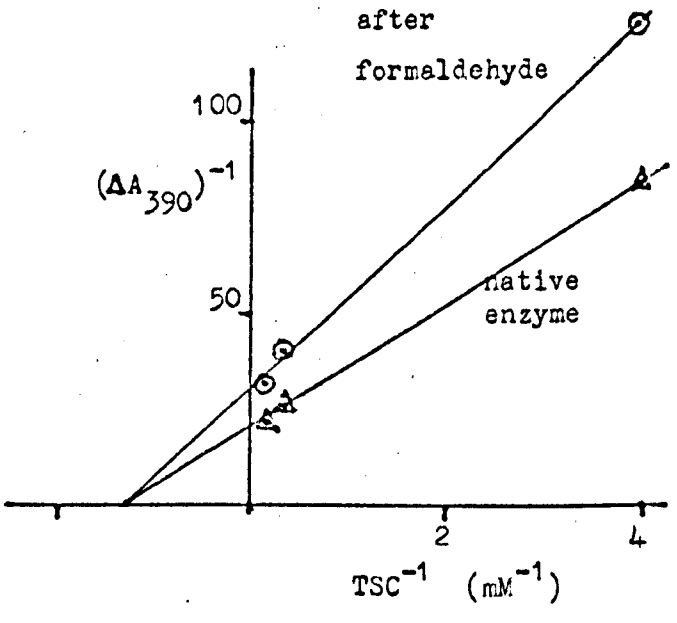
after
formaldehyde
100
$(\Delta A_{390})^{-1}$
50
native
enzyme
2
4
TSC^{-1} (mM^{-1})

PM-ala AT and the enzyme-substrate complex are considerably more labile than PL-ala AT.

The buffer effect was slight and was calculated out on the assumption that the rate was proportional to the buffer concentration. On this basis PM-ala AT inactivation showed three pKs at about pH 5.6, 7.4 and 8.5.

The reaction velocity was unaltered when the enzyme had been acetylated, (under the conditions described in 11.2).

The effect of adding substrate or inhibitors may be complicated Possibly, their binding is reduced in 50 mM formaldehyde. All the same, it is apparent that the binding of substrate or fumarate increases the rate considerably at pH 8 and not at pH 7.

11.4(c) Absorption Spectra

The following experiment was designed to test whether formaldehyde formed a covalent bridge between the amino group of PMP and the protein.

The PM form was incubated with 50 mM formaldehyde until the activity had fallen to 23 %. The non-covalently bound PMP was assayed as described in chapter 2. Figure 11.4 shows the spectra obtained before and after inactivation. The change in the quantity of PMP released was small and not significant. Very little of the coenzyme became covalently bound.

The PL form was incubated with 100 mM aspartate, 50 mM formaldehyde and 50 mM pH 8.0 tris chloride, until the activity had fallen to 38 %. Equal samples of the native and treated ala AT were dialysed overnight against 5 mM ME and 5 mM EDTA at pH 7: there was no change in activity. They were diluted to the same volume; pH 7.0 phosphate was added to 50 mM, and the visible

spectrum was recorded. They were titrated against TSC, as shown in figure 11.5.

The p_{430} had fallen to 74 % in the treated enzyme and in the TSC titration, the spectral change was down to 71 % while the K_{TSC} was unchanged.

11.4(d) Discussion

The pK~5.6 suggests a histidine group of similar pK was involved in the reaction. The position of the pK > 8.5 is most indeterminate: it could be a lysine pK, the aminomethylol pK, the pK of the product, or it could be due to the use of a glycine buffer at high pH. The pK 7.4 is difficult to interpret. If it belonged to a group under attack or was hydrogen-bonded to one, or had an inductive effect, one would expect the velocity to increase with pH. Perhaps it is connected with a conformational change, (that does not occur in the enzyme-substrate complex). The spatial relationship of the two bridged residues is a very important factor.

The higher stability of the PL form suggests that the amino group could belong to the lysine of the internal aldimine, which is free in the PM form and in the enzyme- substrate complex.

The reversible formaldehyde inhibition shows poor binding to the PL form. This too, can be explained by formaldehyde binding to the free lysine from the internal aldimine.

The two phenomena show quite different dependences on the formaldehyde concentration. The inactivation indicates a high K_s atypical of an amino group. The imidazole ring is able to bind formaldehyde and the K_s was estimated as 30 mM (169) and 70 mM (109).

FIGURE 11.6

Inactivation of PL-ala AT, by .3 M nitrite, in 50 mM acetate buffer, at 25°C.

A A graph of ala AT activity with time.

B A graph of $\log(A_t - A_\infty)$ with time. The best straight line was obtained with $A_\infty = 16$.

TABLE 11.2

Inactivation of ala AT, by .3 M nitrite, in 50 mM acetate buffer, at 25°C.

The rate constants for inactivation are given , for different forms of the enzyme, at different nitrite concentrations, and in the presence of two inhibitors.

FIGURE 11.6.

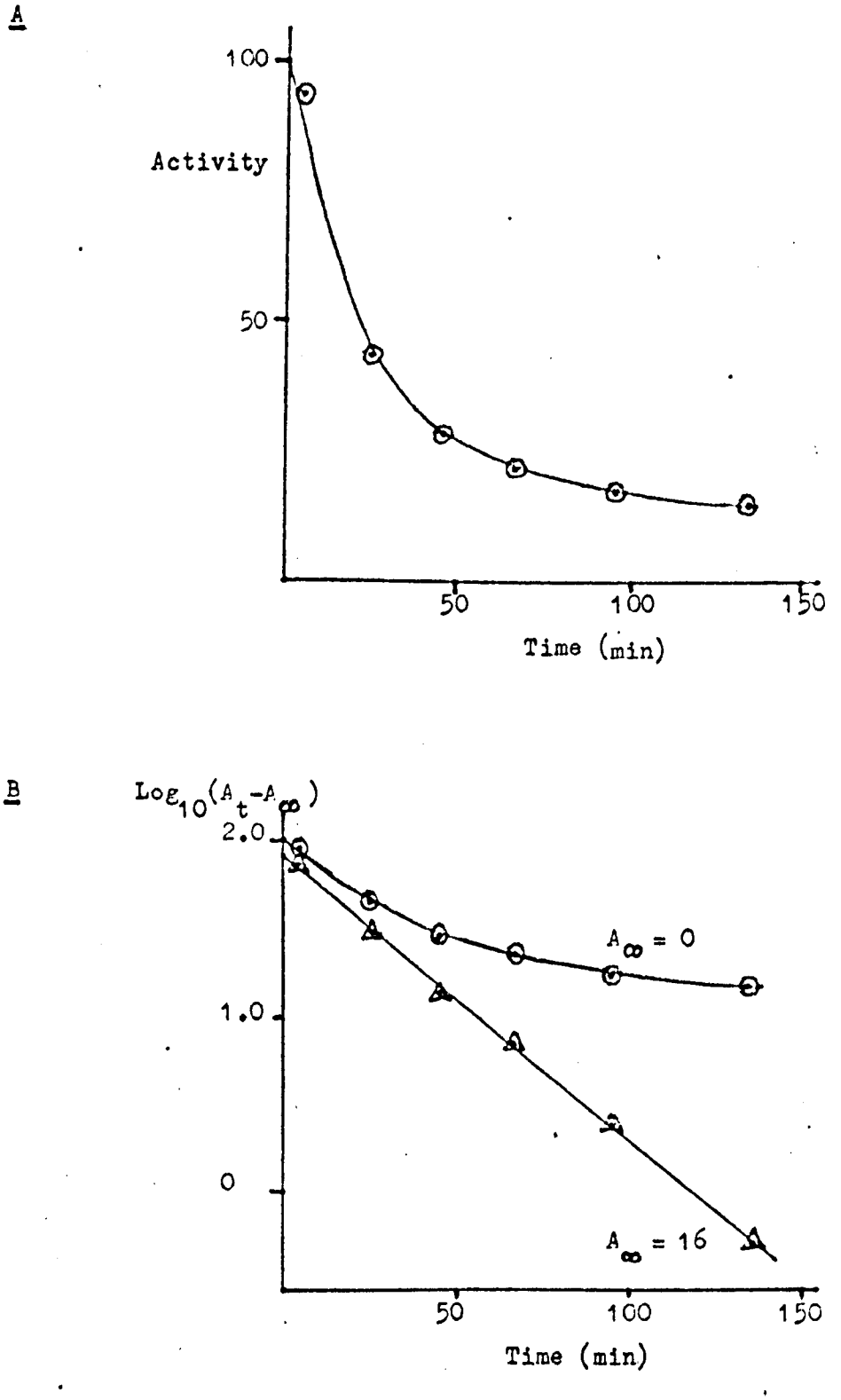
A
100
Activity
50
50
100
150
Time (min)
B
$Log_{10}(A_t - A_\infty)$
2.0
1.0
0
$A_\infty = 0$
$A_\infty = 16$
50
100
150
Time (min)

TABLE 11.2.

Coenzyme	Addition	Nitrite		
		.50M	.30M	.10M
PM		4.7		
PL		1.71	1.88	0.65
PL	5mM TSC		1.66	
PL	.10M Fumarate		0.84	

The spectral experiments show that with PM-ala AT, the PMP does not supply the amino group. With the aspartate- PL ala AT complex, the internal aldimine lysine did not supply the amino group, or the TSC binding would surely have been greatly affected. As the rate of attack was five times slower and included some loss of coenzyme, the inactivation reaction was probably different in the aspartate PL-ala AT complex from what it was in PM-ala AT.

11.5 NITRITE

The reaction of nitrite at low pH has been used to study the roles of tyrosine and amino groups. With tyrosine, a yellow nitrated product is produced (157, 158). The reagent also attacks cysteine residues but this reaction can be reversed by thiols. (135, 136) The attack on amino groups can be specific (199).

Figure 11.6 shows the fall in activity with time when PL- ala AT was incubated with 0.3 M nitrite at pH 5. If it was first order, a residual activity of about 16 % remained.

Table 11.2 shows the effect of different conditions on the rate constant. PM- ala AT was labile. Fumarate gave considerable protection of the PL form; TSC did not.

No experiment in this chapter showed any inactivation that could be attributed to the modification of a lysine that binds the αcarboxyl group of the substrate.

CHAPTER 12

TETRANITROMETHANE

12.1 INTRODUCTION

In 1966, the action of the electrophilic reagent, tetranitromethane, (TNM), was described (165, 183). It nitrates tyrosine, giving 3 nitrotyrosine, which has an absorption peak at 430 nm. It attacks cysteine rapidly, to give the sulphinic acid or the disulphide; (the latter reaction can be reversed by thiol reagents (184). It attacks tryptophan slowly (185).

The first enzyme studied with TNM was carboxypeptidase A (166). Aldolase has since been studied and showed a greater lability when substrate was bound - "syncatalytic effect" (32, 167).

Asp AT was studied. The enzyme-substrate complex, (especially with β hydroxy aspartate), gave a faster production of nitroformate than the free enzyme did (179). It has been suggested that this might be due to a reaction with the deprotonated intermediate.

Holo asp AT is inactivated slowly (178); apo-asp AT rapidly; and the enzyme-substrate complex rapidly (33). In the last two cases (after cysteine treatment), there was an increased inactivation corresponding to one extra modified tyrosine (33, 198). The position of this tyrosine in the primary amino-acid sequence has been determined (20, 162).

There is a syncatalytic modification of a specific cysteine residue, (obtained with other reagents too) (16, 17, 18, 20, 32).

The relationship of these two events to the activity and to

FIGURE 12.1

Inactivation of PL-ala AT, by 0.6 mM tetranitromethane, (TNM), in 50 mM pH 8.0 tris buffer, at 25°C.

A A graph of ala AT activity against time.

B A graph of $\log_{10}(A_t - A_\infty)$ against time. The best straight line was obtained with $A_\infty = 9$.

TABLE 12.1

Inactivation of PL-ala AT, by 0.6 mM TNM, at 25°C.

The rate constants of inactivation are given, for different forms of the enzyme, at different pHs, and in the presence of some substrates and inhibitors.

Results are expressed in 10^{-3}min^{-1}.

FIGURE 12.2

Inactivation of ala AT, by 0.6 mM TNM, at 25°C, in 50 mM buffer. The rate constants of inactivation are plotted against pH. A The increase in the rate constant when L alanine and pyruvate are added to excess, to:

△ PL-ala AT

⊙ PM-ala AT

B A graph of rate constant against pH for:

△ PL-ala AT

⊙ PM-ala AT

\+ ala AT plus L alanine and pyruvate

FIGURE 12.1.

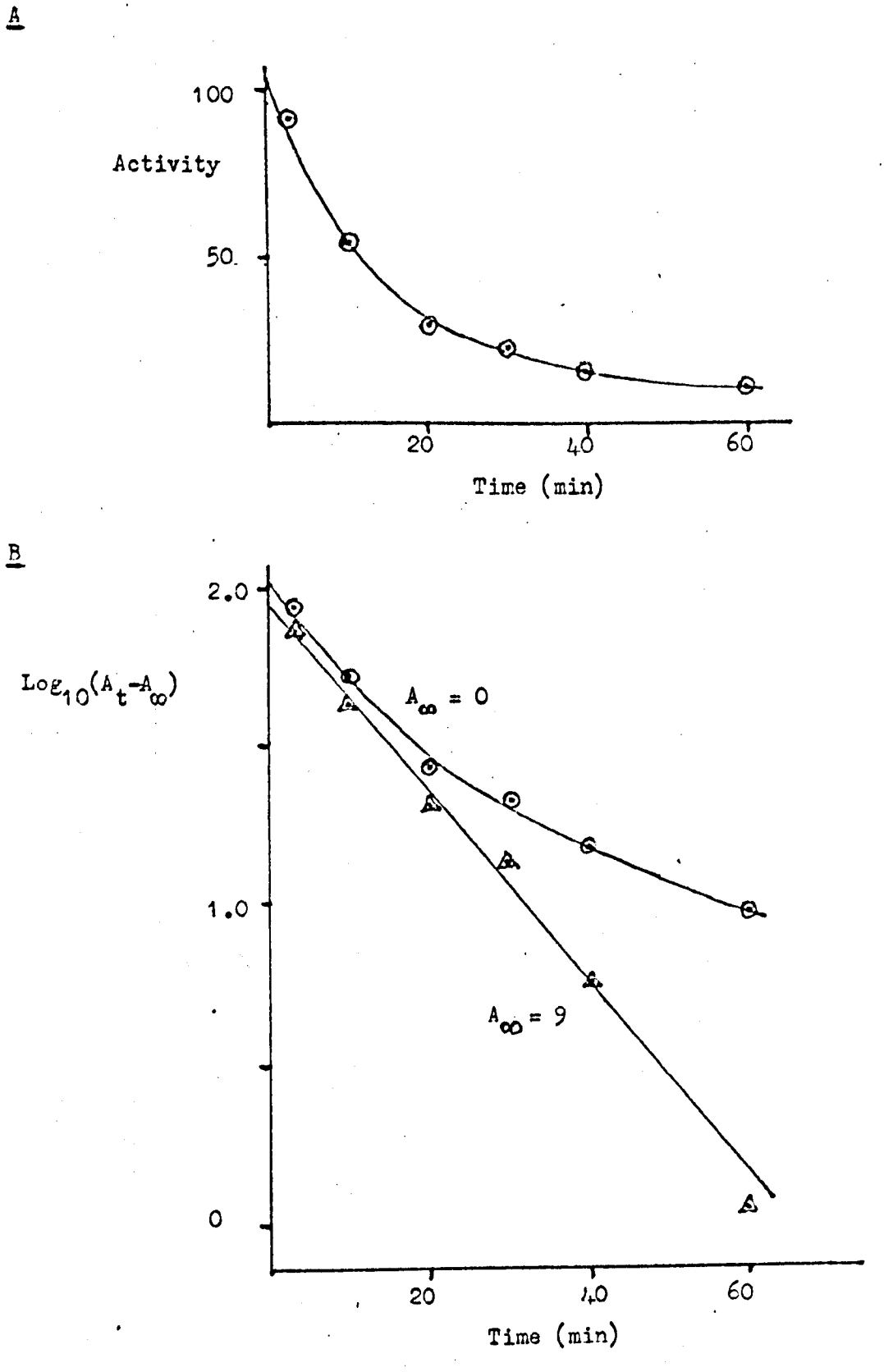
A
100
Activity
50
20
40
60
Time (min)
B
2.0
$Log_{10}(A_t - A_\infty)$
$A_\infty = 0$
1.0
$A_\infty = 9$
0
20
40
60
Time (min)

TABLE 12.1.

pH	6.0	6.5	7.0	7.5	8.0	8.5	9.0
PM-alaAT	8.7		18		55	143	
PL-alaAT	6.5	7.6	13.8	28	55	175	high
PM-alaAT + .070M Fumarate					44		
PL-ala AT + .070M Fumarate			21		46		
+ .002M ∝KG + .060M L Glu					25		
+ .004M ∝KG + .200M L Glu			11.5				
+ .006M ∝KG + .300M L Glu	3.9						
+ .003M Pyr + .100M L Ala				57	92	230	
+ .008M Pyr + .200M L Ala			37				
+ .010M Pyr + .300M L Ala	4.8	10.8					
.008M Pyr + .200M L Ala + .250M Formate			21				
+ .008M Pyr			13.6				
+ .200M L Ala			14.0				
+ .002M ∝KG					53		
+ .060M L Glu					44		
.150M Buffer			13.8				

FIGURE 12.2.

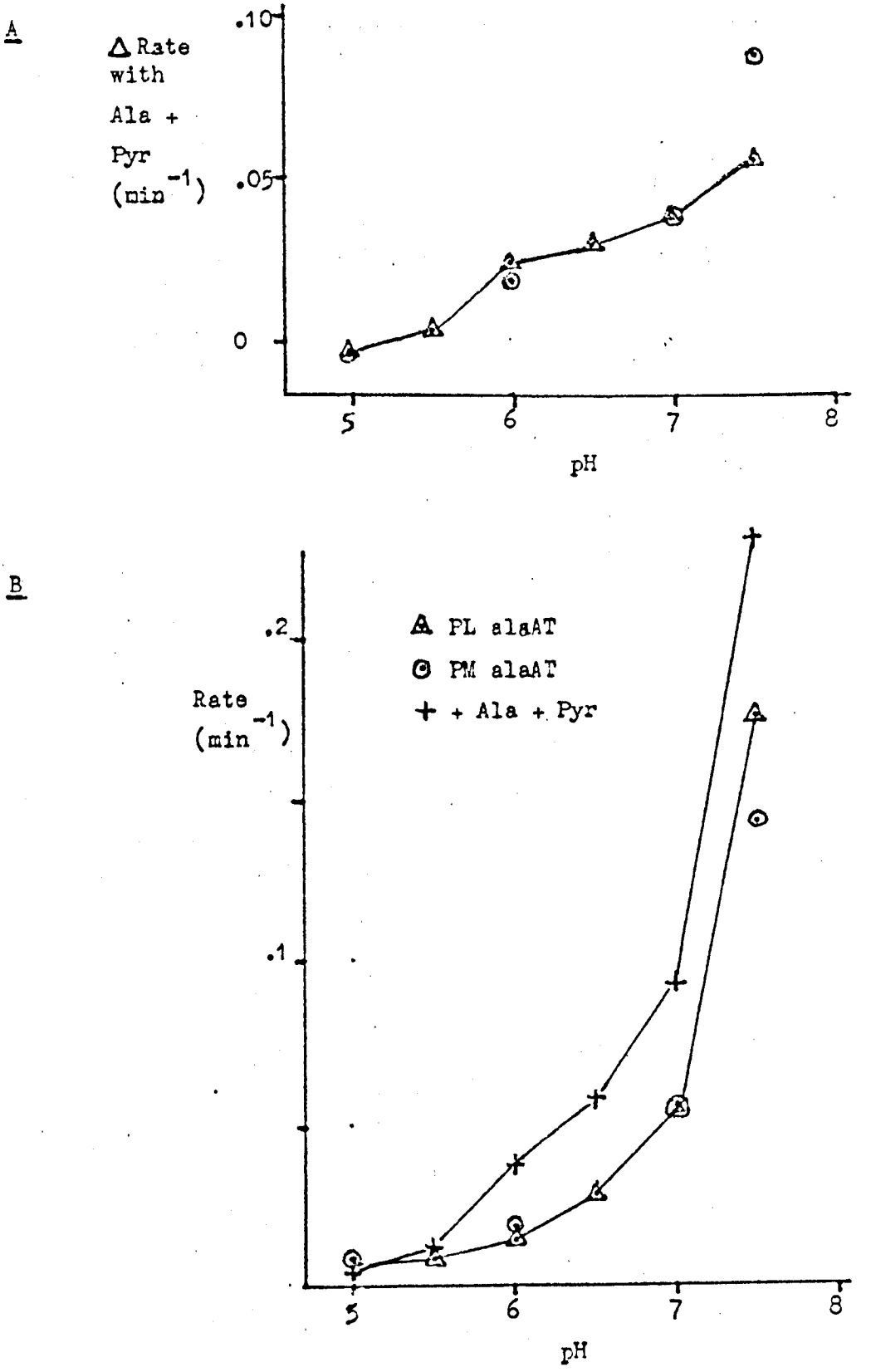
A
Δ Rate with Ala + Pyr (min^{-1})
.10
.05
0
5
6
7
8
pH
B
Rate (min^{-1})
.2
.1
PL alaAT
PM alaAT
+ + Ala + Pyr
5
6
7
8
pH

each other is uncertain. There is evidence that each leads to a partial inactivation and together give complete inactivation (20). It has been suggested that modification of the cysteine is the primary act in the syncatalytic modification (18).

12.2 RESULTS

Figure 12.1 shows the fall in activity with time when ala AT is incubated with 0.6 mM TNM in 50 mM pH 8.0 tris chloride at 25°C. It is not a simple first-order curve. It may be that there is a residual activity of something like 8 %. This was ignored in calculating the rate constant.

Table 12.1 gives the rate constant under different conditions. The PM and PL forms gave similar but different rates. There was no buffer effect. The rate was pH dependent with a pK at over pH 8.5 (figure 12.2).

The results were not all from the most suitable pH; however, it is easy to repeat an assumption of chapter 9; that the binding at the γ carboxyl site has a distinct effect - protection. L alanine plus pyruvate binding labilises the enzyme. However, no simple scheme, incorporating just these two phenomena, will give a quantitative description of the results.

The increased rate with pyruvate plus L alanine, (figure 12.2) was observed only at pH above 6.5. There seemed to be a pK at about pH 5.8.

The inactivation of PL-ala AT at pH 7.0 was followed by the standard and aminobutyrate assays at pH 7.5, (figure 12.3). The reaction was stopped by adding ME to 1 % by volume. Samples were dialysed overnight against 5 mM ME, 5 mM EDTA, and 10 mM pH 7.5 phosphate buffer. In one case, 10 mg/l PLP was added to the

TABLE 12.2

Ala AT was treated with .6 mM TNM, at pH 7.0, 25°C; in some cases substrates or inhibitors were present. After, it was dialysed against various solutions, (see text).

The changes in activity, as measured by the standard and aminobutyrate assays are recorded in the table.

FIGURE 12.3

Inactivation of PL-ala AT, by 0.6 mM TNM, in 50 mM pH 7.0 tris buffer, at 25°C.

A graph of activity in the aminobutyrate assay against the activity in the standard assay.

⊙ inactivated in the absence of fumarate

+ inactivated in the presence of fumarate

TABLE 12.2.

	Assay	Additions			
		—	Fumarate	Pyr L Ala	Pyr L Ala Formate
Native alaAT	Standard	100	100	100	100
	AB	100	100		
After TNM	Standard	15	37.5	6.0	25
	AB	59	80		
Dialysed	Standard	9	26	3.0	12
	AB	38	43		
Dialysed + PLP	Standard	9	23	5.0	12
	AB	39	47		
Dialysed + PMP	Standard	10			

FIGURE 12.3.

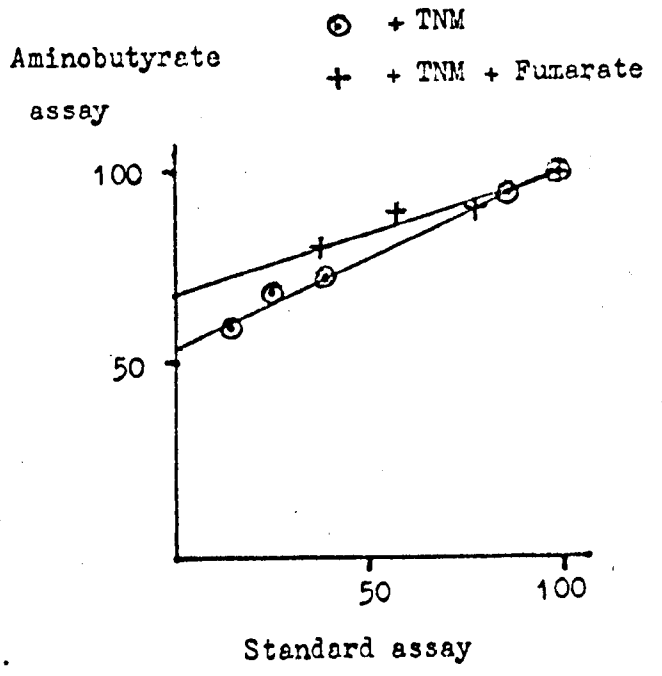
+ TNM
+ TNM + Fumarate
Aminobutyrate assay
100
50
50
100
Standard assay

mixture; in another, 10 mg/l PMP was added.

This experiment was repeated. The incubation with TNM was carried out in the presence of 100 mM fumarate or 8 mM pyruvate plus 200 mM formate. The results are given in table 12.2.

All samples lost activity on dialysis. The percentage loss of activity was similar for each assay and for each experiment. PMP and PLP protection were not significant.

The residual activity for the standard assays were too low for comparison. With the aminobutyrate assay the residual activity was slightly higher in the presence of fumarate, (figure 12.3).

It is possible that more than one inactivating reaction occurs.

12.3 DISCUSSION

The results are difficult to interpret further.

Like asp AT, ala AT with TNM shows a residual activity and the rate is increased in an enzyme-substrate complex.

CHAPTER 13

DISCUSSION

13.1 A MODEL OF ALANINE AMINOTRANSFERASE ACTIVITY

The tentative conclusions from the kinetic and spectral work suggest a still more tentative model for ala AT activity. The details are given below, and are illustrated in figure 13.1. The reasoning behind the model is given in bracketed paragraphs.

A) PL-ala AT contains a PLP-ϵ N lysine imine.

[(156)]

B) The internal aldimine has a pK at pH 7.6.

[This is the spectral pK - as in model PLP-aldimines (58, 62 139, 148).]

C) The pyridine nitrogen is protonated and possibly bound to the protein.

[In free PLP-amino-acid imines, the aldimine pK is about pH 10.5 when the pyridine nitrogen is unprotonated.; it is about pH 8 when the pyridine nitrogen is protonated (62, 91, 148). The low aldimine pK suggests that the pyridine nitrogen pK is raised considerably from the pH 6.3 of the free aldimine. Hydrogen-bonding to the protein might produce such an effect.]

D) The amino-acid substrate gives non-covalent binding at first, binding at two sites.

[Ionic and hydrophobic interactions are much more rapid than covalent ones. More nucleophilic reagents such as hydroxylamine and TSC react more slowly than the substrates. This initial binding orientates the substrate correctly, giving a rapid covalent reaction. The poor binding of D alanine suggests that at least two binding sites are involved initially.]

E) One site is cationic, binding the ∝carboxyl group and is close to the aldimine - it may have a pK at about pH 10.

[Acetate binding at the active site,(like L alanine), raises the aldimine pK by about .6 pH units, suggesting its proximity to to the aldimine. It also indicates that acetate binds like the ∝carboxyl group of the substrate.

The pK 10 could be that of a cationic binding site, (such as lysine).

It could be due to the change in net charge on the protein, that occurs in that pH region and is illustrated by the urea stability experiment. However, at pH 10 to 10.5, there is little change in ϕ_0^{KB} which should be as sensitive to charge and conformational change as the binding parameters.

The poor binding of propylamine demonstrates the strength of ∝carboxyl group binding.]

F) The methyl group of L alanine binds to the protein. The L glutamate ϒcarboxyl group binds to the protein.

[Glycine, with no side group, binds poorly. From the study of the binding of amino-acid analogues, Saier and Jenkins (171)

concluded that there are two side-chain binding groups; one binds the methyl; the other binds the γ carboxyl group.]

G) The amino pK, (of the amino-acid), falls to about pH 8.

[This is due to the neutralisation of the α carboxyl group. Ivanov and Karpeisky suggest the value of pH 7.8 (91). The amino pK of triglycine is pH 8.1.]

H) The internal aldimine pK rises to about pH 8.

[The spectral pK with acetate or fumarate rises to about pH 8.]

I) The amino-group attacks the unsaturated carbon of the aldimine, to give a tetrahedral intermediate and then a substrate aldimine with a free lysyl residue.

[It is the only conceivable covalent reaction of the amino-acid.]

J) The pK of the lysine group released is about pH 9.6

[see chapter 8 and appendix 6.]

K) The phenolic group on the coenzyme is well placed to catalyse the covalent binding.

L) At low pH, the equilibrium favours the formation of the substrate aldimine. At high pH, it may well be that the equilibrium constant is of the order of 1, (despite the fact that the lysine amino group is the more nucleophilic).

[see chapter 8.]

FIGURE 13.1

A diagram of the substrate aldimine in the ala AT-L alanine complex.

A showing possible binding to the protein

B showing possible interaction with a catalytic histidine

FIGURE 13.2

A possible deprotonated species in the ala AT-substrate complex, showing canonical forms.

FIGURE 13.1.

A

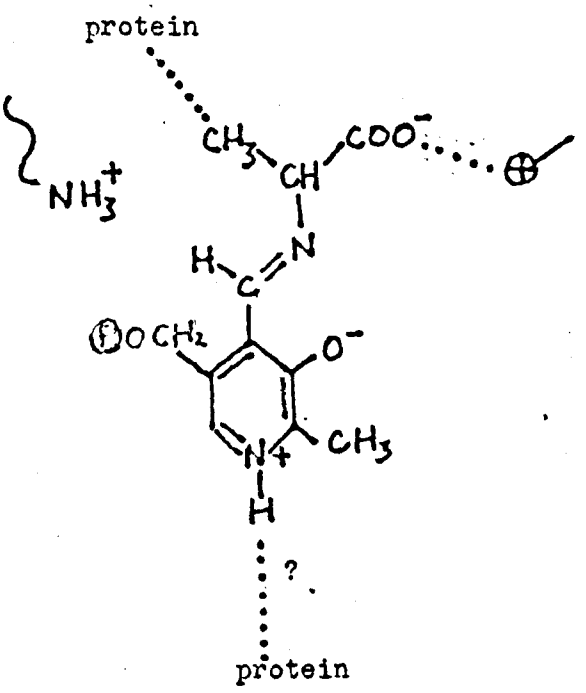

B

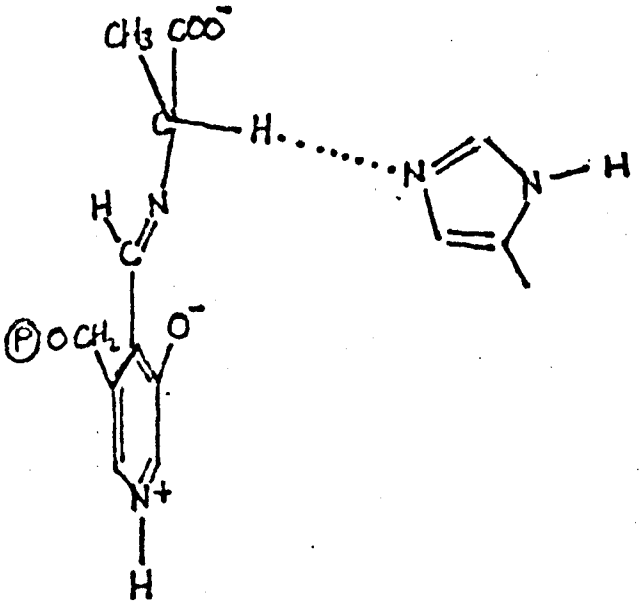

FIGURE 13.2.

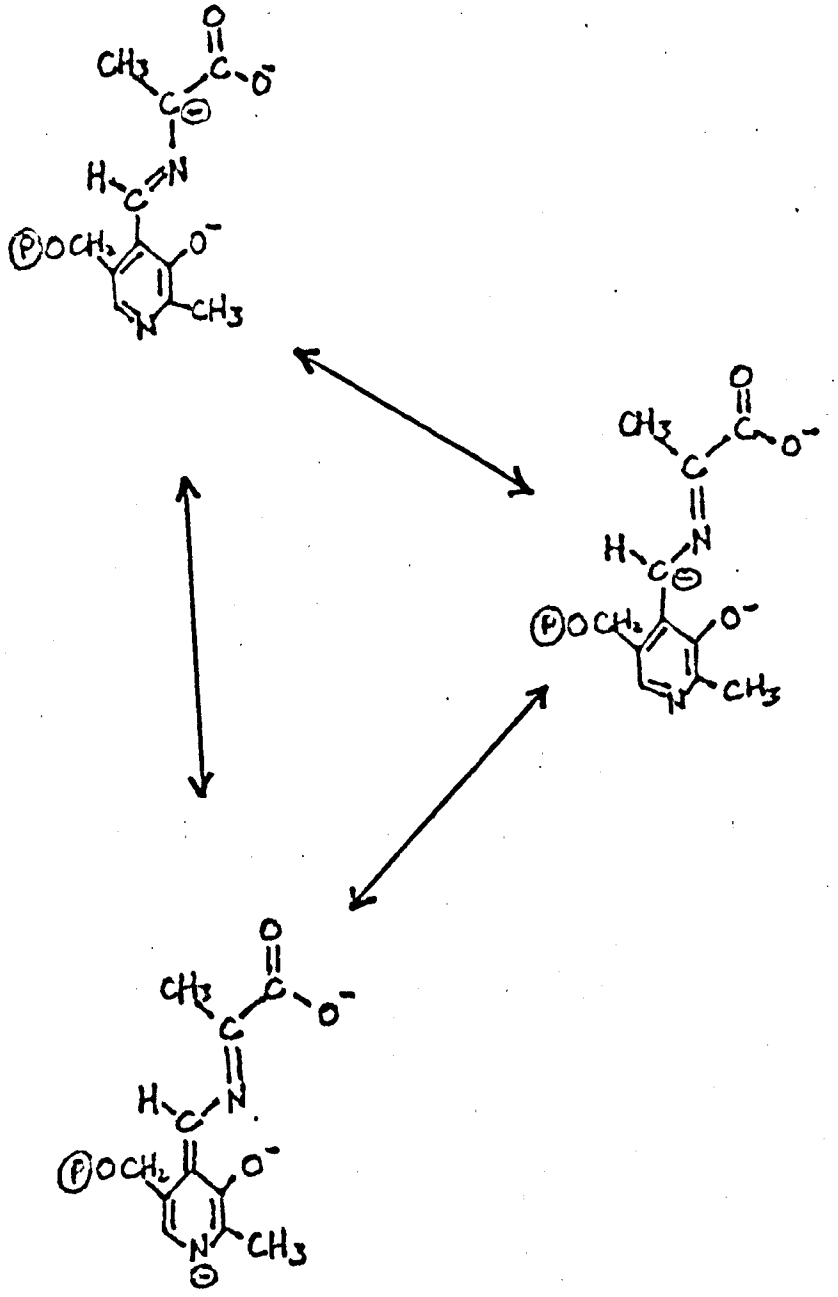

M) Either the coenzyme or the binding sites move through a considerable distance in the course of this initial covalent reaction.

[The amino group must attack the aldimine perpendicular to the plane of the aldimine. The initial separation of the amino nitrogen and aldimine carbon atoms must be over 3.5 Å, (the sum of their van der Waals radii). In the substrate aldimine they lie in the plane of the coenzyme, 1.3 Å apart. The substrate can rotate about its two points of attachment, but a model of a rigid enzyme still will not work.

For asp AT, Ivanov and Karpeisky suggested that the coenzyme rotates (91, 113).]

N) The substrate aldimine pK is about pH 8.

[The spectral pK of the enzyme-substrate complex.]

O) The pyridine nitrogen is still protonated.

[This is because the aldimine pK is still low. The binding parameters show one pK that could belong to the pyridine nitrogen, at pH 6.6. However, the ϕ_0 results show no pK in this region and ϕ_0 would be very sensitive to the state of the pyridine nitrogen.]

P) At some stage in binding, the pK of a histidine falls from pH 5.9 to pH 5.3. Possibly it is caused by steric hindrance from the α carbon proton.

[The identity of this residue is strongly suggested by its role as a base, its low pK and its apparent sensitivity to photo-oxidation. The way in which its pK is lowered is suggested by comparison with the higher pK of the very similar ketimine.

Q) The substrate and coenzyme are completely in one plane, with the α proton perpendicular to that plane.

[The results with cycloglutamate and asp AT suggest a fairly planar arrangement of the ionically bound substrate - with considerable separation of the carboxyl groups (114, 176). The deprotonated species would be greatly stabilised by a rigid planar arrangement (47, 48). It would also account for the transaminase reaction specificity (48).]

R) The histidine abstracts the α proton and the semiquinoid intermediate is formed.

[see chapter 7 and 8.]

S) This intermediate is stabilised considerably by the pyridine nitrogen proton and only slightly by the aldimine proton.

[Figure 13.2 shows three canonical forms of the intermediate. The semiquinoid form carries a negative charge on the pyridine nitrogen, unless that nitrogen atom is protonated. Hence the semiquinoid form is stabilised by the protonation of the pyridine nitrogen. Quantum mechanical calculations show that the protonated intermediate has a large semiquinoid component in its structure. It also shows that protonation of the aldimine nitrogen has little effect (154, 163).]

T) The formyl carbon atom is protonated. The protonation is stereospecific and pH independent at pH 5.5 to 9.0.

[In the reverse reaction, protonation on the side of the intermediate away from the histidine would produce the D amino-acid imine. In this direction, at least, the reaction is

stereo-specific.

There is hardly any evidence concerning the nature of the acidic species. It could be free or structural water. It could be a lysine. It could well be the catalytic histidine, if its pK is considerably raised in the deprotonated form.]

U) In the ketimine formed, the histidyl pK returns to pH 5.7. The ketimine pK is about pH 8.

[see chapter 8.]

V) The ketimine is hydrolysed to PM alaAT and the bound keto-acid.

W) During this hydrolysis, the change outlined in (M) is reversed

[This is for the same reasons as was the introduction of (M).]

X) The keto-acid dissociates.

Y) The PMP amino pK falls to about pH 7.5. The lysine pK is unaltered, (i.e. about pH 9.6). The pK 10, (mentioned in (E)), is found in PM-ala AT. The histidine pK is about pH 5.8.

[The kinetic pKs are identified largely by analogy with the situation in PL-ala AT.]

Z) The reverse reaction is the exact reverse of the forward reaction, if the histidine is the acid and base in both directions. Otherwise, the tautomerisation step, only, is not exactly reversed as the catalytic histidine is the base in both directions.

[ϕ_0 shows that the same base operates in both directions.]

13.2 CONFORMATIONAL CHANGES

The data from the inactivation experiments reveal two distinct conformational changes, produced by substrate binding, as described in chapter 9.

In the urea, heat, rose bengal, (and possibly TNM) inactivation, binding at the γ carboxyl binding site seems to protect the enzyme partially. The diversity of the experiments suggests that binding at this site produces a conformational change. Formate activation seems to operate in this way. As alanine and pyruvate do not bind to this site, it is debatable whether this conformational change is essential for activity. It is very possible that rose-bengal photo-oxidation prevents this conformational change.

In urea and formaldehyde inactivation, a pK of about pH 7.3 is seen - and also in kinetic experiments. In each case it was considered probable that a conformational change was involved. No "conformational pK" is seen in the enzyme-substrate complex, which shows similar stability to PL-ala AT at low pH. Hence substrate (or fumarate) binding may produce a conformational change at high pH.

Such a conformational change might correspond to that described in paragraph M. It should be noted that fumarate produces this change, although this is not specified by the model.

Ivanov and Karpeisky have postulated an attractive theory for asp AT, mainly on the basis of circular dichroism (25, 52, 53, 90, 190, 191). They suggest that in the free enzyme the pyridine nitrogen of the coenzyme is bound to a tyrosyl anion: in the enzyme-substrate complex it is rotated by 40°. The TNM inactivation of asp AT, described in chapter 12, shows the nitration

of an important tyrosyl residue, which is particularly labile in the presence of substrate.

The evidence for such a theory is not very strong in the case of asp AT and almost non-existent for ala AT.

13.3 COMPARISON WITH ASPARTATE AMINOTRANSFERASE

The relationship between asp AT and ala AT is further illuminated by the results described.

A structure of two subunits, with one coenzyme molecule per subunit is indicated for pig heart ala AT, as well as for rat liver ala AT and asp AT.

Ala AT substrate specificity has already been described by Saier and Jenkins (171). It should be noted that ala AT has to provide for more diverse substrate structures than does asp AT. Consequently, several other amino-acids bind well and ala AT distinguishes between amino-acids very well at the tautomerisation step, while asp AT does not (180).

The similarities between their active sites are shown by their TSC (106) and dicarboxylic acid (78, 104) binding. While in PL-ala AT. the spectral pK is raised about 0.5 units by the dicarboxylic acid binding, in PL-asp AT, the spectral pK is raised by about 2 units.

It has been suggested that in asp AT the amino-acid binds better when the aldimine is unprotonated (51, 200): it has also been suggested that some inhibitors bind to a catalytic histidine (39, 97). In ala AT, this is certainly not the case.

The enzyme-substrate complex has a much higher A_{490} in ala AT than in asp AT. This difference may be only quantitative. It is of interest that a substrate aldimine pK has been observed

for ala AT, but not in the few asp AT results. The approximate value of this pK is important for any model.

The methylene-blue photo-oxidation and TNM inactivation results are very similar for the two enzymes, indicating that the similarities in structure extend beyond the coenzyme to the amino-acid residues.

Saier suggested that a conformational change, brought about by binding at a γ carboxyl binding site, exists in both ala AT and asp AT. There is additional evidence for this (98, 108, 146). It is possible that the second conformational effect, postulated in this thesis, occurs in asp AT.

APPENDIX I

DERIVATION OF THE EQUATION, GOVERNING THE ISOTOPE ASSAY.

A and P are the concentrations of unlabelled L alanine and pyruvate and are time-independent for this assay. A* and P* are the concentrations of labelled L alanine and pyruvate.

In the presence of ala AT, L alanine and pyruvate, four reactions are possible.

$$A_1 + P_2 \xrightarrow{v_1} P_1 + A_2 \qquad A + P^* \xrightarrow{v_2} P + A^*$$

$$A^* + P \xrightarrow{v_3} P^* + A \qquad A_1^* + P_2^* \xrightarrow{v_4} P_1^* + A_2^*$$

$dA^*/dt = v_2 - v_3$, where v is the reaction velocity, shown above.

P* and P have identical chemical properties. The probability that any alanine formed is radioactive, is the probability that the pyruvate bound was radioactive.

$\therefore \quad v_2/v_1 = P^*/P$ and

$v_3/v_1 = A^*/A$

$\therefore \quad dA^*/dt = v_1(P^*/P - A^*/A)$

Let $P^* + A^* = x$ and $A' = A^*/x$

Then, $dA^*/dt = v_1((x - A^*)/P - A^*/A)$

$= v_1(x/P - A^*(1/P + 1/A))$

$$\therefore \quad dA'/dt = v_1(1/P - A'(1/P + 1/A))$$

$$\frac{dA'}{(1/P - A'(1/P + 1/A))} = v_1\, dt$$

$$\int_0^{A'} \frac{dA'}{(1/P - A'(1/P + 1/A))} = \int_0^{t} v_1\, dt$$

when $A' = 0$, at time 0

$$\therefore \frac{-\log_e(1/P - A'(1/P + 1/A))}{(1/P + 1/A)} = v_1 t$$

$$\therefore -\log_{10}(1/P - A'(1/P + 1/A)) = 0.4346\,(1/P + 1/A)\, v_1 t$$

$$\therefore \log_{10}P + \log_{10}(1 - A'(1 + P/A)) = -.4346\,(1/P + 1/A)v_1 t$$

In this assay, $A \doteq A + A^*$ and $P \doteq P + P^*$

Hence, v_1 = total activity

Plotting $\log_{10}(1 - A'(1 + P/A))$ against time, gives a gradient of $-.4346(1/P + 1/A)$ x activity.

APPENDIX II

A QUANTITATIVE TREATMENT OF THE RESULTS IN THE PYRIDOXAL 5' PHOSPHATE ASSAY.

This appendix shows how an accurate estimation of PLP was made, despite the fact, that the sample and standard gave differing spectra.

The ratio of the A_{390} for the two spectra in figure 4.7 is 0.74, but this is not the ratio of the concentrations of PLP, because the PLP from the enzyme has an additional component, absorbing at short wavelengths.

If it is assumed that the absorbance of this component varies linearly with wavelength, then its absorbance, $A_c = x + k\lambda$, where λ is the wavelength, and x and k are constants.

The total absorbance, $A_t = A_{PLP} + A_c$, where A_{PLP} is the absorbance due to the PLP.

$$A_t = A_{PLP} + x + k\lambda$$

Consider three equally spaced wavelengths, λ_0, $(\lambda_0 - a)$, and $(\lambda_0 + a)$.

$$\text{Let } f(A_t) = A_{t(\lambda_0)} - 1/2(A_{t(\lambda_0 - a)} + A_{t(\lambda_0 + a)})$$

$$= A_{PLP(\lambda_0)} - 1/2(A_{PLP(\lambda_0 - a)} + A_{PLP(\lambda_0 + a)}) + x + k\lambda_0 - 1/2(x + (\lambda_0 - a)k + x + (\lambda_0 + a)k)$$

$$= A_{PLP(\lambda_0)} - 1/2(A_{PLP(\lambda_0 - a)} + A_{PLP(\lambda_0 + a)})$$

$$= f(A_{PLP})$$

i.e. The function, $f(A_t)$, depends only on the absorbance of PLP.

Set λ_0 = 390 nm. For the two spectra;

a (nm)	$f(A_t)$ (ala AT)	$f(A_t)$ (standard)	ratio
10	.006	.007	.86
20	.0195	.0275	.71
30	.0325	.0475	.69
40	.049	.069	.71
50	.063	.094	.67
60	.073	.106	.69
70	.076	.109	.70

The ratio is constant, within experimental error, which means that the assumption, that $A_c = x + k\lambda$, was a reasonable one.

The mean value, (excepting the first value), was 0.70.

Hence, the final concentration of PLP in the sample was 0.70 times the final concentration in the standard.

APPENDIX III

THE STEADY-STATE EQUATION FOR A PING-PONG MECHANISM, IN THE PRESENCE OF A COMPETITIVE INHIBITOR.

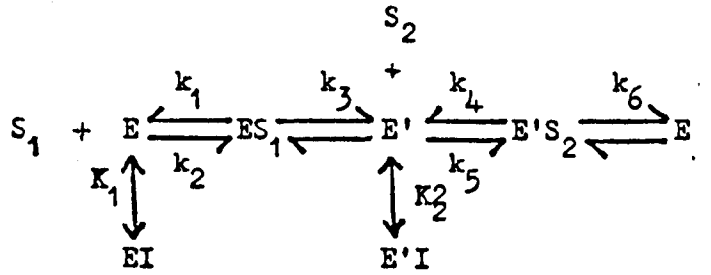

The above reaction scheme is for a ping- pong enzyme mechanism, in the absence of substrate inhibition, and in the presence of one independent inhibitor, I, which binds only to the two free forms of the enzyme.

E and E' are the two free forms of the enzyme.

ES_1 and $E'S_2$ are the enzyme-substrate complexes.

S_1 and S_2 are the two substrates.

EI and E'I are enzyme-inhibitor complexes.

k_i are rate constants.

K_i are dissociation constants.

Since initial rates are measured, product concentrations approach zero under experimental conditions, and the reaction steps $E' \longrightarrow ES_1$ and $E \longrightarrow E'S_2$ do not occur.

A steady state is obtained when the concentration of each enzyme species is constant. For the above scheme, this implies that the rate of each catalytic step is equal (26).

$$\text{Hence } S_1 E k_2 - ES_1 k_1 = ES_1 k_3 = S_2 E' k_5 - E'S_2 k_4 = E'S_2 k_6$$

This gives $E = ES_1 S_1^{-1}(k_1 + k_3)/k_2$

And $E'S_2 = ES_1 k_3/k_6$

And $EI = E \times I/K_1$

And $E'I = E' \times I/K_2$

Total enzyme, $E_t = E + EI + ES_1 + E' + E'I + ES_2$

$\therefore E_t = E(1 + I/K_1) + ES_1 + E'(1 + I/K_2) + ES_2$

$$= ES_1\left[1 + k_3/k_6 + S_1^{-1}(k_1 + k_3)/k_2 \times (1 + I/K_1) + S_2^{-1}(k_3(k_4 + k_6)/k_5k_6) \times (1 + I/K_2)\right]$$

The overall rate of formation of a product, v, equals the rate of any one step.

$\therefore v = ES_1 \times k_3$

$$E_t/v = 1/k_3 + 1/k_6 \quad S_1^{-1}\left(\frac{k_1 + k_3}{k_2k_3}\right)\left(1 + \frac{I}{K_1}\right) + S_2^{-1}\left(\frac{k_4 + k_6}{k_5k_6}\right)\left(1 + \frac{I}{K_2}\right)$$

Let $\phi_0 = 1/k_3 + 1/k_6$ Let $\phi_1 = (k_1 + k_3)/k_2k_3$

Let $\phi_0 = (k_4 + k_6)/k_5k_6$

Then $\frac{E_t}{v} = \phi_0 + \phi_1 S_1^{-1}(1 + I/K_1) + \phi_2 S_2^{-1}(1 + I/K_2)$

A QUASI-EQUILIBRIUM EQUATION FOR A PING-PONG MECHANISM, WITH AN INHIBITOR THAT BINDS TO ALL FORMS OF THE ENZYME.

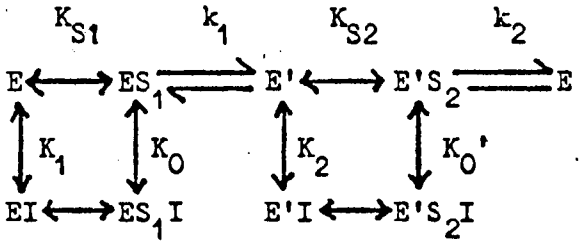

The above is the reaction scheme for a ping-pong enzyme mechanism, in the absence of substrate inhibition, but in the presence of one independent inhibitor, I, which binds to all forms of the enzyme.

E and E' are the two free forms of the enzyme.

S_1 and S_2 are the two substrates.

ES_1 and $E'S_2$ are enzyme-substrate complexes.

EI and E'I are enzyme-inhibitor complexes.

ES_1I and $E'S_2I$ are enzyme-substrate-inhibitor complexes.

k_i are rate constants.

K_i are dissociation constants.

It will be observed that:-

A) Initially, the concentrations of the products are practically zero and the steps, $E' \longrightarrow ES_1$ and $E \longrightarrow E'S_2$ do not occur.

B) The steps, $ES_1I \longrightarrow E'I$ and $E'S_2I \longrightarrow EI$, do not occur at significant rates.

C) There is a quasi-equilibrium between E and ES_1, and Between E' and $E'S_2$.

The last two assumptions are not necessarily true for all systems (140).

Under steady-state conditions,

$$v = ES_1k_1 = E'S_2k_2$$

Hence $$E'S_2 = ES_1 \times k_1/k_2$$

The equilibrium equations give:

$$E = ES_1/S_1 \times K_{S1} \qquad E' = ES_1/S_2 \times k_1/k_2 \times K_{S2}$$

$$EI = E \times I/K_1 \qquad ES_1I = ES_1 \times I/K_0$$

$$E'I = E' \times I/K_2 \qquad E'S_2I = E'S_2 \times I/K_0'$$

As $$E_t = ES_1 + ES_1I + E'S_2 + E'S_2I + E + EI + E' + E'I$$

$$E_t = ES_1(1 + I/K_0) + E'S_2(1 + I/K_0') + E(1 + I/K_1) + E'(1 + I/K_2)$$

$$\frac{E_t}{ES_1} = \left(1 + \frac{I}{K_0}\right) + \frac{k_1}{k_2}\left(1 + \frac{I}{K_0'}\right) + \frac{K_{S1}}{S_1}\left(1 + \frac{I}{K_1}\right) + \frac{K_{S2}}{S_2}\frac{k_1}{k_2}\left(1 + \frac{I}{K_2}\right)$$

$$\frac{E_t}{v} = \frac{1}{k_1}\left(1 + \frac{I}{K_0}\right) + \frac{1}{k_2}\left(1 + \frac{I}{K_0'}\right) + \frac{1}{S_1}\frac{K_{S1}}{k_1}\left(1 + \frac{I}{K_1}\right) + \frac{1}{S_2}\frac{K_{S2}}{k_2}\left(1 + \frac{I}{K_2}\right)$$

Let $\phi_1 = K_{S1}/k_1$ and $\phi_2 = K_{S2}/k_2$

Then $$\frac{E_t}{v} = \frac{1}{k_1}\left(1 + \frac{I}{K_0}\right) + \frac{1}{k_2}\left(1 + \frac{I}{K_0'}\right) + \frac{\phi_1}{S_1}\left(1 + \frac{I}{K_1}\right) + \frac{\phi_2}{S_2}\left(1 + \frac{I}{K_2}\right)$$

A simpler equation can be used when $K_0 = K_0'$ or $k_1 \ll k_2$.

$$\frac{E_t}{v} = \phi_0\left(1 + \frac{I}{K_0}\right) + \frac{\phi_1}{S_1}\left(1 + \frac{I}{K_1}\right) + \frac{\phi_2}{S_2}\left(1 + \frac{I}{K_2}\right)$$

It is unlikely that all the assumptions are completely true for any particular case. However, the parameter, K_O, is easily obtained. If K_O is high, the inhibitor does not bind well to the enzyme-substrate complex and the equation obtained in the first part of this appendix can be used with confidence.

APPENDIX IV

DETERMINATION OF THE REAL BINDING CONSTANT OF AN INHIBITOR, IN THE PRESENCE OF A SECOND INHIBITOR

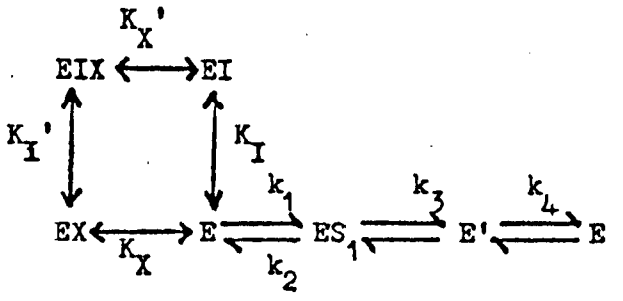

The above is the reaction scheme for a ping-pong enzyme mechanism, in the absence of substrate inhibition, but in the presence of two independent inhibitors, I and X. Neither binds to ES_1.

E is a free form of the enzyme.

ES_1 is an enzyme-substrate complex.

E' is a mixture of the second form of the free enzyme and the second enzyme-substrate complex, $(E'S_2)$

EI, EX, and EIX are inhibitor complexes, with E.

K_i are dissociation constants.

k_i are rate constants. N.B. k_4 is a complex parameter; its value depends on the concentrations of the secondsubstrate, I, and X.

Initially there are no products and the reaction steps, $E \longrightarrow E'$ and $E' \longrightarrow ES_1$, do not occur.

Total enzyme, $E_t = EIX + EX + E + EI + ES_1 + E'$

The steady-state assumption implies that

$$S_1 Ek_1 - ES_1 k_2 = ES_1 k_3 = E' k_4$$

$$E' = ES_1 k_3/k_4$$

$$E = ES_1/S_1 \times (k_2 + k_3)/k_1$$

$$EI = E \times I/K_I$$

$$EIX = E \times XI/K_X K_I'$$

$$EX = E \times X/K_X$$

$$E_t = ES + E' + E(1 + I/K_I + X/K_X + XI/K_X K_I)$$

$$E_t/ES = 1 + k_3/k_4 + (k_2 + k_3)/S_1 k_1 \times (1 + I/K_I + X/K_X + XI/K_X K_I)$$

The overall velocity, $v = ES_1 \times k_3$

$$\therefore E_t/v = 1/k_3 + 1/k_4 + \phi_1/S_1(1 + I/K_I + X/K_X + XI/K_X K_I')$$

where $\phi_1 = (k_2 + k_3)/k_1 \times k_3$

If v^{-1} is plotted against S_1^{-1} at constant I, X and S_2, the gradient, $g = \phi_1(1 + X/K_X + I(1/K_I + X/K_X K_I'))$.

If g is plotted against I at constant X and S_2, the gradient, $g' = \phi_1(1/K_I + X/K_X K_I')$.

If g' is plotted against X, at constant S_2, the intercept on the g' axis is equal to ϕ_1/K_I.

If g is plotted against X, at constant S_2 and $I = 0$, the intercept on the g axis is equal to ϕ_1.

Hence K_I can be obtained, in the presence of X.

APPENDIX V

THE MATHEMATICAL BASIS OF SPECTRAL TITRATIONS

Let $EX \longleftrightarrow E + X$

K is the dissociation constant

Let E be the con-centration of E and EX the concentration of EX. At any wavelength, the total absorbance is A, and the molar absorbance of each chemical is ϵ_i.

Hence $A = E \times \epsilon_E + EX \times \epsilon_{EX}$

At $X = 0$, $EX = 0$, and the absorbance, A_0 is given by

$$A_0 = E_0 \times \epsilon_E$$

$$\Delta A = A - A_0 = EX(\epsilon_{EX} - \epsilon_E)$$

$$\therefore (\Delta A)^{-1} = EX^{-1}(\epsilon_{EX} - \epsilon_E)^{-1}$$

$$EX = E_0(X/(K + X)$$

$$\therefore (\Delta A)^{-1} = E_0^{-1}(\epsilon_{EX} - \epsilon_E)^{-1}(1 + K/X)$$

If $(\Delta A)^{-1}$ is plotted against X^{-1}, the plot is linear.

The intercept on the X^{-1} axis equals $-K^{-1}$.

The intercept on the $(\Delta A)^{-1}$ axis equals $(E_0\epsilon_{EX} - A_0)^{-1}$.

Hence K and ϵ_{EX} can be obtained.

In spectral experiments, one wavelength, (or a linear combination of wavelengths), with a high ΔA was chosen for the determination of K. The graphs at all other wavelengths were drawn to give this same value of K.

This simple titration procedure was used to determine the spectrum of the equilibrium enzyme-substrate complex, (see chapter 8).

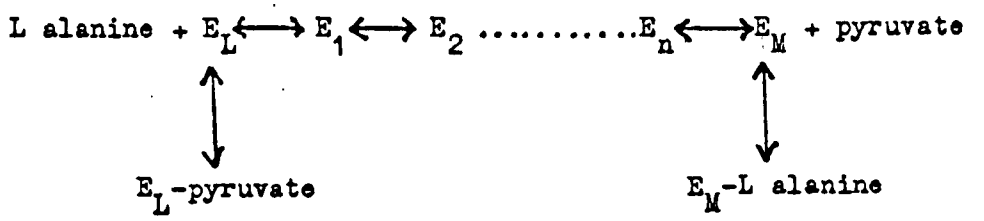

The above scheme shows all the binary complexes that might have been involved in the substrate titration of chapter 8.

E_L-pyruvate and E_M- L alanine are abortive complexes.

E_L and E_M are the PL and PM forms of the free enzyme.

E_1 to E_n are the enzyme-substrate complexes on the catalytic pathway.

At high pyruvate concentration, $E_M = E_M$-L alanine = 0

E_1, E_2.....E_n are in equilibrium, and this equilibrium is independent of substrate concentration.

Let $EX = \sum E_i$. Then the composition of EX is the same throughout the titration.

E_L and E_L-pyruvate are in equilibrium. This Equilibrium is dependent on pyruvate concentration but not on L alanine concentration. Let $E = E_L + E_L$-pyruvate, then the composition of E is the same throughout the titration, as long as the concentration of pyruvate is constant.

Hence, L alanine can be titrated against ala AT at a constant high concentration of pyruvate, and the following equation can be used L alanine + E ⟷ EX

The dissociation constant is very complex and not very useful. $E_0\epsilon_{EX}$ was obtained at each wavelength, giving the spectrum of the equilibrium enzyme-substrate complex.

The titrations were carried out at two very different pyruvate concentrations. If the pyruvate was in excess in each case, then the same spectrum should have been obtained at both pyruvate concentrations. This was the case at every pH.

APPENDIX VI

A SIMPLE MODEL OF THE pH DEPENDENCE OF ϕ_0^{AB} AT HIGH pH

In chapter 8, it is suggested that there are two forms of the aldimine in the enzyme-substrate complex, (A and B); that the equilibrium between them is pH dependent, (due to the difference in the pK of an amino group in the two forms); and that the rate of the tautomerisation step is pH independent at high pH.

It will be shown that such a model can be made to fit the data and that it has certain implications.

For the reaction, $A \overset{K}{\longleftrightarrow} B \xrightarrow{k} C$, where k is a pH independent rate constant and K is a pH dependent equilibrium constant (and the equilibrium is a rapid one), the velocity is given by

$$\phi_0^{AB} = Bk$$

$$B = K/(1 + K)$$

$$\therefore (\phi_0^{AB})^{-1} = k^{-1}(K^{-1} + 1)$$

Now $$K = x(1 + H/K_2)(1 + H/K_1)^{-1}$$

where x is a constant and H is the hydrogen ion concentration.

where A has an ionising group, dissociation constant K_1.

and B has an ionising group, dissociation constant K_2.

$$(\phi_0^{AB})^{-1} = k^{-1}x^{-1}\left(\frac{1 + H/K_1}{1 + H/K_2} + x\right) \qquad \text{——1}$$

at high H $$(\phi_0^{AB})^{-1} = k^{-1}x^{-1}(K_2/K_1 + x) \qquad \text{——2}$$

at low H $$(\phi_0^{AB})^{-1} = k^{-1}x^{-1}(1 + x) \qquad \text{——3}$$

at $H = K_2$, $(\phi_0^{AB})^{-1} = k^{-1}x^{-1}((1 + K_2/K_1)/2 + x)$

i.e. At $H = K_2$, $(\phi_0^{AB})^{-1}$ is exactly half way between its maximum and minimum values,

pK_2 can be obtained for ϕ_0 in the forward, reverse and aminobutyrate assays. Unfortunately, these results, (figure 6.5) do not extend to a sufficiently high pH. Any value for pK_2 from 9.4 to9.8 will do.

For $(\phi_0^{AB})^{-1}$, a very rough estimate has been made for the maximum (250) and minimum (100) values. The pK_2 has been estimated to be about 9.6 and the pK_1 is set at 8.0, (see text).

Substituting these values into the equations, (2) and (3), we get $x = 0.63$ and $k = 0.0104$

Substititing these values into equation (1) we get;

pH	K	B	$(\phi_0^{AB})^{-1}$
low	25	.96	100
8.0	12.5	.93	103
9.0	2.2	.70	139
9.5	1.38	.58	166
10.0	.84	.45	212
high	.63	39	250

These figures are compared with the measured values of $(\phi_0^{AB})^{-1}$ in figure 8.12.

BIBLIOGRAPHY

1) AHLFORS, C.E., and MANSOUR, T.E., J. Biol. Chem., 244, 1247, (1969).

2) ALBERTY, R.A., and MASSEY, V., Biochim. Biophys. Acta, 13, 347, (1954).

3) ALBERTY, R.A., Adv. Enzymol., 17, (1956).

4) ARRIO-DUPONT, M., Biochem. Biophys. Res. Commun., 36, 306, (1969).

5) ARRIO-DUPONT, M., COURNIL, I., and DUIE, P., F.E.B.S. Letters, 11, 144, (1970).

6) ARRIO-DUPONT, M., Eur. J. Biochem., 30, 307. (1972).

7) AULD, D.S., BRUICE, T.C., J. Amer. Chem. Soc., 89, 2090, (1967).

8) AULD, D.S., and BRUICE, T.C., J. Amer. Chem. Soc., 89, 2098, (1967).

9) AURICCHIO, F., and BRUNI, C.B., Biochem. Z., 340, 321, (1964).

10) AZARKH, R.M., BRAUNSTEIN, A.E., PASKHINA, T.S., and TING-SEN, H., Biokhimiya, 25, 471, (1960).

11) BADDILEY, J., and MATHIAS, A.P., J. Chem. Soc. (1952), 2583.

12) BANKS, E.C., DIAMANTIS, A.A., and VERNON, C.A., J. Chem. Soc., (1961), 4235.

13) BANKS, E.C., DOONAN, S.I.LAWRENCE, A.J., and VERNON, C.A., Eur. J. Biochem., 5, 528, (1968).

14) BELLIN, J.S., and YANKUS, C.A., Arch. Biochem. Biophys., 123, 18, (1968).

15) BERTLAND, L.H., and KAPLAN, N.O., Biochem., 9, 2653, (1970)

16) BIRCHMEIER, W., WILSON, K.J., and CHRISTEN, P., F.E.B.S. Letters, 26, 113, (1972).

17) BIRCHMEIER, W., WILSON, K.J., and CHRISTEN, P., J. Biol. Chem., 248

18) BIRCHMEIER, W., ZAORELEK, P.E., and CHRISTEN, P., Biochem. 12, 2874, (1973).

19) BOCHAROV, A.L., IVANOV, V.I., KARPEISKY, M.Y., MAMAEVA, O.K., and FLORENTIEV, V.L., Biochem. Biophys. Res. Commun., 30, 459, (1968).

20) BOCHAROV, A.L., DEMIDKINA, T.V., KARPEISKY, M.Y., and POLYANOVSKY, O.L. Biochem. Biophys. Res. Commun. 50, 377, (1973).

21) BOYDE, T.R.C., Biochem. J. 106, 581, (1968).

22) BRAKE, J.M., and WOLD, F., Biochim. Biophys. Acta, 40, 171, (1960).

23) BRAUNSTEIN, A.E., and KRITSMAN, M.G., Enzymologia, 2, 129, (1937).

24) BRAUNSTEIN, A.E., AZARKH, R.M., and SYUI. T., Biokhimiya, 26, 760, (1961).

25) BREUSOV, Y.N., IVANOV, V.I., KARPEISKY, M.Y., and MOROZOV, Y. Y.V., Biochem. Biophys. Acta, 92, 391, (1964).

26) BRIGGS, G.E., and HALDANE, J.B.S., Biochem. J., 19, 338, (1925).

27) BRUICE, T.C., and TOPPING, R.M., J. Amer. Chem. Soc., 85, 1480, (1963).

28) BRUICE, T.C., and TOPPING, R.M., J. Amer. Chem. Soc., 85, 1489, (1963).

29) BULOS, B., and HANDLER, P., J. Biol. Chem., 240, 3283, (1965).

30) CHENG, S., MICHUDA-KOZAK, C., and MARTINEZ-CARRION, M., J. Biol. Chem., 246, 3623, (1971).

31) CHENG, S., and MARTINEZ-CARRION, M., J. Biol. Chem., 247, 6597, (1965).

32) CHRISTEN, P., and RIORDAN, J.F., Biochem., 7, 1531, (1968).

33) CHRISTEN, P., and RIORDAN, J.F., Biochem., 9, 3025, (1970).

34) CHURCHICH, J.E., Biochem. Biophys. Res. Commun., 28, 857, (1967).

35) CHURCHICH, J.E., and FARELLY, J.G., Biochem. Biophys. Res. Commun. 31, 316, (1968).

36) CHURCHICH, J.E., and FARELLY, J.G., J. Biol. Chem. 244, 3685, (1969).

37) CHURCHICH, J.E., Biochim. Biophys. Acta, 178, 480, (1969).

38) COHEN, P.P., Fed. Proc., 1, 273, (1942).

39) COURNIL, I., and ARRIO-DUPONT, M., Biochem. Biophys. Res. Commun., 43, 40, (1971).

40) CZERLINSKI, G.H., and MALKEWITZ, J., Biochem., 4, 1127, (1965).

41) DALZIEL, K., Biochem. J., 66, 34p. (1957).

42) DAVIES, B.J., Annals N.Y.A.S., 121, 404, (1964).

43) DENISOVA, G.F., and POLYANOVSKY, O.L., F.E.B.S. Letters, 35, 129, (1973).

44) DIXON, M., Biochem. J., 55, 161, (1953).

45) DIXON, M., and WEBB, E.C., The Enzymes, (Longmans and Green), (1964).

46) DUMITRU, I.F., IORDACHESCU, D., and NICULESCU, S., Enzymologia, 42, 79, (1971).

47) DUNATHAN, H.C., Proc. Nat. Acad. Sci., 55, 712, (1966).

48) DUNATHAN, H.C., Adv. Enzymol., 35, 79, (1971).

49) ESIPOVA, N.G., DEMBO, A.T., TUMANYAN, V.G., and POLYANOVSKY, O.L., Mol. Biol., 2, 527, (1968).

50) FARELLY, J.G., and CHURCHICH, J.E., Biochem. Biophys. Acta, 167, 280, (1968).

51) FASELLA, P., GIARTOSIO, A., and HAMMES, G.G., Biochem., 5, 197, (1966).

52) FASELLA, P., and HAMMES, C.G., Biochem., 3, 530, (1964).

53) FASELLA, P., and HAMMES, C.G., Biochem., 4, 801, (1965).

54) FASELLA, P., and HAMMES, C.G., Biochem., 6, 1798. (1967).

55) FELIG, P., WAHREN, L., and LARS, R., Proc. Nat. Acad. Sci., 70, 1775, (1963).

56) FELISS, N., and MARTINEZ-CARRION, M., Biochem. Biophys. Res. Commun., 40, 932, (1970).

57) FINCHAM, J.R.S., and BOULTER, A.B., Biochem. J. 62, 72, (1956).

58) FINSETH, F., and SIZER, I.W., Biochem. Biophys. Res. Commun., 26, 625, (1967).

59) FONDA, M.L., and JOHNSON, R.J., J. Biol. Chem., 245, 2709, (1970).

60) FRAENKEL-CONRAT, H., and OLCOTT, H.S., J. Amer. Chem. Soc., 70, 2673, (1948).

61) FRAENKEL-CONRAT, H., and OLCOTT, H.S., J. Biol. Chem., 174, 827, (1948).

62) FRENCH, T.C., AULD, D.S., and BRUICE, T.C., Biochem., 4, 77, (1965).

63) FRIEDEN, C., and ALBERTY, R.A., J. Biol. Chem., 212, 859, (1955).

64) FURBISH, F.S., FONDA, M.L., and METZLER, D.E., Biochem. 8, 5169, (1969).

65) GALE, E.F., and EPPS, H.M.R., Nature, 152, 327, (1943).

66) GALE, E.F., and EPPS, H.M.R., Biochem. J., 38, 250, (1944).

67) GATEHOUSE, P.W., HOPPER, S., SCHATZ, L., and SEGAL, H.L., J. Biol. Chem., 242, 2319, (1967).

68) GORNALL, A.G., BARDAWILL, C.J., and DAVID, M.M., J. Biol. Chem., 177, 751, (1949).

69) GREEN, D.E., LELOIR, L.F., and NOCITO, V., J. Biol. Chem., 161, 559, (1945).

70) GREIN, L., and PFLEIDERER, G., Biochem. Z., 330, 433, (1958).

71) GRODZENSKY, D.E., Bull. Biol. Med. Exp. U.R.S.S., 9, 116, (1940).

72) GUTFREUND, H., EBNER, K.E., and MENDIOLA, L., Nature, 192, 820, (1961).

73) GUTHRIE, R.D., MEISTER, W., and CRAM, D.J., J. Amer. Chem. Soc., 89, 5288, (1967).

74) HABEEB, A., CASSIDY, H.G., and SINGER, S.J., Biochim. Biophys. Acta, 29, 587, (1958).

75) HAMMES, G.G., and FASELLA, P., J. Amer. Chem. Soc., 84, 4644, (1962).

76) HAMMES, G.G., and HASLAM, J.L., Biochem. 7, 1519, (1968).

77) HAMMES, G.G., and HASLAM, J.L., Biochem., 8, 1591, (1969).

78) HARRIS, H., KALOGERAKOS, T., EVANGELOPOULOS, A.R., and BAYLEY, P.M., Biochem. J. 126, 20p, (1972).

79) HATHAWAY, D.E. MALLINSON, A., and AKINTOWA, D.A.A., Biochem. J., 94, 676, (1965).

80) HAYAISHI, O., and SHIZUTA, Y., Vitamin Horm., 28, 245, (1970).

81) HEINERT, D., and MARTELL, A.E., J. Amer. Chem. Soc., 85, 183, (1963).

82) HEINERT, D., and MARTELL, A.E., J. Amer. Chem. Soc., 85 188, (1963).

83) HENSON, C.P., and CLELAND, W.W., Biochem., 3, 338, (1964).

84) HERBST, R.M., and ENGEL, L.L., J. Biol. Chem., 107, 505, (1934).

85) HOFFEE, P., LIU, C.Y., PUGH, P.L., and HORECKER, B.L., Proc. Nat. Acad. Sci., 57, 107, (1967).

86) HOPPER, S., and SEGAL, H.L., J. Biol. Chem. 237, 3189, (1962)

87) HUCHO, F., MARKAU, U., and SUND, H., Eur. J. Biochem., 32, 69, (1973).

88) HUGHES, R.C., JENKINS, W.T., and FISCHER, E.H., Proc. Nat Acad. Sci., 48, 1615, (1962).

89) IKAWA, M., and SNELL, E.E., J. Amer. Chem. Soc., 76, 653, (1954).

90) IVANOV, V.I., BREUSOV, Y.N., KARPEISKY, M.Y., and POLYANOVSKY O.L., Mol. Biol., 1, 588, (1967).

91) IVANOV, V.I., and KARPEISKY, M.Y., Adv. Enzymol., 32, 21, (1969).

92) JENKINS, W.T., and SIZER, I.W., J. Amer. Chem. Soc., 79, 2655, (1957).

93) JENKINS, W.T., YPHANTIS, D.A., and SIZER, I.W., J. Biol. Chem., 234, 51, (1958).

94) JENKINS, W.T., and SIZER, I.W., J. Biol. Chem., 234, 1179, (1959).

95) JENKINS, W.T., YPHANTIS, D.A., and SIZER, I.W., J. Biol. Chem., 234, 51, (1958).

96) JENKINS, W.T., and SIZER, I.W., J. Biol. Chem., 235, 620, (1960).

97) JENKINS, W.T., J. Biol. Chem. 236, 1121, (1961).

98) JENKINS, W.T., J. Biol. Chem., 236, 474, (1961).

99) JENKINS, W.T., Fed. Proc., 20, 978, (1961).

100) JENKINS, W.T., Biochem. J., 82, 1p, (1962).

101) JENKINS, W.T., Chem. Biol. Aspects of Pyridoxal Catalysis, 139, (1962).

102) JENKINS, W.T., J. Biol. Chem., 239, 1742, (1964).

103) JENKINS, W.T., and TAYLOR, R.T., J. Biol. Chem., 240, 2907, (1965).

104) JENKINS, W.T., D'ARI, L., J. Biol. Chem., 241, 2845, (1966)

105) JENKINS, W.T., D'ARI, L., J. Biol. Chem., 241, 5667, (1966)

106) JENKINS, W.T., and D'ARI, L., Biochem., 5, 2900, (1966).

107) JOHN, R.A., and FASELLA, P., Biochem., 8, 4477, (1969).

108) JOHN, R.A., and TUDBALL, N., Eur. J. Biochem., 31, 135, (1972).

109) KALLEN, R.G., and JENCKS, W.P., J. Biol. Chem., 241, 5864, (1966).

110) KARNI-KATSAMIDAS, I., DIMITROPOULOS, C., and EVANGELOPOULOS, A.E., Eur. J. Biochem., 8, 50, (1969).

111) KARPEISKY, M.Y., BREUSOV, Y.N., KHOMUTOV, R.M., SEVERIN, E.S. and POLYANOVSKY, O.L., Biokhimiya, 28, 286, (1963).

112) KARPEISKY, M.Y., and BREUSOV, Y.N., Biokhimiya, 30, 151, (1965).

113) KARPEISKY, M.Y., and IVANOV, V.I., Nature, 210, 493, (1966).

114) KHOMUTOV, R.M., KOVALEVA, G.K., SEVERIN, E.S., and VDOVINA, L.V., Biokhimiya, 32, 900, (1967).

115) KISTIAKOVSKY, G.B., and SHAW, W.H.R., J. Amer. Chem. Soc., 74, 5015, (1952).

116) KISTIAKOVSKY, G.B., et al., J. Amer. Chem. Soc., 75, 2751, (1953).

117) KOVALEVA, G.K., and SEVERIN, E.S., Biokhimiya, 37, 392, (1972).

118) KRISHNASWAMY, M., UMAKANT, W.K., J. Biol. Chem., 245, 3956, (1970).

119) LOWRY, O.H., ROSEBROUGH, N.J., FARR, L., and RANDALL, R.J., J. Biol. Chem., 193, 265, (1951).

120) MANNING, J.M., KHOMUTOV, R.M., and FASELLA, P., Eur. J. Biochem., 5, 199, (1968).

121) MALETTE, L.E., EXTON, J.H., and PARK, C.R., J. Biol. Chem. 244, 5713, (1969).

122) MANNING, J.M., KHOMUTOV, R.M., and FASELLA, P., Eur. J. Biochem., 5, 199, (1968).

123) MARINI, M.A., and MARTIN, C.J., Eur. J. Biochem., 19, 162, (1972).

124) MARINO, G., PATERNO, M., and DE ROSA, M., F.E.B.S. Letters, 21, 53, (1972).

125) MARTINEZ-CARRION, M., and TIEMEIER, D.C., Biochem., 6, 1715, (1967).

126) MARTINEZ-CARRION, M., TURANO, C., CHIANCONE, E., BOSSA, F., GIARTOSIO, A., RIVA, F., and FASELLA, P., J. Biol. Chem., 242, 2397, (1967).

127) MARTINEZ-CARRION, M., TURANO, C., RIVA, F., and FASELLA, P., J. Biol. Chem., 242, 1426, (1967).

128) MARTINEZ-CARRION, M., and TIEMEIER, D.C., Biochem. 8, 1095, (1969).

129) MARTINEZ-CARRION, M., KUCZENSKY, R., TIEMEIER, D.C., and PETERSON, D.L., J. Biol. Chem., 245, 799, (1970)

130) MARTINEZ-CARRION, M., and PETERSON, D.L., J. Biol. Chem., 245, 806, (1970).

131) MARTINEZ-CARRION, M., TIEMEIER, D.C., and PETERSON, D.L., Biochem., 9, 2574, (1970).

132) MARTINEZ-CARRION, M., CHENG, S., and RELIMPIO, A.M., J. Biol. Chem., 248, 2153, (1973).

133) MASSEY, V., Biochem. J., 55, 172, (1953).

134) MATSUO, Y., J. Amer. Chem. Soc., 79, 2016, (1957).

135) MAURER, P.H., and HEIDELBERGER, M., J. Amer. Chem. Soc., 73, 2070, (1951).

136) MAURER, P.H., and HEIDELBERGER, M., J. Amer. Chem. Soc., 74, 1089, (1952).

137) MEISTER, A., SOBER, H.A., and PETERSON, E.A., J. Biol. Chem., 206, 89, (1953).

138) METZLER, D.E., IKAWA, M., and SNELL, E.E., J. Amer. Chem. Soc., 76, 648, (1954).

139) METZLER, D.E., J. Amer., Chem. Soc., 79, 485, (1957).

140) MICHAELIS, L., and MENTEN, M.L., Biochem. Z., 49, 333, (1913).

141) MICHUDA, C.M., and MARTINEZ-CARRION, M., J. Biol. Chem., 244, 5920, (1969).

142) MICHUDA, C.M., and MARTINEZ-CARRION, M., J. Biol. Chem., 245, 262, (1970).

143) MORINO, Y., and KAGAMIYAMA, H., and WADA, H., J. Biol. Chem., 239, 943, (1964).

144) MORINO, Y and SNELL, E.E., Proc. Nat. Acad. Sci., 57, 1692, (1967).

145) MORINO, Y., and WATANABE, T., Biochem., 8, 3412, (1969).

146) MORINO, Y., and MITSOHIRO, O., Biochem. Biophys. Res. Commun., 47, 498, (1972).

147) MORINO, Y., and OKAMOTO, M., Biochem., 11, 3196, (1972).

148) NAGANO, K., and METZLER, D.E., J. Amer. Chem. Soc., 89, 2891, (1967).

149) NAIR, P.M., VAIDYANATHAN, C.S., Arch. Biochem. Biophys., 104, 405, (1964).

150) NEUBERGER, A., Biochem. J., 38, 309, (1944).

151) NISHII, Y., SHIMIZU, T., and ANDO, S., Bitamin, 40, 442, (1969).

152) OKAMOTO, M., and MORINO, Y., Biochem., 11, 3188, (1972).

153) OSTER, G., BELLIN, J.S., KIMBALL, R.W., and SCHRADER, M.E., J. Amer. Chem. Soc., 81, 5095, (1959).

154) PERAULT, A., PULLMAN, B., and VALDEMORO, C., Biochim. Biophys. Acta, 45, 555, (1961).

155) PETERSON, E.A., and SOBER, H.A., J. Amer. Chem. Soc., 76, 169, (1954).

156) PFLEIDERER,G., STOCK, A., ORTANDERL, F., and MELLA, K., Eur. J. Biochem., 5, 18, (1968).

157) PHILPOT, J.S., and SMALL, P.A., Biochem. J., 32, 534, (1938).

158) PHILPOT, J.S., and SMALL, P.A., Biochem. J., 32, 542, (1938).

159) POLYANOVSKY, O.L., Biokhimiya, 27, 623, (1962).

160) POLYANOVSKY, O.L., and KEIL, B.A., Biokhimiya, 28, 307, (1963).

161) POLYANOVSKY, O.L., ZAGYANSKY, Y.A., and TUMERMAN, L.A., Mol. Biol., 4, 458, (1970).

162) POLYANOVSKY, O.L., DEMIDKINA, T.V., and EGOROV, C.A., F.E.B.S. Letters, 23, 262, (1972).

163) PULLMAN, B., Chem. Biol. Aspects Pyridoxal Catalysis, 103 (1962).

165) RIORDAN, J.F., SOKOLOVSKY,M., and VALLEE, B.L., J. Amer. Chem. Soc., 88, 4104, (1966).

166) RIORDAN, J.F., SOKOLOVSKY, M., and VALLEE, B.L., Biochem. 6, 358 , (1967).

167) RIORDAN, J.F., and CHRISTEN, P., Biochem. 7, 1525, (1968).

168) RYAN, E., and FOTTRELL, P.F., F.E.B.S. Letters, 23, 73, (1972).

169) SAIDEL, L.J., and CARINO, R.L., Fed. Proc., 25, 796, (1966).

170) SAIER, M.H., and JENKINS, W.T., J. Biol. Chem., 242, 91, (1967).

171) SAIER, M.H., and JENKINS, W.T., J. Biol. Chem., 242, 101, (1967).

172) SCHIRCH, L.G., and MASON, M., J. Biol. Chem., 238, 1032, (1963).

173) SCHIRCH, L.G., and SLOTTER, R.A., Biochem., 5, 3175, (1966).

174) SEGAL, H.L. BEATTIE, D.S., and HOPPER, S., J. Biol. Chem., (1962).

175) SEVERIN, E.S., GULYAEV, N.N., KHURS, E.N., and KHOMUTOV, R.M. Biochem. Biophys. Res. Commun., 35, 38, (1969).

176) SEVERIN, E.S., KOVALEVA, G.K., and SASCHENKA, L.P., Biokhimiya, 37, 385, (1972).

177) SHAPIRO, A.L., VINUELA, E., and MAIZE,, J.V., Biochem. Biophys. Res. Commun., 28, 815, (1967).

178) SHLIAPNIKOV, S.V., BOCHAROV, A.L., DZEDZIELA, D.A., and KARPEISKY, M.Y., Mol. Biol., 3, 709, (1969).

179) SHLIAPNIKOV, S.V., and KARPEISKY, M.Y., Eur. J. Biochem., 11, 424, (1969).

180) SHRAWDER, E., and MARTINEZ-CARRION, M., J. Biol. Chem., 247, 2486, (1972).

181) SHRAWDER,E., and MARTINEZ-CARRION, M., J. Biol. Chem., 248, 2141, (1973).

182) SHRAWDER, E., and MARTINEZ-CARRION, M., J. Biol. Chem., 248, 2147, (1973).

183) SOKOLOVSKY, M., RIORDAN, J.F., and VALLEE, B.L., Biochem., 5, 3582, (1966).

184) SOKOLOVSKY, M., HARELL, D., and RIORDAN, J.F., Biochem. 8, 4740, (1969).

185) SOKOLOVSKY, M., FUCHS, M., and RIORDAN, J.F., F.E.B.S. Letters, 7, 167, (1970).

186) STANKEWITZ, M.J., CHENG,S., and MARTINEZ-CARRION, M., Biochem., 10, 2877, (1971).

187) THANASSI, J.W., BUTLER, A.R., and BRUICE, T.C., Biochem., 4, 1463, (1965).

188) TORCHINSKY, Y.M., Biokhimiya, 27, 778, (1962).

189) TORCHINSKY, Y.M., Biokhimiya, 29, 458, (1964).

190) TORCHINSKY, Y.M., and KORENEVA, L.G., Biochim. Biophys. Acta, 79, 426, (1964).

191) TORCHINSKY, Y.M., and MALAKHOVA, E.A., Dokl. Akad. Nauk. S.S.R., 178, 722, (1968).

192) TORCHINSKY, and SINITSYNA, N.I., Mol. Biol., 4, 256, (1970).

193) TORCHINSKY, Y.M., ZUFAROV, R.A., AGALAROVA, M.B., and SEVERIN, E.S., F.E.B.S. Letters, 28, 302, (1972).

194) TUDBALL, N., and THOMAS, P., Biochem. J., 128, 41, (1972).

195) TURANO, C., and RIVA, F., Ital. J. Biochem., 13, 304, (1964).

196) TURANO, C., GIARTOSIO, A., RIVA, F., BARONCELLI, V., BOSSA, F., Arch. Biochem. Biophys., 117, 678, (1966).

197) TURANO, C., GIARTOSIO, A., RIVA., F., and BARONCELLI, V., Biochem. J. 104, 970, (1967).

198) TURANO, C., BARRA, D., BOSSA, F., FERRARER, A., and GIARTOSIO, A., Eur. J. Biochem., 23, 349, (1971).

199) VAN VANUKIS, H., LEIKHIM, E., DELANEY, R., LEVINE, L., BROWN, R.K., J. Biol. Chem., 235, 3430, (1960).

200) VELICK, S.F., and VAYDA, J., J. Biol. Chem., 237, 2109, (1962).

201) WADA, H., WATANABE, T., and MIYATAKA, A., Biochem. Biophys. Res, Commun., 43, 1318, (1971).

202) WEBER, K., and OSBORN, M., J. Biol. Chem., 244, 4406, (1969).

203) WEIL, L., GORDON, W.G., and BUCHERT, A.R., Arch. Biochem. Biophys., 33, 90, (1951).

204) WEIL, L., and BUCHERT, A.R., Arch. Biochem. Biophys., 34, 1, (1952).

205) WEIL, L., BUCHERT, A.R., and MAHER, J., Arch. Biochem. Biophys,. 40, 245, (1952).

206) WEIL, L., JAMES, S., and BUCHERT, A.R., Arch. Biochem. Biophys., 46, 266, (1953).

207) WEIL, L.: and SEIBLES, T.S., Arch. Biochem. Biophys., 54, 368, (1955).

208) WESTHEAD, E.W., Fed. Proc., 22, 594, (1963).

209) WESTHEAD, E.W., Biochem. 4, 2139, (1965).

210) WILSON, D.G., KING, K.W., and BURRIS, R.H., J. Biol. Chem., 863, (1954).

211) WROBLEWSKY, F., and LADUE, J.S., Proc. Soc. Exp. Biol. N. Y., 21, 569, (1956).

212) BEIS, I.D., M. Sc. thesis, University of Warwick, (1970)